

SYNTHESIS AND ELECTROCHEMICAL CHARACTERIZATION OF NOVEL
BRIDGED DIFERROCENE TAGGED ALKANETHIOL SELF-ASSEMBLED
MONOLAYERS

by

Carolyn Ann Pugh

Submitted in Partial Fulfillment of the Requirements

for the Degree of

Master of Science

in the

Chemistry

Program

YOUNGSTOWN STATE UNIVERSITY

May, 2001

SYNTHESIS AND ELECTROCHEMICAL CHARACTERIZATION OF NOVEL
BRIDGED DIFERROCENE TAGGED ALKANETHIOL SELF-ASSEMBLED
MONOLAYERS

Carolyn Ann Pugh

I hereby release this thesis to the public. I understand this thesis will be housed at the Circulation Desk of the University Library and will be available for public access. I also authorize the University or other Individuals to make copies of this thesis as needed for scholarly research.

Signature:

Carolyn A. Pugh 5.7.01
Carolyn A. Pugh, Student Date

Approvals:

Larry S. Curtin 5/5/01
Dr. Larry S. Curtin, Thesis Advisor Date

James H. Mike 5/7/01
Dr. James H. Mike, Committee Member Date

Timothy R. Wagner 5/7/01
Dr. Timothy R. Wagner, Committee Member Date

Peter J. Kasvinsky 5/7/01
Dr. Peter J. Kasvinsky, Dean of Graduate Studies Date

Abstract

A diferrocene tagged alkanethiol monolayer was synthesized via a four part reaction procedure to produce 6-(diferrocenylhexanylethyl)pentanethiol. Monolayers were adsorbed onto a polycrystalline gold electrode by soaking in a solution of the thiol. Cyclic voltammetric experiments were done to determine the heterogeneous electron transfer rate constant, k° . Formal potentials, surface coverages and FWHM values were investigated to determine the thermodynamic properties of the thiol monolayer.

Single crystal X-ray crystallography was performed on three compounds synthesized throughout the reaction pathway. These experiments provided information regarding symmetry and unit cell packing of the molecules, as well as the relative positions of the ferrocenes with respect to one another.

This research provides preliminary voltammetric data on alkanethiol monolayers tagged with dimeric ferrocenes. Introduction of another electroactive moiety within the monolayer can dramatically alter the shape of the voltammograms. Formal potentials, FWHM data and electrochemical kinetics were similar to those reported in the literature. Analysis of surface coverages indicates that only 40% of the outer ferrocenes are electrochemically accessible. A possible explanation for this unusual phenomenon is suggested.

Acknowledgements

I would first like to acknowledge my fearless leader, Larry, who has put up with my “perfectionist” tendencies for two years and never once complained. Larry I thank you for introducing me to the realm of electrochemistry. It took many explanations and discussions and I thank you for your patience and contributing to my growth as a scientist.

The X-ray expert, Dr. Wagner (“Tim Dog”), who without his help my crystallography skills would be quite poor. I also thank him for taking the time to review my thesis. Also, the crystallography chapter would not have come to fruition without the help of Dr. Casey Raymond at Kent State University.

Dr. Mike who has provided me with his wisdom and guidance throughout my YSU career. He opened my eyes to the wonderful world of chemistry. I also thank him for reviewing my thesis on such short notice.

My Mom, Dad and comedic brother, Jimmy (“Ladies Man”) who have emotionally and financially supported me through my college years. Without them, I would not be the person that I am today. Thank you for your unconditional love and patience, for without it, I don’t think I would have come this far.

YSU chemistry has given me everlasting friendships that I will cherish forever. Erica, my cohort in crime, who has entertained me in both undergraduate and graduate school. Chemistry would not have been fun or interesting without her. Thank you for all your help with everything. I will cherish the memories of the fire we caused. Rhea, my workout buddy and sister, thanks for all the coffee talks and your endless advice with X-ray. The Curtin research group, Jeff, Val, Wendy, Rick, for making each day different as

well as “interesting”. Joni, thanks for your help with the Excel spreadsheets. I knew your CPA skills would benefit this thesis in some way.

Ray (“Ray Dog” and “Log Off Hoff”) for your knowledge on everything. You are invaluable to the chemistry department and I am forever grateful for all of your help. Bruce Levinson, for the use of the LC/MS in the Center for Biomedical and Environmental Research, I also thank you for knowing all of the answers to my questions and helping with the spectroscopic data.

Finally, to my fiancé, Buck. Your endless love, understanding and patience gave me the strength to do what I do everyday. You are such an integral part of my life and I have the rest of my life to prove to you how important you are to me. I thank you for loving me and sticking by my side through all of the stressful times. Thank you for all of your help. Just remember, chemistry is what brought us together, which makes me love it even more.

I consider myself extremely blessed to have had this opportunity as a chemistry graduate student. Not many people get to experience the world of chemistry that I have and I am so fortunate to have done so. I have met extraordinary people at YSU and each of them in some way has shaped the person and scientist that I am today. I am also blessed with wonderful family and friends, and dog (Amos), who have always been there for me. I want the people who read this work, to know how grateful and appreciative I am to have had these experiences and the great individuals that touched my life. Thank you.

Table of Contents

Title Page	i
Signature Page	ii
Abstract	iii
Acknowledgements	iv
Table of Contents	vi
List of Tables	x
List of Figures	xii
CHAPTER ONE INTRODUCTION	1
Introduction to Self Assembled Monolayers	1
Self Assembled Monolayer Formation	2
Langmuir-Blodgett (LB) Films	5
Organosilanes	7
Alkanethiol SAMs	7
Electrochemistry	12
Cyclic Voltammetry	13
Monolayer Electrochemistry	22
Monomeric Ferrocene Alkanethiol Monolayers	28
Dimeric Ferrocene Alkanethiol Monolayers	32
Research Proposal	37
References	39
CHAPTER TWO SYNTHESIS AND CHARACTERIZATION	40
Chemicals	40

Instrumentation	43
Synthesis of 1,6-diferrocenylhexane-1,6-dione and 1-ferrocenyl-carbonyl-2-ferrocenylcyclopentene	43
Spectroscopic Data for 1,6-diferrocenylhexane-1,6-dione	44
Spectroscopic Data for 1-ferrocenylcarbonyl-2-ferrocenylcyclopentene	45
Synthesis of 1,6-diferrocenylhexane and 1,6-diferrocenylhexane-1-one	45
Spectroscopic Data for 1,6-diferrocenylhexane	46
Spectroscopic Data for 1,6-diferrocenylhexane-1-one	47
Synthesis of 6-(diferrocenylhexanylecarbonyl)pentanebromide	47
Spectroscopic Data for 6-(diferrocenylhexanylecarbonyl)pentanebromide	48
Synthesis of 6-(diferrocenylhexanylecarbonyl)pentanethiol	48
Spectroscopic Data for 6-(diferrocenylhexanylecarbonyl)pentanethiol	49
Results and Discussion	50
Characterization of 1,6-diferrocenylhexane-1,6-dione	50
Characterization of 1-ferrocenylcarbonyl-2-ferrocenylcyclopentene	54
Characterization of 1,6-diferrocenylhexane	62
Characterization of 1,6-diferrocenylhexane-1-one	73
Characterization of 6-(diferrocenylhexanylecarbonyl)pentanebromide	77
Characterization of 6-(diferrocenylhexanylecarbonyl)pentanethiol	88
Conclusion	95
References	100
CHAPTER THREE X-RAY CRYSTALLOGRAPHY	101
Experimental	101
Instrumentation	102

X-ray Diffraction Analysis of 1,6-diferrocenylhexane-1,6-dione	103
X-ray Diffraction Analysis of 1-ferrocenylcarbonyl-2-ferrocenylcyclopentene	113
X-ray Diffraction Analysis of 1,6-diferrocenylhexane	115
Results and Discussion	115
Characterization of 1,6-diferrocenylhexane-1,6-dione	115
Characterization of 1-ferrocenylcarbonyl-2-ferrocenylcyclopentene	143
Characterization of 1,6-diferrocenylhexane	145
Conclusion	147
References	150
CHAPTER FOUR ELECTROCHEMISTRY	151
Chemicals	151
Instrumentation	152
Electrode Preparation	152
Solution Voltammetry	153
Monolayer Preparation	153
Solution Voltammetry of 1,6-diferrocenylhexane-1,6-dione	154
Solution Voltammetry of 1-ferrocenylcarbonyl-2-ferrocenylcyclopentene	154
Solution Voltammetry of 1,6-diferrocenylhexane	157
Solution Voltammetry of 1,6-diferrocenylhexane-1-one	157
Monolayer Voltammetry of 6-(diferrocenylhexanylethynyl)pentanethiol	157
Results and Discussion	163
Analysis of Solution Voltammetry	163

Analysis of 6-(diferrocenylhexanylethyl)pentanethiol Self-Assembled Monolayer Voltammetry	165
Conclusion	176
References	177
Appendix A	178
Appendix B	187
Appendix C	214
Appendix D	222

LIST OF TABLES

TABLE		PAGE
2.1	Assigned Fragments from 1,6-diferrocenylhexane-1,6-dione Mass Spectrum	57
2.2	Assigned Fragments from 1-ferrocenylcarbonyl-2-ferrocenylcyclopentene Mass Spectrum	66
2.3	Assigned Fragments from 1,6-diferrocenylhexane Mass Spectrum	72
2.4	Assigned Fragments from 1,6-diferrocenylhexane-1-one Mass Spectrum	80
2.5	Assigned Fragments from 6-(diferrocenylhexanylecarbonyl)pentanebromide Mass Spectrum	90
2.6	Assigned Fragments from 6-(diferrocenylhexanylecarbonyl)pentanethiol Mass Spectrum	98
3.1	Crystal Data and Structure Refinement Results for 1,6-diferrocenylhexane-1,6-dione	104
3.2	Atomic Coordinates and Equivalent Isotropic Displacement Parameters for 1,6-diferrocenylhexane-1,6-dione	107
3.3	Anisotropic Displacement Parameters for 1,6-diferrocenylhexane-1,6-dione	108
3.4	Bond Lengths [Å] for 1,6-diferrocenylhexane-1,6-dione	109
3.5	Bond Angles [degrees] for 1,6-diferrocenylhexane-1,6-dione	110
3.6	Hydrogen Coordinates and Isotropic Displacement Parameters for 1,6-diferrocenylhexane-1,6-dione	112
3.7	Crystal Data and Structure Refinement for 1-ferrocenylcarbonyl-2-ferrocenylcyclopentene	114
3.8	Atomic Coordinates and Equivalent Isotropic Displacement Parameters for 1-ferrocenylcarbonyl-2-ferrocenylcyclopentene	119
3.9	Bond Lengths [Å] for 1-ferrocenylcarbonyl-2-ferrocenylcyclopentene	121

3.10	Bond Angles [\AA] for 1-ferrocenylcarbonyl-2-ferrocenylcyclopentene	123
3.11	Anisotropic Displacement Parameters for 1-ferrocenylcarbonyl-2-ferrocenylcyclopentene	129
3.12	Hydrogen Coordinates and Isotropic Displacement Parameters for 1-ferrocenylcarbonyl-2-ferrocenylcyclopentene	131
3.13	Crystal Data and Structure Refinement for 1,6-diferrocenylhexane	133
3.14	Atomic Coordinates and Equivalent Isotropic Displacement Parameters for 1,6-diferrocenylhexane	136
3.15	Bond Lengths [\AA] for 1,6-diferrocenylhexane	137
3.16	Bond Angles [degrees] for 1,6-diferrocenylhexane	138
3.17	Anisotropic Displacement Parameters for 1,6-diferrocenylhexane	140
3.18	Hydrogen Coordinates and Isotropic Displacement Parameters for 1,6-diferrocenylhexane	141
A-1	Equations of Mean Plane for 1,6-diferrocenylhexane-1,6-dione for C1 to C5	179
A-2	Equations of Mean Plane for 1,6-diferrocenylhexane-1,6-dione for C6 to C10	179
A-3	Equations of Mean Plane for 1,6-diferrocenylhexane-1,6-dione for C6 to C10 and O1	179
A-4	Observed and Calculated Structure Factors for 1,6-diferrocenylhexane-1,6-dione	180
B-1	Equations of Mean Plane for 1-ferrocenylcarbonyl-2-ferrocenylcyclopentene for C6 to C11 and O1	188
B-2	Equations of Mean Plane for 1-ferrocenylcarbonyl-2-ferrocenylcyclopentene for C32 to C37 and O2	188
B-3	Equations of Mean Plane for 1-ferrocenylcarbonyl-2-ferrocenylcyclopentene for C12 to C21	189
B-4	Equations of Mean Plane for 1-ferrocenylcarbonyl-2-ferrocenylcyclopentene for C38 to C47	189

B-5	Equations of Mean Plane for 1-ferrocenylcarbonyl-2-ferrocenyl-cyclopentene for C1 to C5	190
B-6	Equations of Mean Plane for 1-ferrocenylcarbonyl-2-ferrocenyl-cyclopentene for C6 to C10	190
B-7	Equations of Mean Plane for 1-ferrocenylcarbonyl-2-ferrocenyl-cyclopentene for C17 to C21	190
B-8	Equations of Mean Plane for 1-ferrocenylcarbonyl-2-ferrocenyl-cyclopentene for C22 to C26	191
B-9	Equations of Mean Plane for 1-ferrocenylcarbonyl-2-ferrocenyl-cyclopentene for C27 to C31	191
B-10	Equations of Mean Plane for 1-ferrocenylcarbonyl-2-ferrocenyl-cyclopentene for C32 to C36	191
B-11	Equations of Mean Plane for 1-ferrocenylcarbonyl-2-ferrocenyl-cyclopentene for C43 to C47	192
B-12	Equations of Mean Plane for 1-ferrocenylcarbonyl-2-ferrocenyl-cyclopentene for C48 to C52	192
B-13	Equations of Mean Plane for 1-ferrocenylcarbonyl-2-ferrocenyl-cyclopentene for C12 to C16	192
B-14	Equations of Mean Plane for 1-ferrocenylcarbonyl-2-ferrocenyl-cyclopentene for C38 to C42	193
B-15	Observed and Calculated Structure Factors for 1-ferrocenyl-carbonyl-2-ferrocenylcyclopentene	194
C-1	Equations of Mean Plane for 1,6-diferrocenylhexane for C1 to C5	215
C-2	Equations of Mean Plane for 1,6-diferrocenylhexane for C6 to C10	215
C-3	Observed and Calculated Structure Factors for 1,6-diferrocenyl-hexane	216
D-1	Solution Voltammetry Data for 1,6-diferrocenylhexane-1,6-dione	223

D-2	Solution Voltammetry Data for 1-ferrocenylcarbonyl-2-ferrocenyl-cyclopentene	224
D-3	Solution Voltammetry Data for 1,6-diferrocenylohexane	225
D-4	Solution Voltammetry Data for 1,6-diferrocenylohexane-1-one	226
D-5	Monolayer Voltammetry Data for Thiol-First Electrode	227
D-6	Monolayer Voltammetry Data for Thiol-Second Electrode	228
D-7	Monolayer Voltammetry Data for Thiol-Third Electrode	229

LIST OF FIGURES

FIGURE		PAGE
1.1	Schematic representation of components of a self-assembled monolayer and interactions involved	3
1.2	The formation of a monolayer through Langmuir-Blodgett techniques	6
1.3	An organosilane self-assembled monolayer	8
1.4	An alkanethiol self-assembled monolayer on Au	10
1.5	Potential versus time profile and resulting voltammogram for a reversible redox couple	14
1.6	Representation of (a) reduction and (b) oxidation process of a species in solution	17
1.7	Theoretical cyclic voltammogram of a reversible surface confined species	23
1.8	Possible self-assembled monolayer defects	25
1.9	Plot of $n\Delta E_p$ versus $1/m$ based on Laviron's tabulated values	27
1.10	Voltammogram for mixed monolayers of $\text{FcCO}_2(\text{CH}_2)_{11}\text{SH}$ and $\text{CH}_3(\text{CH}_2)_{15}\text{SH}$	29
1.11	Cyclic voltammogram for 6-(1,2-diferrocenylethylcarbonyl)-pentanethiol	33
2.1	Schematic of Synthetic Pathway	41
2.2	^1H NMR spectrum of 1,6-diferrocenylhexane-1,6-dione	51
2.3	^{13}C NMR spectrum of 1,6-diferrocenylhexane-1,6-dione	52
2.4	^{13}C NMR spectrum close up from 70-85 ppm of 1,6-diferrocenylhexane-1,6-dione	54
2.5	IR spectrum of 1,6-diferrocenylhexane-1,6-dione	55
2.6	Mass spectrum of 1,6-diferrocenylhexane-1,6-dione	56

2.7	¹ H NMR spectrum of 1-ferrocenylcarbonyl-2-ferrocenylcyclopentene	58
2.8	¹³ C NMR spectrum of 1-ferrocenylcarbonyl-2-ferrocenylcyclopentene	60
2.9	¹³ C NMR spectrum close up from 69-82 ppm of 1-ferrocenylcarbonyl-2-ferrocenylcyclopentene	61
2.10	APT spectrum of 1-ferrocenylcarbonyl-2-ferrocenylcyclopentene	63
2.11	IR spectrum of 1-ferrocenylcarbonyl-2-ferrocenylcyclopentene	64
2.12	Mass spectrum of 1-ferrocenylcarbonyl-2-ferrocenylcyclopentene	65
2.13	¹ H NMR spectrum of 1,6-diferrocenylhexane	67
2.14	¹³ C NMR spectrum of 1,6-diferrocenylhexane	69
2.15	IR spectrum of 1,6-diferrocenylhexane	70
2.16	Mass spectrum of 1,6-diferrocenylhexane	71
2.17	¹ H NMR spectrum of 1,6-diferrocenylhexane-1-one	74
2.18	¹³ C NMR spectrum of 1,6-diferrocenylhexane-1-one	75
2.19	¹³ C NMR close up from 65-95 ppm of 1,6-diferrocenylhexane-1-one	76
2.20	IR spectrum of 1,6-diferrocenylhexane-1-one	78
2.21	Mass spectrum of 1,6-diferrocenylhexane-1-one	79
2.22	¹ H NMR spectrum close up from 1.2-2.0 ppm of 6-(diferrocenylhexanylecarbonyl)pentanebromide	82
2.23	¹ H NMR spectrum close up from 2.3-3.5 ppm of 6-(diferrocenylhexanylecarbonyl)pentanebromide	83
2.24	¹ H NMR spectrum close up from 4.0-4.6 ppm of 6-(diferrocenylhexanylecarbonyl)pentanebromide	84
2.25	¹³ C NMR spectrum of 6-(diferrocenylhexanylecarbonyl)pentanebromide	86

2.26	¹³ C NMR spectrum close up from 25-42 ppm and 65-80 ppm of 6-(diferrocenylhexanycarbonyl)pentanebromide	87
2.27	Mass Spectrum of 6-(diferrocenylhexanycarbonyl)pentanebromide	89
2.28	¹ H NMR spectrum close up from 1.2-3.0 ppm of 6-(diferrocenylhexanycarbonyl)pentanethiol	91
2.29	¹ H NMR spectrum close up from 4.0-4.6 ppm of 6-(diferrocenylhexanycarbonyl)pentanethiol	93
2.30	¹³ C NMR spectrum close up from 25-45 ppm and 68-77 ppm of 6-(diferrocenylhexanycarbonyl)pentanethiol	94
2.31	¹³ C NMR spectrum of 6-(diferrocenylhexanycarbonyl)pentanethiol	96
2.32	Mass Spectrum of 6-(diferrocenylhexanycarbonyl)pentanethiol	97
3.1	ORTEP plot of 1,6-diferrocenylhexane-1,6-dione (50% ellipsoids)	105
3.2	Unit cell of 1,6-diferrocenylhexane-1,6-dione	106
3.3	ORTEP plot of 1-ferrocenylcarbonyl-2-ferrocenylcyclopentene (50% ellipsoids)	116
3.4	ORTEP plot of 1-ferrocenylcarbonyl-2-ferrocenylcyclopentene (50% ellipsoids)	117
3.5	Unit cell of 1-ferrocenylcarbonyl-2-ferrocenylcyclopentene	118
3.6	ORTEP plot of 1,6-diferrocenylhexane (50% ellipsoids)	134
3.7	Unit cell of 1,6-diferrocenylhexane	135
3.8	ORTEP plot of 1-ferrocenylcarbonyl-2-ferrocenylcyclopentene (50% ellipsoids) demonstrating coplanarity of carbonyl with adjacent Cp ring	144
3.9	ORTEP plot of 1-ferrocenylcarbonyl-2-ferrocenylcyclopentene (50% ellipsoids) demonstrating coplanarity of cyclopentene ring with adjacent Cp ring	146

4.1	Cyclic voltammogram of 1.0 mM 1,6-diferrocenylhexane-1,6-dione with 0.1 M TBAP in CH ₃ CN	155
4.2	Cyclic voltammogram of 1.0 mM 1-ferrocenylcarbonyl-2-ferrocenylcyclopentene with 0.1 M TBAP in CH ₃ CN	156
4.3	Cyclic voltammogram of 1.0 mM 1,6-diferrocenylhexane with 0.1 M TBAP in CH ₃ CN	158
4.4	Cyclic voltammogram of 1.0 mM 1,6-diferrocenylhexane-1-one with 0.1 M TBAP in CH ₃ CN	159
4.5	Poor cyclic voltammogram of 1.0 mM 6-(diferrocenylhexanylcarbonyl)pentanethiol	160
4.6	Cyclic voltammogram of 1.0 mM 6-(diferrocenylhexanylcarbonyl)pentanethiol	162
4.7	Plot of $i_{p,a}$ versus $v^{1/2}$ of 1,6-diferrocenylhexane-1,6-dione for the 25 mV/sec to 200 mV/sec scan rates	166
4.8	Plot of $i_{p,a}$ versus $v^{1/2}$ of 1-ferrocenylcarbonyl-2-ferrocenylcyclopentene for the 25 mV/sec to 200 mV/sec scan rates	167
4.9	Plot of $i_{p,a}$ versus $v^{1/2}$ of 1,6-diferrocenylhexane for the 25 mV/sec to 200 mV/sec scan rates	168
4.10	Plot of $i_{p,a}$ versus $v^{1/2}$ of 1,6-diferrocenylhexane-1-one for the 25 mV/sec to 200 mV/sec scan rates	169
4.11	Plot of ΔE_p versus v for 6-(diferrocenylhexanylcarbonyl)pentanethiol	171
4.12	Plot of $i_{p,a}$ versus v for 6-(diferrocenylhexanylcarbonyl)pentanethiol for the 25 mV/sec to 200 mV/sec scan rates	171
4.13	Cyclic voltammogram of 6-(diferrocenylhexanylcarbonyl)pentanethiol monolayer at 100 mV/sec (blue) and 100 sweeps (red) at 100 mV/sec. Blue: Before extended cycling; Red: After extended cycling	175

CHAPTER ONE

INTRODUCTION

Introduction to Self-Assembled Monolayers

Self-assembled monolayers (SAMs) have become a popular and convenient method for studying the chemistry of interfaces at the molecular level. The term self-assembly arises from the fact that molecules or atoms will assemble themselves in an ordered fashion, without machine or human manipulation. SAMs have potential applications in a variety of areas such as chemical and biochemical sensors, protective coatings, and molecular scale electronics.¹ Devices constructed using SAM technology could allow the machines and computers of the future to be drastically reduced in size while becoming increasingly more complex because of microscale electronics.

Although self-assembly has gained much attention recently, it is a phenomenon that nature has inspired. Simple, or thermodynamic self-assembly, can be exemplified in a raindrop. The drop takes a spherical shape because of the instability of the molecules on the exterior of the sphere in contact with air, while those on the interior exhibit more stability. The laws of thermodynamics govern that to keep the drop stable, the exterior surface area needs to be minimal. The water molecules will therefore assemble themselves into a spherical shape to minimize the surface area in contact with the air. Monolayer chemistry has the same fundamental principles as that of simple self-assembly, but the breadth of SAM chemistry is much more extensive.²

Another type of self-assembly, which pertains to more complicated situations, i.e. living organisms, is called coded self-assembly. Coded designates that self-assembly occurs through a set of instructions contained within the system. For example, cell reproduction is based on the genetic code of DNA within the cell. The cell will “follow” the instructions encoded on the DNA and reproduce to form another fully functioning cell without external manipulation. The ability of a system, as simple as a raindrop or as complex as a human cell, to “build” itself into an energetically stable state presents many advantages.²

Self-Assembled Monolayer Formation

Formation of self-assembled monolayers occurs spontaneously when a surface is exposed to a solution containing the species that will be adsorbed onto the substrate. The part of the molecule that adsorbs onto the surface is referred to as the head group (see Figure 1.1) and this generally occurs through an exothermic chemisorption process, producing strong interactions between the head group and the surface. The energy evolved during chemisorption lies in the tens of kilocalories per mole.³ Thermodynamics usually dictates that the head group molecules will “assemble” themselves at all available sites on the substrate, forming a close packed monolayer. The majority of monolayer systems contain an alkyl chain attached to the head group to promote close packing and order within the monolayer. As a result of close packing of the adsorbate molecules, van der Waals interactions occur between neighboring molecules. The van der Waals energies are slightly less than ten kilocalories per mole, and contribute to the overall stability of the monolayer.³ These van der Waals interactions between neighboring molecules become a driving force for monolayer

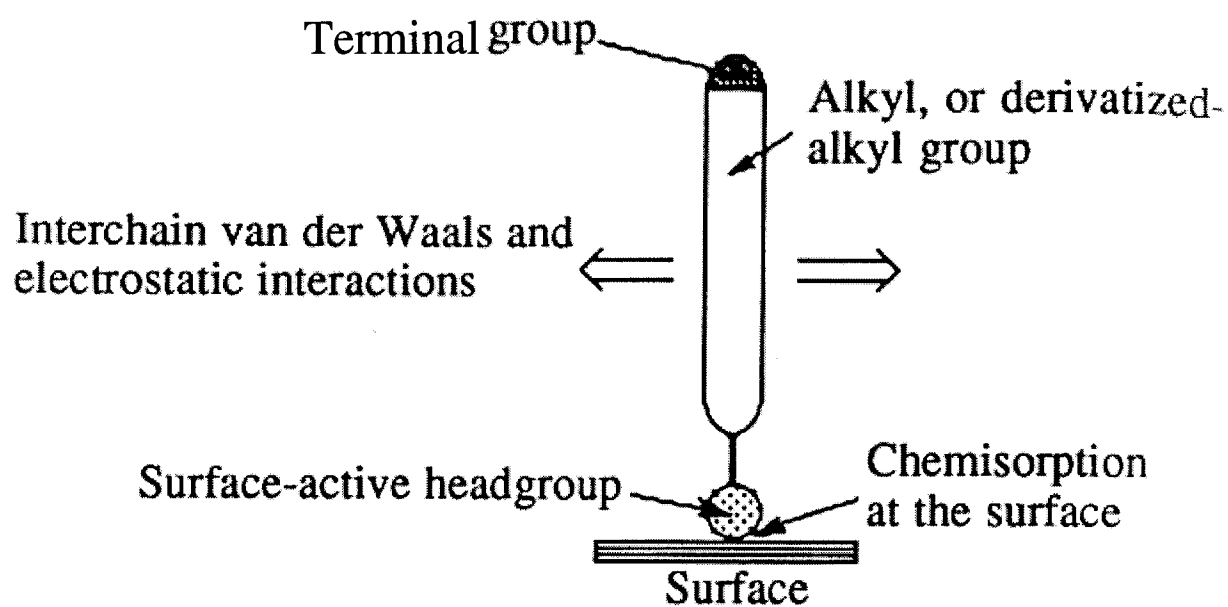


Figure 1.1: Schematic representation of the components of a self-assembled monolayer and the interactions involved. Reprinted from reference 3.

ordering on a surface.

The choice of head and terminal groups for the monolayer is limitless and is usually based on the desired properties that are to be investigated. The stability of the monolayer is usually determined by the strength of head group-substrate bond. The size of head and terminal groups can drastically affect the extent of ordering within the monolayer. Groups larger in size attached to a small alkyl chain do not pack as efficiently on the surface and van der Waals forces between adjacent chains are less effective, therefore the ordering of the monolayer is poor. Larger functionalities allow room for more defects, which translates into poor ordering. Defects associated with large head and terminal groups are corrected for by including molecules similar in nature to the alkyl chain connecting both groups. Smaller functionalities allow for more ordered monolayers because the molecules can pack on the surface much more efficiently, thereby increasing lateral van der Waals interactions.

The polarity of the terminal group can alter the chemical and physical properties of the monolayer. The polarity will dictate the type of surface, i.e. hydrophobic or hydrophilic, that will be constructed. For example, a methyl terminal group produces a hydrophobic surface, while a hydroxyl group produces a hydrophilic one. The desired chemical and physical properties depend on the application, i.e. sensing of hydronium ions may entail a pyridine group. The choice of head and terminal groups and the length of the alkyl chain allows the ability to tailor properties of the interface that is to be studied.

There are various ways to prepare self-assembled monolayers, each having inherent advantages and disadvantages.³ Some of the techniques can be used to form multilayer assemblies, but the focus will remain on the formation of monolayers. The three most

common methods used to prepare monolayers are Langmuir-Blodgett techniques and adsorption of organosilanes and alkanethiols to substrates.

Langmuir-Blodgett (LB) Films

The oldest and most studied process of monolayer preparation is that of Langmuir-Blodgett techniques.³ Although LB film preparation is not necessarily a self-assembly technique, it was the first technique that allowed the study and construction of ordered molecular assemblies. LB films usually consist of amphiphilic molecules in solution that are transferred to a solid substrate, from the solvent-air interface. The hydrophilic portion of the molecule resides at the water interface while the hydrophobic portion resides at the air interface. Experimentally, the conditions are controlled to the highest degree of sensitivity. The most common film preparation technique is called vertical deposition. The substrate, commonly glass, quartz, or silicon wafers, is placed into the amphiphilic solution, usually water, and moved through it, creating a film on the substrate surface. The film is then compressed in a Langmuir trough creating the solvent-air interface (see Figure 1.2). The monolayer is relatively unstable due to the absence of a chemical bond between the head group and the surface. Thus the adsorbate molecules are mobile on the surface. The motion causes instability and defect sites to be introduced, which can ultimately affect the overall properties of the monolayer. Another drawback to this technique is that the same surface is not created each time the process is performed. This process however, will form a film on a surface that is one molecule thick. Film instability and poor reproducibility are major disadvantages, thus LB techniques are rarely used for real devices.³

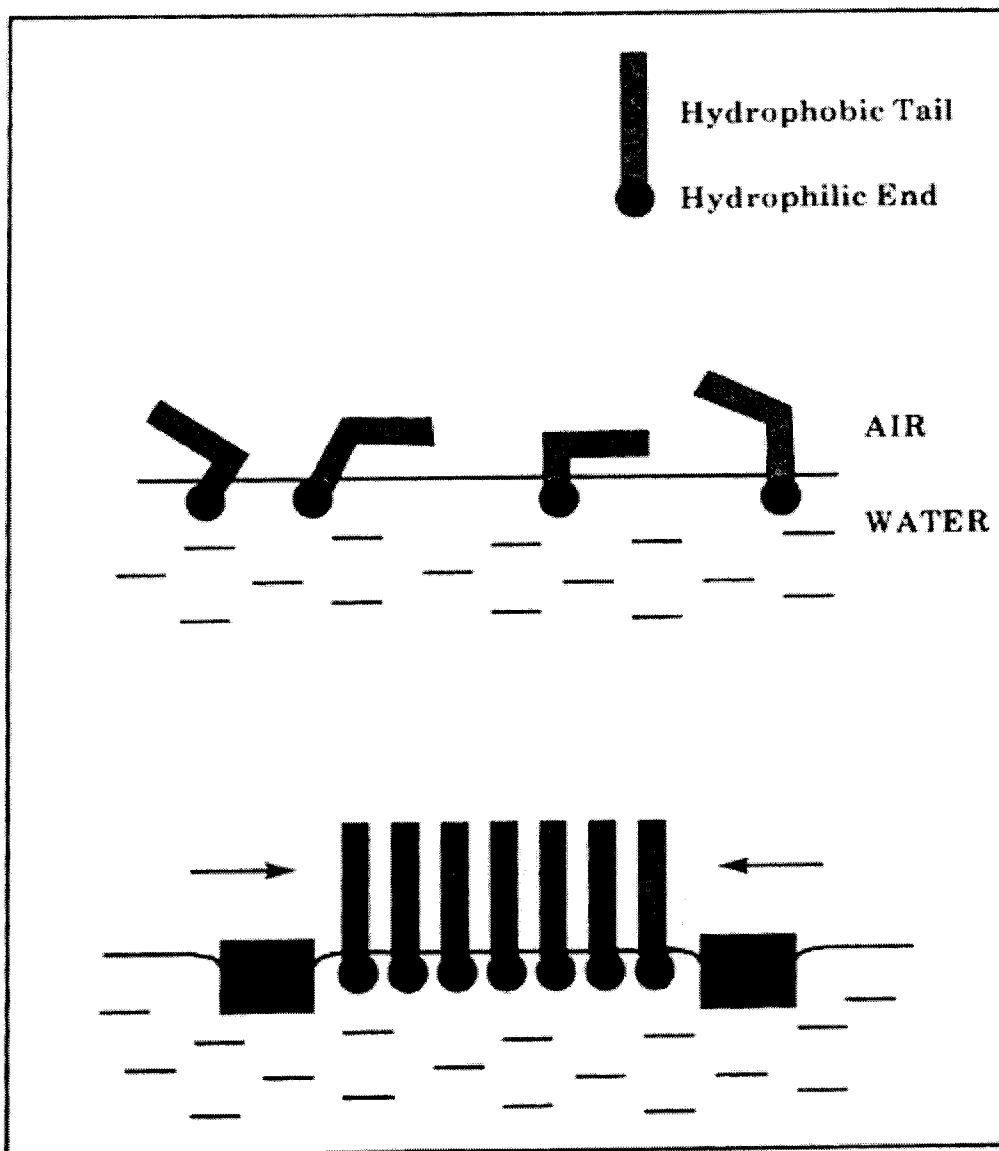


Figure 1.2: The formation of a monolayer through Langmuir-Blodgett techniques.
Reprinted from reference 4.

Organosilanes

Monolayer preparation can also take place through a reaction involving trichloroalkylsilanes or triethoxyalkylsilanes with a hydroxylated surface, usually silica, or platinum.³ The chlorine-silicon or ethoxy-silicon bond reacts with free hydroxyls on the surface, creating a complex silicon-oxygen bond network. A robust monolayer is formed due to the silanes covalently bonding to the hydroxylated surface, as well as Si-O-Si crosslinking between neighboring alkylsilanes (see Figure 1.3). A polymer network is created, producing a strong monolayer, but due to the large head group, the alkyl chains have some degree of movement and the films are disordered. Disorder is also introduced when the siloxanes cross link with a contaminant or bond to different points on the surface. Water sensitivity is also a problem during film preparation that can cause disorder. LB films do not possess this degree of order or strength, so organosilanes have the potential for more applications. The organosilane molecules, due to the size of their head group, cannot close pack on the substrate surface, and therefore van der Waals forces between the alkyl chains are less effective. Reproducibility, as with LB films, is also a problem because the same surface is not produced each time. Murray⁴ demonstrated that alkylsilane films are disordered by constructing a ferrocene terminated alkylsilane monolayer. The results of the study demonstrated that electron transfer between the ferrocene and a platinum electrode was rapid on the voltammetric time scale, indicating extensive disorder in the film. Although organosilanes form a more robust monolayer than LB techniques, the poor ordering is a major disadvantage.

Alkanethiol SAMs

SAMs formed from alkanethiols offer significant advantages over other monolayer

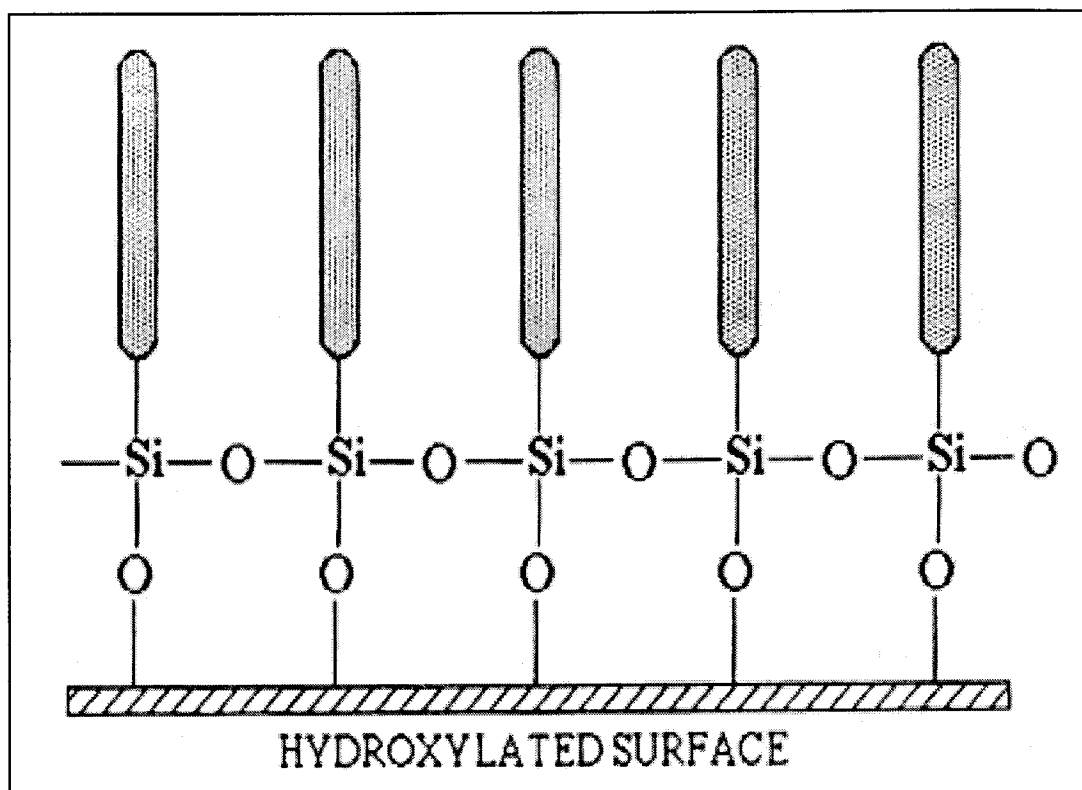


Figure 1.3: An organosilane self-assembled monolayer. Reprinted from reference 3.

systems in terms of stability, ease of preparation, and order on the molecular level.

Unlike organosilanes, alkanethiols are not water sensitive and polymeric in nature.

Alkanethiols form a stronger covalent bond to the adsorbing surface (30-40 kcal/mol), than the Si-O-Si bond network, thereby creating a much more stable monolayer.³ Self-assembled monolayers formed from alkanethiols are quite advantageous, not only in ease of construction and stability, but are excellent systems for studying a species in a well-defined environment.

Alkanethiol self-assembled monolayers consist of an alkane chain of variable length connected to a thiol head group, which is commonly bound to a gold surface, with the terminal group pointing away from the surface (see Figure 1.4). Nuzzo and Allara found that the primary driving force for alkanethiol monolayer formation is a strong gold-sulfur covalent bond, 30-40 kcal/mol, as stated previously.^{3,5} A secondary driving force for the formation of highly ordered monolayers occurs via van der Waals interactions between adjacent alkyl chains. Alkanethiols tend to close pack on the gold surface and will “assemble” themselves on the surface until all available sites are occupied. This will form, in some cases, a crystalline monolayer. The alkyl chains become extremely close to one another and the van der Waals interactions between them hold the monolayer together in an extended all *trans* configuration. Longer alkyl chains yield more van der Waals forces between them, resulting in more highly ordered structures. Monolayers containing less than eight methylene units are disordered, eight to twelve methylene units are somewhat ordered, and chains containing twelve or more methylene units are crystalline. The extent of ordering in SAMs has been studied via x-ray and neutron diffraction, ellipsometry, STM (scanning tunneling microscopy), contact angle

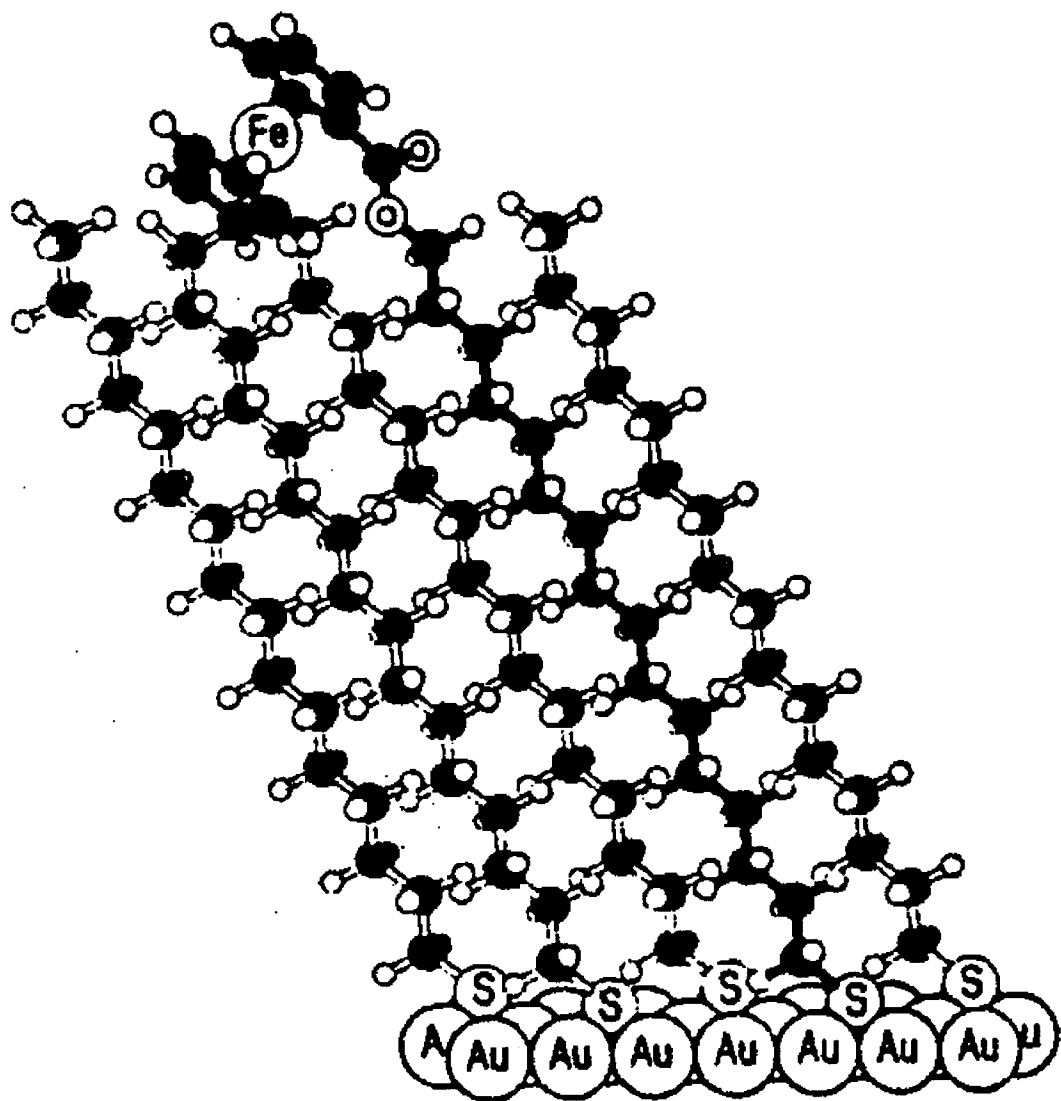


Figure 1.4: An alkanethiol self-assembled monolayer on gold. Reprinted from reference 6.

measurements, surface IR, and electrochemical methods.^{1,3,7-11}

As stated previously, the choice of the head group can effect the extent of ordering and stability in the monolayer. Bain³ studied various head groups such as sulfur, phosphorous, mercury, amines, and cyano functionalities adsorbed onto a gold surface. The study concluded that sulfur and phosphorous produced the strongest covalent bond with gold. However, sulfur created a more closely packed and better ordered monolayer than phosphorous. Sulfur also produces strong bonds to silver, copper, and platinum, but gold is commonly chosen because it exhibits only one stable oxidation state.

The biggest advantage of alkanethiols is that synthetically they are easily attached to a variety of terminal groups. However, the size of the terminal group effects the ordering, i.e. large terminal groups translate into less order. The polarity of the head group can also effect the properties displayed by the monolayer. The physical nature of the film dictates the type of surface that is constructed. Chidsey⁶ demonstrated that a polar, ester linked ferrocene terminated alkanethiol, produced better electrochemical data than a non-polar linked alkanethiol.

The attachment of an electroactive molecule ω to the thiol head group allows for the electrochemical study of alkanethiol monolayers. An electroactive molecule is one that is capable of undergoing either oxidation or reduction. Attachment of such a molecule can provide information on the relationship between the structure and properties of the monolayer. Examples of typical electroactive molecules used in alkanethiol SAMs are ferrocenes, ruthenium pentaamines, anthroquinones, and porphyrins. Ideally, the electroactive molecule should be synthetically easy to couple to an alkanethiol and be both chemically and electrochemically reversible. Monolayers can also be constructed of

electroinactive functionalities such as methyl, hydroxyl, and acetyl groups. Electroactive monolayers, however, are more commonly studied because the insulating alkane chain separates the electroactive portion of the molecule from the electrode surface at a fixed distance. This characteristic of the monolayer allows the study of electrochemical kinetics and thermodynamics as a function of alkane chain length in a well-defined environment.

Electrochemistry

Electrochemistry is a discipline of chemistry that can encompass a variety of applications such as electrophoresis, batteries, digital displays and fuel cells.¹² Although each of these applications is quite different, the fundamental principles of electrochemistry are the same throughout. Electrochemistry probes the relationship between the electronic structure and the physical and chemical properties of a molecule. The majority of electrochemical studies are done to obtain thermodynamic and kinetic information on electron transfer. Thermodynamic studies typically yield information regarding the formal potential, E° , of an electroactive species and ion-pairing effects. Determination of heterogeneous electron transfer rate constants, k° 's, or the rate of coupled homogeneous chemical reactions, are examples of kinetic parameters obtained via electrochemical methods.

Electrochemical reactions occur when one molecule is oxidized and another is reduced. Electrochemical experiments occur in cells in which two electrodes are required, one for the oxidation reaction and the other for the reduction. The two electrodes are the cathode, at which a species is reduced and the anode, where oxidation occurs. During a typical electrochemical experiment, only one reaction, either oxidation

or reduction, is of interest. The working electrode detects the half reaction of interest, while the other half reaction occurs at the counter electrode. Thus, current flows between the working and counter electrodes. The working and counter electrodes are generally made of inert metals such as platinum, gold, mercury, or glassy carbon. Both the working and counter electrodes can be made of the same material while performing the experiment. A reference electrode is used to control the potential of the working electrode. A high input impedance is placed between the working and reference electrodes so that just enough current flows between them to measure the potential difference. The reference electrode has a potential that is constant, allowing the potential of the working electrode to be accurately known at all times during the experiment. Common reference electrodes include the standard calomel (SCE), silver/silver chloride, and nonaqueous silver/silver nitrate electrodes. Typically this three-electrode arrangement is used because a two-electrode arrangement would not allow for the potential of the working electrode to be accurately known.¹²

Cyclic Voltammetry

Cyclic voltammetry is the most common linear sweep technique in electrochemistry. A typical CV experiment involves the application of a linear potential ramp to an electrode at a given scan rate, v . The potential of the electrode is increased to a predetermined switching potential, E_{λ} , at which point the electrode potential is decreased (see Figure 1.5) back to the initial potential. A current response is observed as a result of analyte oxidation or reduction during the potential sweep.

Solution electrochemistry is much more complicated than monolayer electrochemistry due to mass transport effects. Mass transport deals with the delivery of

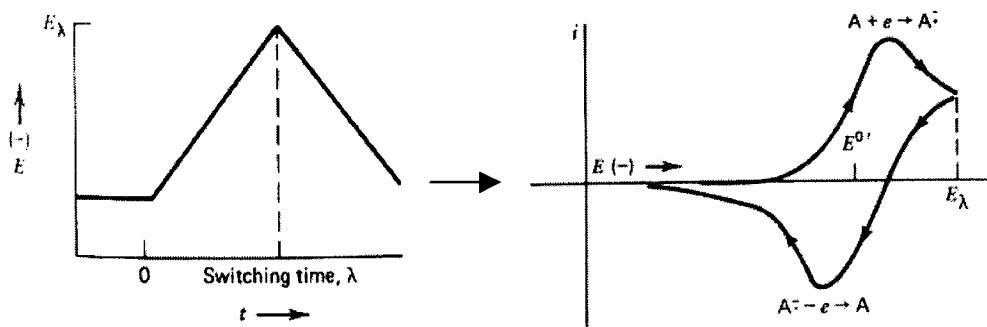


Figure 1.5: Potential versus time profile and the resulting voltammogram for a reversible redox couple. Reprinted from reference 12.

analyte molecules to the electrode/solution surface, which must be considered in solution voltammetry experiments. Mass transport affects the current drawn in response to a changing electrode potential and affects the overall shape of the voltammogram. There are three types of mass transport: diffusion, migration and hydrodynamic. Hydrodynamic mass transport results from stirring the solution or rotating the electrode throughout the experiment. Solution electrochemistry is typically done in a quiescent environment to remove effects due to hydrodynamic mass transport. Migrational mass transport deals with the motion of ions under the influence of a potential gradient. Ions will migrate in response to a change in electrode potential, which gives rise to non-faradaic currents. Solutions are generally prepared with a large excess of non-electroactive supporting electrolyte. A large excess of electrolyte supplies charge-compensating ions, which migrate in response to a change in the electrode potential. Since there are many more electrolyte ions, migration of the analyte is minimized. Data from a CV experiment where migrational mass transport is not minimized is more difficult to analyze because of the analyte molecules acting as charge carriers.

Diffusional mass transport is defined as the motion of a species under the influence of a concentration gradient. A concentration gradient is generated at the electrode surface as a result of oxidation and reduction of the analyte. Diffusion is a relatively slow process, which is responsible for delivering more analyte to the electrode surface to undergo electron transfer. When electron transfer is fast with respect to diffusion, concentration polarization is observed. This affects the shape of the voltammogram by causing peak tailing. However, if the electron transfer is slow with respect to diffusion, kinetic polarization predominates and the rate of electron transfer can be determined. A graphical representation of diffusion controlled electron transfer is demonstrated by plotting the peak currents, i_p , (cathodic or anodic) versus the square root of scan rate, $v^{1/2}$. If the electron transfer is diffusion controlled, the plot will be linear.

There are two types of currents encountered in an electrochemical experiment, non-faradaic and faradaic. Non-faradaic currents are generated from the motion of charge compensating ions migrating toward the electrode due to the potential gradient generated at the working electrode. Non-faradaic currents limit the sensitivity and time scale of the experiment. Faradaic currents arise from electron transfer and are therefore associated with oxidation and/or reduction of the analyte. Typically, these are the focus of a cyclic voltammetry experiment, because faradaic currents can be analyzed to obtain thermodynamic and kinetic information. Faradaic and non-faradaic are terms derived from Faraday's Law, which explains that the amount of electricity generated is directly proportional to the number of electrons transferred.

A CV experiment begins at a potential that is not sufficient to reduce the analyte in solution. Thus, only non-faradaic currents are observed. As the potential is made more

negative, the energy of the electrons in the metal increases until the potential becomes sufficiently negative for electron transfer from the electrode to the analyte to be energetically favorable (see Figure 1.6). As the analyte is reduced, an increase in current occurs, i.e. faradaic currents and the current increases until the surface concentration of the analyte is driven to zero, at which point it reaches a maximum. The current then decreases due to concentration polarization, until the switching potential is reached. The scan is then reversed and the energy of electrons in the metal decreases until it is energetically favorable for an electron to be transferred from the analyte to the electrode. Thus, the analyte is oxidized and an increase in faradaic current is observed. The current continues to increase until the surface concentration of the reduced form of the analyte reaches zero. At this point, the current reaches a maximum and subsequently decreases due to concentration polarization.

Cyclic voltammetry is commonly performed on electroactive substances to determine the formal potential, $E^{\circ'}$, a thermodynamic property that is characteristic of the analyte. The formal potential is the potential at which electron transfer occurs. This provides information concerning the electronic structure of the analyte. The formal potential is experimentally determined as:

$$E^{\circ'} = (E_{p,a} + E_{p,c})/2$$

The formal potential of an electroactive molecule, $E^{\circ'}$, can be used to calculate the relative amounts of oxidized and reduced species. For $O + ne^- \rightarrow R$, the Nernst equation states that:

$$E = E^{\circ'} + (RT)/(nF) \ln [O]/[R]$$

where E is the potential of the cell, $E^{\circ'}$ is the formal potential, R is the ideal gas constant

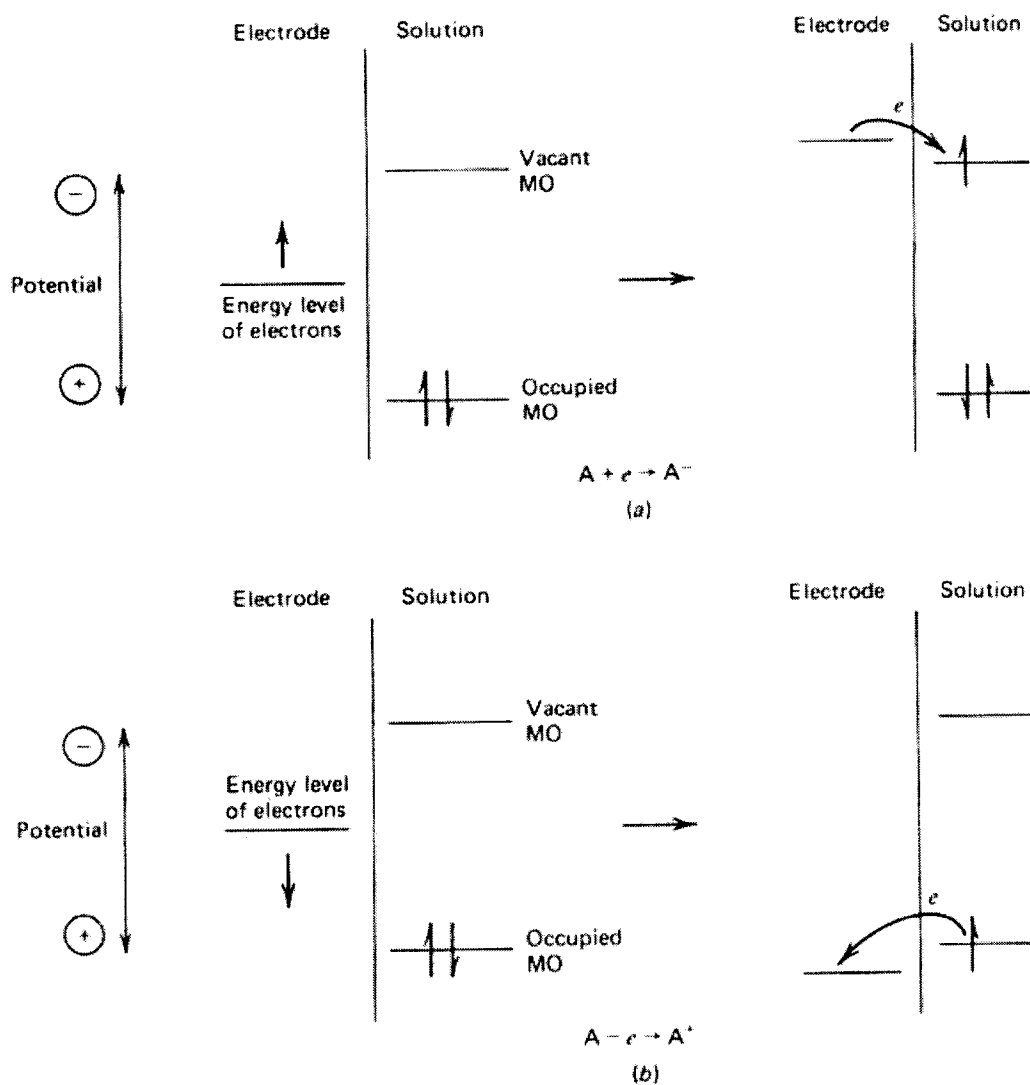


Figure 1.6: Representation of (a) reduction and (b) oxidation process of a species in solution. Reprinted from reference 12.

($8.314 \text{ J/mol}\cdot\text{K}$), T is the temperature in Kelvin, n is the number of electrons transferred, F is Faraday's constant, $[O]$ is the surface concentration of the oxidized species and $[R]$ is the surface concentration of the reduced form of molecule. The Nernst equation can be used to relate the kinetics of a system to the relative concentrations of the oxidized or reduced forms of the analyte.

Electron transfer kinetics are generally investigated using cyclic voltammetric methods. There are two very distinct areas in the study of electron transfer kinetics, reversible and irreversible. A grey area exists, known as quasi-reversible electron transfer, but the focus will remain on systems that are purely reversible or totally irreversible. CV is used to investigate the reversibility or irreversibility of an electron transfer, both chemically and electrochemically. Each of these areas has different criteria in data analysis to determine if the electron transfer is reversible or irreversible and of what type, chemical or electrochemical.

In an electrochemically reversible system, electron transfer is rapid on the voltammetric time scale. Thus, the Nernst equation is obeyed at all potentials. Electrochemical reversibility is indicated in a cyclic voltammetry experiment when ΔE_p , ($E_{p,a} - E_{p,c}$), is equal to $57/n \text{ mV}$ and is independent of scan rate. Another test for electrochemical reversibility is a Nernst plot of $\log(i_{p,c} - i)/i$ in the rising portion of the cathodic wave versus potential. If the slope is equal to $57/n \text{ mV}$ and the y intercept is equal to the formal potential of the analyte, the electron transfer is electrochemically reversible. In practice, ΔE_p for a reversible couple is typically about $70/n \text{ mV}$ and independent of scan rate, due to problems with solution resistance.

An irreversible system is one in which heterogeneous electron transfer kinetics are slow. Due to slow charge transfer kinetics, an overpotential must be applied in the cathodic and anodic directions in order to induce electron transfer. The overpotential is the amount of extra potential needed to observe a current response equal to that of a reversible electron transfer. ΔE_p values increase with increasing scan rate for electrochemically irreversible systems. The rate constant is obtained based on how ΔE_p increases with increasing scan rate. For a totally irreversible electron transfer, k° can be obtained from the Butler-Volmer equation. The Butler-Volmer equation is stated as follows:

$$i = nFAk^\circ [C_O e^{-\alpha n f \eta} - C_R e^{-(1-\alpha) n f \eta}]$$

where i is the current, n is the number of electrons transferred, F is Faraday's constant, A is the electrode surface area, k° is the heterogeneous electron transfer rate constant, C_O is the surface concentration of oxidized form of the analyte, C_R is the surface concentration of reduced form of the analyte, α is the electron transfer coefficient (usually 0.5), f is F/RT , and η is the overpotential.

Chemical reversibility deals with the chemical stability of the analyte. For example, if ten molecules are oxidized in the forward sweep of the experiment and all ten are re-oxidized in the reverse sweep, this is a chemically reversible couple. Chemically reversible systems are observed when small deviations from $E^{o'}$ drives the forward or reverse reaction, and only that reaction. The test for chemical reversibility is that the ratio of the peak currents, i.e. $i_{p,a}/i_{p,c}$, should be equal to one at all scan rates.

If the analyte molecules cannot be re-oxidized in the reverse sweep, due for example to a homogeneous decomposition reaction, then this is referred to as a chemically

irreversible process. A decomposition reaction may produce another species from the unstable reduced analyte, which may or may not be electroactive, i.e. $O + ne^- \rightarrow R \rightarrow Z$. Rate constants for the decomposition reaction, as well as mechanistic information can be determined with CV.

Cyclic voltammetry is a very powerful tool for obtaining k_{chem} , the rate constant for a homogeneous chemical reaction, as well as providing mechanistic information. Cyclic voltammetry provides two different methods of obtaining the value of k_{chem} . The first method involves decreasing the time scale of the experiment by increasing the scan rate. Increasing the scan rate allows less time for the decomposition reaction to occur, thereby altering the shape of the voltammogram. Ideally, the time scale of the experiment is adjusted to the same range as that of k_{chem} . To obtain the value of k_{chem} , a working curve of $i_{p,a}/i_{p,c}$ versus $\log v^{1/2}$ as a function of k_{chem} is constructed. When the working curve matches the data from the CV experiment, k_{chem} is determined. The mechanism of the chemical reaction can be obtained by proposing a reasonable pathway, and using digital methods to simulate the CV experiment. When the digital simulation matches the experimental CV, the proposed mechanism may be the correct one. The proposed mechanism must be checked with an independent method because two different mechanisms may give rise to the same simulated CV. It is, however, unlikely to produce the same simulation for an independent experiment, i.e., chronoamperometry or rotated ring disk electrochemistry. The main disadvantage of performing high scan rate voltammetry is that high-speed electronics are required, which tend to be expensive.

Another method of acquiring k_{chem} is to perform low temperature electrochemistry. Running the CV experiment at low temperatures slows the kinetics of the chemical step

down until k_{chem} decreases into a measurable range. An advantage to low temperature CV is that the experiment need not be as sophisticated and commercially available potentiostats can be used. A major disadvantage to this technique is high iR drop at low temperatures, which makes it difficult to accurately know the potential of the working electrode. In addition, the presence of a large solution iR can mimic slow electron transfer kinetics, making it impossible to extract k_{chem} . Other problems include the solubility of the analyte, a decrease in the diffusion coefficient, and aqueous solutions generally cannot be used.

Both of the described methods are useful in acquiring k_{chem} . Generally, with either technique, the shape of the voltammogram changes in a similar fashion, with increasing scan rates or decreasing temperatures. At low scan rates or high temperature, the cathodic wave is present, but no anodic wave. This is because upon reduction, the analyte quickly decomposes to Z and cannot be re-oxidized back to O. At intermediate scan rates or temperatures, some of R decomposes to Z, but a small portion is also re-oxidized, as evident from a small anodic peak. At high scan rates or low temperatures, the analyte appears to be reversible because there is not sufficient time for R to decompose to Z.

The basic principles of solution electrochemistry and cyclic voltammetry have been presented. The majority of studies done on electroactive molecules concentrate on the kinetics and thermodynamics of a system. Monolayers are model systems for exploring such areas. The responses generated from electrochemical experiments, typically cyclic voltammetry, on monolayer systems are quite different and will be discussed.

Monolayer Electrochemistry

Electrochemistry performed on self-assembled monolayers produces different responses than when the analyte is dissolved in solution. The largest difference is the fact that the analyte molecules are surface confined, so diffusional mass transport has no effect on the voltammetry. The absence of diffusion is indicated by a linear plot of i_p versus scan rate, providing evidence that the species is adsorbed to the electrode surface. Cyclic voltammetry is a common technique used to study SAMs, but other methods, i.e. chronoamperometry, are used as well. The potential versus time profile for a surface confined species is the same as solution CV, but data analysis is quite different.

A linear potential ramp is applied to the working electrode and the current is measured as a function of the applied potential (see Figure 1.5). The voltammogram generated from a monolayer has observable differences when compared to one generated from a solution experiment (see Figure 1.7). One distinct feature is that peak tailing does not occur due to the absence of diffusional mass transport. The result is a voltammogram which closely resembles that observed in a thin layer electrochemical cell.

The terminal groups used in SAMs are generally chosen so that they are chemically reversible, resulting in symmetric peak shapes. Chemically reversible monolayers produce $i_{p,a}/i_{p,c}$ equal to one, as in solution electrochemistry. Deviation from unity suggests chemical irreversibility due to a homogeneous reaction taking place.

Electrochemically reversible monolayers usually produce symmetric peaks on the voltammogram and ΔE_p should theoretically be 0 mV and independent of scan rate. In practice, ΔE_p is usually ten to twenty mV for a reversible couple due to the effects of solution iR. For a reversible reaction, the rate at which electron transfer occurs is too

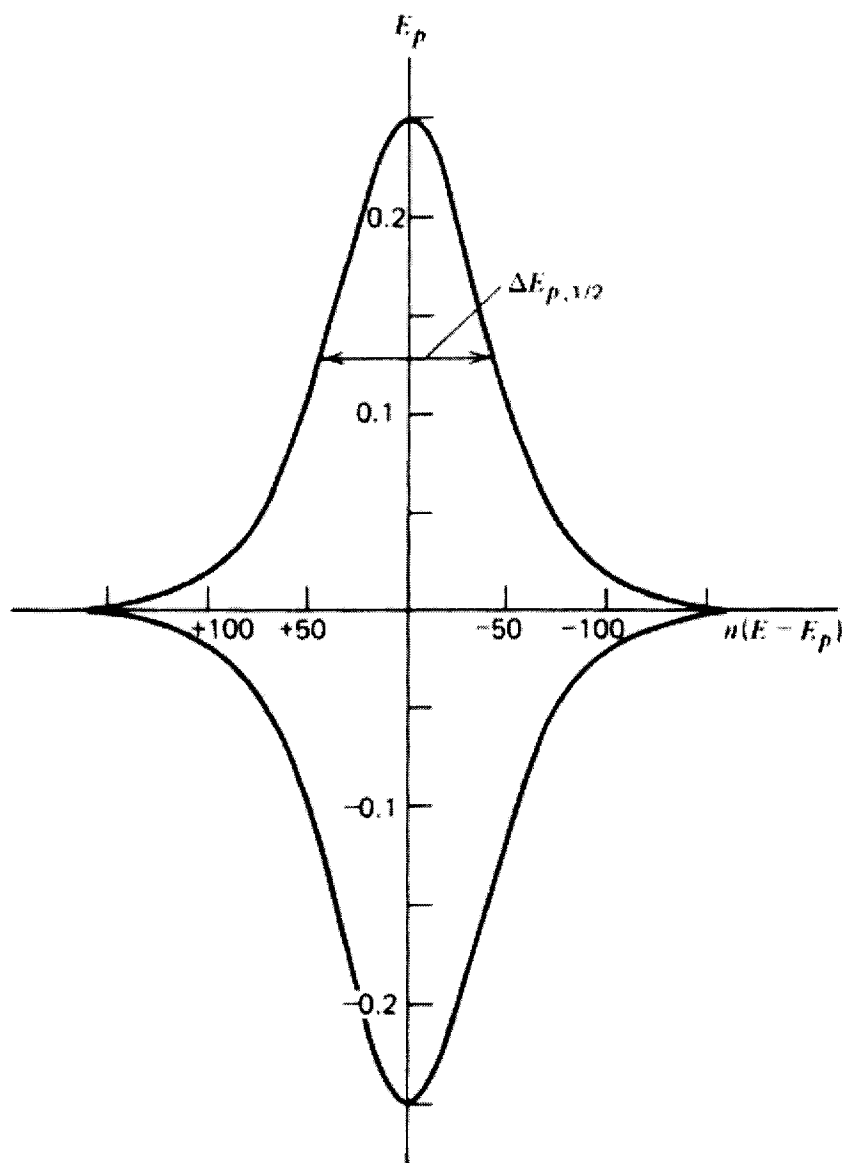
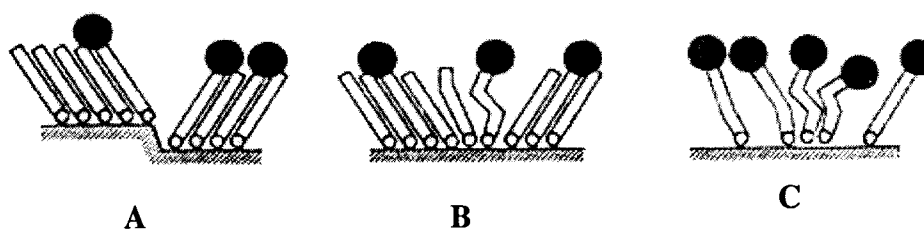


Figure 1.7: Theoretical cyclic voltammogram of a reversible surface confined species.
Reprinted from reference 7.

rapid to be measured on the voltammetric time scale and k° cannot be extracted. Rapid electron transfer kinetics can be an indication of defect sites embedded within the monolayer (see Figure 1.8). The monolayer may contain functionalities that can be folded over on themselves because they are located at step or other defect sites. Therefore, a small portion of the electroactive groups are closer to the electrode surface, resulting in a more rapid electron transfer. Electrons in more ordered regions of the monolayer can “hop” to this defect site, rather than tunneling through the insulating alkane chain. Collard and Fox¹³ demonstrated that defect sites in ferrocene alkanethiol monolayers, could be eliminated by soaking the electrode in a solution of electroinactive alkanethiols. The electroactive alkanethiols located at defect sites are replaced by the electroinactive species, resulting in decreased faradaic currents and more order. Under the appropriate conditions, k° can be measured for diluted electroactive SAMs. This process of exchanging sites is known as dilution and is a common method to introduce more order into the monolayer. Fully loaded films are generally reversible because of disorder, but dilution isolates the redox sites so that a single rate constant can be calculated.

Electrochemically irreversible monolayers provide information regarding heterogeneous electron transfer kinetics. Electron transfers in monolayers containing long alkane chains or films that are diluted with electroinactive alkanethiol, are typically kinetically slow due to the insulating alkane chain. For an irreversible electron transfer, ΔE_p increases with increasing scan rate. In order to extract a rate constant, electron transfer should occur to and from isolated, independent molecules. Interactions between the redox active groups, gives rise to a broad distribution of rate constants and a single



- A:** Impurities or crystal defects (boundaries, steps) on a gold surface
- B:** Alkanethiol two-dimensional crystal domain boundary
- C:** Steric interactions between ferrocene-substituted alkanethiols in neighboring monolayer lattice sites

Figure 1.8: Possible self-assembled monolayer defects. Reprinted from reference 13.

rate constant cannot be extracted.

As with solution voltammetry, the Butler-Volmer equation can be used to determine the value of k° . However, the equation is rearranged to neglect effects from diffusion and the equation is based on monolayer surface coverage, Γ , instead of concentration.

Laviron¹⁴ developed a mathematical model based on the Butler-Volmer equation, which established the relationship of how ΔE_p increases with increasing scan rate. A plot of how ΔE_p varies with scan rate demonstrates that the rate constant, k° , is inversely proportional to the slope of the curve. The rate constant is solved for with the following equation:

$$1/m = (nFv)/(RTk^\circ)$$

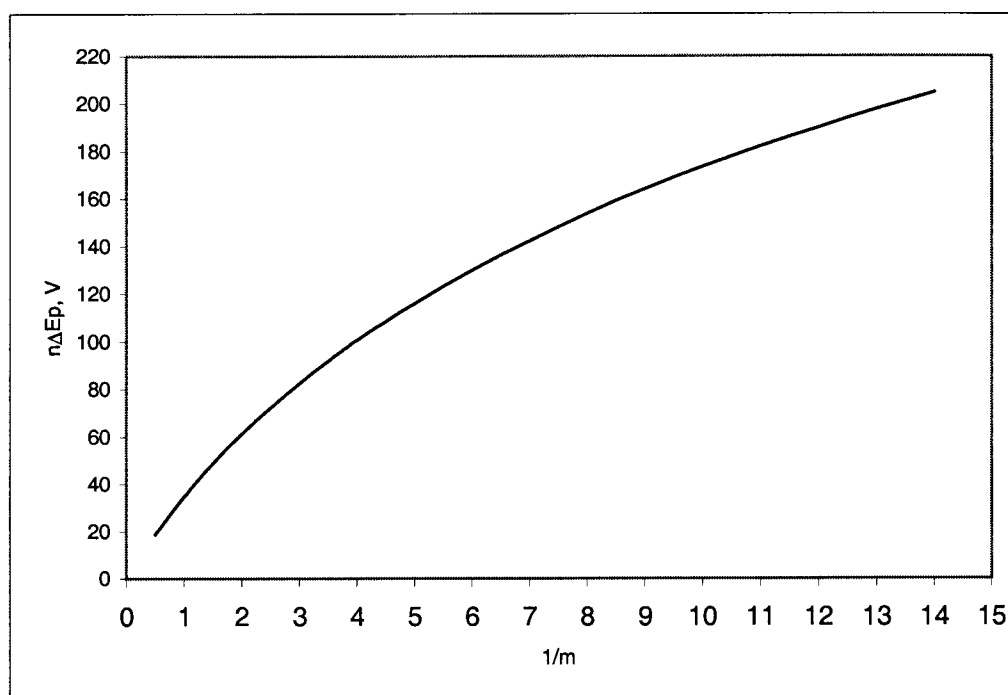
Laviron tabulated the values for $1/m$ and $n\Delta E_p$ at various scan rates, so that rate constants could be easily extracted (see Figure 1.9) by measuring ΔE_p as a function of scan rate.¹⁴

Surface coverage of the monolayer is also an important factor, which can be calculated from the voltammogram. The surface coverage is defined as:

$$\Gamma = Q/(nFA)$$

where Q is the charge passed during oxidation or reduction. The extent of coverage can affect the overall thermodynamic and kinetic properties of the monolayer. Surface coverage is determined by integrating the peak areas of the cathodic and anodic waves and dividing by the scan rate, number of electrons transferred and Faraday's constant.

The charge passed is directly proportional to the number of sites occupied on the substrate surface. The value obtained indicates if the monolayer is close packed on the surface. If the coverage is too low, the possibility of disorder is higher. If the surface coverage is too high, this indicates the presence of multi-layers or non-specific adsorption



1/m	0.5	0.8	1	1.5	2	2.5	3	3.5	4	5
$n\Delta E_p$ (mV)	19	27	34.8	48.8	61.2	72.2	82.4	91.8	100.6	116

1/m	6	7	8	9	10	11	12	13	14
$n\Delta E_p$ (mV)	130	142	154	164	173.4	182	190	197.6	204.6

Figure 1.9: Plot of $n\Delta E_p$ versus $1/m$ based on Laviron's tabulated values to determine the rate constant of a redox couple. Reprinted from reference 14.

of redox active molecules. Thus, at high or low surface coverages, the voltammogram displays broad peaks, due to the presence of defect sites, and calculation of a rate constant is difficult.

The ordering of the monolayer, a thermodynamic property, can be quantified on the voltammogram using full width at half-maximum values (FWHM). Theoretical values for FWHM are $90/n$ mV and values above this indicate that the species within the monolayer are disordered or are interacting with one another. Undiluted films usually produce broadened peaks on the voltammogram and FWHM values much greater than $90/n$ mV, complicating the task of extracting a rate constant. Dilution of the monolayer with electroinactive alkanethiols, removes electroactive molecules from defect sites, resulting in voltammetric waves displaying FWHM values of $90/n$ mV.

Self-assembled monolayer studies provide fundamental information regarding electron transfer in a well-defined environment. Monolayers used to study electron transfer rates are typically constructed of ferrocene linked to the electrode surface via an alkanethiol. Ferrocene is commonly chosen because it is a reversible, outer sphere redox couple. Another advantage of using ferrocene is that synthetically it is easy to attach to the alkanethiol chain. Although SAMs can be constructed from a variety of redoxactive molecules, i.e. ruthenium pentaamine, anthroquinones, porphyrins and viologens, the focus throughout will remain on those constructed of ferrocene alkanethiols.

Monomeric Ferrocene Alkanethiol Monolayers

Ferrocene terminated alkanethiol SAMs are widely studied to determine the rate of electron transfer. Chidsey¹⁵ constructed the first ferrocene terminated alkanethiol monolayer. Shown in Figure 1.10 is a voltammogram of monomeric ferrocene

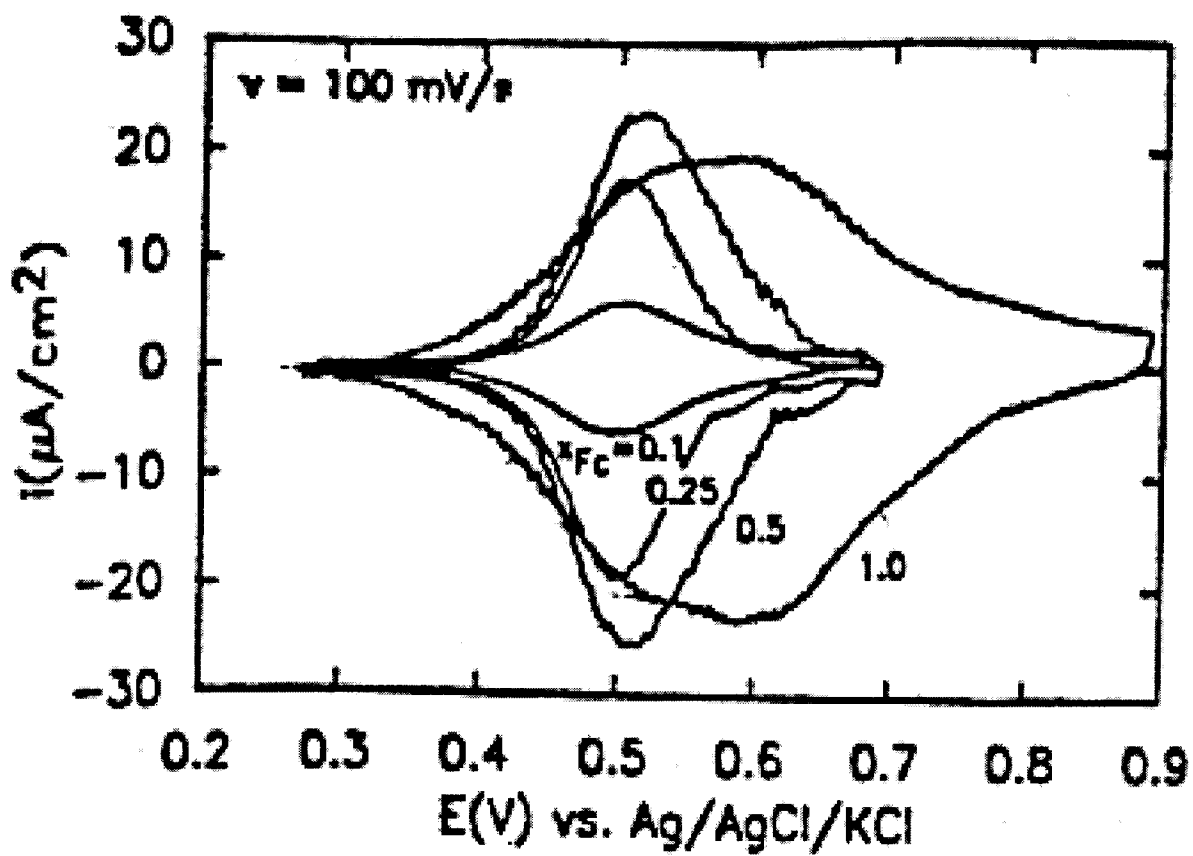


Figure 1.10: Voltammogram for mixed monolayers of $\text{FcCO}_2(\text{CH}_2)_{11}\text{SH}$ and $\text{CH}_3(\text{CH}_2)_{15}\text{SH}$. Reprinted from reference 15. The broadened outer wave represents the undiluted film.

alkanethiols diluted with unsubstituted alkanethiols. The broadened peaks displayed by the fully loaded films demonstrate that there are many defect sites present in the monolayer. As the film is diluted, the peaks narrow, as evident from the voltammograms. The peaks on the voltammogram are also symmetrical, which is typical for monolayer chemistry. Ferrocene containing SAMs are typically chemically reversible as demonstrated by Chidsey.¹⁵ The ratio of the peak currents for the voltammograms shown in Figure 1.10 is equal to one for fully loaded and diluted films, confirming that the reaction is chemically reversible.

The CV's for the fully loaded and partially diluted films displayed ΔE_p values which were independent of scan rate, indicating electrochemical reversibility. A rate constant could not be extracted because of the presence of defect sites in the films. When the ratio of $\text{Cp}_2\text{FcCO}_2(\text{CH}_2)_{11}\text{SH}$ to undecanethiol was 1:15, ΔE_p increased with increasing scan rate, indicating an electrochemically irreversible electron transfer. Using the method of Laviron¹⁴, a heterogeneous electron transfer rate constant of 5.2 s^{-1} was obtained. This indicated the effectiveness of monolayer dilution for slowing electron transfer kinetics into a measurable range.

In a separate study, Chidsey⁶ constructed diluted films having a longer alkane chain of sixteen methylene units. The ferrocene was connected to the alkanethiol via an ester group. The results of this study demonstrated that the currents obtained at high overpotentials were lower than those predicted by Butler-Volmer theory. Thus, the more general Marcus-Hush theory, in conjunction with the density of states in the metal, was needed to provide an accurate rate constant. Using this method, Chidsey obtained a heterogeneous electron transfer rate constant of 1.3 s^{-1} for the ferrocenes in the

monolayer. Thus, the rate of electron transfer was shown to decrease with an increase in alkane chain length. Although this research does not provide extensive information on the distance dependence of electron transfer, it does demonstrate that separating a reversible redox couple from an electrode with an insulator slows the electron transfer kinetics into a measurable range.

Finklea¹⁶ et al. also investigated the distance dependence of electron transfer in SAMs by attaching ruthenium pentaamine to alkyl chains of ten, eleven, and fifteen methylene units. The results demonstrated that the electron transfer rate between the electrode and the ruthenium decreased exponentially with increasing distance. Based on Tafel plots, the mechanism of electron transfer was found to occur through bond tunneling, i.e. through the alkyl chain, rather than through space.

The surface coverage for SAMs constructed from ferrocene alkanethiols was also calculated for Chidsey's fully loaded films. He obtained a value of 5.8×10^{-10} mol/cm². This value is typical for ferrocene containing monolayers and indicates close packing of the molecules on the surface. The value is somewhat high due to the broad peaks on the voltammogram and integration yielding a large area. Theoretically, ferrocene alkanethiols are modeled as 6.6 Å spheres and a surface coverage of 7.71×10^{-10} is calculated. For a fully loaded close packed film, there is some agreement between the experimental and theoretical values. Differences are most likely due to different solvation spheres around the molecules in the thiol coating solution.

The FWHM values for Chidsey's ferrocene containing films were approximately 230 mV for the cathodic and anodic waves. These values were much greater than the theoretical value of $90/n$ mV, indicating that the ferrocenes were interacting with one

another. The high FWHM value is evident from the extremely broadened peak on the voltammogram shown in Figure 1.10. The broadened waves for fully loaded films therefore could not allow for a single rate constant to be determined. Hence, the film had to be diluted in order to determine k° .

Dimeric Ferrocene Alkanethiol Monolayers

Many self-assembled alkanethiol monolayers containing monomeric ferrocenes have been synthesized and studied electrochemically,^{6,13,15,16} but alkanethiol monolayers containing dimeric ferrocenes have not been extensively reported. The effect of another electroactive substituent within the monolayer can have profound effects on the observed thermodynamic and kinetic properties.

The study of dimeric ferrocene alkanethiols on gold has concentrated on investigating the effect of another electroactive site within the monolayer. The ability of a system to contain mixed valence functionalities is attractive because the properties of the mixed valent state are often not the sum of those of the monovalent states. Monolayers containing two ferrocenes have been reported by Filler¹⁷ and Kubo¹⁸ et al. These studies will be the focus throughout this section.

Filler¹⁷ et al. constructed a variety of diferrocenylolethane tagged alkanethiol SAMs having different chain lengths of six, twelve, and sixteen methylene units between the electrode surface and the inner ferrocene. Voltammograms for the six-carbon derivative are shown in Figure 1.11. The voltammograms for monolayer films containing two ferrocenes are not drastically different than those containing one ferrocene. The most noticeable difference is that the voltammogram displays two waves in both the anodic and cathodic directions. The peaks are reasonably symmetric, with the first redox wave

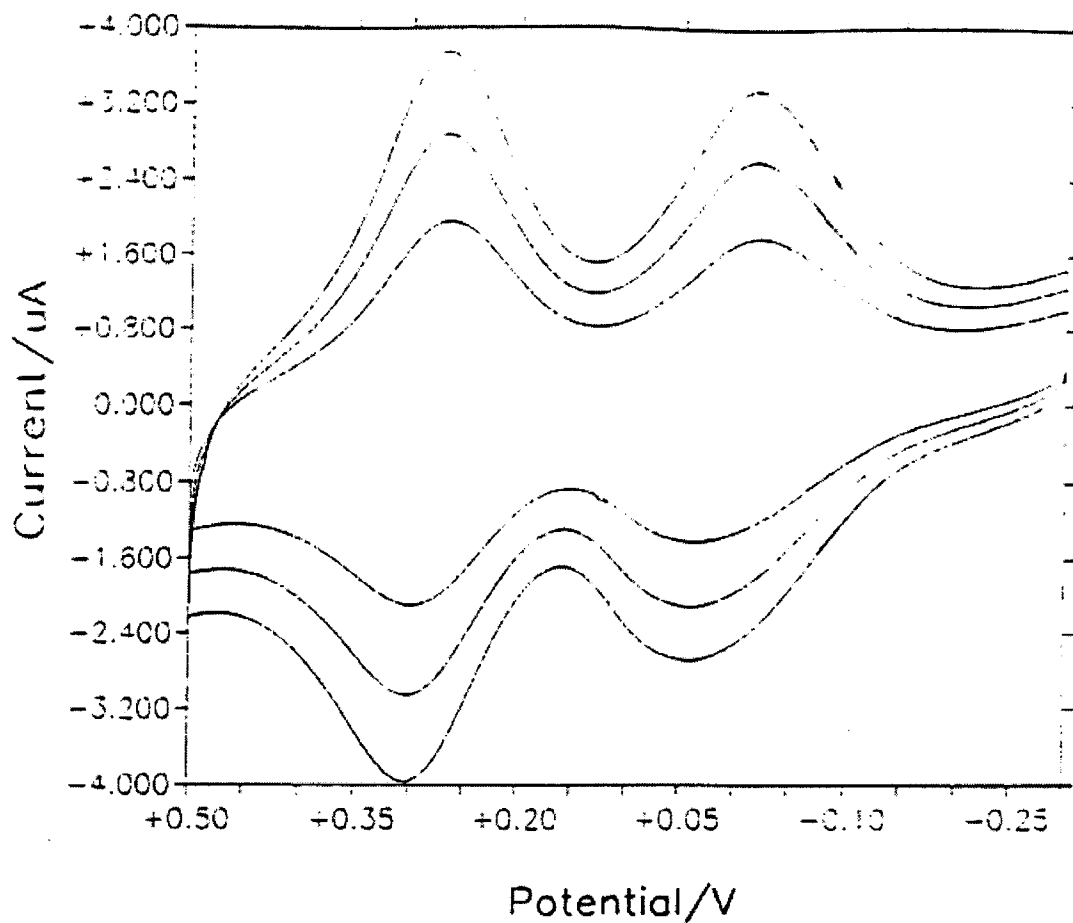


Figure 1.11: Cyclic voltammogram for 6-(1,2-diferrocenylethylcarbonyl)pentanethiol. Working electrode: Gold; Counter electrode: Silver wire; Reference electrode; Ag wire. Reprinted from reference 17.

diferrocenylethane group was modeled as a 12 Å sphere. The measured surface coverages indicated the formation of a closely packed monolayer on the surface.

The ordering of the monolayer was probed by examining FWHM values. The monolayer having a six-carbon chain between the inner ferrocene and the electrode produced a value of 150 mV for the first redox wave and 124 mV for the second redox wave. The twelve-carbon derivative demonstrated values of 105 mV for both redox waves. FWHM values for the fifteen-carbon chain could not be determined due to poorly resolved redox waves. While the FWHM values for the diferrocenylethane monolayers were larger than the theoretical value of $90/n$ mV, they were much smaller than those reported for monomeric ferrocenes, further indicating ordered films.

Kubo¹⁸ et al. constructed alkanethiol SAMs containing biferrocene. Two symmetrical one electron transfers were observed, with the first wave centered at 197 mV and the second at 600 mV. The oxidation of the outer ferrocene occurred at lower potentials, as seen with Filler's compounds, due to the presence of an electron withdrawing carbonyl substituent on the inner ferrocene.

The major difference between the biferrocene films synthesized by Kubo and those containing 1,2-diferrocenylethane terminal groups, was that oxidation of the biferrocene group was found to be chemically irreversible. When the potential scan was limited to 500 mV, so that only the outer ferrocene was oxidized, the peak current ratios deviated from unity, indicating a chemically irreversible process. The results demonstrated that the homogeneous chemical reaction followed second order kinetics. When the potential was scanned to 900 mV, both redox waves were observed. The peak current ratios again

deviated from unity. However, when the larger potential limit was used, the reaction was found to obey first order kinetics.

Two rate constants for the biferrocene monolayer were obtained by the method of Laviron. The outer ferrocene produced a more rapid rate constant of $0.93(\pm 0.02) \text{ s}^{-1}$, compared to a slower value of $0.64(\pm 0.02) \text{ s}^{-1}$ for the inner ferrocene. The electron transfer for the outer ferrocene occurred more rapidly, despite the fact it is farther from the electrode surface. Upon oxidation of the outer ferrocene, a counter ion from the electrolyte solution must supply a charge compensating anion to the ferricenium cation. A charge compensating anion must also be supplied when the inner ferrocene is oxidized. Kubo speculated that forcing an anion past the anion located at the outer ferrocene was limiting the rate of the electron transfer. This inversion of rate constants was not observed in the diferrocenylethane tagged monolayers studied by Filler.

Kubo et al. obtained a surface coverages of $4.6 \times 10^{-10} \text{ mol/cm}^2$ which were similar to those obtained for monomeric ferrocenes. This indicated the formation of a closely packed monolayer.

The biferrocene films produced FWHM values of approximately 100 mV. The peaks were relatively narrow and the values were in close agreement with the theoretical value of $90/n \text{ mV}$. This provided evidence that the ferrocenes were non-interacting, allowing the extraction of a single rate constant.

Monolayer chemistry is widely studied to obtain fundamental thermodynamic and kinetic information concerning the rate of electron transfers. They have become increasingly attractive systems to model electron transfer because of the ability to tailor the interface on the molecular level. Various methods of tailoring include monolayers

containing two, rather than one ferrocene, altering the distance from the ferrocene to the electrode surface, or altering the distance between the two ferrocenes. The latter approach has not been reported in the literature, and is the focus of the research outlined in this thesis.

Research Proposal

The goal of this research endeavor is to increase the alkane chain length separating two ferrocenes to explore the extent of communication between them and the possible increase in order through the attachment of an alkane chain on the backside of inner ferrocene. Effects of the bridging alkane chain will be quantified through the determination of heterogeneous electron transfer rate constants, surface coverages, and FWHM values. Another area of interest is the possibility of a thermodynamic price for oxidation of the inner ferrocene due to ion migration into a non-polar alkane environment. The data obtained will be compared to the previous studies done by Chidsey, Filler and Kubo. Although, this is a novel area of self-assembled monolayer chemistry, the fundamental principles described previously are the same.

1,6-diferrocenylhexane will be synthesized, tagged with an alkanethiol, purified and adsorbed onto a polycrystalline gold electrode. The electrochemical properties of SAMs constructed from this molecule will be probed via the previously explained cyclic voltammetry method. The cyclic voltammograms should produce four peaks and provide thermodynamic and kinetic data for comparison with the literature.

X-ray crystallography will be used to provide pertinent structural information concerning the diferrocenylhexane head group and packing orientation on the gold surface. Single crystal X-ray diffraction data will be obtained for any of the compounds

synthesized during the pathway to the final alkanethiol product. The orientation of the ferrocenes with respect to each other, as well as the unit cell-packing scheme, will be the focus of such experiments.

Cyclic voltammetry provides a wide range of information concerning self-assembled monolayers. A single experiment can allow extraction of heterogeneous electron transfer rate constants, thermodynamic properties such as the formal potential of each ferrocene, and how well the monolayer covers the gold electrode surface. The structural characteristics of the monolayer are found indirectly by performing this simple electrochemical experiment. The research presented will provide information useful to future endeavors in interfacial chemistry.

REFERENCES

1. Brett, C. *Electrochemistry Principles, Methods and Applications*; Oxford University Press: New York, **1993**.
2. Whitesides, G.M. *Sci. Am.* **1995**, *, 146-149.
3. Ulman, A. *An Introduction to Ultrathin Organic Films*; Academic Press: New York, **1994**.
4. Murray, R. *Molecular Design of Electrode Surfaces*; Wiley: New York, **1992**.
5. Nuzzo, R.G., Allara, D.L. *J. Am. Chem. Soc.*, **1983**, 105, 4481-4483.
6. Chidsey, C.E.D. *Science*, **1991**, 251, 919-921.
7. Bard, A., Faulkner, L. *Electrochemical Methods*; Wiley: New York, **1980**.
8. Gale, R. *Spectroelectrochemistry-Theory and Practice*; Plenum: New York, **1988**.
9. Evans, D. *J. Chem. Educ.* **1983**, 60, 290-293.
10. Kuwana, T., Heineman, W. *Acc. Chem. Res.* **1976**, 9, 241-248.
11. Heineman, W. *J. Chem. Educ.* **1983**, 60, 305-308.
12. Bard, A., Faulkner, L. *Electrochemical Methods*, 2nd ed. Wiley: New York, **2000**.
13. Collard, D.M., Fox, M.A. *Langmuir*; **1991**, 7, 1192-1197.
14. Laviron, E. *J. Electroanal. Chem.* **1979**, 101, 19-28.
15. Chidsey, C.E.D., Bertozzi, C.R., Putvinski, T.M., Mujcsce, A.M. *J. Am. Chem. Soc.*, **1990**, 112, 4301-4306.
16. Finklea, H.O., Hanshew, D.D. *J. Am. Chem. Soc.* **1992**, 114, 3173-3181.
17. Filler, William J. Characterization of Diferrocene Tagged Self-Assembled Alkanethiol Monolayers, M.S. Thesis, Temple University, Philadelphia, August 1996.
18. Kubo, K., Kondow, H., Nishihara, H. *Electrochemistry*. **1999**, 67, 1129-1131

CHAPTER TWO

SYNTHESIS AND CHARACTERIZATION

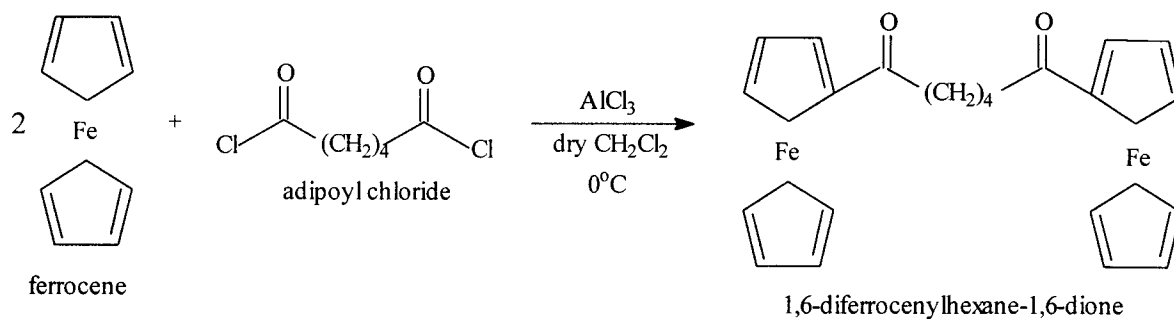
The production of a compound containing two ferrocene moieties bridged by a six-carbon chain is synthetically quite involved (see Figure 2.1). SAMs containing monomeric ferrocenes have been extensively studied¹⁻⁴, but little attention has been paid to monolayers containing oligomeric ferrocenes.

The initial step was a Friedel-Crafts acylation, in which adipoyl chloride, in the presence of AlCl_3 in dry methylene chloride, was used to link the two ferrocenes together. The two carbonyls in the bridge were reduced under Clemmensen reduction conditions, using a zinc-mercury amalgam and HCl in toluene. Upon reduction, another Friedel-Crafts acylation was performed with 6-bromohexanoyl chloride, under the same conditions as above. The final step in the reaction sequence was a nucleophilic displacement of bromide with thiolacetic acid, followed by displacement of acetic acid from the thioacetyl group using dilute NaOH.

Chemicals

Adipoyl chloride (Aldrich, 99%), aluminum chloride (Aldrich, 98%), argon (Praxair, 99.999%), 6-bromohexanoyl chloride (Aldrich, 97%), calcium hydride (Aldrich, 95%), deuterated chloroform (Aldrich, 99%), ethanol (Pharmco, absolute, 100%), ethyl acetate (Pharmco, 99.98%), ferrocene (Aldrich, 98%), hexane (Pharmco, 99.99%), hydrochloric acid (Fisher, certified ACS plus), magnesium sulfate (Fisher, certified ACS, 99%), mercuric chloride (Mallinckrodt, 98%), silica gel (Aldrich, 200-400 mesh, 60 Å), sodium

Step One: Friedel-Crafts Acylation



Step Two: Clemmensen Reduction

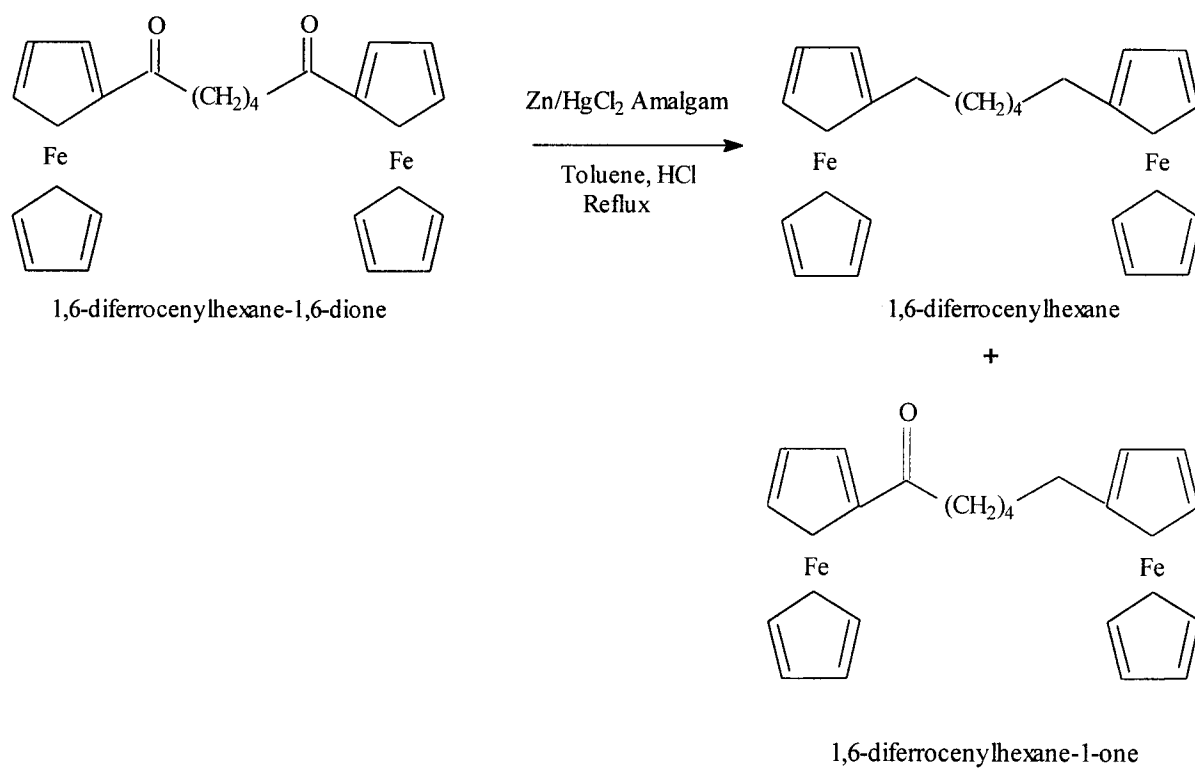
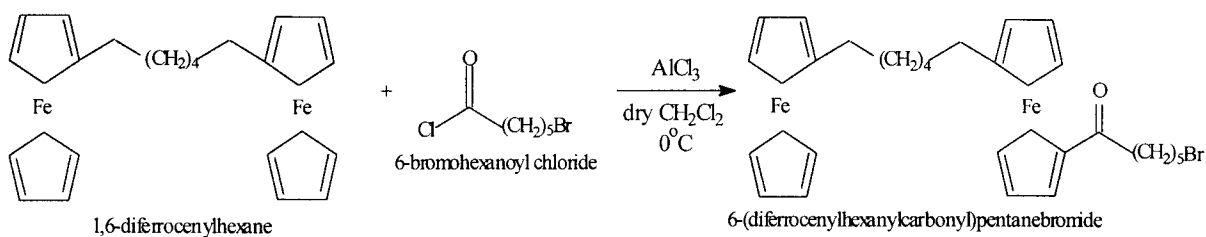


Figure 2.1: Schematic of Synthetic Pathway

Step Three: Friedel-Crafts Acylation



Step Four: Thiolation

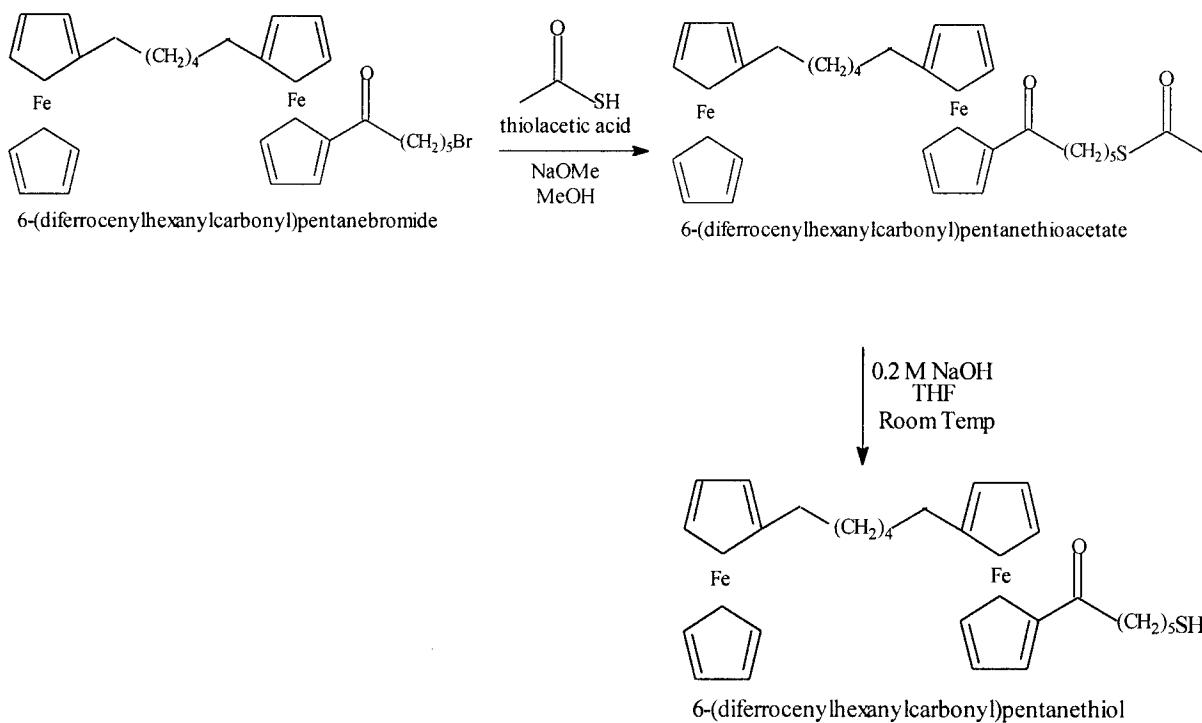


Figure 2.1, Continued: Schematic of Synthetic Pathway

chloride (Fisher, certified ACS, 99%), sodium hydroxide (Fisher, 97%), sodium sulfate (Fisher, certified ACS, 99%), tetrahydrofuran (Fisher, 99%), thiolacetic acid (Aldrich, 95%), toluene (Fisher, certified ACS, 99.9%) and zinc dust (Aldrich, 98%) were used as received.

Methylene chloride (Fisher, certified ACS, Fisher, 99.9%) was distilled over CaH_2 under nitrogen and used immediately. Methanol (Pharmco, 99.89%) was also distilled and used immediately. For reactions in which an inert atmosphere was required, pre-purified argon was delivered via a Schlenk line. Where appropriate, glassware was oven dried overnight at 110 °C and cooled under flowing argon. An overhead mechanical stirrer was used for reactions in which vigorous stirring was required.

Instrumentation

^1H and ^{13}C NMR spectra were obtained using a Varian-Gemini 2000 400 MHz NMR spectrometer using a deuterium lock, with chemical shifts reported as parts per million (ppm) downfield from TMS. IR spectra were obtained using an FT/IR 410 JASCO spectrometer, with the sample prepared as a KBr pellet and peak positions reported in wavenumbers. Direct probe mass spectrometry was performed using a Finnigan Model GCQ ion-trap spectrometer utilizing electron ionization to fragment the molecule.

Synthesis of 1,6-diferrocenylhexane-1,6-dione and 1-ferrocenylcarbonyl-2-ferrocenylcyclopentene

A modified version of the Friedel-Crafts acylation described by Chidsey², was used to prepare 1,6-diferrocenylhexane-1,6-dione and 1-ferrocenylcarbonyl-2-ferrocenylcyclopentene. Ferrocene (61.23 g, 0.329 mol) was dissolved in 700 mL of dry methylene chloride and cooled in an ice bath for fifteen minutes. Adipoyl chloride (24 mL, 0.165

mol) and anhydrous aluminum chloride (43.64 g, 0.327 mol) were added to the dissolved ferrocene. The reaction changed immediately from orange to deep purple. The ice bath was removed after fifteen minutes. After one and half-hours of stirring, 250 mL of deionized water was added dropwise via an addition funnel. The reaction began to slowly reflux and the color gradually turned back to orange. After an additional hour of stirring, the organic phase was extracted with deionized water until the aqueous layer was colorless, followed by three extractions with brine solution. The product was dried overnight over anhydrous sodium sulfate. The solvent was removed under reduced pressure and the crude product was purified via column chromatography using silica gel as the stationary phase and 75%/25% hexane/ethyl acetate as the eluent. Upon purification, two products were isolated. The first product ($R_f = 0.7$, 56% yield) was 1-ferrocenylcarbonyl-2-ferrocenylcyclopentene, while the second ($R_f = 0.5$, 28% yield) was 1,6-diferrocenylhexane-1,6-dione.

Spectroscopic Data for 1,6-diferrocenylhexane-1,6-dione

$^1\text{H NMR}$ (400 MHz, CDCl_3 , ppm) 1.799 (broad m, 4H, peak E), 2.774 (t, 4H, peak D), 4.201 (s, 10H, peak A), 4.499 (t, 4H, peak B), 4.798 (t, 4H, peak C)

$^{13}\text{C NMR}$ (400 MHz, CDCl_3 , ppm) 25.715 (2C, peak G), 40.850 (2C, peak F), 70.492 (10C, peak A), 70.939 (4C, peak B), 73.352 (4C, peak C), 80.159 (2C, peak D), 205.191 (2C, peak E)

IR spectroscopy ($\nu_{\text{max}}/\text{cm}^{-1}$) 3000-2950 (CH_2 stretching), 1658.48 (C=O stretching), 1453.10 (CH_2 bending), 1258.32 (C-C bending), 1069.33 (CH stretching), 827.31 (C=C stretching)

Mass spectrometry: parent ion peak at 482 m/z

Spectroscopic Data for 1-ferrocenylcarbonyl-2-ferrocenylcyclopentene

¹H NMR (400 MHz, CDCl₃, ppm) 1.256 (m, 2H, peak E), 2.076 (q, 1H, peak F), 2.888 (t, 2H, peak D), 4.072 (s, 5H, peak I), 4.105 (s, 2H, peak H), 4.162 (s, 5H, peak A), 4.194 (s, 2H, peak G), 4.418 (s, 2H, peak B), 4.668 (s, 2H, peak C)

¹³C NMR (400 MHz, CDCl₃, ppm) 24.349 (1C, peak I), 38.765 (1C, peaks H), 39.189 (1C, peak G), 69.567 (2C, peak L), 69.977 (2C, peak M), 70.250 (5C, peak N), 70.933 (5C, peak A), 71.570 (2C, peak B), 73.255 (2C, peak C), 80.181 (1C, peak D), 81.312 (1C, peak K), 136.984 (1C, peak J), 142.143 (1C, peak F), 203.248 (1C, peak E)

IR spectroscopy ($\nu_{\max}/\text{cm}^{-1}$) 3000-2950 (CH₂ stretching), 1631.48 (C=O stretching), 1444.42 (CH₂ bending), 1270.86 (C-C bending), 1103.08 (CH stretching), 823.46 (C=C stretching)

Mass spectrometry: parent ion peak at 464 m/z.

Synthesis of 1,6-diferrocenylhexane and 1,6-diferrocenylhexane-1-one

A Clemmensen reduction was carried out on the purified 1,6-diferrocenylhexane-1,6-dione to reduce the carbonyls into methylene groups according to the method of Creager³. The 1,6-diferrocenylhexane-1,6-dione (8.49 g, 0.018 mol) was dissolved in 100 mL of toluene and transferred to a three neck round bottom flask. A zinc-mercury amalgam was prepared by dissolving mercuric chloride (1.20 g, 0.00442 mol) in 30 mL of deionized water, followed by addition of zinc dust (17.59 g, 0.269 mol). Deionized water (30 mL) and concentrated hydrochloric acid (12 M, 47 mL, 1.54 mol) were added to the solution and the mixture was heated to reflux under static argon for six hours. An overhead mechanical stirrer was used to ensure the biphasic mixture was in proper contact with the amalgam at all times throughout the reaction. After two and a half hours, an additional

portion of HCl (12 mL, 0.394 mol) was added, followed by a similar addition two and half hours later. The reaction was allowed to stir for another hour. Once the mixture had cooled to room temperature, the organic portion was extracted three times with deionized water, followed by three extractions with brine solution. The resulting crude product was then dried over anhydrous sodium sulfate overnight and the solvent was removed under reduced pressure. The product was purified using column chromatography with silica gel as the stationary phase and 75%/25% hexane/ethyl acetate as the mobile phase. Two products were isolated, those being the fully reduced product, 1,6-diferrocenylhexane ($R_f = 0.6$, 76 % yield), and the monoreduced product, 1,6-diferrocenylhexane-1-one ($R_f = 0.4$, yield 8.8%). Both products were isolated and fully characterized.

Spectroscopic Data for 1,6-diferrocenylhexane

^1H NMR (400 MHz, CDCl_3 , ppm) 1.337 (broad m, 4H, peak F), 1.500 (broad m, 4H, peak E), 2.308 (t, 4H, peak D), 4.054 (m, 4H, peak C), 4.071 (m, 4H, peak B), 4.106 (m, 10H, peak A)

^{13}C NMR (400 MHz, CDCl_3 , ppm) 22.799 (2C, peak G), 29.620 (4C, peak F), 31.175 (4C, peak E), 67.114 (4C, peak C), 68.169 (4C, peak B), 68.594 (10C, peak A), 89.617 (2C, peak D)

IR spectroscopy ($\nu_{\text{max}}/\text{cm}^{-1}$) 2917.77 cm^{-1} -2847.38 cm^{-1} (CH_2 stretching), 1393.32 cm^{-1} (CH_2 bending), 1104.05 cm^{-1} (C-C bending), 1020.16 cm^{-1} (CH stretching), 815.74 cm^{-1} (C=C stretching)

Mass spectrometry: parent ion peak occurs at 454 m/z

Spectroscopic Data for 1,6-diferrocenylhexane-1-one

¹H NMR (400 MHz, CDCl₃, ppm) 1.408 (t, 2H, peak F), 1.555 (t, 2H, peak G), 1.725 (t, 2H, peak E), 2.347 (t, 2H, peak H), 2.695 (t, 2H, peak D), 4.050 (m, 1H, peak I), 4.073 (m, 2H, peak J), 4.102 (s, 5H, peak K), 4.192 (s, 5H, peak A), 4.487 (s, 2H, peak B), 4.777 (s, 2H, peak C)

¹³C NMR (400 MHz, CDCl₃, ppm) 25.700 (1C, peak G), 30.722 (1C, peaks H and I), 32.361 (1C, peak J), 40.896 (1C, peak F), 68.278 (2C, peak L), 69.325 (2C, peak M), 69.711 (2C, peak N), 70.478 (2C, peak A), 70.895 (5C, peak B), 73.277 (5C, peak C), 80.280 (1C, peak D), 90.462 (1C, peak K), 205.403 (1C, peak E)

IR spectroscopy ($\nu_{\max}/\text{cm}^{-1}$) 2927.89 cm^{-1} (CH₂ stretching), 1675.84 cm^{-1} (C=O stretching), 1454.06 cm^{-1} (CH₂ bending), 1248.68 cm^{-1} (C-C bending), 1103.57 cm^{-1} (C-C stretching), 1025.46 cm^{-1} (CH stretching), 817.67 cm^{-1} (C=C stretching)

Mass spectrometry: parent ion peak at occurs at 468 m/z

Synthesis of 6-(diferrocenylhexanylecarbonyl)pentanebromide

Another Friedel Crafts acylation, as reported by Chidsey², was carried out on the purified 1,6-diferrocenylhexane. A 300 mL, oven-dried round bottom flask was cooled under flowing argon and 40 mL of dry methylene chloride was used to dissolve the 1,6-diferrocenylhexane (6.02 g, 0.0133 mol). The flask was stoppered and cooled in an ice bath for fifteen minutes. The 6-bromohexanoyl chloride (2.0 mL, 0.0131 mol) was added and the ice bath was removed. Anhydrous AlCl₃ (1.80g, 0.0135 mol) was then added to the mixture, which immediately turned from orange to deep purple. The mixture was stirred for one and half-hours under static argon and then quenched with 27 mL of deionized water, added via an additional funnel. The solution was then stirred for an

additional half-hour. The organic phase was extracted three times with deionized water until the aqueous layer was colorless, followed by three extractions with brine solution. The resulting organic phase was dried over anhydrous MgSO_4 , filtered, and the solvent was removed under reduced pressure. The crude product was purified using column chromatography with silica gel as the stationary phase and 80%/20% hexane/ethyl acetate as the eluent. Five products were isolated after running several columns. The second compound ($R_f = 0.6$, 0.5% yield) was the desired product, 6-(diferrocenylhexanylethylcarbonyl)pentanebromide.

Spectroscopic Data for 6-(diferrocenylhexanylethylcarbonyl)pentanebromide

^1H NMR (400 MHz, CDCl_3 , ppm) 1.254 (broad s, 2H, peak F), 1.352 (t, 4H, peak M), 1.540 (m, 4H, peak E), 1.731 (t, 2H, peak L), 1.928 (q, 2H, peak N), 2.300 (t, 4H, peak D), 2.786 (m, 2H, peak K), 3.445 (t, 2H, peak O), 4.029 (broad d, 2H, peak C), 4.047 (broad d, 2H, peak B), 4.086 (s, 5H, peak A), 4.111 (s, 4H, peaks G and H), 4.408 (q, 2H, peak I), 4.589 (q, 2H, peak J)

^{13}C NMR (400 MHz, CDCl_3 , ppm) 24.676 (2C, peak G), 29.349 (1C, peak P), 30.669 (2C, peak F), 30.814 (2C, peak E), 32.331 (1C, peak Q), 34.000 (1C, peak O), 35.009 (1C, peak R), 41.215 (1C, peak N), 68.141 (2C, peak C), 69.218 (2C, peak B), 69.628 (5C, peak A), 70.758 (2C, peak H), 71.350 (2C, peak I), 71.722 (2C, peak J), 74.484 (2C, peak K), 76.949 (1C, peak L), 93.231 (2C, peak D), 206.260 (1C, peak M)

Mass spectrometry: The parent ion peak occurs at 631 m/z

Synthesis of 6-(diferrocenylhexanylethylcarbonyl)pentaneethiol

The purified product was thiolated by dissolving sodium methoxide (0.03 g, 0.555 mmol) in 25 mL of distilled methanol according to the method of Hickman⁵ et al.

Thiolacetic acid (35 μ L, 0.037 g, 0.388 mmol) was added to the methanol via a syringe. The 6-(diferrocenylhexanylethylcarbonyl)pentanebromide (0.15 g, 0.238 mmol) was dissolved in 25 mL of freshly distilled methanol and added to the reaction flask. The reaction was refluxed under static argon for eighteen hours. The methanol was removed under reduced pressure and the product was collected as an orange syrup. The crude product was purified via column chromatography with silica gel as the stationary phase and 60%/40% hexane/ethyl acetate as the mobile phase. The purified thioacetate salt (0.020 g, 0.0319 mmol) was dissolved in 10 mL of deoxygenated tetrahydrofuran. Two drops of deoxygenated 0.2 M NaOH (0.04 g in 50 mL deionized water) was added and the solution was stirred at room temperature overnight. The THF was removed under reduced pressure and the product was purified via column chromatography using a silica gel as the stationary phase and 60%/40% hexane/ethyl acetate as the eluent. The final product, 6-(diferrocenylhexanylethylcarbonyl)pentanethiol ($R_f = 0.5$, 75 % yield), was isolated and fully characterized.

Spectroscopic Data for 6-(diferrocenylhexanylethylcarbonyl)pentanethiol

^1H NMR (400 MHz, CDCl_3 , ppm) 1.240 (s, 1H, peak P), 1.258 (m, 4H, peak F), 1.353 (t, 4H, peak M), 1.501 (m, 2H, peak N), 1.573 (m, 4H, peak E), 1.742 (t, 2H, peak L), 2.294 (t, 4H, peak D), 2.494 (m, 2H, peak O), 2.784 (m, 2H, peak K), 4.039 (m, 2H, peak C), 4.062 (m, 2H, peak B), 4.094 (broad m, 5H, peak A), 4.130 (s, 2H, peak G), 4.147 (s, 2H, peak H), 4.404 (q, 2H, peak I), 4.595 (q, 2H, peak J)

^{13}C NMR (400 MHz, CDCl_3 , ppm) 25.108 (2C, peak G), 29.630 (1C, peak P), 30.434 (1C, peak Q), 30.677 (2C, peak F), 30.821 (2C, peak E), 31.595 (1C, peak O), 33.181 (1C, peak R), 41.306 (1C, peak N), 68.126 (2C, peak C), 69.203 (2C, peak B), 69.605

(5C, peak A), 70.743 (2C, peak H), 71.350 (2C, peak I), 71.783 (2C, peak J), 74.438 (2C, peak K), 76.995 (1C, peak L), 93.193 (2C, peak D), 206.420 (1C, peak M)

Mass spectrometry: The parent ion peak occurs at 585 m/z

RESULTS AND DISCUSSION

Characterization of 1,6-diferrocenylhexane-1,6-dione

The ^1H NMR of 1,6-diferrocenylhexane-1,6-dione in CDCl_3 is shown in Figure 2.2. The broad peak at 1.255 ppm is from the hexane used to purify the product. The inner methylene protons on the six-carbon chain joining the two ferrocenes show a broad signal at 1.799 ppm (peak E). The protons neighboring the carbonyl were shifted downfield to 2.774 ppm (peak D) due to the electron withdrawing carbonyl substituent. The protons on the bottom cyclopentadienyl (Cp) ring showed a strong singlet at 4.201 ppm (peak A). This peak will recur throughout the following ^1H NMR assignments and will be very distinguishable from other peaks. The two protons on the top Cp ring that are two bonds away from the carbonyl shows a triplet at 4.798 ppm (peak C) and the protons three bonds away from the carbonyl show a triplet at 4.499 ppm (peak B). Protons in this region are common for carbonyl substituted ferrocene compounds.

^{13}C NMR of 1,6-diferrocenylhexane-1,6-dione was also performed in CDCl_3 and is shown in Figure 2.3. The carbons in the methylene bridge that are the farthest from the oxygen should be shifted upfield with the adjacent carbons downfield. The methylene carbon two bonds away from the carbonyl is located at 25.715 ppm (peak G) while the carbon one away is at 40.850 ppm (peak F). The region in the ^{13}C spectra between 70 and 80 ppm had to be magnified to assign the remaining peaks, as shown in Figure 2.4. The bottom Cp ring carbons are at 70.492 ppm (peak A), which is a characteristic peak

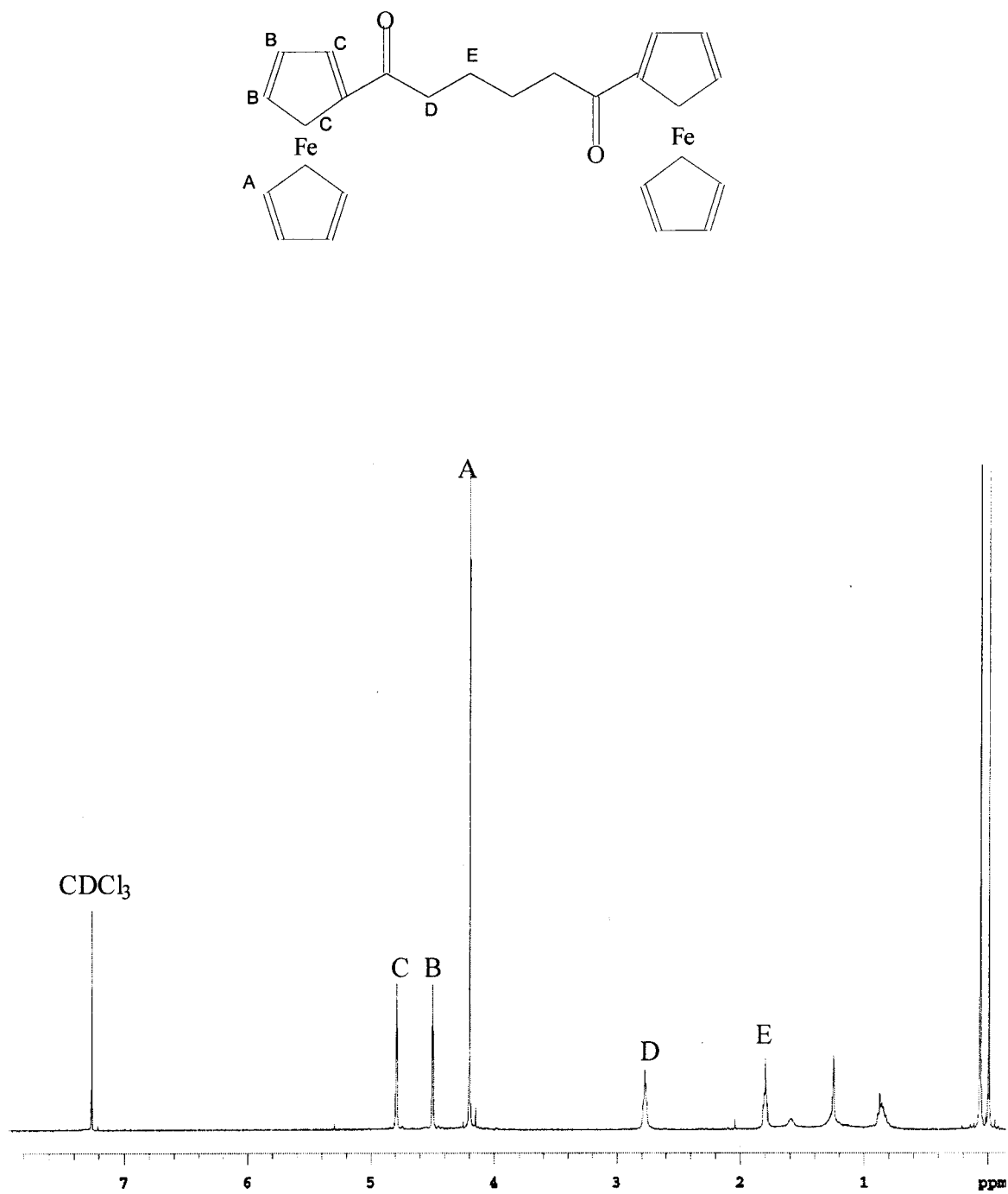


Figure 2.2: ^1H NMR spectrum of 1,6-diferrocenylhexane-1,6-dione

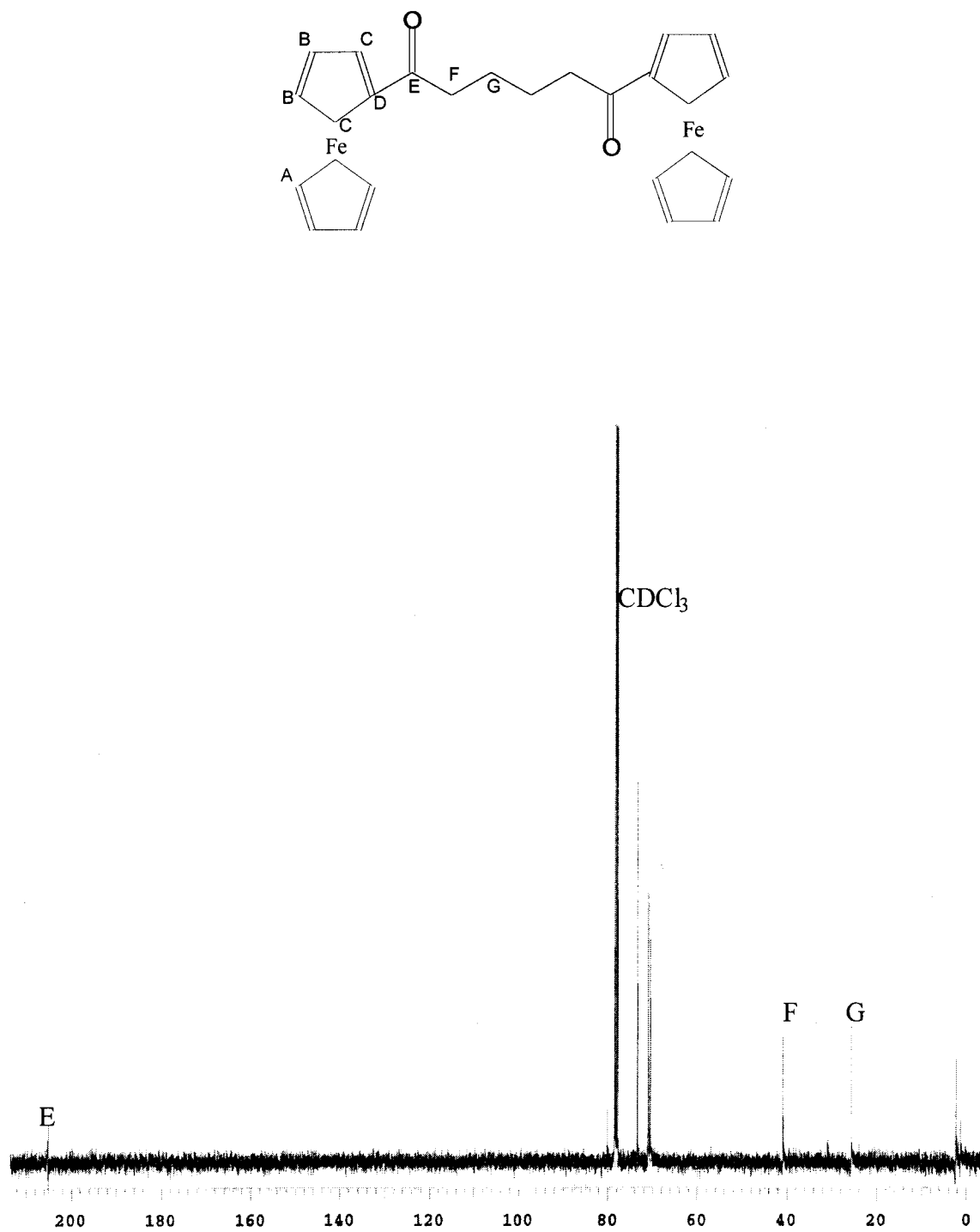


Figure 2.3: ^{13}C NMR spectrum of 1,6-diferrocenylhexane-1,6-dione

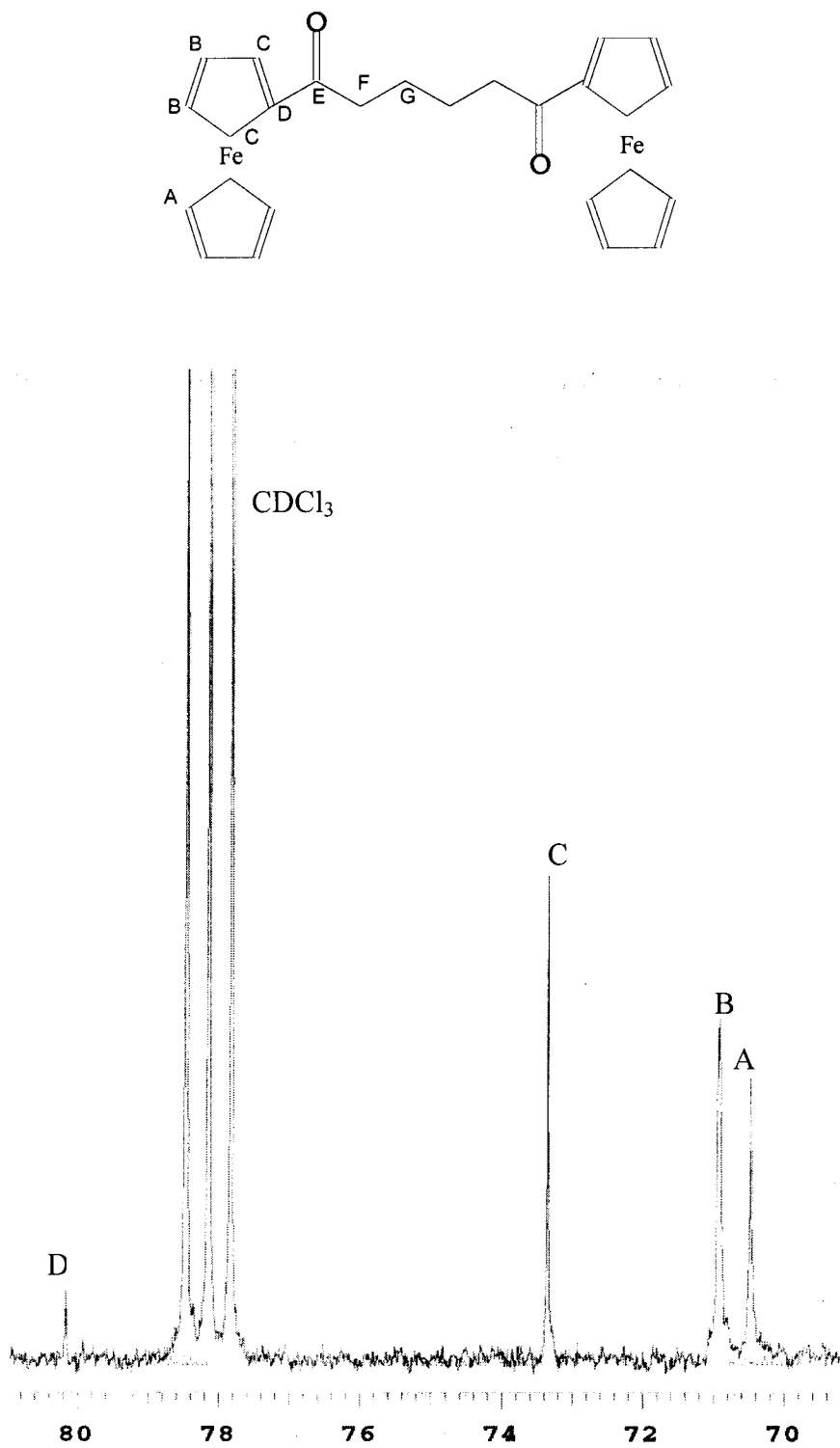


Figure 2.4: ^{13}C NMR spectrum close up from 70-85 ppm of 1,6-diferrocenylhexane-1,6-dione

in the ferrocene compounds. The carbons in the top Cp ring that are two and three bonds away from the carbonyl show chemical shifts at 73.352 ppm (peak C) and 70.939 ppm (peak B), respectively. The carbon in the Cp ring directly attached to the carbonyl, shows a low intensity peak at 80.159 ppm (peak D). The low intensity is due to the fact no protons are attached to that carbon. The carbonyl carbon was easily assigned at 205.191 ppm (peak E).

The IR spectrum, shown in Figure 2.5, was assigned with close attention to a strong absorbing carbonyl stretch at 1658.48 cm^{-1} . Stretching from the C=C bonds in the Cp rings occurs between 3000 and 2950 cm^{-1} , with CH_2 bending from the methylenes at 1453.10 cm^{-1} . Single carbon-carbon bonds in the methylene bridge occurred at 1258.32 cm^{-1} and 827.31 cm^{-1} . CH stretching at 1069.33 cm^{-1} was attributed to the Cp rings.

Direct probe mass spectrometry on 1,6-diferrocenylohexane-1,6-dione dissolved in CH_2Cl_2 was performed and the results are shown in Figure 2.6. The parent ion peak is easily assigned at 482 m/z. A common feature in fragmenting of ferrocene compounds, is the loss of a bottom Cp ring. This is evident from the peak at 417 m/z. Refer to Table 2.1 for the assignments of the remaining major fragments.

Characterization of 1-ferrocenylcarbonyl-2-ferrocenylcyclopentene

The ^1H NMR spectrum of 1-ferrocenylcarbonyl-2-ferrocenylcyclopentene in CDCl_3 is shown in Figure 2.7. The protons the farthest upfield at 1.256 (peak E) are located at the apex of the cyclopentene ring. The protons adjacent to the apex are located at 2.706 ppm (peak F) and 2.888 ppm (peak D). Peak D is shifted downfield from the other protons due to the carbonyl substituent. The large singlet at 4.072 ppm (peak I) is assigned to the bottom Cp ring protons closest to the cyclopentene ring. The other unsubstituted Cp

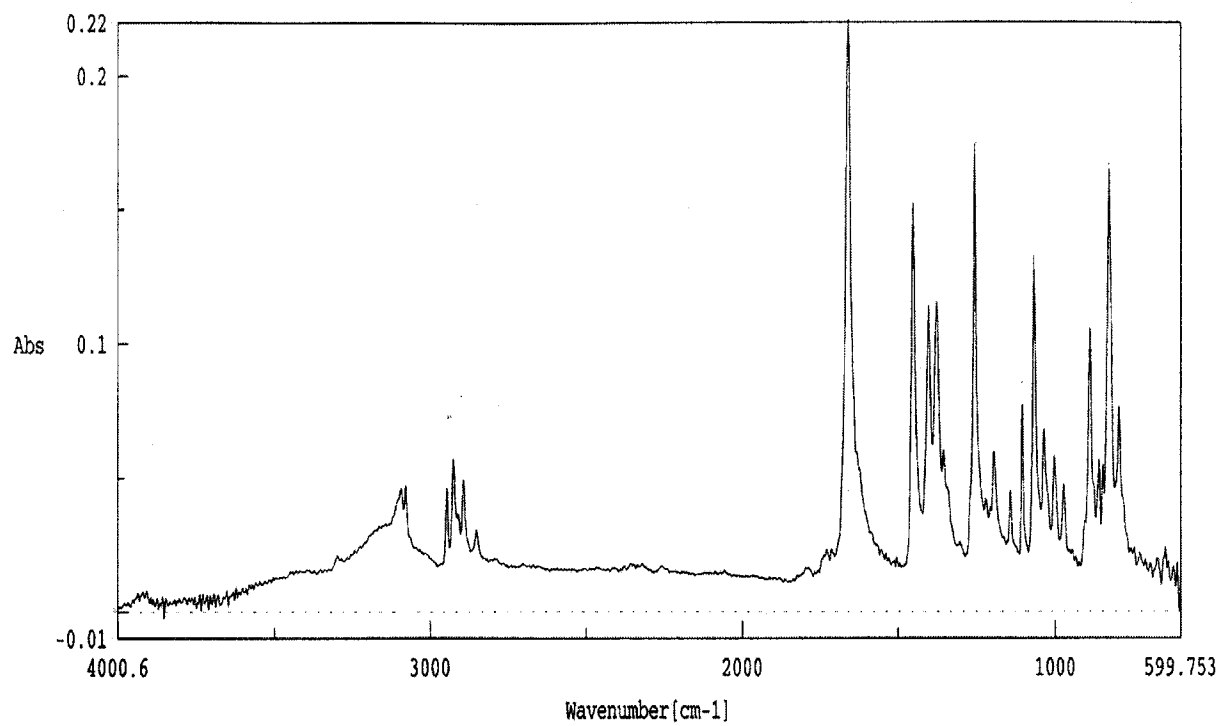


Figure 2.5: IR spectrum of 1,6-diferrocenylhexane-1,6-dione

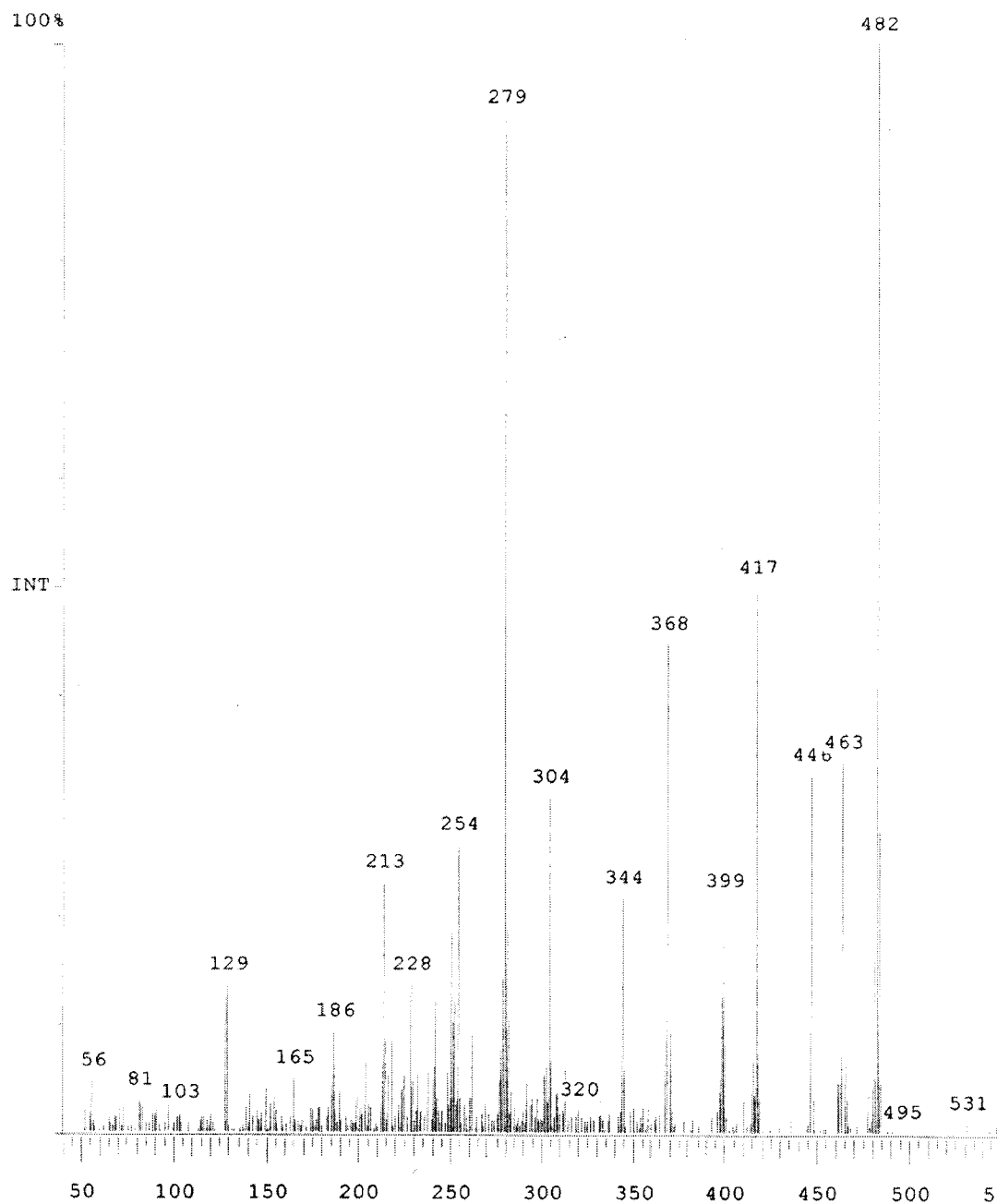
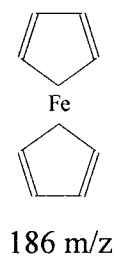
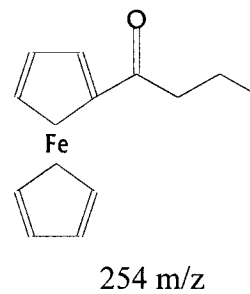
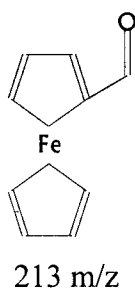
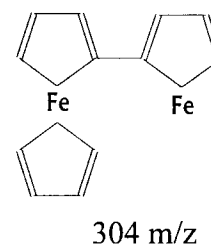
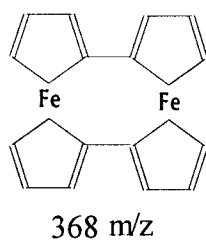
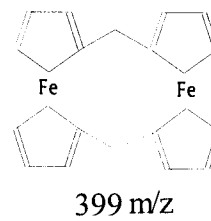
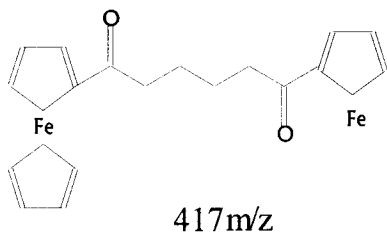


Figure 2.6: Mass spectrum of 1,6-diferrocenylhexane-1,6-dione

Table 2.1

Assigned Fragments from 1,6-diferrocenylhexane-1,6-dione Mass Spectrum

Fragments

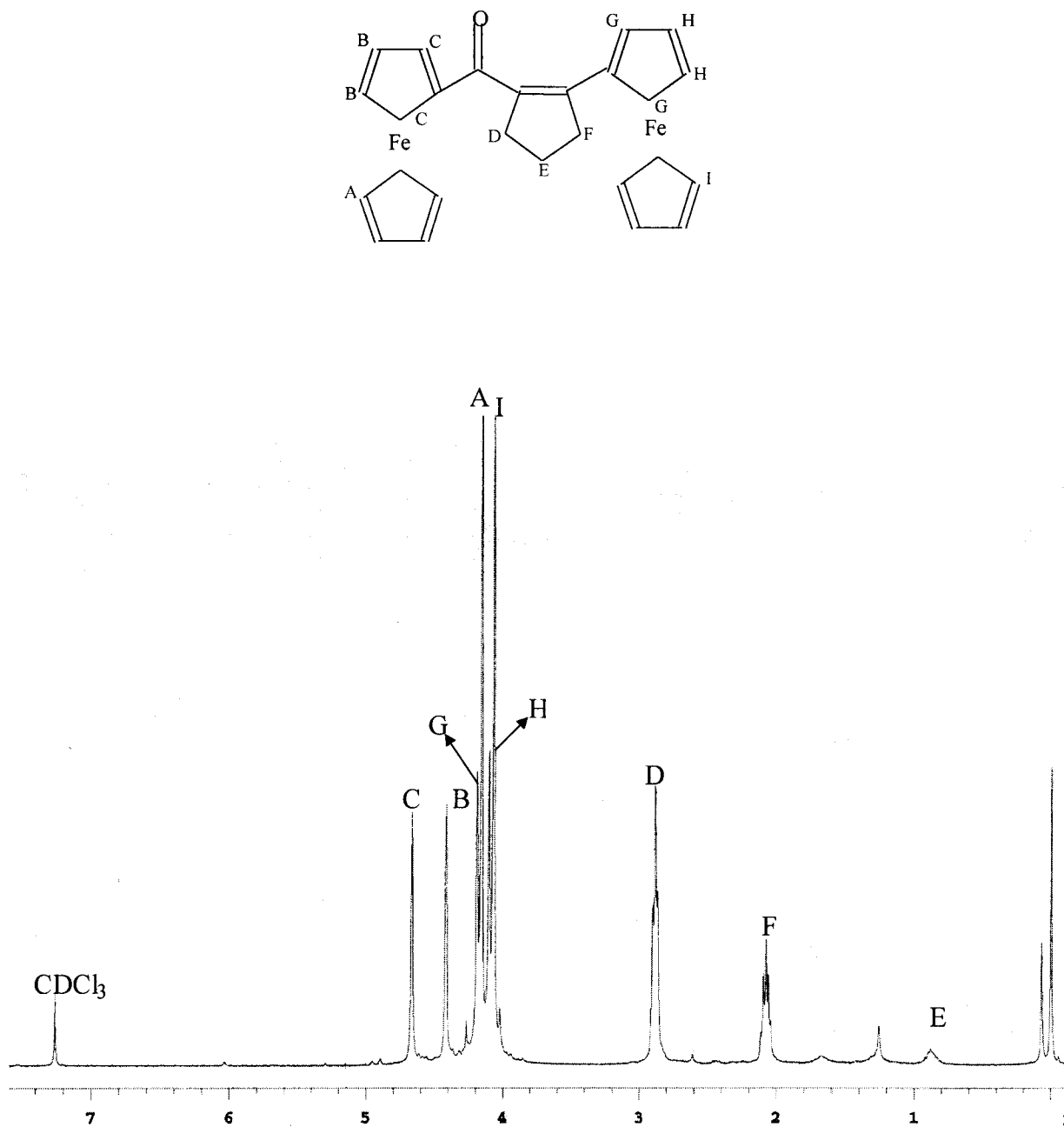


Figure 2.7: ¹H NMR spectrum of 1-ferrocenylcarbonyl-2-ferrocenylcyclopentene

ring protons are a singlet at 4.162 ppm (peak A). The protons on the top Cp ring adjacent to the cyclopentene ring are shown in the same region at 4.105 ppm (peak H) and 4.194 ppm (peak G). However, the similar protons on the other Cp ring are shifted downfield due to the proximity of the electron withdrawing carbonyl substituent. The protons two and three bonds away from the carbonyl are shown at 4.668 ppm (peak C) and 4.418 ppm (peak B), respectively.

The ^{13}C NMR spectrum of 1-ferrocenylcarbonyl-2-ferrocenylcyclopentene in CDCl_3 is shown in Figure 2.8. The methylene carbon at the apex of the five-membered ring showed a peak at 38.765 ppm (peak H). The adjacent methylene carbons at 24.349 ppm (peak I) and 39.189 ppm (peak G) were extremely close to one another, but peak G was shifted downfield due to the proximity of the carbonyl substituent. The ^{13}C spectra in the region from 70 to 80 ppm was expanded and is shown in Figure 2.9. The carbons in the top Cp ring directly attached to the cyclopentene ring demonstrated chemical shifts at 69.567 ppm (peak L) and 69.977 ppm (peak M), which were one and two bonds away, respectively. The carbons on the lower Cp ring attached to the cyclopentene ring were found downfield slightly at 70.250 ppm (peak N). The characteristic peak at 70.933 ppm (peak A) was assigned to the bottom Cp ring carbons of the ferrocene attached to the carbonyl. The four carbons in the upper ring that were two and three bonds away from the carbonyl were downfield from peak A at 73.255 ppm (peak C) and 71.570 ppm (peak B), respectively. The carbon in the ferrocene ring to which the carbonyl is directly attached is located at 80.181 ppm (peak D) while the carbon in the other Cp ring attached to the cyclopentene is at 81.312 ppm (peak K). The sp^2 carbons in the five-membered ring to which the ferrocene and carbonyl are directly attached, are located at

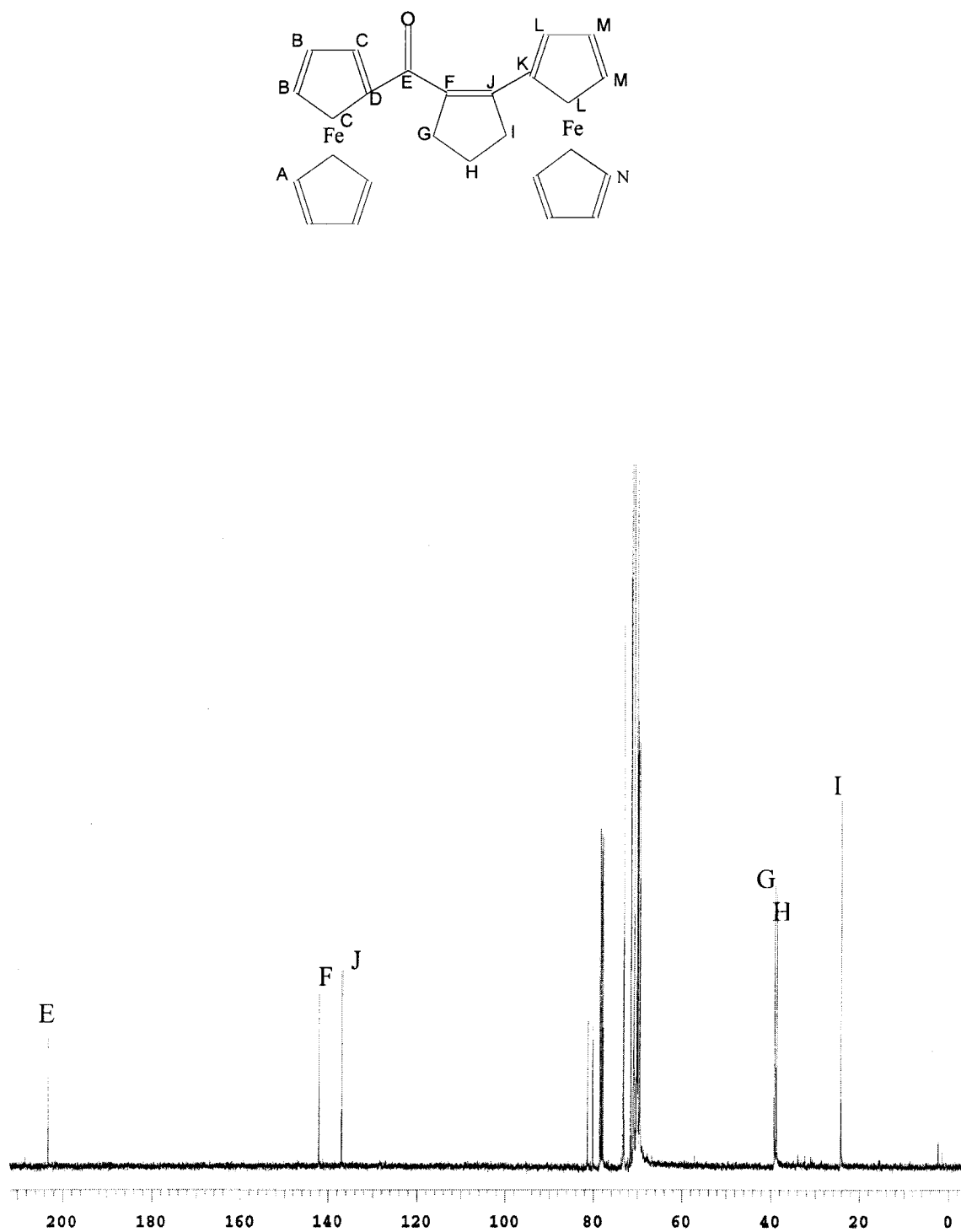


Figure 2.8: ^{13}C NMR spectrum of 1-ferrocenylcarbonyl-2-ferrocenylcyclopentene

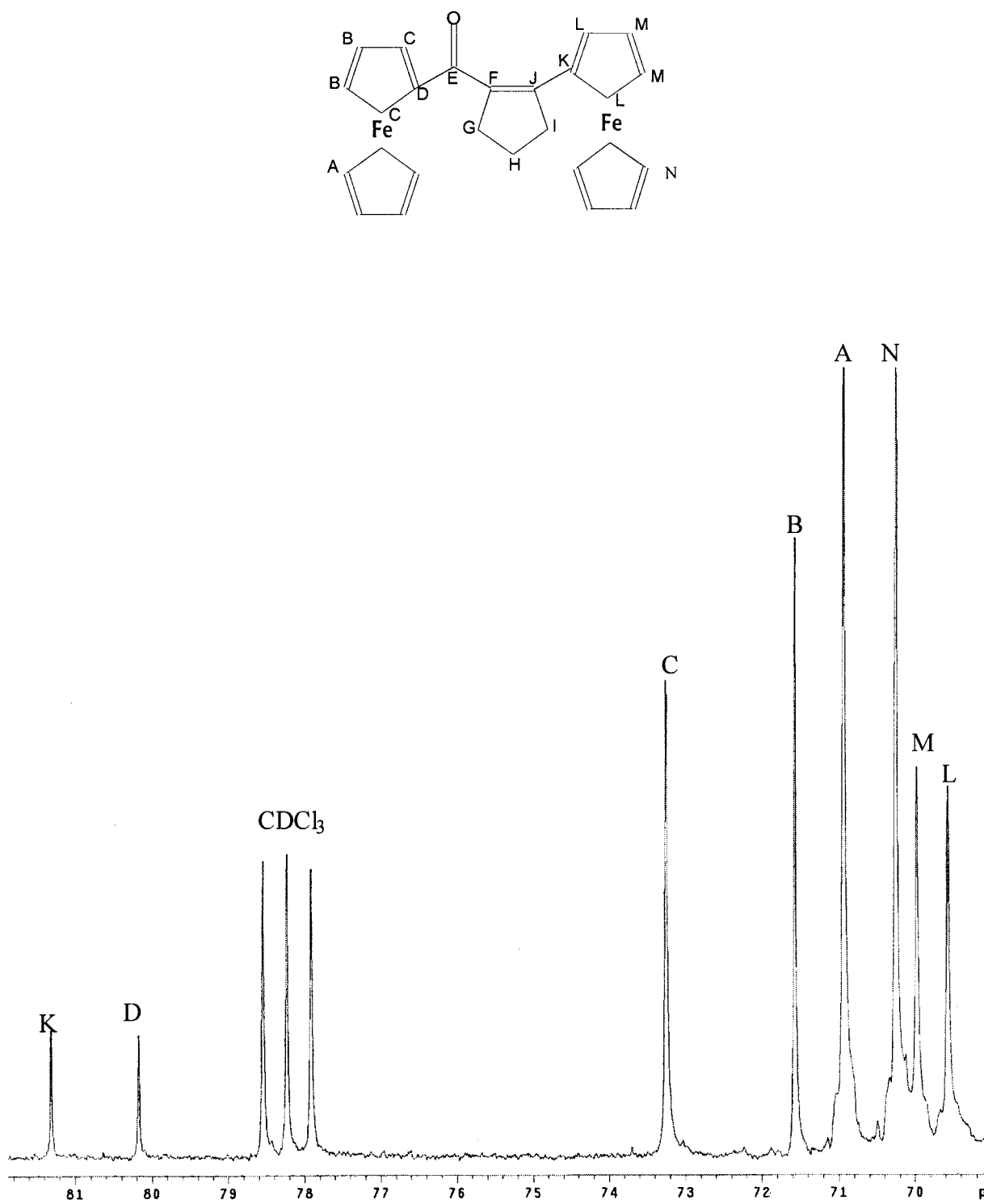


Figure 2.9: ^{13}C NMR spectrum close up from 69-82 ppm of 1-ferrocenylcarbonyl-2-ferrocenylcyclopentene

136.984 ppm (peak J) and 142.143 ppm (peak F), respectively. Lastly, the carbonyl carbon displays the characteristic chemical shift at 203.248 ppm (peak E).

To aid the in the ^{13}C NMR assignments, due to the complexity of this molecule, an Attached Proton Test (APT) was performed. Spectra of this nature will distinguish between carbons that have even or odd numbered protons attached to it. Carbons with even number of protons attached, i.e. zero or two, will show chemical shifts that point up, while carbons with odd number of carbons attached, i.e. one or three, will display chemical shifts that point down. This spectrum confirmed the ^{13}C NMR assignments and is shown in Figure 2.10.

The IR spectrum is shown in Figure 2.11 and displays a strong carbonyl stretch at 1631.48 cm^{-1} . Methylene stretching and bending from the Cp rings appears at $3000\text{-}2950\text{ cm}^{-1}$ and 1444.42 cm^{-1} , respectively. Unsaturated carbon bending from the methylene bridge was evident from the peak at 1270.86 cm^{-1} and saturated carbons in the Cp rings displayed absorbances at 832.46 cm^{-1} . The C-H stretching from the Cp rings were assigned to the peak at 1103.08 cm^{-1} .

Direct probe mass spectrometry analysis indicated that the parent ion peak occurred at 464 m/z and is shown in Figure 2.12. The next major fragment, 399 m/z, was due to the loss of a bottom Cp ring. The assignment of the remaining fragments is shown in Table 2.2.

Characterization of 1,6-diferrocenylhexane

The ^1H NMR spectrum of 1,6-diferrocenylhexane in CDCl_3 is shown in Figure 2.13. The inner methylene protons in the carbon bridge were located upfield at 1.337 ppm (peak F). The next two methylene protons were shifted downfield to 1.500 ppm (peak E)

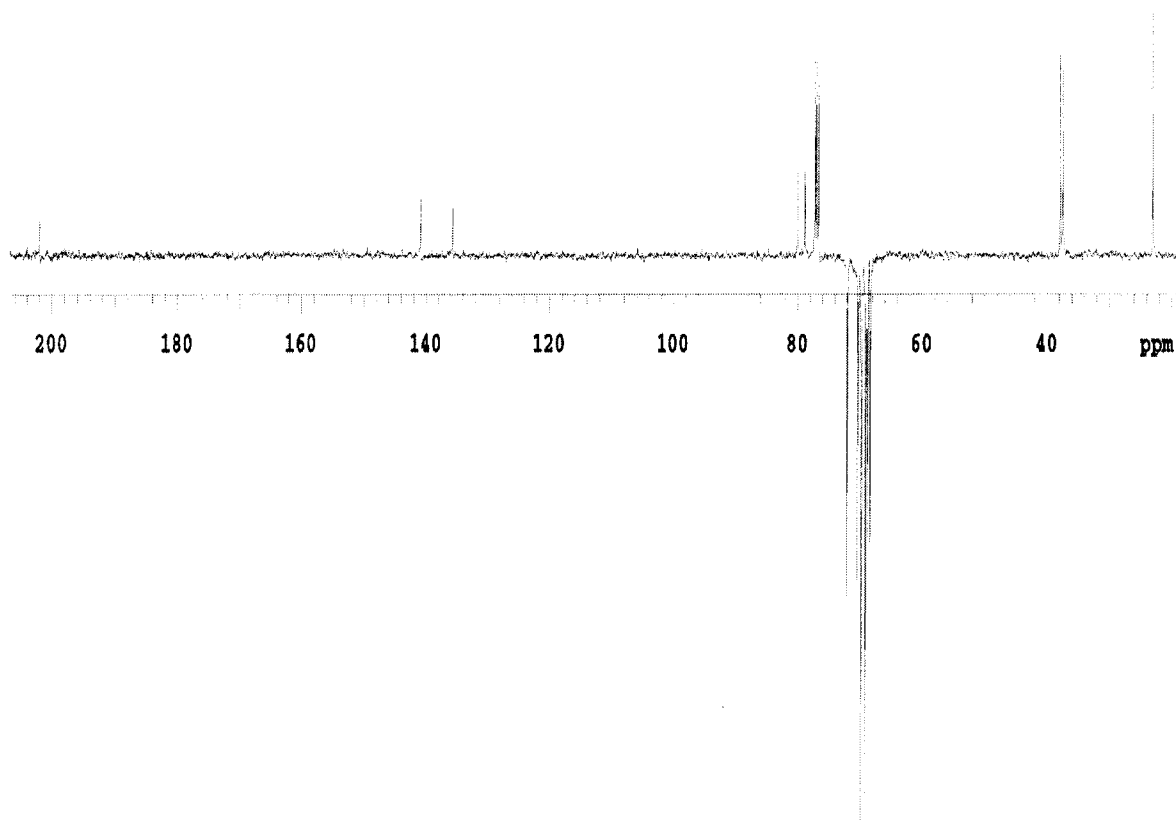


Figure 2.10: APT spectrum of 1-ferrocenylcarbonyl-2-ferrocenylcyclopentene

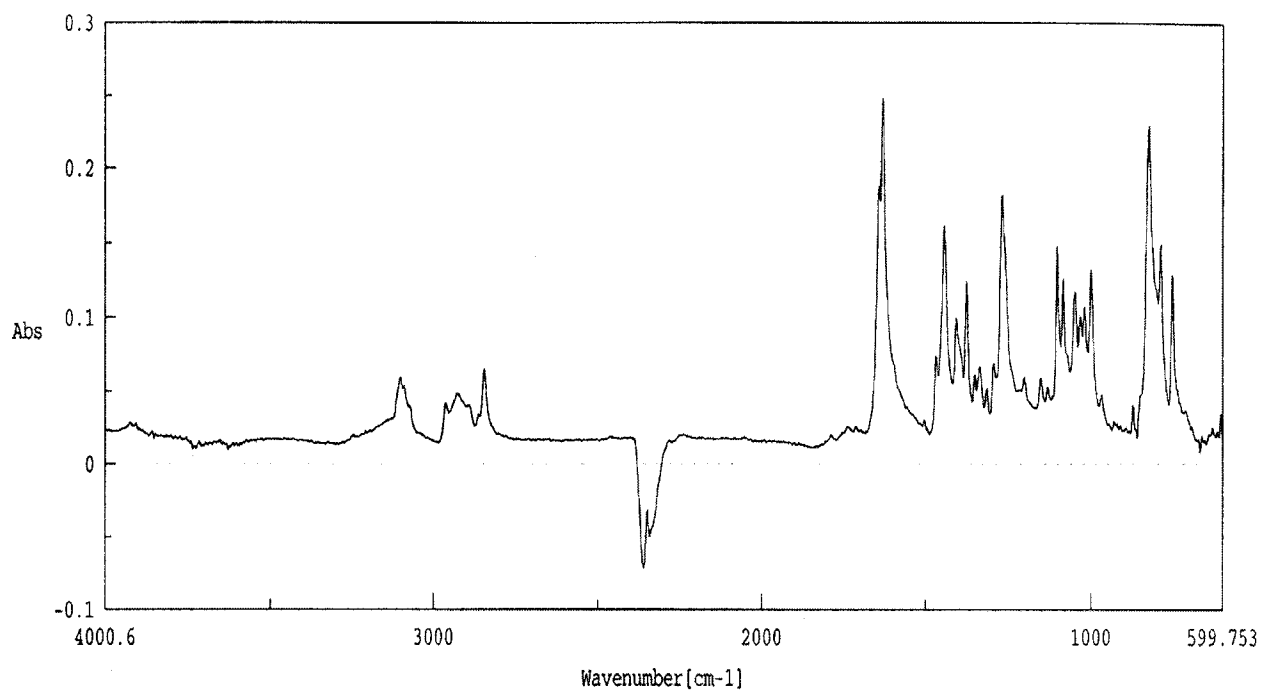


Figure 2.11: IR spectrum of 1-ferrocenylcarbonyl-2-ferrocenylcyclopentene

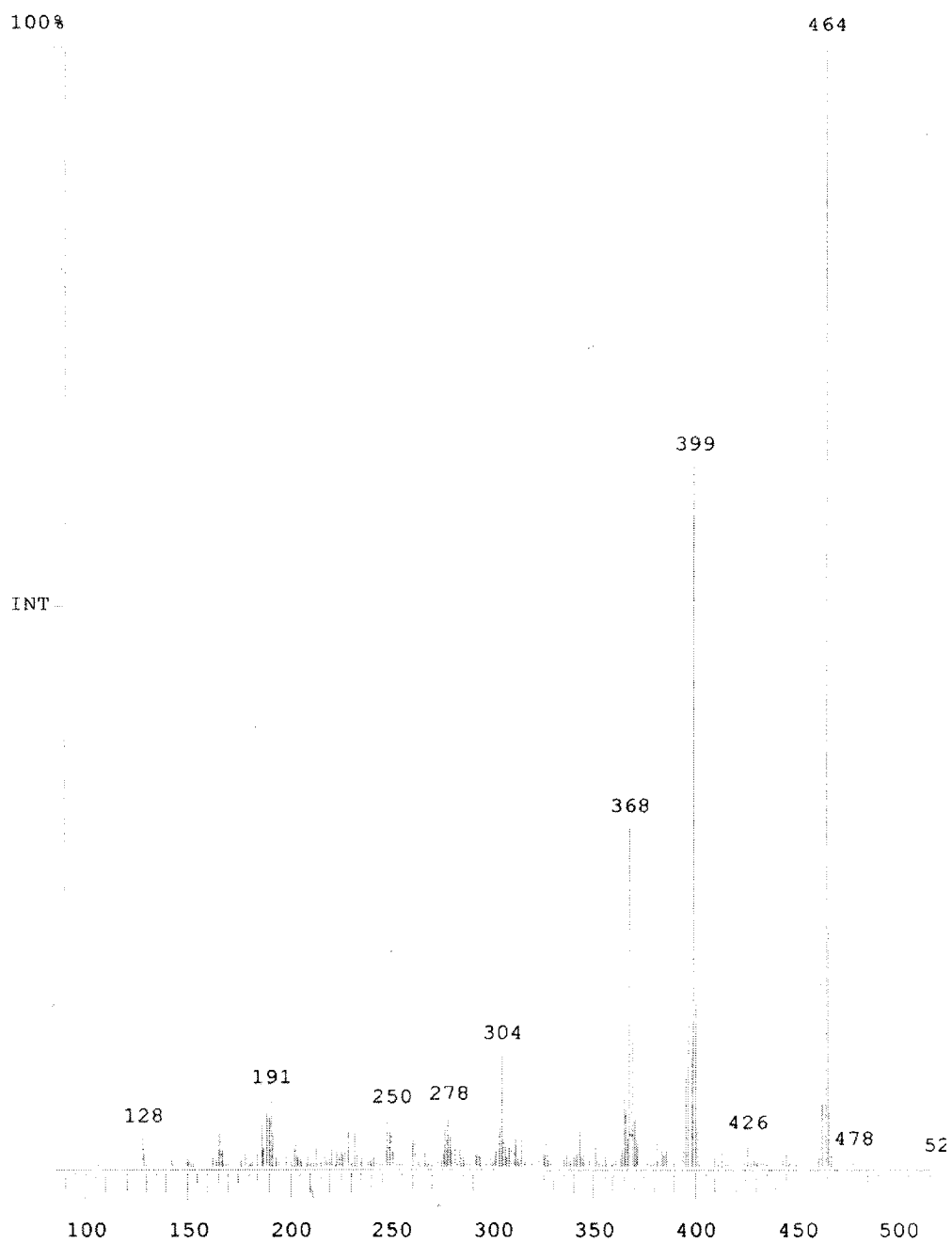
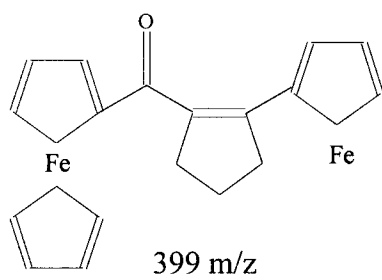
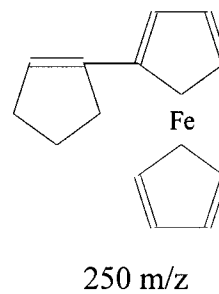
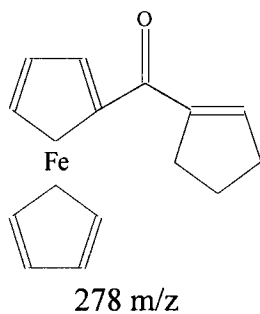
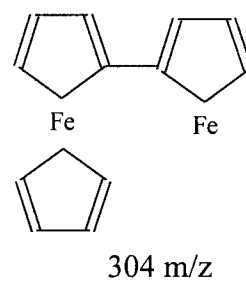
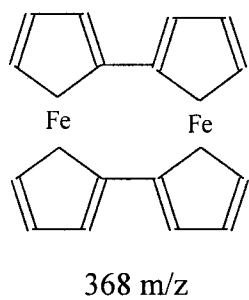
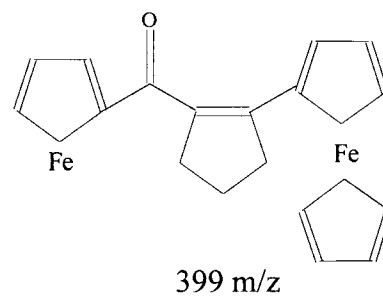


Figure 2.12: Mass spectrum of 1-ferrocenylcarbonyl-2-ferrocenylcyclopentene

Table 2.2

Assigned Fragments from 1-ferrocenylcarbonyl-2-ferrocenylcyclopentene Mass Spectrum**Fragments**

or



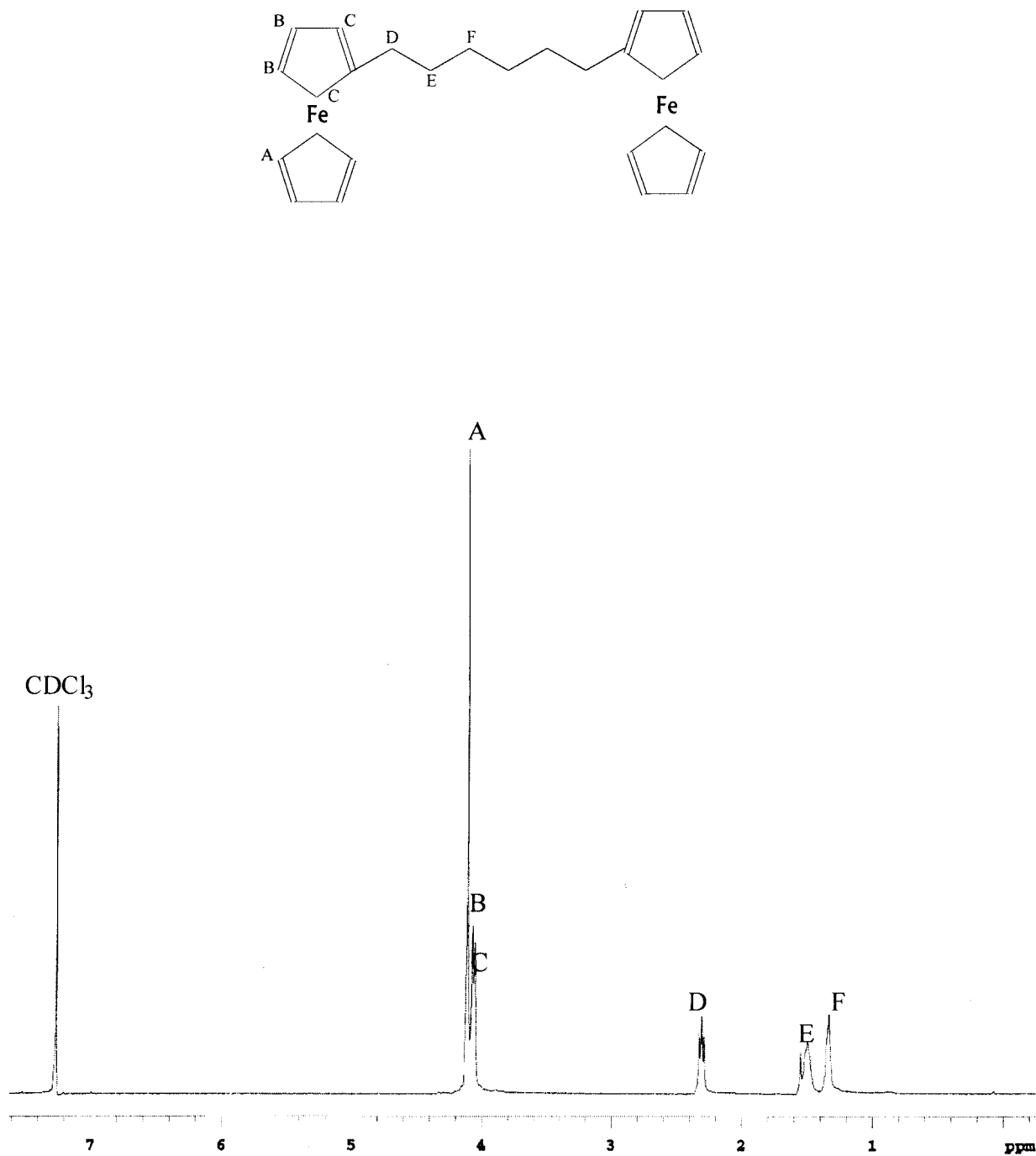


Figure 2.13: ^1H NMR spectrum of 1,6-diferrocenylhexane

and 2.303 ppm (peak D). The protons on the top Cp ring were shifted upfield by the electron donating alkyl substituent showing chemical shifts of 4.054 ppm (peak C) and 4.071 ppm (peak B). This was an indication that the reduction was successful. The Cp protons on the bottom ring gave a strong singlet at 4.106 ppm (peak A), as expected.

The ^{13}C NMR spectrum of 1,6-diferrocenylhexane was performed in CDCl_3 and is shown in Figure 2.14. The inner most methylene carbons in the bridge were shifted upfield to 22.799 ppm (peak G) as compared to 1,6-diferrocenylhexane-1,6-dione. The next two peaks were the carbons located one and two bonds away from the ferrocene at 31.175 ppm (peak E) and 29.620 ppm (peak F), respectively. The carbons in the top Cp ring one bond away from the electron donating bridge show a chemical shift value of 67.114 ppm (peak C) and the carbons two bonds away occur at 68.169 ppm (peak B). The five carbons in the bottom Cp ring were indicated by the intense peak at 68.594 ppm (peak A). The carbon in the top Cp ring to which the methylene bridge is bonded, shows a chemical shift of 89.617 ppm (peak D). The absence of the carbonyl peak around 200 ppm also indicated that the reduction was successful.

The IR spectrum is shown in Figure 2.15 and displays no carbonyl stretch at approximately 1600 cm^{-1} . The methylene stretching from the Cp rings showed peaks at 2917.77 cm^{-1} and 2847.38 cm^{-1} . Single carbon-carbon bond stretching from the methylene bridge occurred at 1104.05 cm^{-1} . The C-H stretching from the Cp rings was evident at 1020.16 cm^{-1} . Unsaturated carbon-carbon bond stretching from the Cp rings was assigned to the peak at 815.74 cm^{-1} .

Shown in Figure 2.16 is the mass spectrum of the fully reduced product and shows the parent ion peak at 454 m/z. The fragment assignments are shown in Table 2.3.

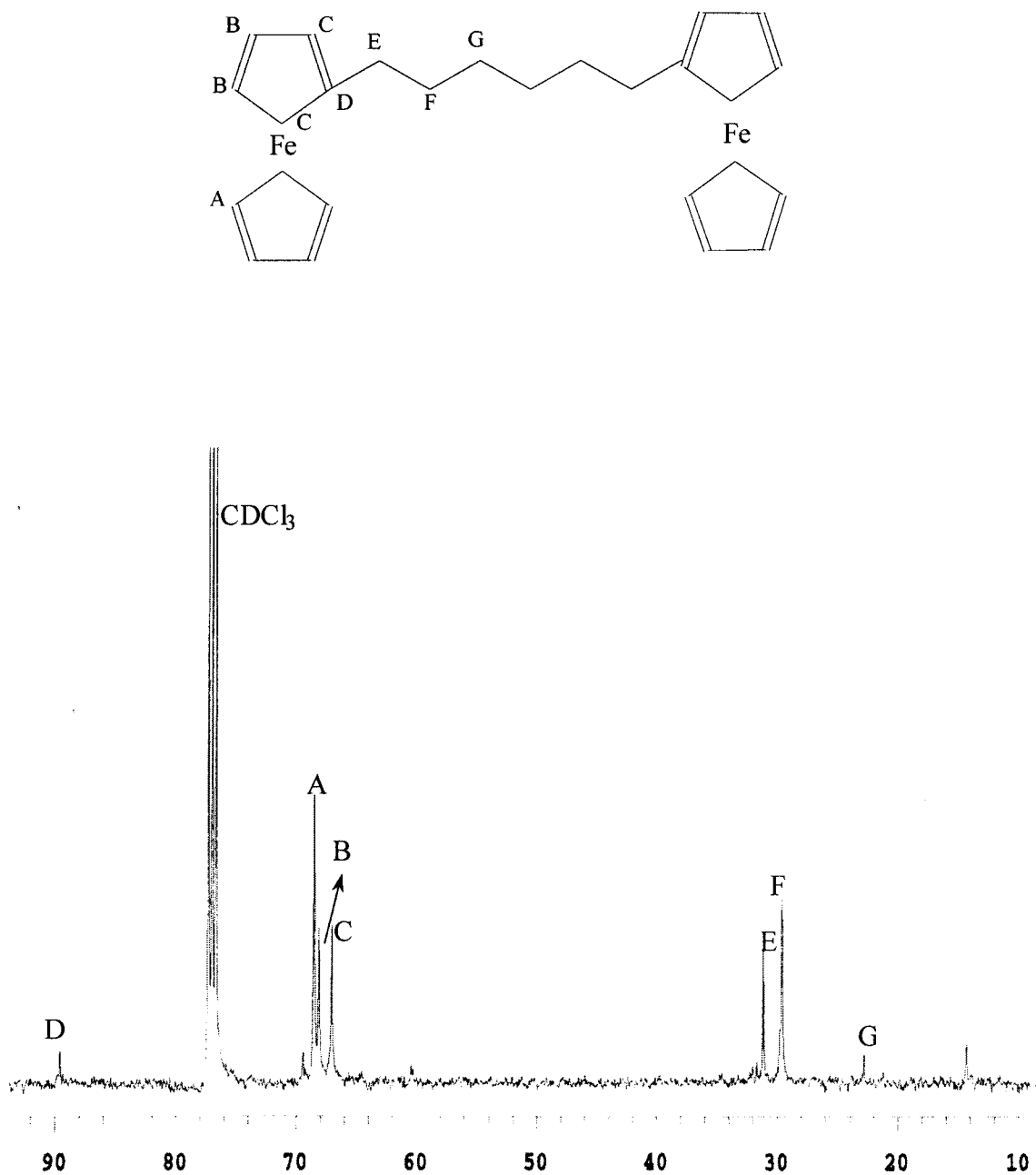


Figure 2.14: ^{13}C NMR spectrum of 1,6-diferrocenylhexane

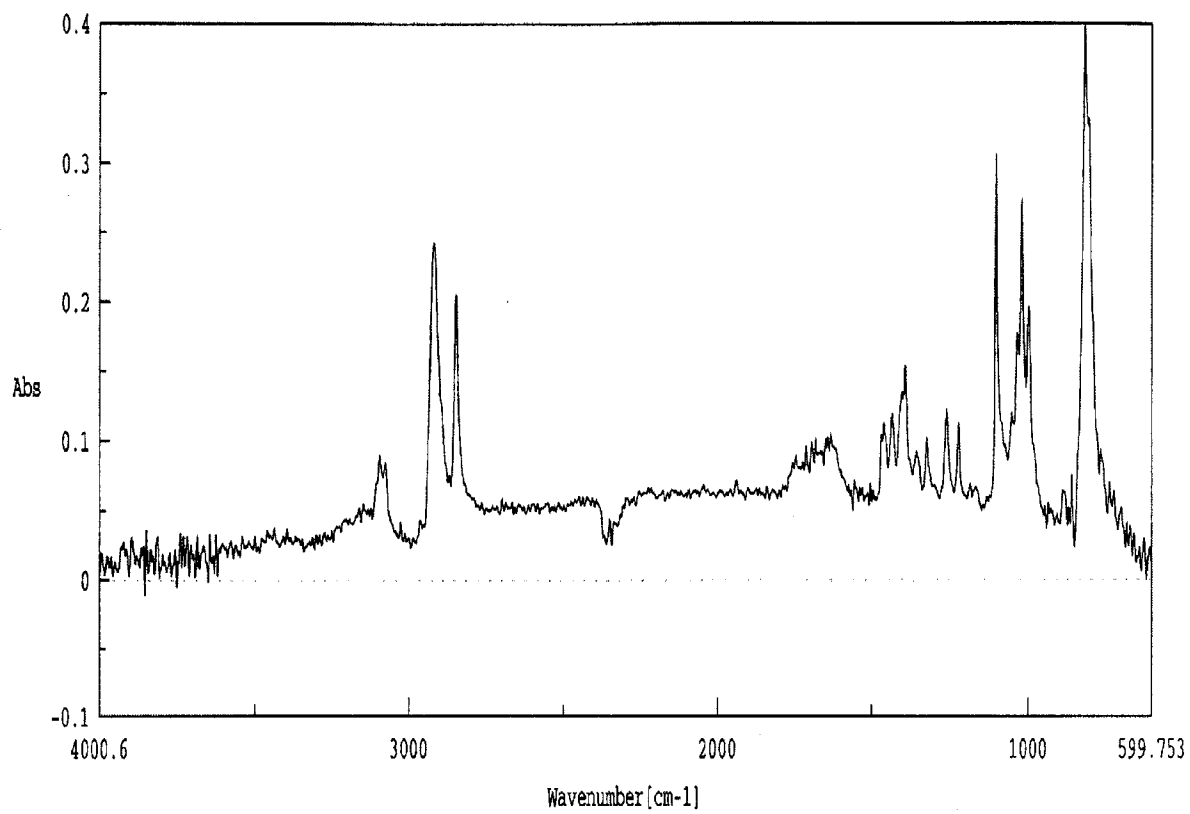


Figure 2.15: IR spectrum of 1,6-diferrocenylhexane

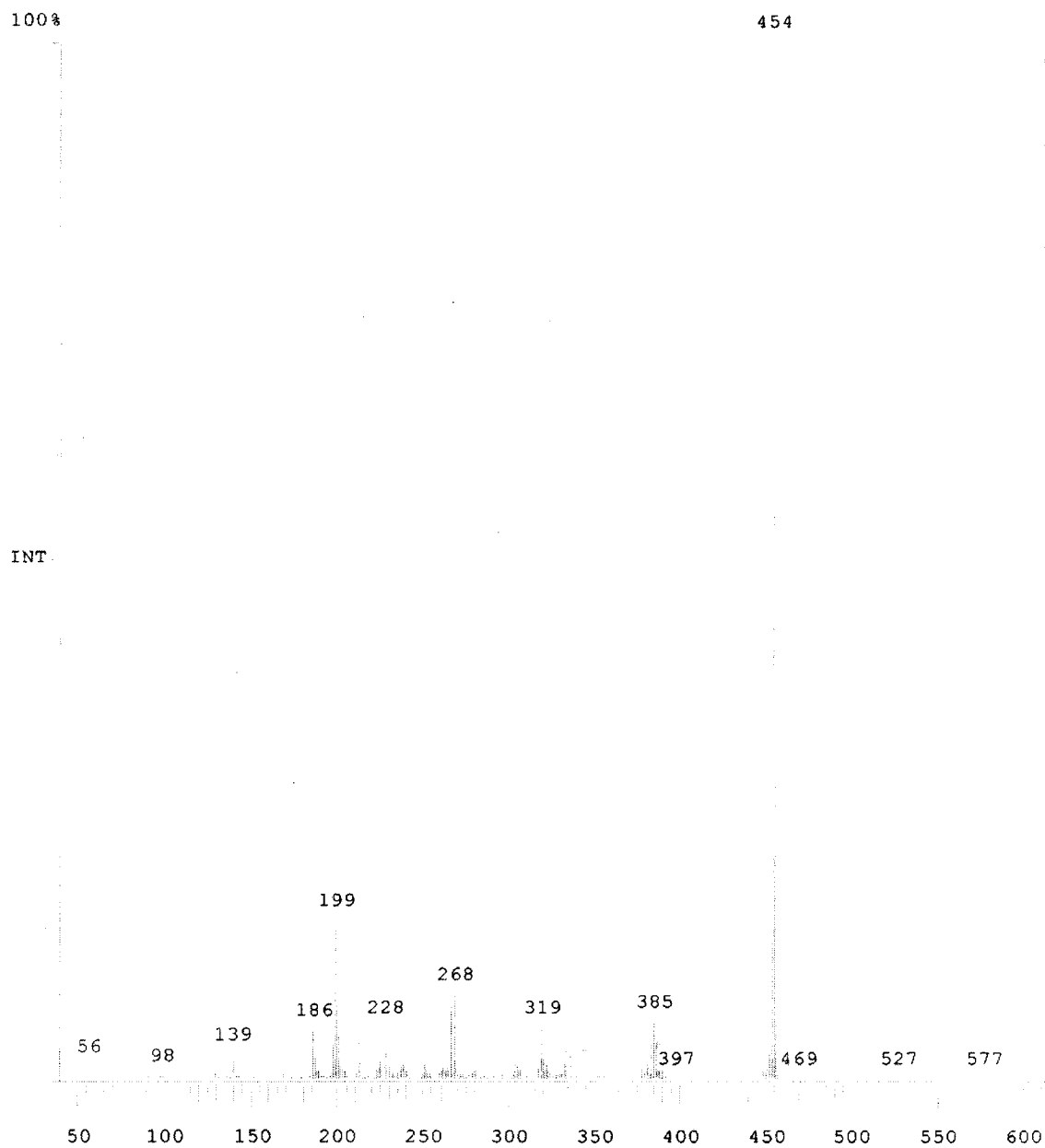
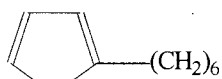


Figure 2.16: Mass spectrum of 1,6-diferrocenylhexane

Table 2.3

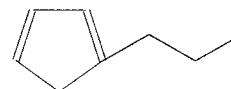
Assigned Fragments from 1,6-diferrocenylhexane Mass Spectrum

Fragments

Fe



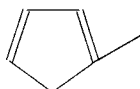
268 m/z



Fe



228 m/z



Fe



199 m/z



Fe



186 m/z

Characterization of 1,6-diferrocenylhexane-1-one

The ^1H NMR spectrum of 1,6-diferrocenylhexane is shown in Figure 2.17. The three peaks close to one another and the furthest upfield were assigned to the methylene protons on the three inner carbons in the bridge. The innermost protons showed a broad triplet at 1.408 ppm (peak F) while the adjacent protons were triplets at 1.555 ppm (peak G) and 1.725 ppm (peak E). Peak E was shifted downfield due to the carbonyl. The two protons adjacent to the top alkyl substituted Cp ring demonstrated a chemical shift of 2.347 ppm (peak H) while the peak at 2.695 ppm (peak D) was assigned to the protons closest to the carbonyl. The top Cp ring protons attached to the six carbon chain two and three bonds away, were evident in the spectrum at 4.073 ppm (peak J) and 4.050 ppm (peak I). The two intense singlets at 4.102 ppm (peak K) and 4.192 ppm (peak A) were attributed to the protons on the bottom Cp rings. Peak A was shifted downfield slightly because of the proximity to the carbonyl. The protons located on the top Cp ring that are two and three bonds away from the carbonyl display chemical shifts at 4.777 ppm (peak C) and 4.487 ppm (peak B), respectively.

The ^{13}C NMR spectrum of 1,6-diferrocenylhexane-1-one is shown in Figure 2.18. The methylene carbon two bonds away from the carbonyl was the peak furthest upfield at 25.700 ppm (peak G). The peak at 30.722 ppm (peaks H and I) was assigned to the next two carbons in the methylene bridge. The peaks were superimposed on one another due to the similar environment of each carbon. The next peak at 32.361 ppm (peak J) is due to the carbon one bond away from the ferrocene. The carbon adjacent to the carbonyl was shifted downfield the most, with respect to the other carbons in the bridge at 40.896 ppm (peak F). Figure 2.19 is an expanded view of the ^{13}C NMR spectrum from 65-95

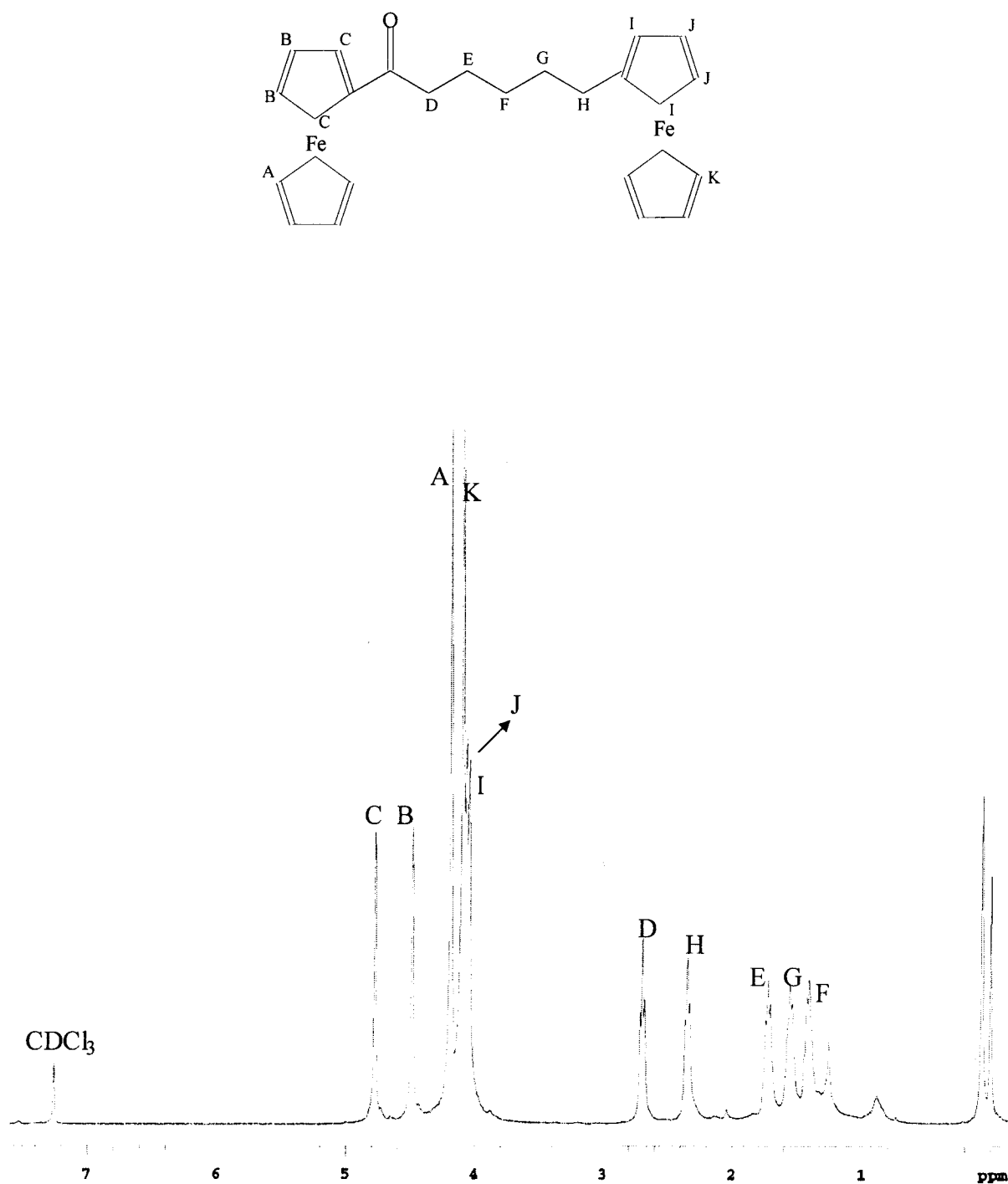


Figure 2.17: ^1H NMR spectrum of 1,6-diferrocenylhexane-1-one

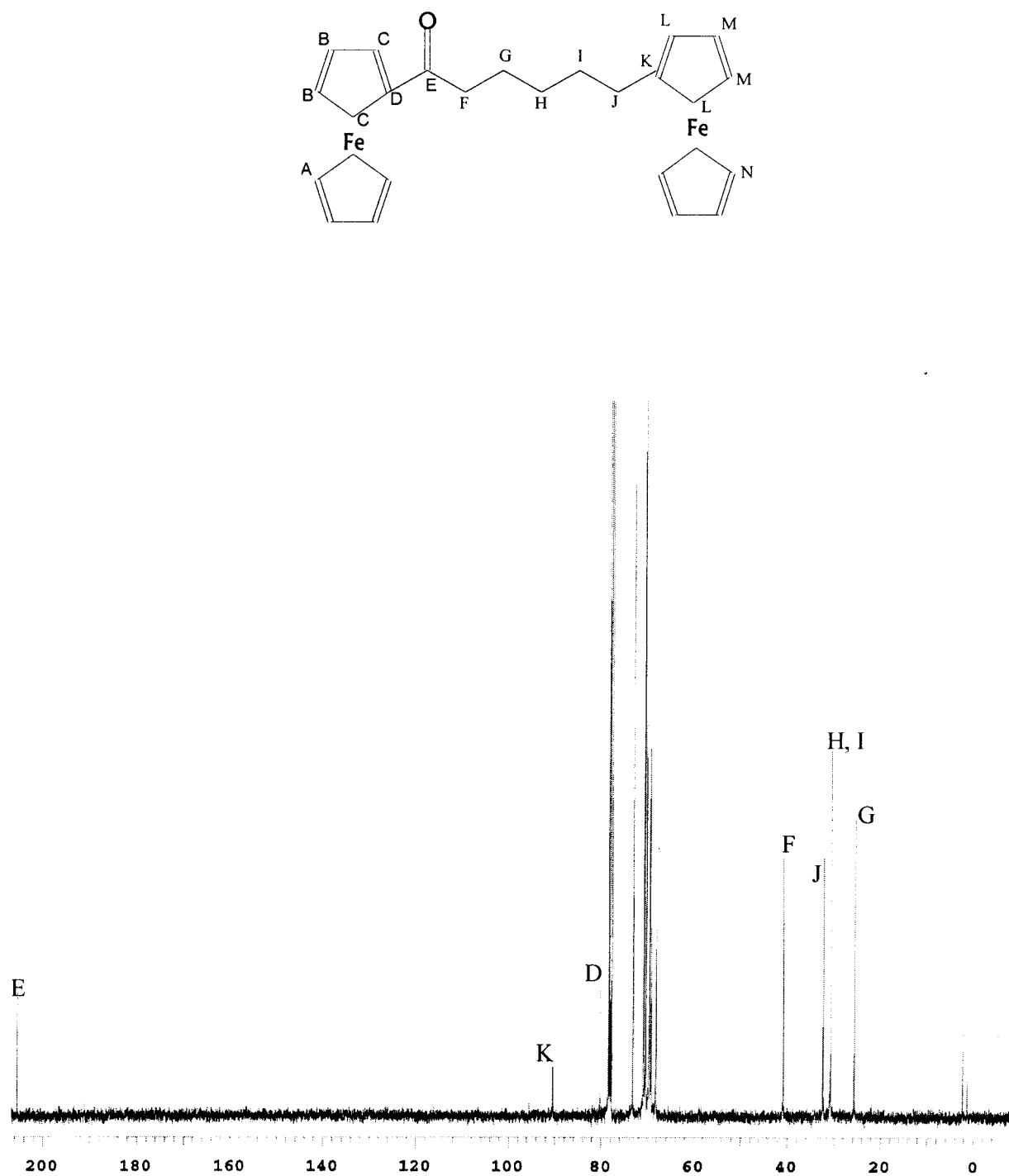


Figure 2.18: ^{13}C NMR spectrum of 1,6-diferrocenylhexane-1-one

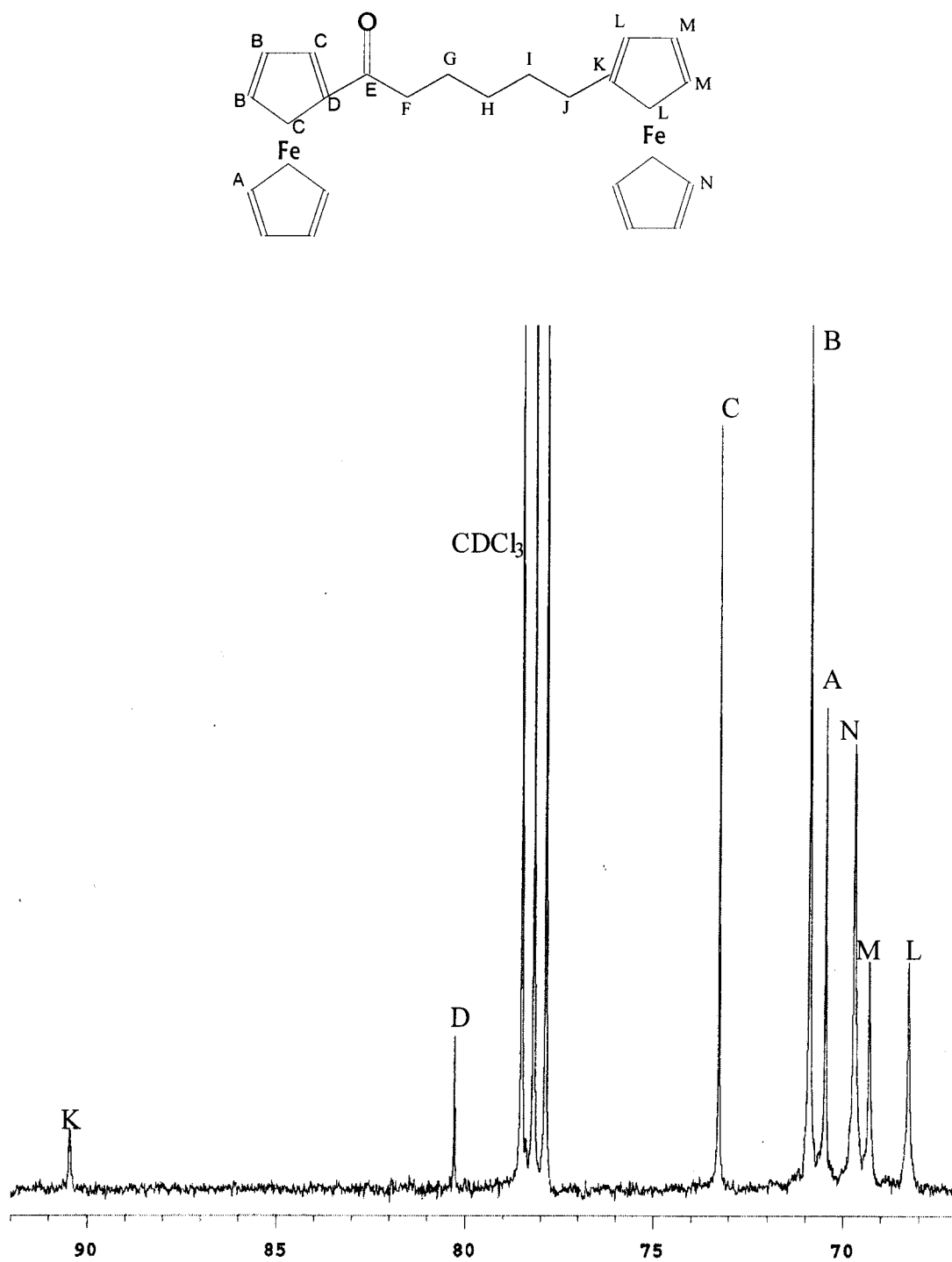


Figure 2.19: ^{13}C NMR spectrum close up from 65-95 ppm of 1,6-diferrocenylhexane-1-one

ppm. The top Cp carbons on the ferrocene attached to the methylene bridge are located at 68.278 ppm (peak L) and 69.325 ppm (peak M). The carbons closest to the electron donating methylene bridge are shifted upfield (peak L) more than the adjacent carbons in the ring (peak M). The carbons in the bottom alkyl substituted Cp ring appear at 69.711 ppm (peak N). The bottom Cp ring carbons attached to the carbonyl display a chemical shift of 70.478 ppm (peak A) downfield with respect to the other bottom Cp ring carbons. The top Cp ring carbons three bonds away from the carbonyl occur at 70.895 ppm (peak B) and two bonds away occur at 73.277 ppm (peak C). The carbon in the top Cp ring attached directly to the carbonyl carbon is located at 80.280 ppm (peak D). The other Cp ring carbon attached to the methylene bridge is downfield at 90.462 ppm (peak K). The carbonyl carbon is easily seen at 205.403 ppm (peak E).

The IR spectrum of 1,6-diferrocenylhexane-1-one is shown in Figure 2.20. The carbonyl stretching peak is easily assigned at 1675.84 cm^{-1} . Methylene stretching occurs at 2927.89 cm^{-1} from the six-carbon chain bridging the two ferrocenes and methylene bending is assigned at 1454.06 cm^{-1} . Single carbon-carbon bond bending and stretching in the methylene bridge, occurs at 1248.68 cm^{-1} and 1103.57 cm^{-1} , respectively. Stretching from the CH groups is assigned to the peak at 1025.46 cm^{-1} . Unsaturated carbon bond stretching from the Cp ring carbons is assigned to the 817.67 cm^{-1} peak.

The mass spectrum obtained from direct probe analysis displayed the parent ion peak at 468 m/z and is shown in Figure 2.21. The loss of a bottom Cp ring is evident from the peak at 403 m/z. The remaining fragments were assigned and can be seen in Table 2.4.

Characterization of 6-(diferrocenylhexanycarbonyl)pentanebromide

The NMR assignments for 6-(diferrocenylhexanycarbonyl)pentanebromide were

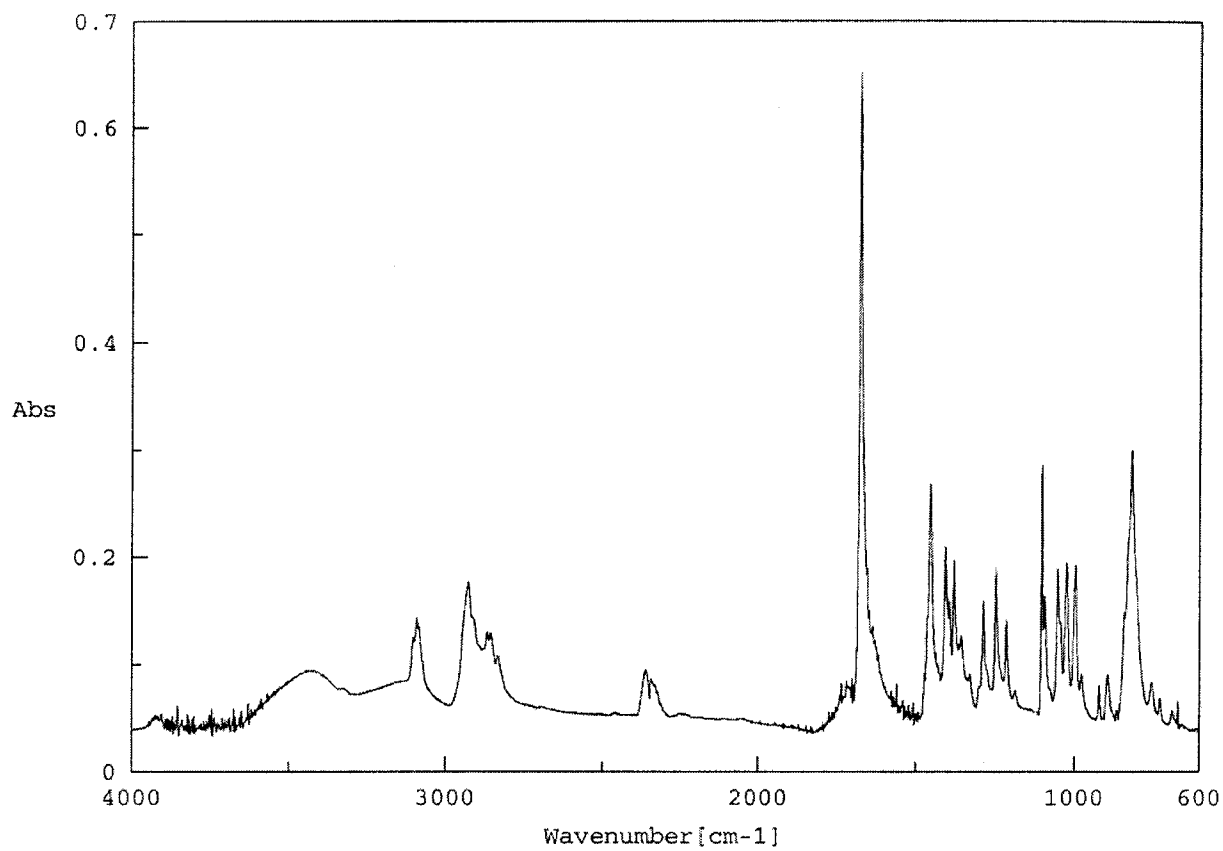


Figure 2.20: IR spectrum of 1,6-diferrocenylhexane-1-one

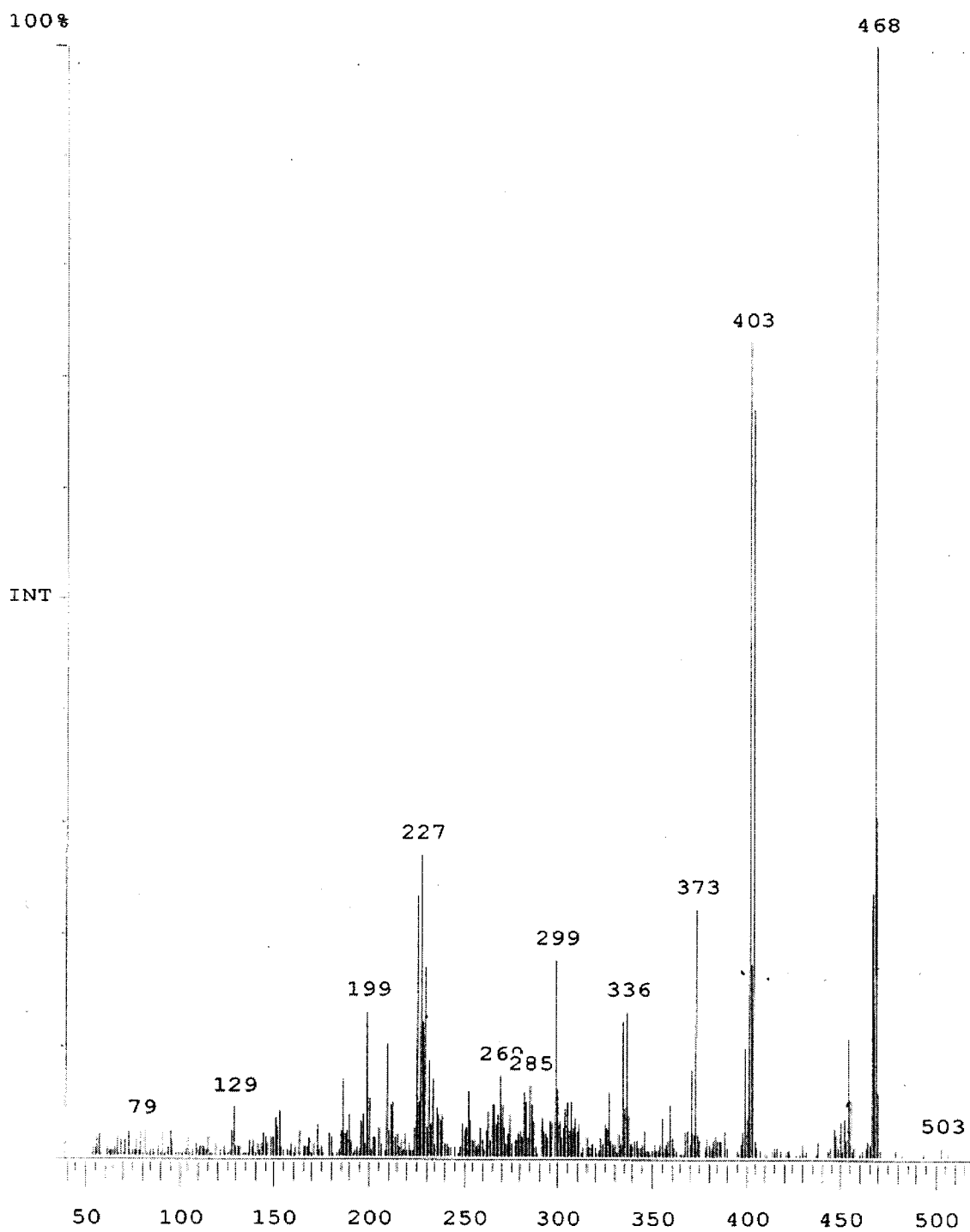
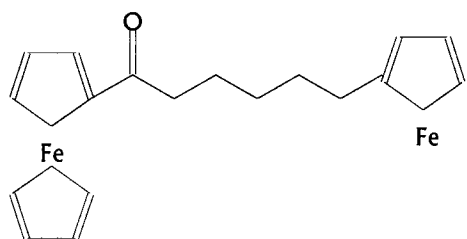


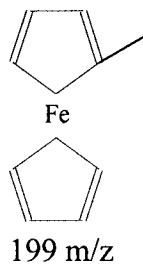
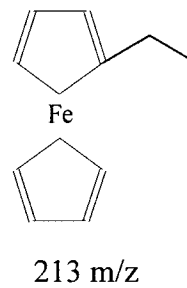
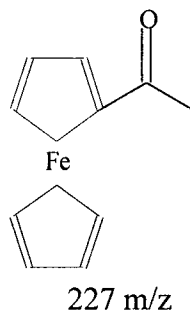
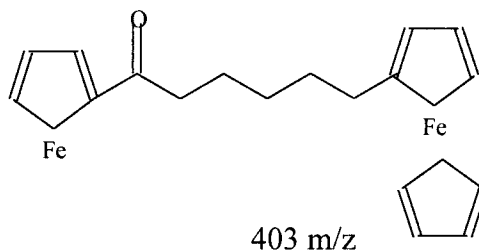
Figure 2.21: Mass spectrum of 1,6-diferrocenylhexane-1-one

Table 2.4

Assigned Fragments from 1,6-diferrocenylhexane-1-one Mass Spectrum

Fragments

or



somewhat difficult due to the broad multiplets upfield. A portion of the ^1H NMR from 1.2 ppm to 2.0 ppm is shown in Figure 2.22. The four center methylene protons in the bridge joining the two ferrocenes show a chemical shift of 1.254 ppm (peak F). The broad triplet at 1.352 ppm (peak M) was assigned to the methylene protons three away from the bromine. The methylene protons two bonds away from the top Cp rings display a broad multiplet at 1.540 ppm (peak E). The multiplet downfield at 1.731 ppm (peak L) is associated with protons located two carbons away from the carbonyl on the bottom ring. The pentet at 1.928 ppm (peak N) are the protons two away from the bromine. Shown in Figure 2.23 is the ^1H NMR spectrum from 2.3 ppm to 3.5 ppm. The broad triplet at 2.300 ppm (peak D) are the protons adjacent to the top Cp rings. The protons neighboring the carbonyl show a chemical shift downfield at 2.786 ppm (peak K) due to the electron withdrawing nature of the oxygen. The protons adjacent to the bromine are shifted downfield at 3.445 ppm (peak O). The remaining ^1H NMR spectrum is shown in Figure 2.24. The protons that are on the top Cp ring of the ferrocene with no substitution on the bottom ring, show characteristic chemical shifts values of 4.029 ppm (peak C) and 4.047 ppm (peak B). The intense signal at 4.086 ppm (peak A) are the five protons on the bottom unsubstituted Cp ring. The other top Cp ring protons are shifted downfield slightly because of the carbonyl substituted on the lower ring at 4.111 ppm (peaks G and H). The protons on the bottom Cp ring attached to the carbonyl that are two and three bonds away are at 4.589 ppm (peak J) and 4.408 ppm (peak I), respectively. These chemical shift values are similar in nature to those reported for 1,6-diferrocenylhexane and 1,6-diferrocenylhexane-1-one.

A portion of the ^{13}C NMR spectrum of 6-(diferrocenylhexan-1-yl)pentane-

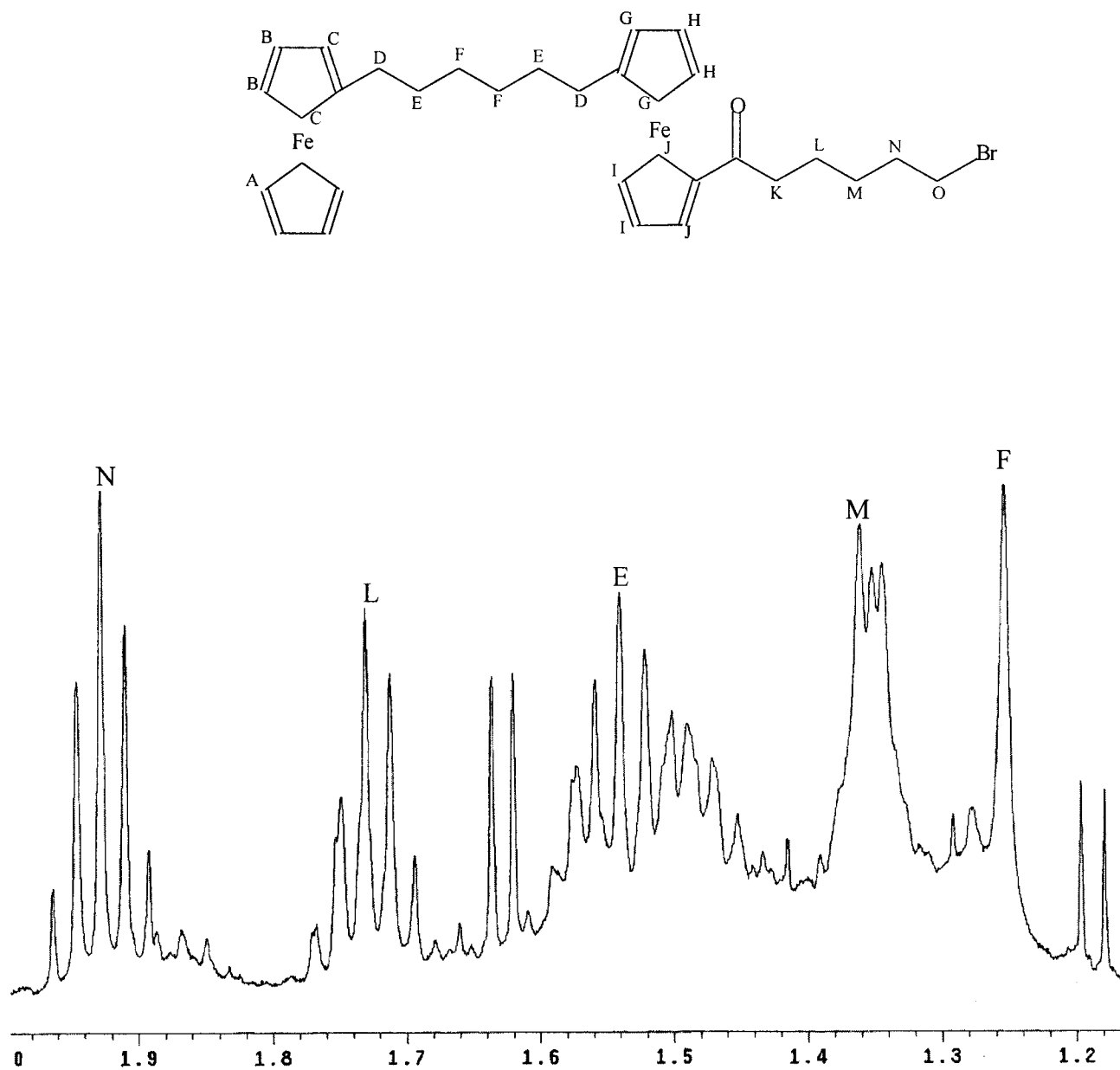


Figure 2.22: ^1H NMR spectrum close up from 1.2-2.0 ppm of 6-(diferrocenylhexanoyl)pentanebromide

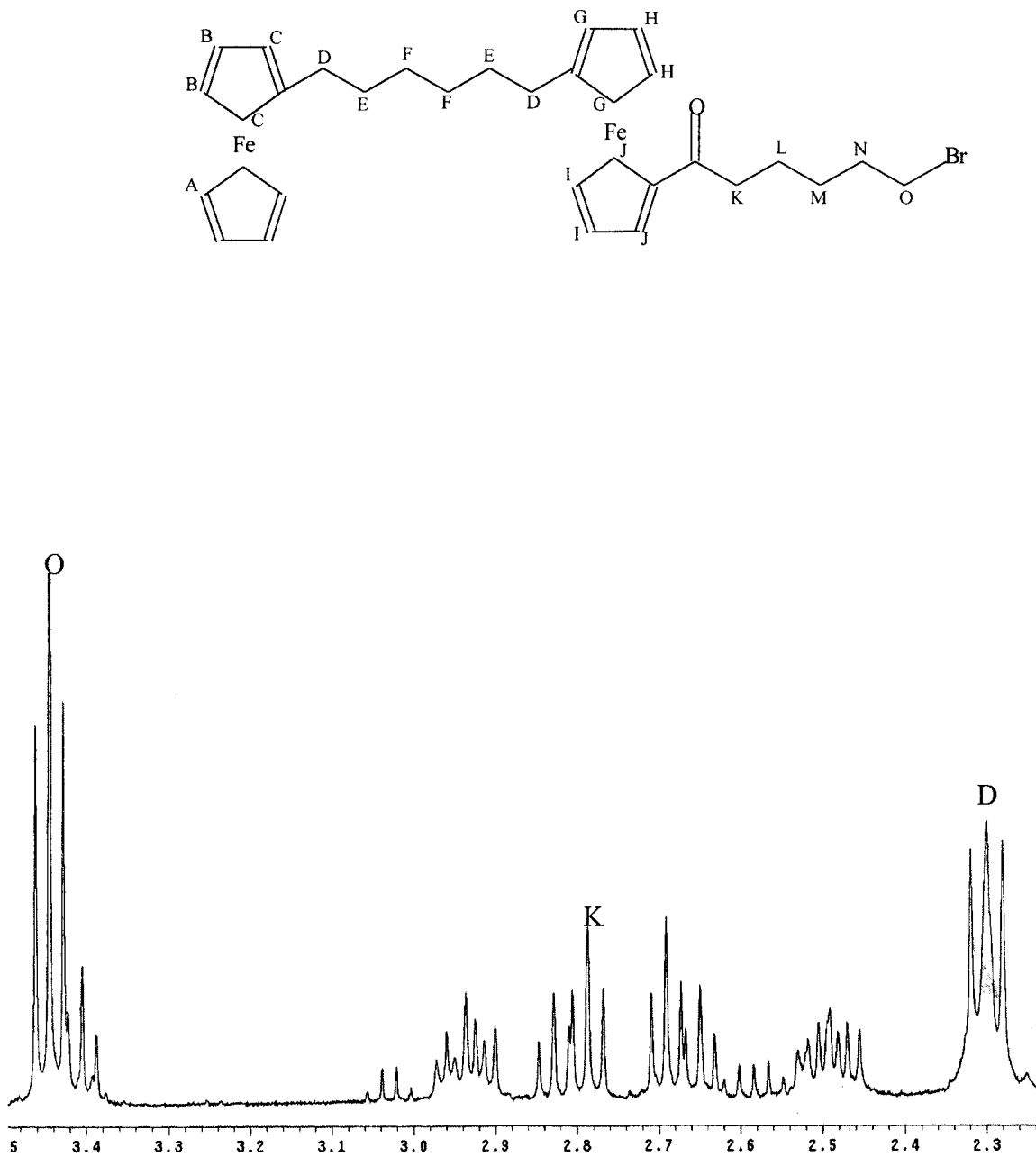


Figure 2.23: ^1H NMR spectrum close up from 2.3-3.5 ppm of 6-(diferrocenylhexanoyl)pentanebromide

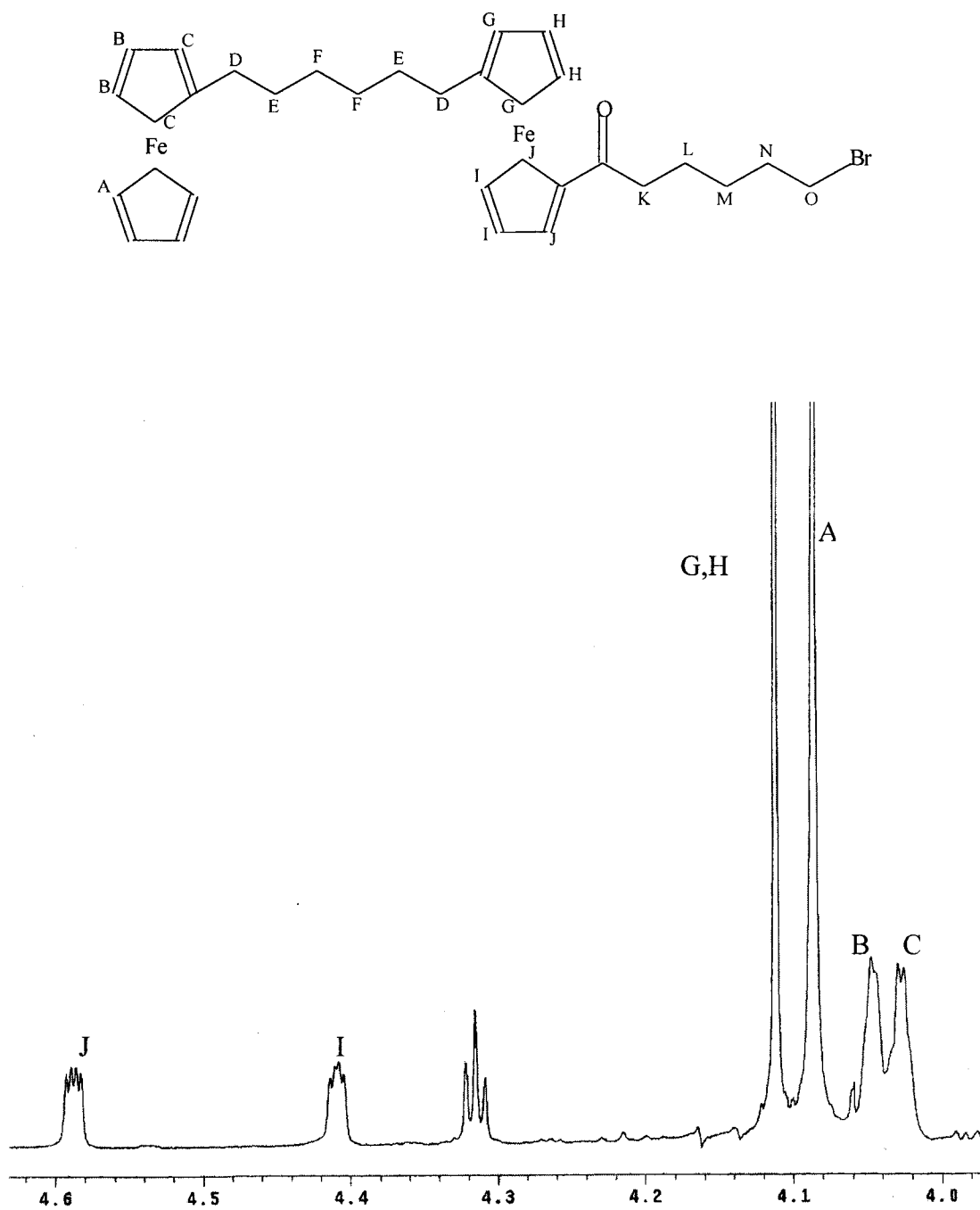


Figure 2.24: ^1H NMR spectrum close up from 4.0-4.6 ppm of 6-(diferrocenylhexanoyl)pentanebromide

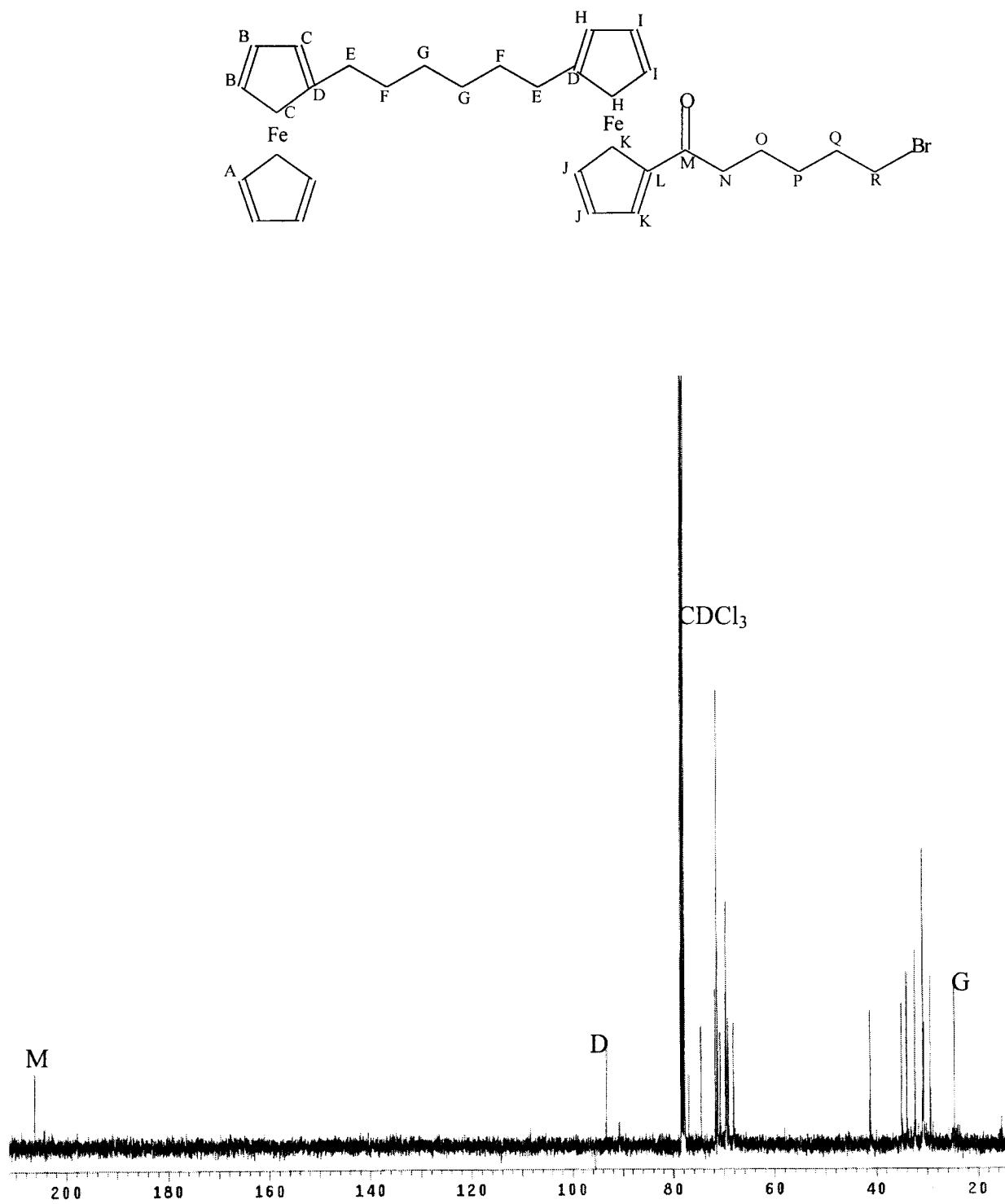


Figure 2.25: ^{13}C NMR spectrum of 6-(diferrocenylhexanoyl)pentanebromide

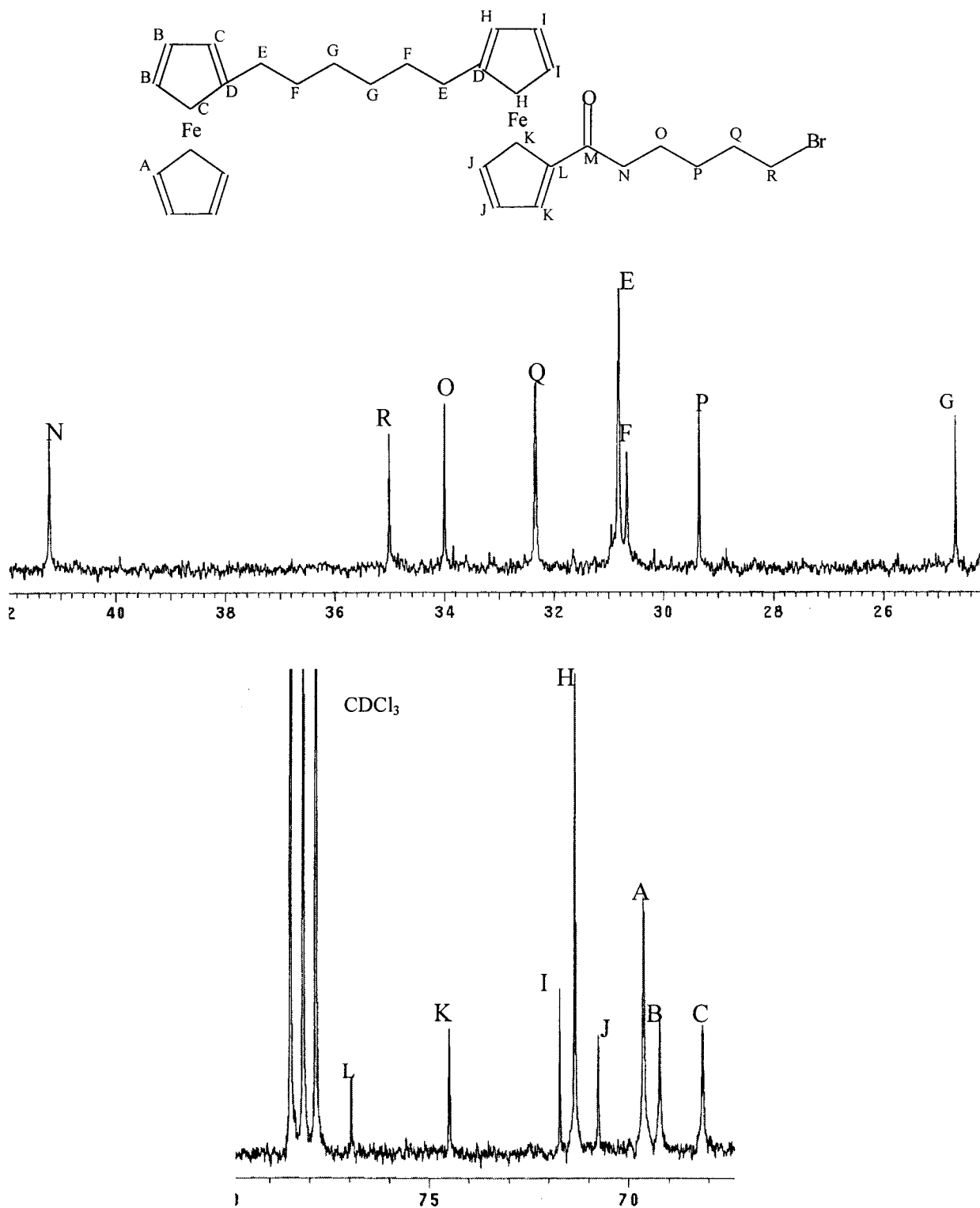


Figure 2.26: ^{13}C NMR spectrum close up from 25-42 ppm and 65-80 ppm
6-(diferrocenylhexanylcarbonyl)pentanebromide

chemical shift of 76.949 ppm (peak L). The remaining carbons are seen in Figure 2.25 of the full carbon spectrum. The carbons in the top Cp rings to which the methylene bridge is attached are located at 93.231 ppm (peak D). The carbonyl carbon is easily assigned at 206.260 ppm (peak M).

The mass spectrum of 6-(diferrocenylhexanoyl)pentanebromide is shown in Figure 2.27. The parent ion peak is located at 630 m/z with the next major peak at 550 m/z, indicating the loss of the bromine. The loss of the bottom Cp ring, common in these types of compounds, was assigned to 485 m/z. The loss of the entire six-carbon chain on the bottom Cp ring was evident from the peak at 453 m/z. The remaining fragments are assigned in Table 2.5.

Characterization of 6-(diferrocenylhexanoyl)pentanethiol

The ^1H NMR spectrum of 6-(diferrocenylhexanoyl)pentanethiol in CDCl_3 is located in Figure 2.28. The peak assignments were similar to those of the 6-(diferrocenylhexanoyl)pentanebromide. The proton attached to the thiol was difficult to assign because of the various overlapping multiplets located upfield. The peak at 1.240 ppm (peak P) was assigned to the proton attached to the sulfur. The four protons on the bridging inner methylene carbons were near peak P at 1.258 ppm (peak F). The broad triplet at 1.353 ppm (peak M) was assigned to the inner protons that are located three bonds away from the thiol. Protons that are two bonds away from the thiol, demonstrate a chemical shift of 1.501 ppm (peak N). The protons that are located on the carbons in the methylene bridge that are two bonds away from the top Cp rings are located at 1.573 ppm (peak E). The chemical shift located at 1.742 ppm (peak L) were assigned to the protons two bonds away from the carbonyl. The broad triplet at 2.294

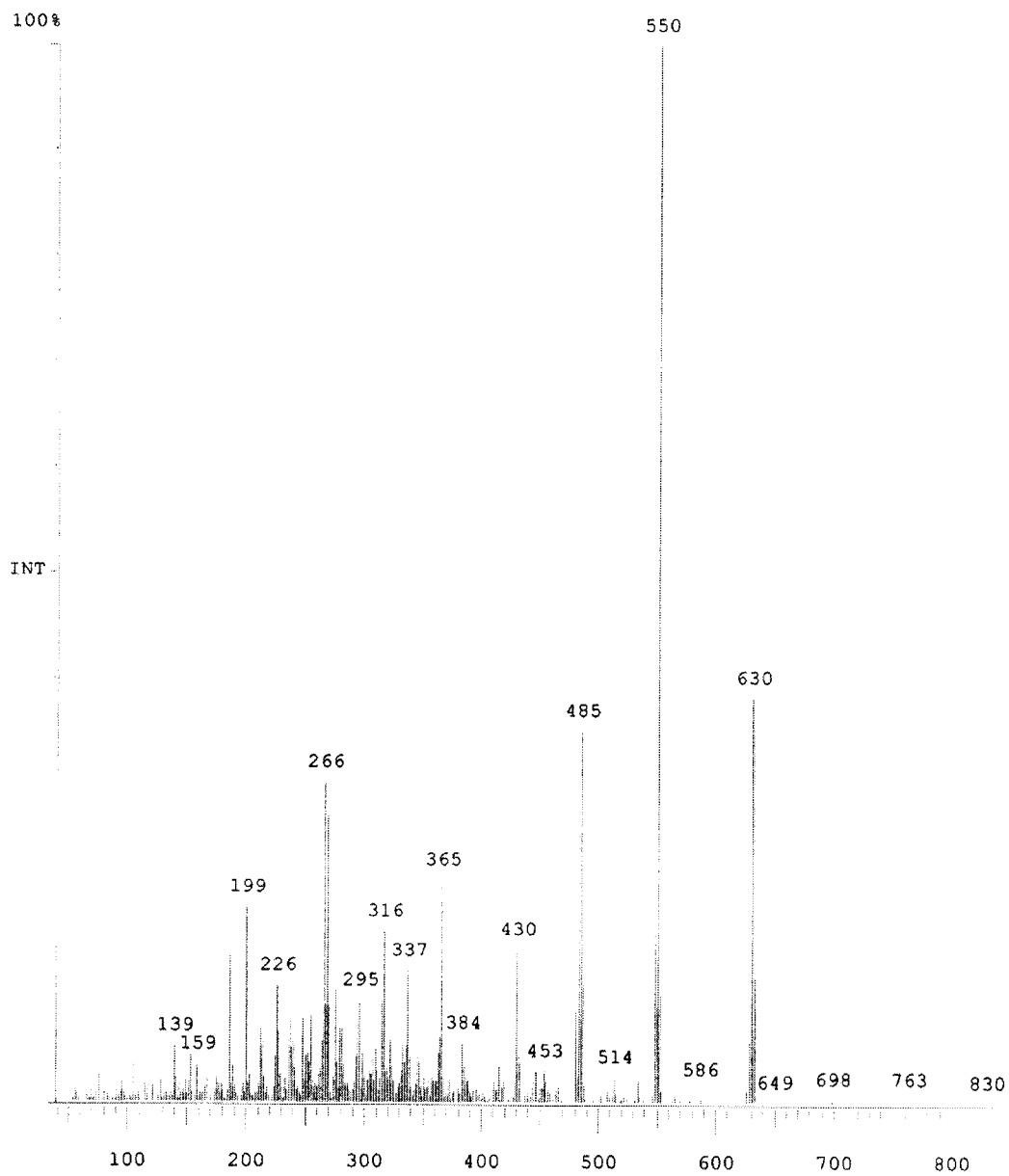
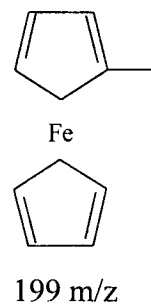
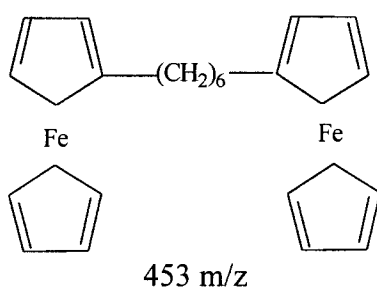
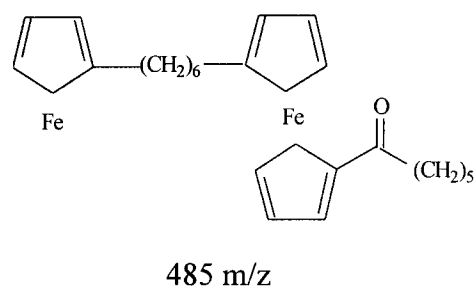
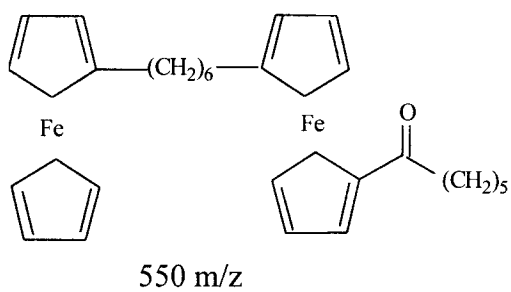


Figure 2.27: Mass spectrum of 6-(diferrocenylhexanylecarbonyl)pentanebromide

Table 2.5

**Assigned Fragments from 6-(diferrocenylhexanycarbonyl)pentanebromide
Mass Spectrum****Fragments**

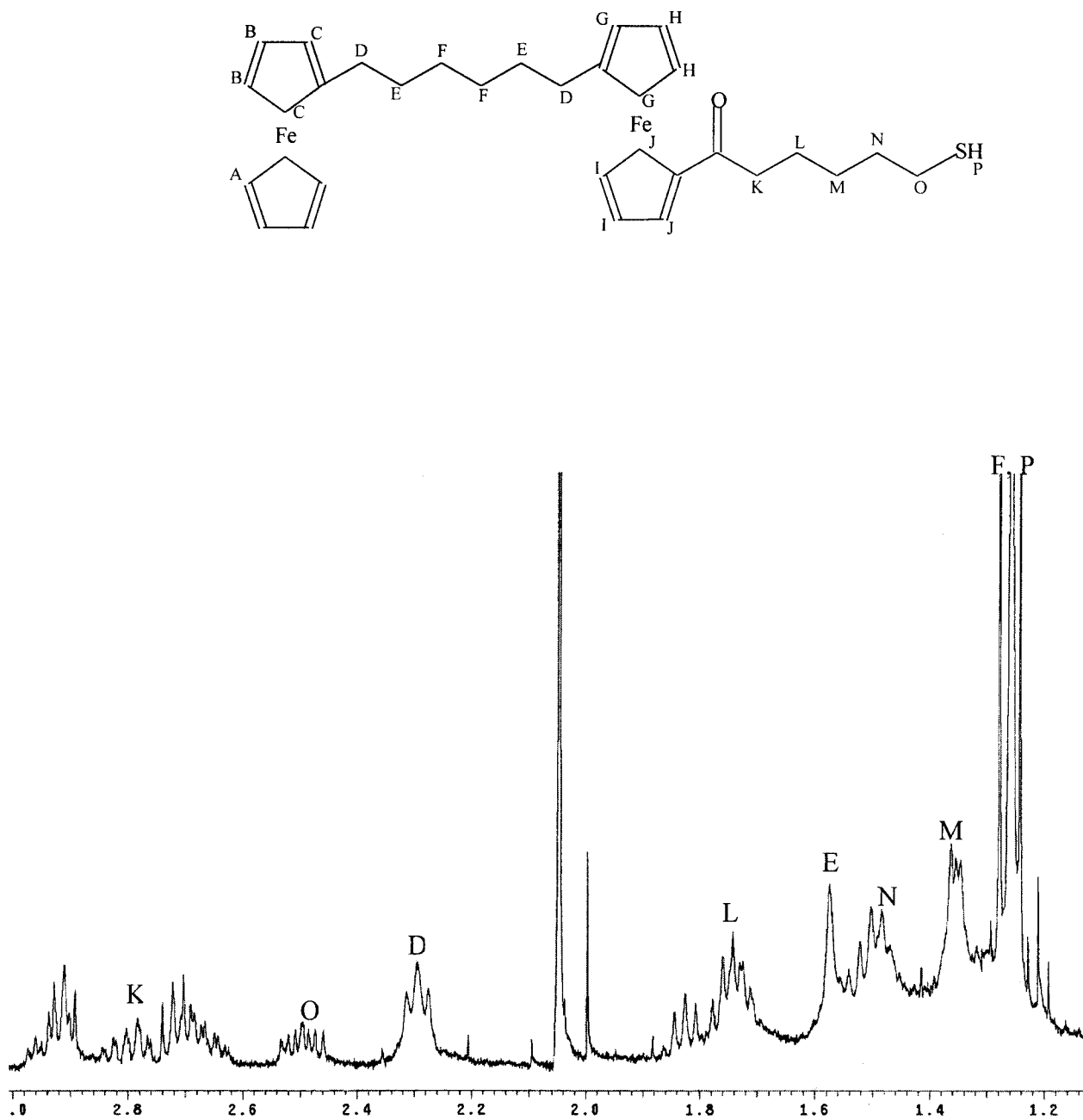


Figure 2.28: ^1H NMR spectrum close up from 1.2-3.0 ppm of 6-(diferrocenylhexanoyl)pentanethiol

ppm (peak D) were result of the protons in the methylene bridge adjacent to the top Cp rings. The multiplet at 2.494 ppm (peak O) were the protons on the carbon next to the sulfur. Another broad multiplet downfield at 2.784 ppm (peak K) is assigned to the protons adjacent to the carbonyl. Figure 2.29 is a close up from 1.2 ppm to 3.0 ppm to expand the various multiplets. The top Cp ring protons of the ferrocene without bottom ring substitution were characteristic at 4.039 ppm (peak C) and 4.062 ppm (peak B). The strong singlet at 4.094 ppm (peak A) were the five protons on the bottom Cp ring. The other top Cp ring protons were located at 4.130 ppm (peak G) and 4.147 ppm (peak H). Peak H was shifted downfield because of the proximity of the carbonyl. The remaining four protons on the bottom substituted Cp ring that are two and three bonds away from the carbonyl are located at 4.595 ppm (peak J) and 4.404 ppm (peak I), respectively.

The ^{13}C NMR spectrum in CDCl_3 of 6-(diferrocenylhexanylcarbonyl)pentanethiol is shown in Figure 2.30. The innermost carbons in the methylene bridge are located the farthest upfield at 25.108 ppm (peak G). The carbon three bonds away from the thiol are downfield at 29.630 ppm (peak P) while the carbon two bonds away from the thiol was assigned at 30.434 ppm (peak Q). The remaining carbons in the methylene bridge that are one and two bonds away from the top Cp rings are at 30.821 ppm (peak E) and 30.677 ppm (peak F), respectively. The carbon two bonds away from the carbonyl was shifted downfield to 31.595 ppm (peak O) relative to the previous chemical shifts due to the carbonyl. The carbon that is directly attached to the thiol displays a chemical shift of 33.181 ppm (peak R). The carbon adjacent to the carbonyl was significantly shifted downfield from the other peaks at 41.306 ppm (peak N). The carbons in the top Cp ring

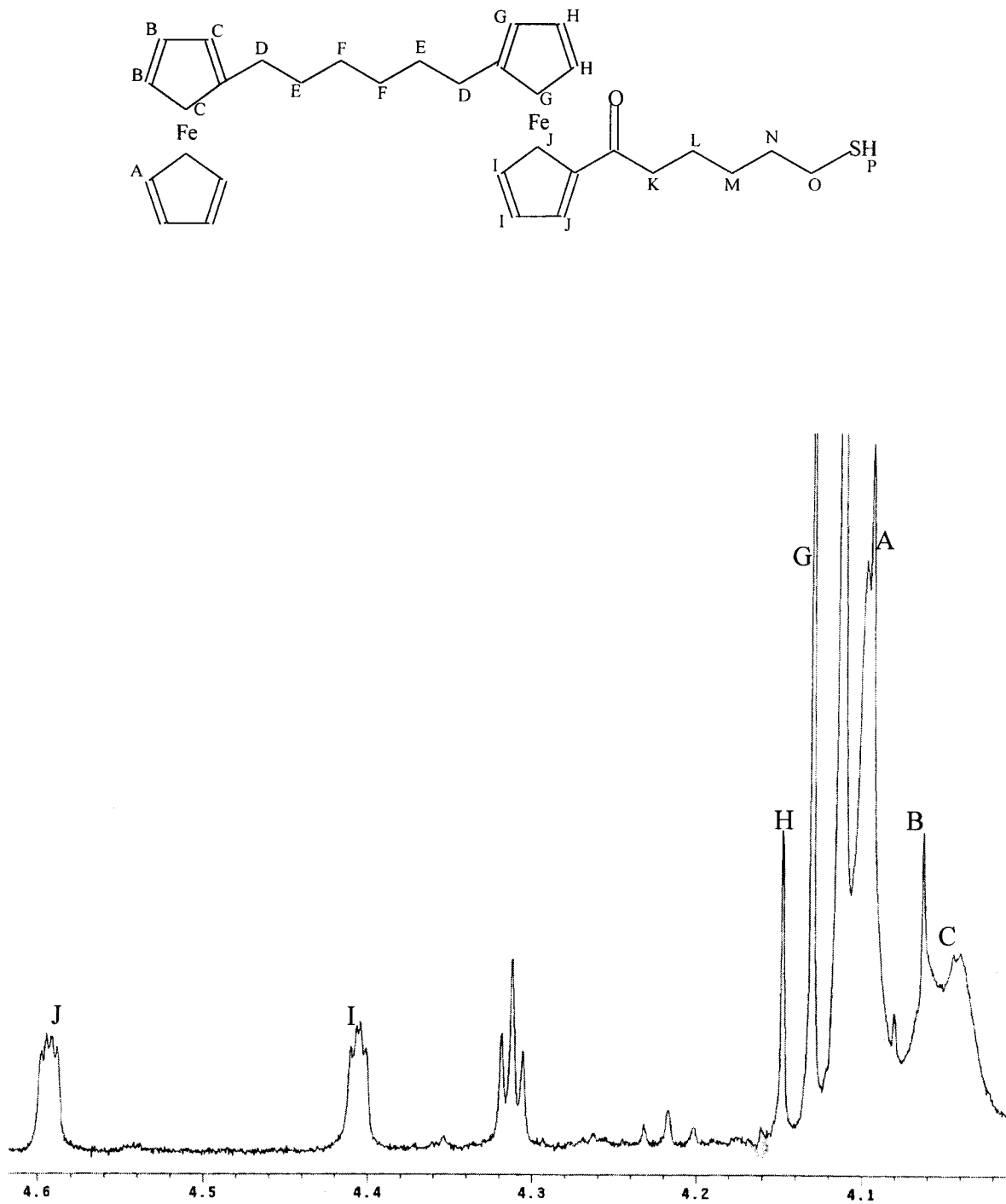


Figure 2.29: ^1H NMR spectrum close up from 4.0-4.6 ppm of 6-(diferrocenylhexanecarbonyl)pentanethiol

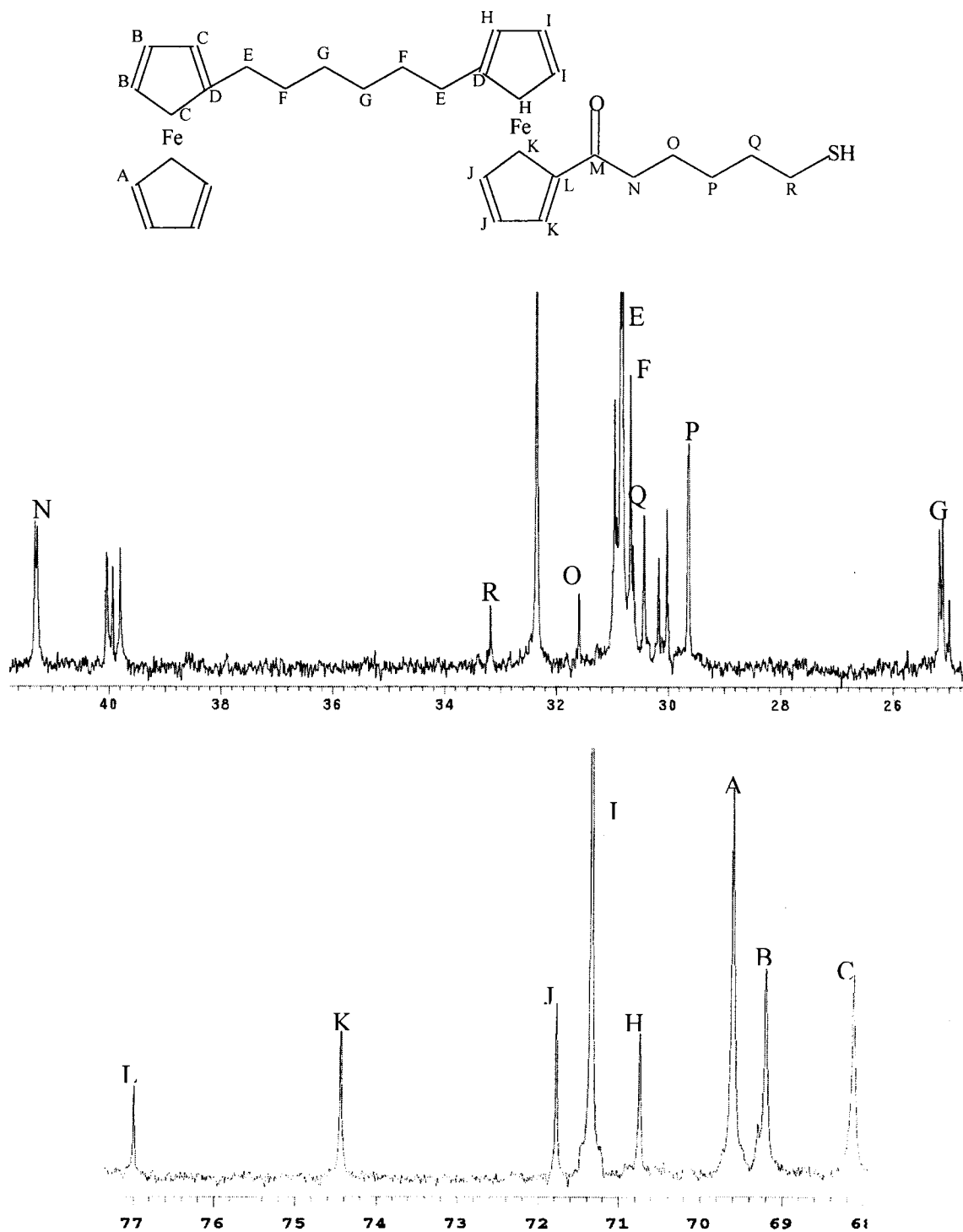


Figure 2.30: ^{13}C NMR spectrum close up from 25-45 ppm and 68-77 ppm of 6-(diferrocenylhexanoyl)pentanethiol

demonstrated characteristic chemical shifts at 68.126 ppm (peak C) and 69.203 ppm (peak B), which are two and three bonds away from the methylene bridge, respectively. The strong signal at 69.605 ppm (peak A) is assigned to the five carbons on the bottom unsubstituted Cp ring. The other top Cp ring carbons with bottom ring substitution are located at 70.743 ppm (peak H) and 71.350 ppm (peak I). The chemical shifts at 71.783 ppm (peak J) and 74.438 ppm (peak K) are due to the carbons in the bottom ring that are three and two bonds away from the carbonyl, respectively. The carbon in the Cp ring attached directly to the carbonyl is located at 76.995 ppm (peak L). Figure 2.31 displays the entire ^{13}C NMR spectrum in which the remaining two peaks were assigned. The low intensity signal at 93.193 ppm (peak D) was assigned to the carbons in the top Cp rings to which the methylene bridge is directly attached. The distinct peak at 206.420 ppm (peak M) was easily assigned to the carbonyl carbon.

The mass spectrum of 6-(diferrocenylhexanylcarbonyl)pentanethiol in CH_2Cl_2 is shown in Figure 2.32 and the parent ion peak is easily seen at 584 m/z. The other major fragment at 453 m/z results from the loss of the entire six-carbon thiol chain substituted on the lower Cp ring. The remaining fragments are assigned in Table 2.6.

Conclusion

The synthetic pathway as presented in Figure 2.1 was carried out to produce the final thiolated product, 6-(diferrocenylhexanylcarbonyl)pentanethiol. The intermediate products in all the reactions were purified via column chromatography and fully characterized using ^1H , ^{13}C NMR, IR, and mass spectrometry. The ^1H and ^{13}C NMR values were similar to those reported in the literature.¹⁻⁴ The reported spectroscopic data verifies that all the products were synthesized, as expected. For three of the compounds,

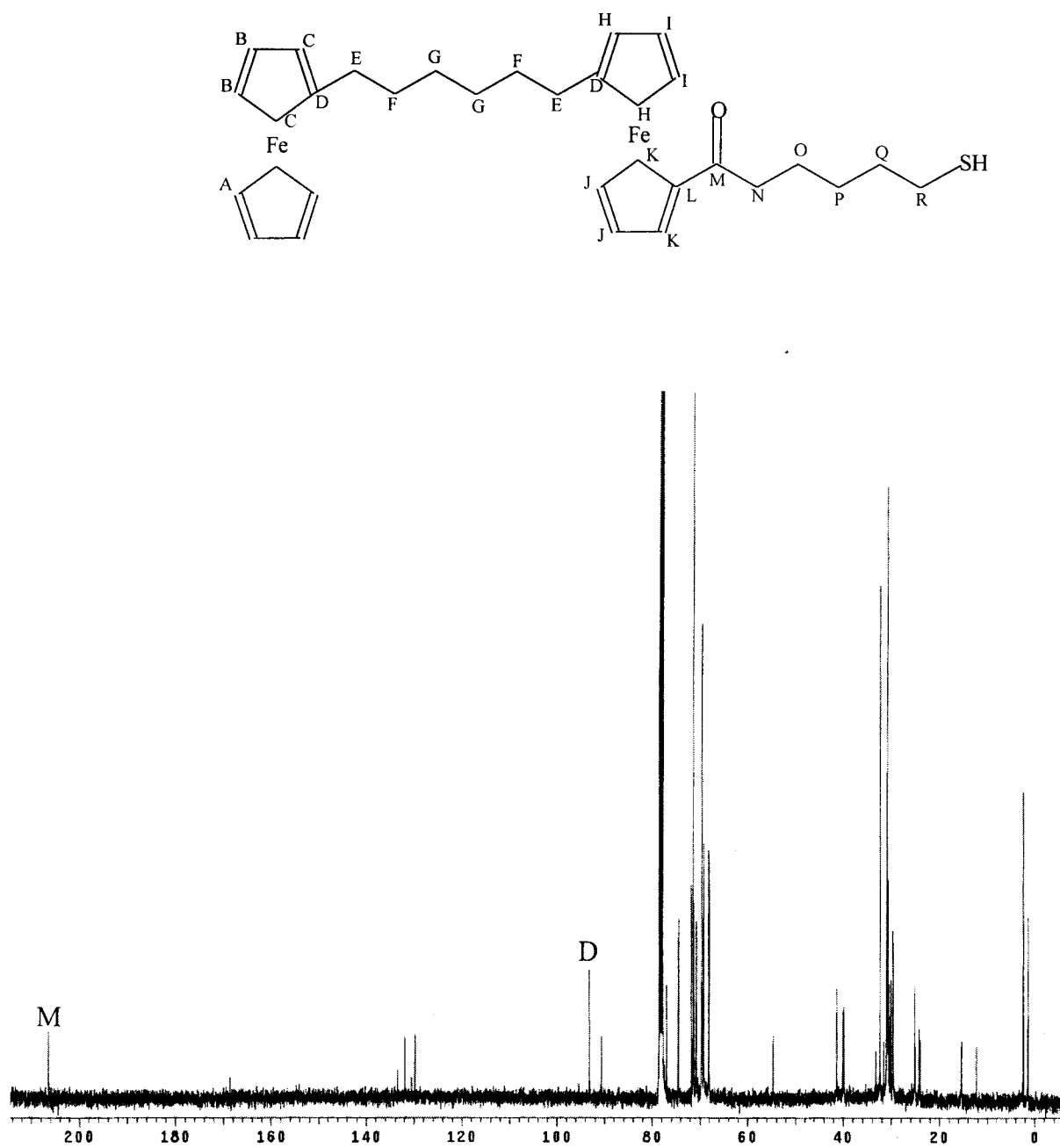


Figure 2.31: ^{13}C NMR spectrum of 6-(diferrocenylhexanoyl)pentanethiol

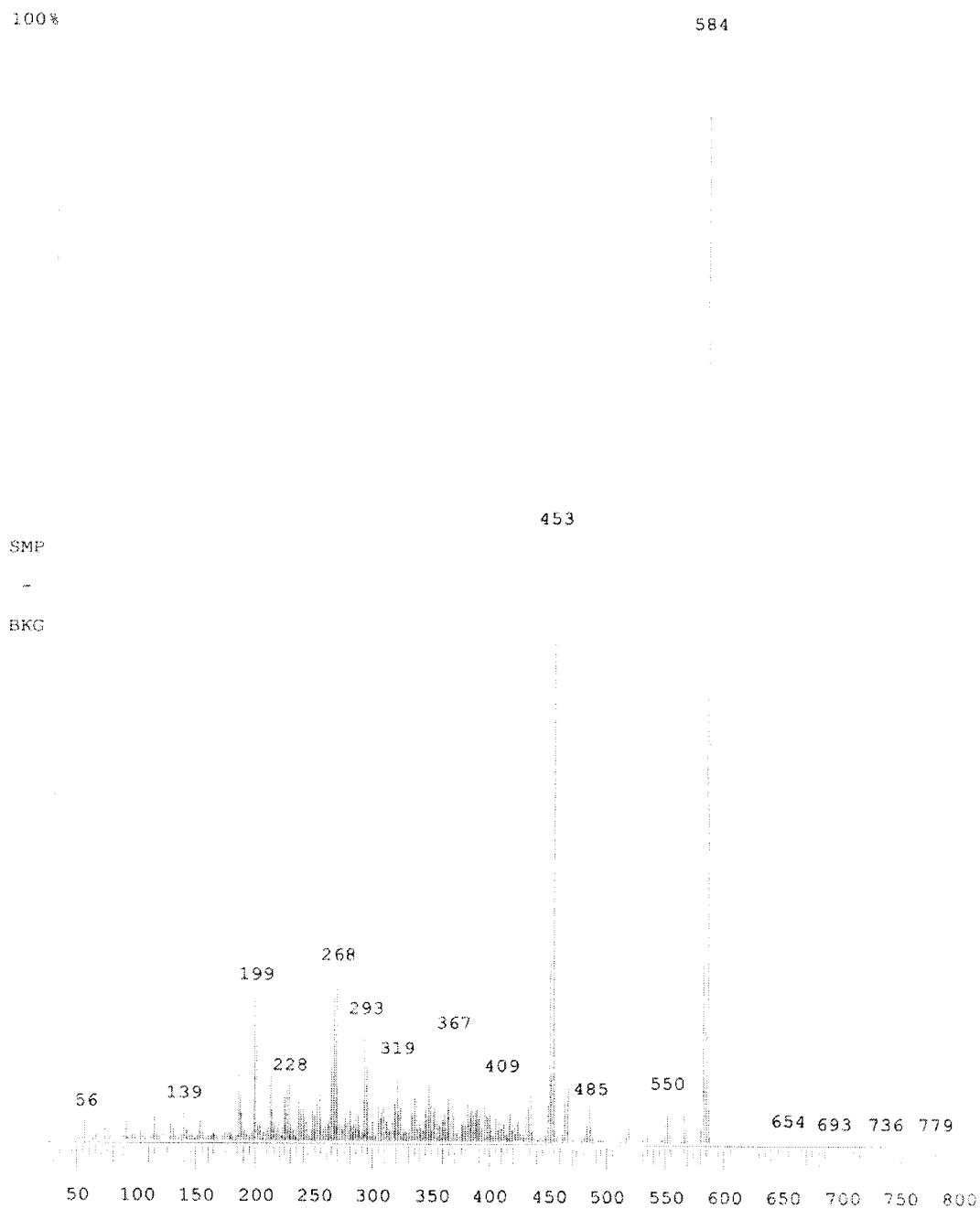
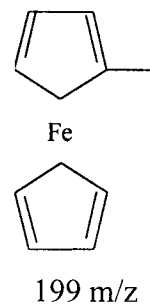
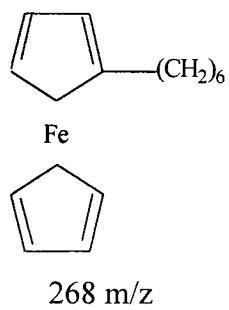
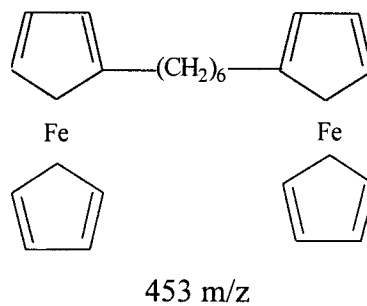
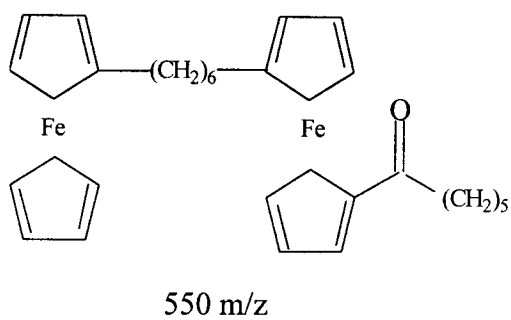


Figure 2.32: Mass spectrum of 6-(diferrocenylhexanylcarbonyl)pentanethiol

Table 2.6

Assigned Fragments from 6-(diferrocenylhexanylcarbonyl)pentanethiol Mass Spectrum**Fragments**

the spectroscopic data was further supported by single crystal X-ray diffraction analysis.

REFERENCES

1. Chidsey, C.E.D. *Science*, **1991**, 251, 919-921.
2. Chidsey, C.E.D., Bertozzi, C.R., Putvinski, T.M., Muijsce, A.M. *J. Am. Chem. Soc.*, **1990**, 112, 4301-4306.
3. Creager, S.E., Rowe, G.K. *J. Electroanal. Chem.* **1997**, 420, 291-299.
4. Rowe, G.K., Creager, S.E. *Langmuir*, **1991**, 7, 2307-2312.
5. Hickman, J.J., Ofer, D., Zou, C., Wrighton, M.S., Laibinis, P.E., Whitesides, G.M. *J. Am. Chem. Soc.*, **1991**, 1128-1132.

CHAPTER THREE

X-RAY CRYSTALLOGRAPHY

Single crystals of 1,6-diferrocenylhexane-1,6-dione, 1-ferrocenylcarbonyl-2-ferrocenylcyclopentene, and 1,6-diferrocenylhexane were obtained and X-ray crystallography was used to deduce their respective solid state structures. The crystal data for 1,6-diferrocenylhexane-1,6-dione and 1,6-diferrocenylhexane produced similar results, each belonging to the monoclinic crystal system and having space groups of $P2(1)/n$ and $P2(1)/c$, respectively.

An unexpected chiral reaction product, 1-ferrocenylcarbonyl-2-ferrocenylcyclopentene, was the most interesting. Single crystal X-ray crystallographic analysis demonstrated that the molecule contained two chiral centers. The BASF parameter was approximately 50%, indicating a nearly racemic mixture. The X-ray data for 1-ferrocenylcarbonyl-2-ferrocenylcyclopentene indicates that the triclinic crystal has a space group of $P1$.

Experimental

All crystals were grown via kinetically controlled solvent evaporation. Both the 1,6-diferrocenylhexane-1,6-dione and 1-ferrocenylcarbonyl-2-ferrocenylcyclopentene crystals precipitated out of a 75%/25% hexane/ethyl acetate solvent system, while the 1,6-diferrocenylhexane precipitated out of a an 80%/20% hexane/ethyl acetate solvent system. The crystals were examined under an optical microscope to observe their quality before mounting. The crystals that were chosen had clean edges with no observable cracks throughout. Crystals were mounted on the end of a glass capillary using epoxy.

Attempts were made to obtain X-ray quality single crystals of 1,6-diferrocenylhexane-1-one, but proved to be unsuccessful.

Instrumentation

The X-ray diffraction data for 1,6-diferrocenylhexane-1,6-dione was collected on a Siemens P4 Single Crystal Diffractometer equipped with a serial detector utilizing molybdenum radiation ($\text{MoK}\alpha$, $\lambda=0.71073 \text{ \AA}$). A copper radiation source could not be utilized because the iron centers in ferrocene absorb the emitted radiation. XSCANS operating program from Bruker (Siemens) was used for data collection in which photo, hemisphere, fractional and thin shell searches were performed. Prior to theta:2theta data collection, Bravais lattice and Laue group symmetry routines determined crystal lattice symmetry and refined the unit cell parameters. Empirical psi scans corrected for absorption in the collected data. Structure refinement was done with Bruker SHELXTL-XP and SHELXTL-XL software packages, and tables of bond lengths, angles and structure factors were prepared using SHELXTL-XCIF.

Data collection for the remaining two crystals, 1-ferrocenylcarbonyl-2-ferrocenylcyclopentene and 1,6-diferrocenylhexane, was done on a Bruker SMART 1k CCD Single Crystal Diffractometer at Kent State University. Mo radiation ($\text{MoK}\alpha$, $\lambda=0.71073 \text{ \AA}$) in a 2.4 kW fine focus sealed tube was used as the source of the X-rays. The crystals of these two compounds were much smaller in size, and data collection would have taken significantly more time with a serial detector than with a Bruker CCD detector. A complete sphere of data was collected in 1800 frames, with an exposure time of ten seconds per frame and a width of 0.30° with ω scans. Approximately 450 frames of data were used to determine the initial unit cell parameters. Bravais lattice and Laue

symmetry were determined in a program called SMART that refined the final cell. All of the generated data was integrated in SAINT and empirical absorption correction was performed using SADABS (written by George Sheldrick, University of Göttingen, 1996). Structure refinement and results for both structures were also done using the Bruker SHELXTL-XP, SHELXTL-XL, and SHELXTL-XCIF software package.

X-ray Diffraction Analysis of 1,6-diferrocenylhexane-1,6-dione

Single crystals of 1,6-diferrocenylhexane-1,6-dione were obtained following purification via column chromatography in which the crystals precipitated out of 75%/25% hexane/ethyl acetate. The crystal was centered in the X-ray beam and a twenty-minute rotation photo was obtained. The total number of reflections found was 6669, of which 3072 were unique. Upon completion of data collection, empirical psi-scans were performed to correct for absorption effects, including corrections for absorption by the glass capillary.

Direct Methods structure solution yielded the resulting structure in which all non-hydrogen atoms were assigned anisotropically. All hydrogen atoms were refined isotropically and convergence was achieved for all atomic positions with an R value of 0.1094 for all data. The high symmetry of the molecule produced a monoclinic crystal belonging to the P2(1)/n space group. Crystal structure data and refinement results are shown in Table 3.1. An ORTEP plot of 50% ellipsoids and the unit cell, generated in SHELXTL-XP, of 1,6-diferrocenylhexane-1,6-dione are shown in Figure 3.1 and Figure 3.2, respectively. The bond lengths, angles, and anisotropic and isotropic displacement coordinates as well as the hydrogen coordinates, are found in Tables 3.2 to 3.6.

Table 3.1

Crystal Data and Structure Refinement for 1,6-diferrocenylhexane-1,6-dione

Empirical formula	C ₂₆ H ₂₆ Fe ₂ O ₂
Formula weight	482.17
Temperature	293(2) K
Wavelength	0.71073 Å
Crystal system, space group	Monoclinic, P2(1)/n
Unit cell dimensions	a = 5.7654(5) Å alpha = 90° b = 22.7859(16) Å beta = 101.778(6)° c = 8.2065(5) Å gamma = 90°
Volume	1055.39(13) Å ³
Z, Calculated density	2, 1.517 Mg/m ³
Absorption coefficient	1.395 mm ⁻¹
F(000)	500
Crystal size	0.05 x 0.42 x 0.18 mm
Theta range for data collection	1.79 to 29.99 deg.
Limiting indices	-8 ≤ h ≤ 8, -32 ≤ k ≤ 32, -11 ≤ l ≤ 11
Reflections collected / unique	6669 / 3072 [R(int) = 0.0765]
Completeness to theta = 29.99	100.0 %
Absorption correction	Empirical
Max. and min. transmission	0.5460 and 0.4435
Refinement method	Full-matrix least-squares on F ²
Hydrogen Atom Positions	Refined
Data / restraints / parameters	3072 / 0 / 189
Goodness-of-fit on F ²	0.958
Final R indices [I > 2σ(I)]	R1(F) ^a = 0.0521, wR2(F ²) ^b = 0.1329
R indices (all data)	R1(F) ^a = 0.1094, wR2(F ²) ^b = 0.1779
Extinction coefficient	0.011(3)
Largest diff. peak and hole	0.660 and -0.958 e.Å ⁻³

$${}^a R_1(F) = \frac{\sum ||F_o| - |F_c||}{\sum |F_o|} \text{ with } F_o > 4.0\sigma(F).$$

$${}^b wR_2(F^2) = \frac{[\sum [w(F_o^2 - F_c^2)^2] / \sum [w(F_o^2)^2]]^{1/2}}{\sigma^2(F_o)^2 + (W \cdot P)^2 + T \cdot P}, \text{ where } P = (\text{Max}(F_o^2, 0) + 2F_c^2) / 3, W = 0.1000, \text{ and } T = 0.00.$$

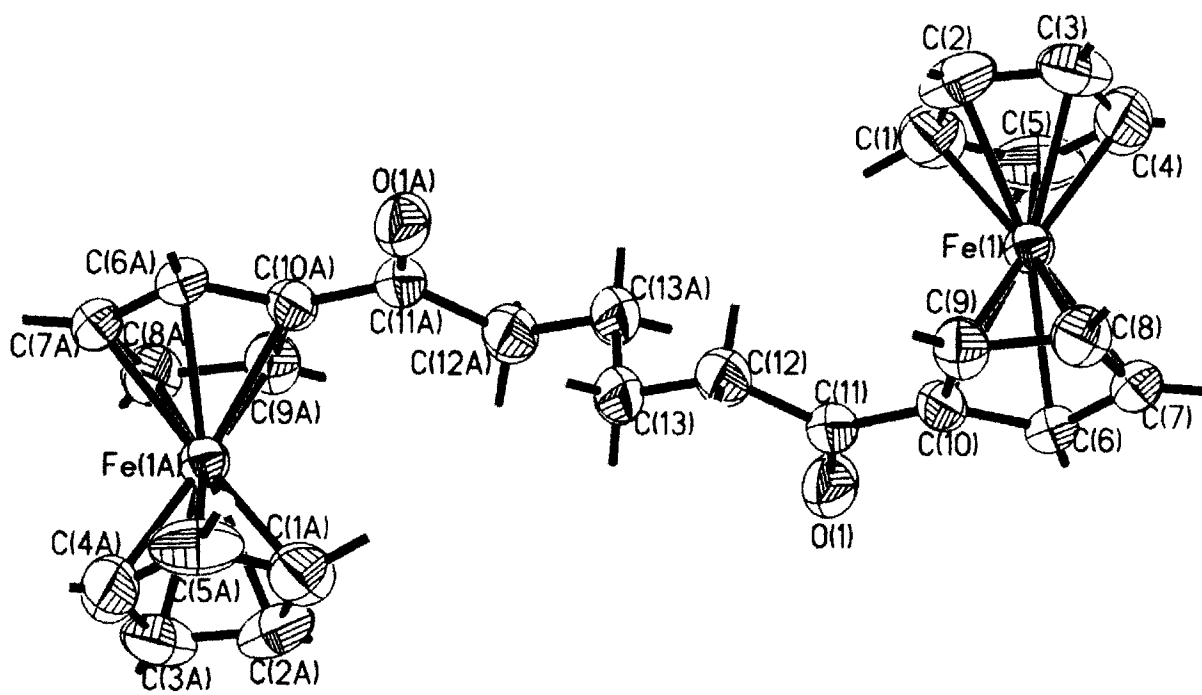


Figure 3.1: ORTEP plot of 1,6-diferrocenylhexane-1,6-dione (50% ellipsoids)

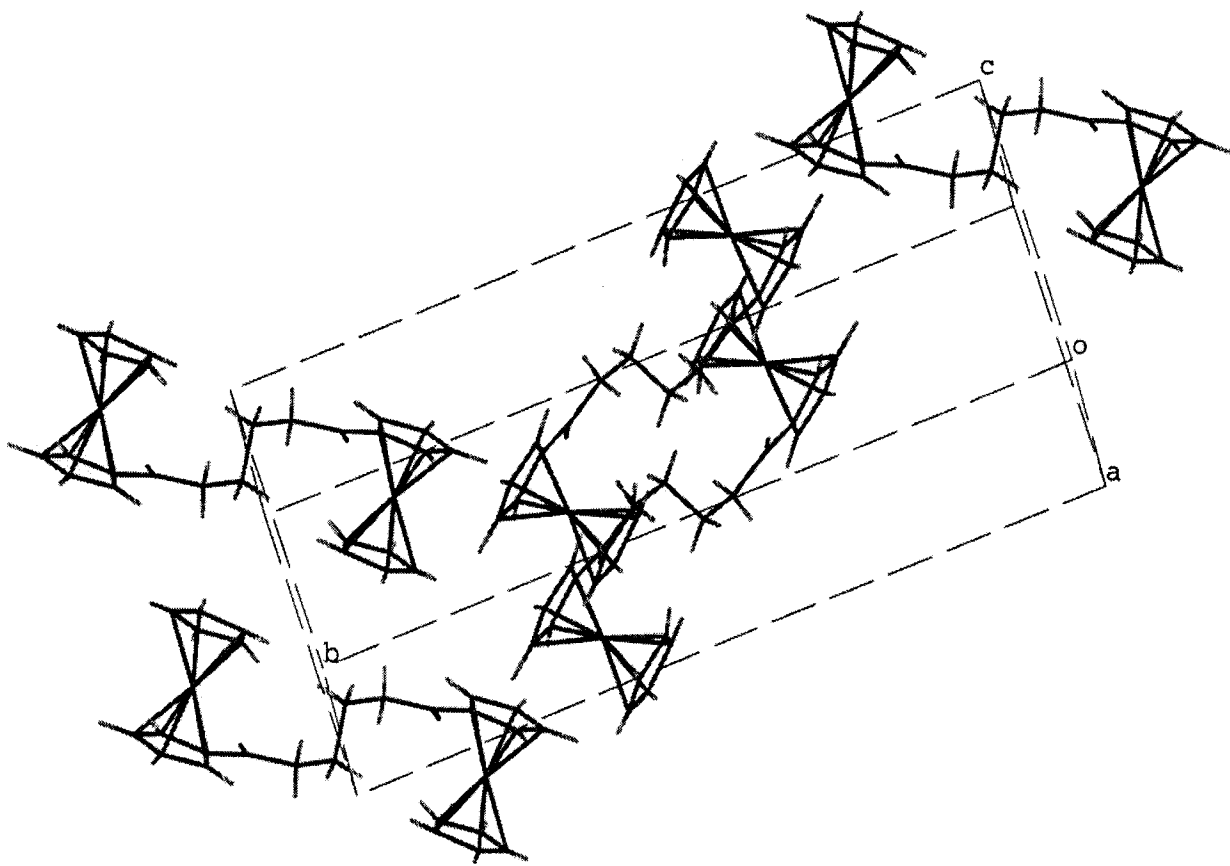


Figure 3.2: Unit cell of 1,6-diferrocenylhexane-1,6-dione

Table 3.2

Atomic Coordinates ($\times 10^4$) and Equivalent Isotropic Displacement Parameters ($\text{\AA}^2 \times 10^3$) for 1,6-diferrocenylhexane-1,6-dione. $U(\text{eq})$ is defined as one third of the trace of the orthogonalized U_{ij} tensor.

Atom Number	x	y	z	$U(\text{eq})$
Fe(1)	7845(1)	1520(1)	4558(1)	36(1)
O(1)	3861(6)	1224(1)	356(4)	56(1)
C(1)	6619(12)	719(2)	5089(6)	66(2)
C(2)	8972(12)	770(2)	5830(7)	66(2)
C(3)	9281(11)	1239(2)	6910(6)	62(1)
C(4)	7070(15)	1485(3)	6848(7)	70(2)
C(5)	5361(10)	1170(3)	5724(7)	73(2)
C(6)	6129(8)	2080(2)	2753(4)	40(1)
C(7)	7918(9)	2389(2)	3873(5)	48(1)
C(8)	10128(9)	2119(2)	3870(5)	50(1)
C(9)	9755(8)	1639(2)	2740(5)	45(1)
C(10)	7233(7)	1609(2)	2040(4)	38(1)
C(11)	5974(8)	1163(2)	927(4)	40(1)
C(12)	7277(8)	622(2)	531(5)	46(1)
C(13)	5774(10)	167(2)	-484(5)	51(1)

Table 3.3

Anisotropic Displacement Parameters ($\text{Å}^2 \times 10^3$) for 1,6-diferrocenylhexane-1,6-dione. The anisotropic displacement factor exponent takes the form: $-2 \pi^2 [h^2 a^{*2} U_{11} + \dots + 2 h k a^* b^* U_{12}]$

Atom Number	U11	U22	U33	U23	U13	U12
Fe(1)	39(1)	34(1)	34(1)	2(1)	6(1)	-2(1)
O(1)	61(2)	43(2)	57(2)	-6(1)	-6(2)	2(2)
C(1)	94(4)	50(3)	52(2)	9(2)	12(3)	-28(3)
C(2)	73(4)	53(3)	75(3)	30(3)	21(3)	18(3)
C(3)	66(3)	72(3)	41(2)	18(2)	-5(2)	-8(3)
C(4)	121(6)	50(3)	52(3)	3(2)	47(3)	5(3)
C(5)	52(3)	92(4)	73(3)	44(3)	11(3)	-7(3)
C(6)	50(2)	33(2)	37(2)	6(1)	5(2)	4(2)
C(7)	72(3)	31(2)	40(2)	3(2)	5(2)	-4(2)
C(8)	54(3)	44(2)	51(2)	3(2)	7(2)	-17(2)
C(9)	48(2)	46(2)	45(2)	-1(2)	19(2)	-6(2)
C(10)	45(2)	37(2)	31(2)	1(1)	6(2)	-4(2)
C(11)	50(2)	35(2)	35(2)	2(1)	6(2)	-1(2)
C(12)	51(3)	48(2)	41(2)	0(2)	15(2)	0(2)
C(13)	79(3)	41(2)	39(2)	-3(2)	21(2)	5(2)

Table 3.4

Bond lengths [Å] for 1,6-diferrocenylhexane-1,6-dione

Fe(1)-C(4)	2.021(5)
Fe(1)-C(5)	2.041(5)
Fe(1)-C(10)	2.034(3)
Fe(1)-C(1)	2.037(5)
Fe(1)-C(2)	2.038(5)
Fe(1)-C(9)	2.045(4)
Fe(1)-C(3)	2.042(4)
Fe(1)-C(6)	2.049(4)
Fe(1)-C(8)	2.052(4)
Fe(1)-C(7)	2.060(4)
C(12)-C(13)	1.491(6)
C(12)-C(11)	1.513(6)
C(12)-H(12B)	0.93(4)
C(12)-H(12A)	0.83(4)
O(1)-C(11)	1.221(5)
C(10)-C(9)	1.451(6)
C(9)-C(8)	1.421(6)
C(6)-C(7)	1.420(6)
C(6)-H(6)	1.01(5)
C(6)-C(10)	1.432(5)
C(8)-C(7)	1.416(7)
C(8)-H(8)	1.03(5)
C(7)-H(7)	1.00(5)
C(1)-C(2)	1.374(9)
C(1)-C(5)	1.417(9)
C(1)-H(1)	1.06(8)
C(3)-C(2)	1.376(8)
C(3)-C(4)	1.384(9)
C(3)-H(3)	0.95(9)
C(2)-H(2)	0.82(7)
C(4)-C(5)	1.402(9)
C(4)-H(4)	0.60(5)
C(5)-H(5)	1.19(5)
C(13)-C(13)#1	1.516(9)
C(13)-H(13A)	0.94(4)
C(13)-H(13B)	0.94(5)

Symmetry transformations used to generate equivalent atoms:

#1 -x+1,-y,-z

Table 3.5

Bond Angles [degrees] for 1,6-diferrocenylhexane-1,6-dione

C(4)-Fe(1)-C(5)	40.4(3)	C(2)-Fe(1)-C(6)	161.5(2)
C(4)-Fe(1)-C(10)	157.4(3)	C(9)-Fe(1)-C(6)	69.07(18)
C(5)-Fe(1)-C(10)	121.5(2)	C(3)-Fe(1)-C(6)	157.1(2)
C(4)-Fe(1)-C(1)	67.2(2)	C(4)-Fe(1)-C(8)	123.9(2)
C(5)-Fe(1)-C(1)	40.7(3)	C(5)-Fe(1)-C(8)	160.0(3)
C(10)-Fe(1)-C(1)	108.11(18)	C(10)-Fe(1)-C(8)	69.06(17)
C(4)-Fe(1)-C(2)	66.3(3)	C(1)-Fe(1)-C(8)	157.6(3)
C(5)-Fe(1)-C(2)	67.2(3)	C(2)-Fe(1)-C(8)	122.8(2)
C(10)-Fe(1)-C(2)	125.1(2)	C(9)-Fe(1)-C(8)	40.58(17)
C(1)-Fe(1)-C(2)	39.4(2)	C(3)-Fe(1)-C(8)	108.0(2)
C(4)-Fe(1)-C(9)	159.8(3)	C(6)-Fe(1)-C(8)	68.30(19)
C(5)-Fe(1)-C(9)	158.1(2)	C(4)-Fe(1)-C(7)	108.2(2)
C(10)-Fe(1)-C(9)	41.69(17)	C(5)-Fe(1)-C(7)	124.0(2)
C(1)-Fe(1)-C(9)	122.5(2)	C(10)-Fe(1)-C(7)	68.67(15)
C(2)-Fe(1)-C(9)	108.8(2)	C(1)-Fe(1)-C(7)	161.2(3)
C(4)-Fe(1)-C(3)	39.8(3)	C(2)-Fe(1)-C(7)	157.4(2)
C(5)-Fe(1)-C(3)	67.8(2)	C(9)-Fe(1)-C(7)	68.27(19)
C(10)-Fe(1)-C(3)	160.8(2)	C(3)-Fe(1)-C(7)	122.2(2)
C(1)-Fe(1)-C(3)	66.9(2)	C(6)-Fe(1)-C(7)	40.44(16)
C(2)-Fe(1)-C(3)	39.4(2)	C(8)-Fe(1)-C(7)	40.3(2)
C(9)-Fe(1)-C(3)	123.8(2)	C(13)-C(12)-C(11)	115.4(4)
C(4)-Fe(1)-C(6)	122.1(2)	C(13)-C(12)-H(12B)	110(2)
C(5)-Fe(1)-C(6)	107.5(2)	C(11)-C(12)-H(12B)	106(2)
C(10)-Fe(1)-C(6)	41.05(15)	C(13)-C(12)-H(12A)	110(3)
C(1)-Fe(1)-C(6)	125.1(2)	C(11)-C(12)-H(12A)	106(3)
H(12B)-C(12)-H(12A)	109(4)	C(9)-C(10)-Fe(1)	69.6(2)
C(6)-C(10)-C(11)	124.9(4)	C(11)-C(10)-Fe(1)	121.8(3)
C(6)-C(10)-C(9)	107.2(3)	O(1)-C(11)-C(10)	119.4(4)
C(9)-C(10)-C(11)	127.7(4)	O(1)-C(11)-C(12)	120.7(4)
C(6)-C(10)-Fe(1)	70.1(2)	C(8)-C(9)-Fe(1)	70.0(2)
C(10)-C(11)-C(12)	119.8(4)	C(10)-C(6)-H(6)	126(3)
C(8)-C(9)-C(10)	107.5(4)	Fe(1)-C(6)-H(6)	125(2)
C(10)-C(9)-Fe(1)	68.7(2)	C(9)-C(8)-C(7)	108.6(4)
C(8)-C(9)-H(9)	128(3)	C(9)-C(8)-Fe(1)	69.4(2)
C(10)-C(9)-H(9)	124(3)	C(7)-C(8)-Fe(1)	70.2(3)
Fe(1)-C(9)-H(9)	132(3)	C(9)-C(8)-H(8)	121(3)
C(7)-C(6)-C(10)	108.1(4)	C(7)-C(8)-H(8)	131(3)
C(7)-C(6)-Fe(1)	70.2(2)	Fe(1)-C(8)-H(8)	130(2)
C(10)-C(6)-Fe(1)	68.9(2)	C(8)-C(7)-C(6)	108.6(4)
C(7)-C(6)-H(6)	126(2)	C(8)-C(7)-Fe(1)	69.6(2)

Table 3.5., Continued

C(6)-C(7)-Fe(1)	69.4(2)	C(1)-C(2)-H(2)	131(4)
C(8)-C(7)-H(7)	128(3)	Fe(1)-C(2)-H(2)	111(4)
C(6)-C(7)-H(7)	123(3)	C(3)-C(4)-C(5)	109.6(5)
Fe(1)-C(7)-H(7)	127(3)	C(3)-C(4)-Fe(1)	70.9(3)
C(2)-C(1)-C(5)	107.9(5)	C(5)-C(4)-Fe(1)	70.6(3)
C(2)-C(1)-Fe(1)	70.3(3)	C(3)-C(4)-H(4)	126(6)
C(5)-C(1)-Fe(1)	69.8(3)	C(5)-C(4)-H(4)	125(6)
C(2)-C(1)-H(1)	133(5)	Fe(1)-C(4)-H(4)	127(5)
C(5)-C(1)-H(1)	117(5)	H(5)-C(5)-C(4)	149(3)
Fe(1)-C(1)-H(1)	113(4)	H(5)-C(5)-C(1)	106(3)
C(2)-C(3)-C(4)	107.1(5)	C(4)-C(5)-C(1)	105.7(5)
C(2)-C(3)-Fe(1)	70.1(3)	H(5)-C(5)-Fe(1)	126(3)
C(4)-C(3)-Fe(1)	69.2(3)	C(4)-C(5)-Fe(1)	69.0(3)
C(2)-C(3)-H(3)	113(5)	C(1)-C(5)-Fe(1)	69.5(3)
C(4)-C(3)-H(3)	140(5)	C(12)-C(13)-C(13)#1	113.2(4)
Fe(1)-C(3)-H(3)	122(5)	C(12)-C(13)-H(13A)	113(3)
C(3)-C(2)-C(1)	109.7(6)	C(13)#1-C(13)-H(13A)	105(3)
C(3)-C(2)-Fe(1)	70.5(3)	C(12)-C(13)-H(13B)	106(3)
C(1)-C(2)-Fe(1)	70.3(3)	C(13)#1-C(13)-H(13B)	112(3)
C(3)-C(2)-H(2)	117(4)	H(13A)-C(13)-H(13B)	109(4)

Symmetry transformations used to generate equivalent atoms:

#1 -x+1,-y,-z

Table 3.6

Hydrogen coordinates ($\times 10^4$) and Isotropic Displacement Parameters ($\text{Å}^2 \times 10^3$) for 1,6-diferrocenylhexane-1,6-dione.

Atom Number	x	y	z	U(eq)
H(1)	5710(160)	490(30)	4020(100)	120(30)
H(2)	10170(120)	640(30)	5560(70)	72(18)
H(3)	10900(150)	1310(30)	7410(100)	120(30)
H(4)	6860(110)	1690(20)	7260(70)	46(17)
H(5)	3320(90)	1090(20)	5120(70)	620(30)
H(6)	4380(80)	2170(19)	2530(50)	45(12)
H(7)	7590(90)	2740(20)	4540(60)	65(15)
H(8)	11810(90)	2240(20)	4460(50)	51(12)
H(9)	10900(90)	1406(18)	2390(50)	44(12)
H(12A)	8300(70)	740(17)	30(50)	26(9)
H(12B)	8010(70)	462(16)	1550(50)	26(9)
H(13A)	4710(80)	325(19)	-1390(60)	42(11)
H(13B)	6830(90)	-80(20)	-880(60)	54(13)

X-ray Diffraction Analysis of 1-ferrocenylcarbonyl-2-ferrocenylcyclopentene

The data set for this crystal was obtained with the help of Dr. Casey Raymond at Kent State University using the Bruker CCD system. The crystal was centered in the X-ray path and a one-minute rotation photo was taken. A full data set was collected, integrated, and corrected for absorption, as stated previously. A total of 9526 total reflections were collected, with 8551 of those being unique.

Prior to X-ray analysis, it was not known that this molecule was chiral. Structure refinement indicated that the molecule was chiral with the value of the BASF parameter being approximately 50%, indicating a nearly racemic mixture. The triclinic crystal is a part of the P1 space group due to the low symmetry of the molecule. Direct methods were used for structure refinement using SHELXTL software. The majority of non-hydrogen atoms were easily assigned anisotropically, but C16, C17, C36, and C37 were initially non-positive definite, meaning these atoms had negative mean square thermal displacement parameters. Since the structure has two molecules in the asymmetric unit, the non-positive definite atoms were constrained to have the same parameters as their symmetrical component in the other molecule using a command called EADP. This command allowed anisotropic refinement of these atoms, and refinement converged upon to an R value of 0.1335. The majority of hydrogen atoms were refined isotropically, while the remaining were assigned using the HFIX command. The constraint on the assigned hydrogens was removed, but refinement attempts proved unsuccessful. Therefore, the constraint was reinstated and the hydrogen atoms emerged as expected. Crystal data and refinement results are summarized in Table 3.7 and ORTEP plots of 1-ferrocenylcarbonyl-2-ferrocenylcyclopentene displaying 50% ellipsoids are shown in

Table 3.7

Crystal Data and Structure Refinement for 1-ferrocenylcarbonyl-2-ferrocenylcyclopentene

Empirical formula	C ₂₆ H ₂ Fe ₂ O
Formula weight	464.15
Temperature	293(2) K
Wavelength	0.71073 Å
Crystal system, space group	Triclinic, P1
Unit cell dimensions	a = 8.4097(6) Å alpha = 93.7510(10)° b = 10.3097(8) Å beta = 100.6130(10)° c = 12.1100(9) Å gamma = 98.2110(10)°
Volume	1016.86(13) Å ³
Z, Calculated density	2, 1.516 Mg/m ³
Absorption coefficient	1.441 mm ⁻¹
F(000)	480
Crystal size	0.02 x 0.05 x 0.10 mm
Theta range for data collection	1.72 to 28.29 deg.
Limiting indices	-11 ≤ h ≤ 11, -13 ≤ k ≤ 13, -16 ≤ l ≤ 15
Reflections collected / unique	9546 / 8551 [R(int) = 0.0277]
Completeness to theta = 28.29	97.4 %
Absorption correction	None
Refinement method	Full-matrix least-squares on F ²
Hydrogen Atom Positions	Mixed Refinement and Constrained
Data / restraints / parameters	8551 / 3 / 500
Goodness-of-fit on F ²	1.008
Final R indices [I > 2σ(I)]	R1(F) ^a = 0.0651, wR2(F ²) ^b = 0.1202
R indices (all data)	R1(F) ^a = 0.1335, wR2(F ²) ^b = 0.1460
Absolute structure parameter	0.46(5)
Largest diff. peak and hole	0.514 and -0.357 e.Å ⁻³

$${}^a R_1(F) = \frac{\sum |F_o| - \sum |F_c|}{\sum |F_o|} \text{ with } F_o > 4.0\sigma(F).$$

$${}^b wR_2(F^2) = \left[\frac{\sum [w(F_o^2 - F_c^2)^2]}{\sum w(F_o^2)^2} \right]^{1/2} \text{ with } F_o > 4.0\sigma(F), \text{ and } w^{-1} = \sigma^2(F_o)^2 + (W \cdot P)^2 + T \cdot P, \text{ where } P = (\text{Max}(F_o^2, 0) + 2F_c^2)/3, W = 0.0599, \text{ and } T = 0.14.$$

Figures 3.3 and 3.4. Figure 3.5 displays the unit cell, followed by tables of bond lengths, angles, and anisotropic displacement parameters in Tables 3.8 to 3.12. Appendix B includes the structure factor tables generated in XCIF.

X-ray Diffraction Analysis of 1,6-diferrocenylhexane

Data collection for this crystal was also performed at Kent State University under the supervision of Dr. Casey Raymond. Data collection generated 1800 frames of data in which 9429 reflections were generated and 2594 were unique. Data integration and empirical absorption correction were performed in SAINT and SADABS, respectively.

Due to the high symmetry of the fully reduced product, the crystal belonged to the monoclinic crystal system, just as 1,6-diferrocenylhexane-1,6-dione, with a space group of P2(1)/c. Direct methods were used for crystal structure refinement and all non-hydrogen atoms were assigned isotropically. However, only H6, H11A, and H11B could be refined. The remaining hydrogen positions were calculated using the HFIX constraint. The constraint was removed and refinement of the hydrogen positions was again attempted, but failed. Thus the HFIX constraint had to be reinstated to include all of the hydrogens in the structure. The final structure converged to a final R value of 0.0960 for all data. The crystal data and refinement results are shown in Table 3.13. An ORTEP plot of the fully reduced molecule displaying 50% ellipsoids is shown in Figure 3.6, followed by the orientation in the unit cell in Figure 3.7. Crystal data and refinement results, as well as bond lengths and angles can be found in Table 3.14 to Table 3.18.

RESULTS AND DISCUSSION

Characterization of 1,6-diferrocenylhexane-1,6-dione

The bond lengths for the structure were compared to those reported in the

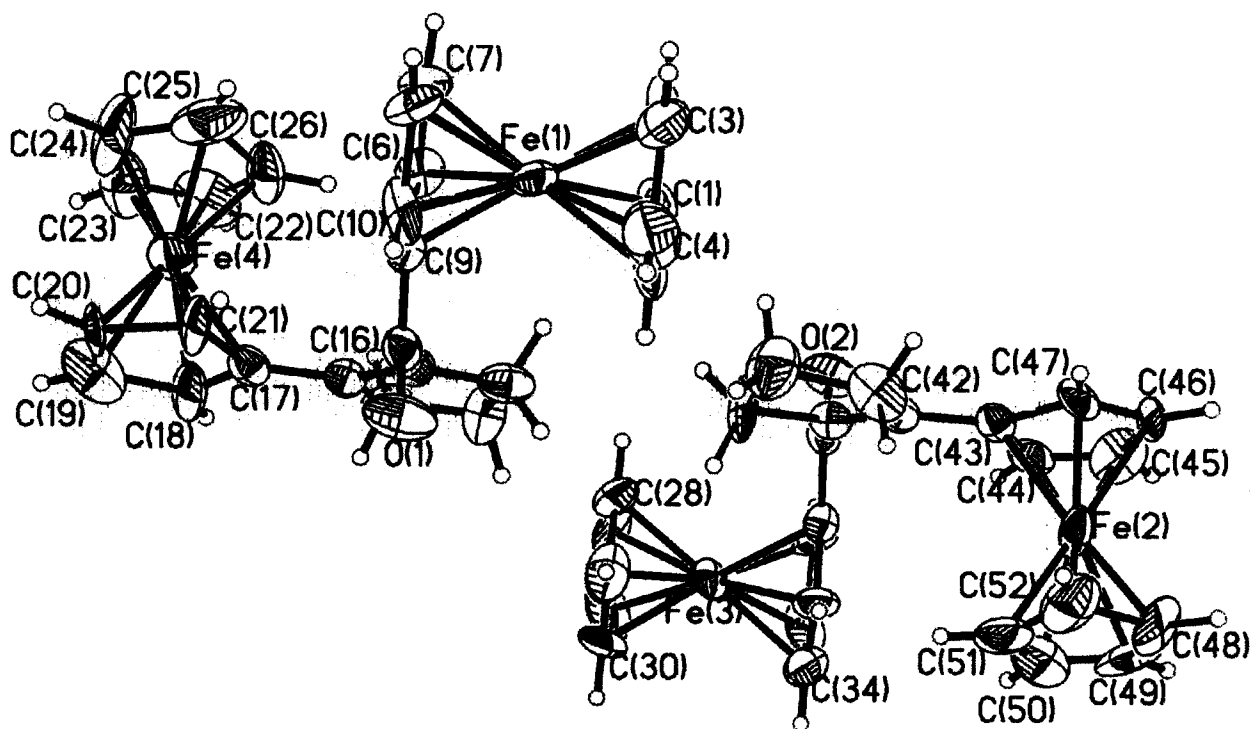


Figure 3.3: ORTEP plot of 1-ferrocenylcarbonyl-2-ferrocenylcyclopentene (50% ellipsoids)

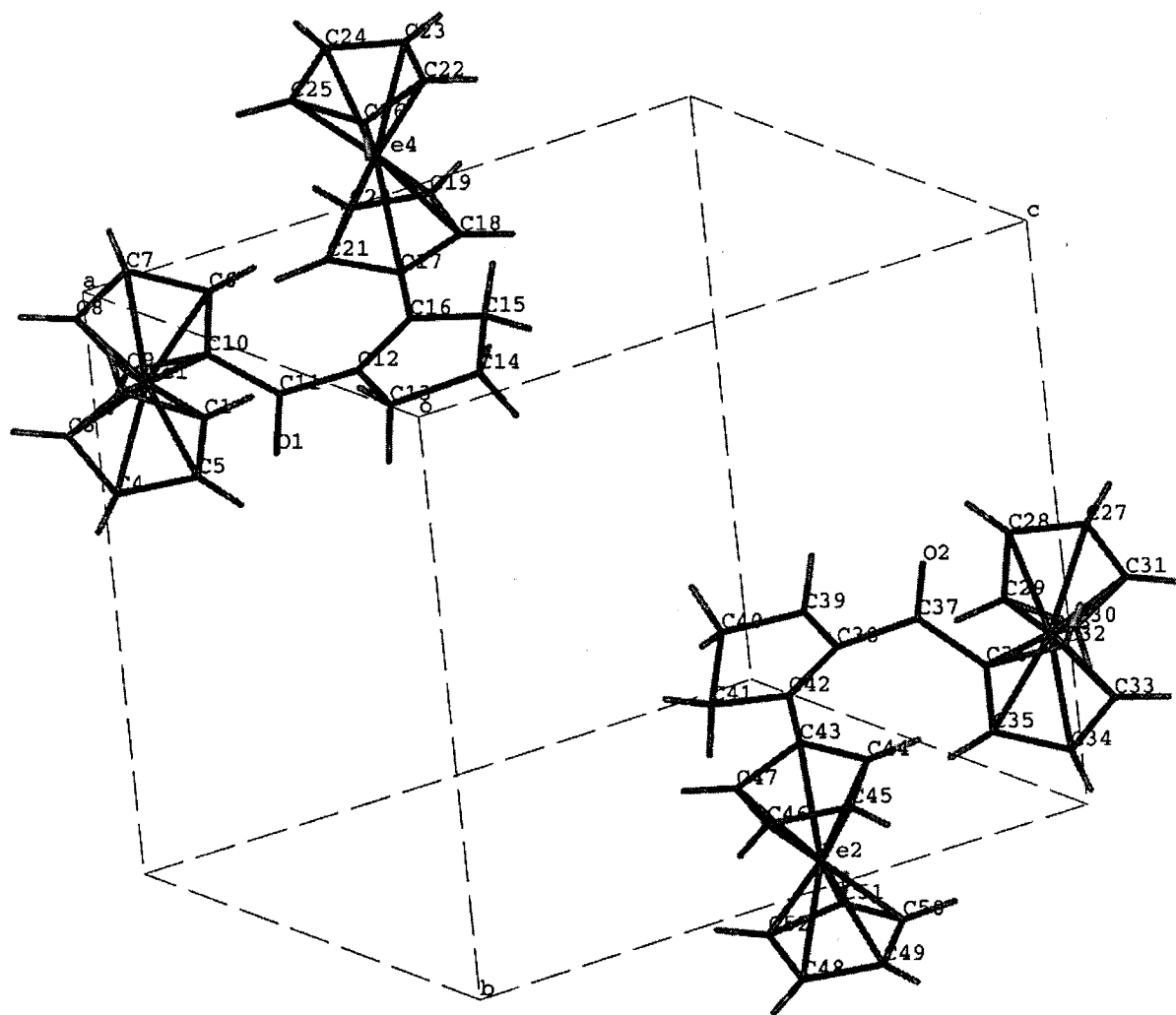


Figure 3.5: Unit cell of 1-ferrocenylcarbonyl-2-ferrocenylcyclopentene

Table 3.8

Atomic Coordinates ($\times 10^4$) and Equivalent Isotropic Displacement Parameters ($\text{\AA}^2 \times 10^3$) for 1-ferrocenylcarbonyl-2-ferrocenylcyclopentene. U(eq) is defined as one third of the trace of the orthogonalized Uij tensor.

Atom Number	x	y	z	U(eq)
Fe(1)	1921(2)	2590(1)	1845(1)	39(1)
Fe(2)	3650(2)	10946(2)	7547(1)	47(1)
Fe(3)	-1512(2)	6399(1)	8915(1)	39(1)
Fe(4)	-3243(2)	-1959(2)	3210(2)	52(1)
O(1)	-2537(14)	2717(13)	1505(10)	64(3)
O(2)	3053(14)	6330(12)	9344(9)	57(3)
C(1)	3022(16)	3900(15)	3272(13)	46(4)
C(2)	4220(20)	3494(16)	2620(15)	67(5)
C(3)	3940(20)	3833(14)	1551(16)	64(5)
C(4)	2440(20)	4478(18)	1449(18)	76(6)
C(5)	2026(17)	4462(13)	2555(11)	47(4)
C(6)	775(17)	965(12)	2399(11)	40(3)
C(7)	1940(20)	637(16)	1721(15)	52(4)
C(8)	1522(19)	1009(13)	629(12)	46(4)
C(9)	98(16)	1594(13)	622(9)	47(4)
C(10)	-363(18)	1558(13)	1682(11)	35(1)
C(11)	-1686(18)	2088(13)	2089(12)	36(1)
C(12)	-1854(16)	2045(13)	3281(12)	37(3)
C(13)	-1049(16)	3096(13)	4149(11)	47(4)
C(14)	-1780(20)	2766(15)	5240(11)	50(4)
C(15)	-2801(17)	1461(12)	4903(11)	49(4)
C(16)	-2854(16)	1087(13)	3689(12)	34(1)
C(17)	-3783(17)	-90(14)	3136(12)	36(1)
C(18)	-4915(19)	-848(14)	3566(12)	54(4)
C(19)	-5680(20)	-1982(17)	2759(16)	78(6)
C(20)	-4963(16)	-1894(12)	1823(13)	58(5)
C(21)	-3740(17)	-676(12)	2015(10)	43(3)
C(22)	-2120(20)	-2510(20)	4677(14)	76(6)
C(23)	-2900(20)	-3534(17)	4042(16)	78(5)
C(24)	-2270(30)	-3622(17)	3087(19)	113(10)
C(25)	-960(30)	-2440(20)	3126(17)	94(7)
C(26)	-1040(20)	-1712(15)	4212(13)	57(4)
C(27)	-2110(20)	4544(14)	9369(16)	65(5)
C(28)	-1490(20)	4500(13)	8422(16)	74(5)
C(29)	-2670(20)	5143(17)	7640(16)	73(5)

Table 3.8, Continued

C(30)	-3790(18)	5537(17)	8169(18)	73(6)
C(31)	-3360(20)	5160(20)	9286(18)	84(6)
C(32)	367(16)	7391(11)	10094(12)	47(4)
C(33)	-1050(20)	7968(16)	10088(15)	66(5)
C(34)	-1560(20)	8403(16)	9028(15)	54(5)
C(35)	-489(17)	8096(14)	8361(13)	50(4)
C(36)	746(18)	7451(13)	8995(12)	35(1)
C(37)	2059(17)	6822(13)	8656(12)	36(1)
C(38)	2302(16)	6951(13)	7467(10)	31(3)
C(39)	1380(20)	5856(13)	6533(12)	62(5)
C(40)	2260(30)	6085(18)	5639(15)	76(5)
C(41)	3138(18)	7554(15)	5808(9)	55(4)
C(42)	3186(16)	7840(13)	7079(11)	34(1)
C(43)	4249(17)	9081(14)	7720(12)	36(1)
C(44)	4288(16)	9735(15)	8778(12)	46(3)
C(45)	5360(20)	10847(16)	8983(11)	63(5)
C(46)	6138(16)	11010(12)	8033(14)	58(5)
C(47)	5481(16)	9983(14)	7265(13)	50(4)
C(48)	3240(30)	12650(17)	6850(20)	106(9)
C(49)	2570(30)	12569(18)	7811(18)	91(7)
C(50)	1430(20)	11490(20)	7607(16)	68(5)
C(51)	1330(20)	10864(17)	6627(17)	68(5)
C(52)	2510(30)	11454(17)	6009(16)	76(6)

Table 3.9

Bond lengths [Å] for 1-ferrocenylcarbonyl-2-ferrocenylcyclopentene

Fe(1)-C(7)	2.012(16)	O(2)-C(37)	1.253(18)
Fe(1)-C(9)	2.028(11)	C(1)-C(5)	1.32(2)
Fe(1)-C(10)	2.027(14)	C(1)-C(2)	1.48(2)
Fe(1)-C(6)	2.027(11)	C(1)-H(1)	0.9300
Fe(1)-C(5)	2.044(12)	C(2)-C(3)	1.35(2)
Fe(1)-C(4)	2.040(18)	C(2)-H(2)	0.9300
Fe(1)-C(2)	2.050(15)	C(3)-C(4)	1.50(3)
Fe(1)-C(3)	2.074(16)	C(3)-H(3)	0.9300
Fe(1)-C(8)	2.070(14)	C(4)-C(5)	1.44(2)
Fe(1)-C(1)	2.101(13)	C(4)-H(4)	0.9300
Fe(2)-C(47)	2.015(14)	C(5)-H(5)	0.9300
Fe(2)-C(51)	2.046(17)	C(6)-C(7)	1.45(2)
Fe(2)-C(50)	2.035(18)	C(6)-C(10)	1.405(19)
Fe(2)-C(49)	2.049(15)	C(6)-H(6)	0.9300
Fe(2)-C(52)	2.068(17)	C(7)-C(8)	1.40(2)
Fe(2)-C(48)	2.043(14)	C(7)-H(7)	0.9300
Fe(2)-C(44)	2.052(15)	C(8)-C(9)	1.41(2)
Fe(2)-C(45)	2.059(15)	C(8)-H(8)	0.9300
Fe(2)-C(43)	2.070(14)	C(9)-C(10)	1.409(17)
Fe(2)-C(46)	2.057(13)	C(9)-H(9)	0.9300
Fe(3)-C(29)	1.957(17)	C(10)-C(11)	1.46(2)
Fe(3)-C(31)	2.002(15)	C(11)-C(12)	1.479(19)
Fe(3)-C(30)	2.011(16)	C(12)-C(16)	1.381(18)
Fe(3)-C(33)	2.026(16)	C(12)-C(13)	1.455(19)
Fe(3)-C(28)	2.011(14)	C(13)-C(14)	1.594(19)
Fe(3)-C(32)	2.024(14)	C(13)-H(13A)	0.9700
Fe(3)-C(35)	2.046(15)	C(13)-H(13B)	0.9700
Fe(3)-C(36)	2.030(14)	C(14)-C(15)	1.478(19)
Fe(3)-C(27)	2.045(13)	C(14)-H(14A)	0.9700
Fe(3)-C(34)	2.069(16)	C(14)-H(14B)	0.9700
Fe(4)-C(23)	1.995(16)	C(15)-C(16)	1.486(19)
Fe(4)-C(26)	1.995(15)	C(15)-H(15A)	0.9700
Fe(4)-C(19)	2.020(17)	C(15)-H(15B)	0.9700
Fe(4)-C(24)	2.011(19)	C(16)-C(17)	1.40(2)
Fe(4)-C(18)	2.024(16)	C(17)-C(18)	1.35(2)
Fe(4)-C(20)	2.016(12)	C(17)-C(21)	1.459(19)
Fe(4)-C(22)	2.009(13)	C(18)-C(19)	1.46(2)
Fe(4)-C(21)	2.050(13)	C(18)-H(18)	0.9300
Fe(4)-C(17)	2.046(14)	C(19)-C(20)	1.38(2)
Fe(4)-C(25)	2.06(2)	C(19)-H(19)	0.9300
O(1)-C(11)	1.200(18)	C(20)-C(21)	1.482(16)

Table 3.9, Continued

C(20)-H(20)	0.9300	C(37)-C(38)	1.503(18)
C(21)-H(21)	0.9300	C(38)-C(42)	1.266(18)
C(22)-C(23)	1.28(3)	C(38)-C(39)	1.555(16)
C(22)-C(26)	1.36(2)	C(39)-C(40)	1.43(2)
C(22)-H(22)	0.9300	C(39)-H(39A)	0.9700
C(23)-C(24)	1.36(3)	C(39)-H(39B)	0.9700
C(23)-H(23)	0.9300	C(40)-C(41)	1.57(2)
C(24)-C(25)	1.51(3)	C(40)-H(40A)	0.9700
C(24)-H(24)	0.9300	C(40)-H(40B)	0.9700
C(25)-C(26)	1.49(2)	C(41)-C(42)	1.540(17)
C(25)-H(25)	0.9300	C(41)-H(41A)	0.9700
C(26)-H(26)	0.9300	C(41)-H(41B)	0.9700
C(27)-C(31)	1.29(3)	C(42)-C(43)	1.53(2)
C(27)-C(28)	1.34(2)	C(43)-C(44)	1.40(2)
C(27)-H(27)	0.9300	C(43)-C(47)	1.498(18)
C(28)-C(29)	1.49(3)	C(44)-C(45)	1.331(19)
C(28)-H(28)	0.9300	C(44)-H(44)	0.9300
C(29)-C(30)	1.33(3)	C(45)-C(46)	1.43(2)
C(29)-H(29)	0.9300	C(45)-H(45)	0.9300
C(30)-C(31)	1.43(3)	C(46)-C(47)	1.34(2)
C(30)-H(30)	0.9300	C(46)-H(46)	0.9300
C(31)-H(31)	0.9300	C(47)-H(47)	0.9300
C(32)-C(33)	1.40(2)	C(48)-C(49)	1.38(3)
C(32)-C(36)	1.428(19)	C(48)-C(52)	1.53(3)
C(32)-H(32)	0.9300	C(48)-H(48)	0.9300
C(33)-C(34)	1.40(2)	C(49)-C(50)	1.34(3)
C(33)-H(33)	0.9300	C(49)-H(49)	0.9300
C(34)-C(35)	1.37(2)	C(50)-C(51)	1.30(2)
C(34)-H(34)	0.9300	C(50)-H(50)	0.9300
C(35)-C(36)	1.443(19)	C(51)-C(52)	1.44(3)
C(35)-H(35)	0.9300	C(51)-H(51)	0.9300
C(36)-C(37)	1.46(2)	C(52)-H(52)	0.9300

Table 3.10

Bond Angles [degrees] for 1-ferrocenylcarbonyl-2-ferrocenylcyclopentene

C(7)-Fe(1)-C(9)	67.2(6)	C(5)-Fe(1)-C(1)	37.0(6)
C(7)-Fe(1)-C(10)	68.4(6)	C(4)-Fe(1)-C(1)	67.7(7)
C(9)-Fe(1)-C(10)	40.7(5)	C(2)-Fe(1)-C(1)	41.8(6)
C(7)-Fe(1)-C(6)	42.1(6)	C(3)-Fe(1)-C(1)	68.5(7)
C(9)-Fe(1)-C(6)	68.5(5)	C(8)-Fe(1)-C(1)	160.6(6)
C(10)-Fe(1)-C(6)	40.6(5)	C(47)-Fe(2)-C(51)	130.4(7)
C(7)-Fe(1)-C(5)	159.9(6)	C(47)-Fe(2)-C(50)	165.0(7)
C(9)-Fe(1)-C(5)	126.1(6)	C(51)-Fe(2)-C(50)	37.0(7)
C(10)-Fe(1)-C(5)	110.6(6)	C(47)-Fe(2)-C(49)	155.5(8)
C(6)-Fe(1)-C(5)	123.8(5)	C(51)-Fe(2)-C(49)	64.9(7)
C(7)-Fe(1)-C(4)	156.0(7)	C(50)-Fe(2)-C(49)	38.2(8)
C(9)-Fe(1)-C(4)	108.6(7)	C(47)-Fe(2)-C(52)	107.5(7)
C(10)-Fe(1)-C(4)	125.0(7)	C(51)-Fe(2)-C(52)	40.9(7)
C(6)-Fe(1)-C(4)	160.7(7)	C(50)-Fe(2)-C(52)	67.6(8)
C(5)-Fe(1)-C(4)	41.4(7)	C(49)-Fe(2)-C(52)	70.9(8)
C(7)-Fe(1)-C(2)	107.6(7)	C(47)-Fe(2)-C(48)	122.7(9)
C(9)-Fe(1)-C(2)	159.0(6)	C(51)-Fe(2)-C(48)	66.0(8)
C(10)-Fe(1)-C(2)	158.6(6)	C(50)-Fe(2)-C(48)	64.3(8)
C(6)-Fe(1)-C(2)	122.3(7)	C(49)-Fe(2)-C(48)	39.5(8)
C(5)-Fe(1)-C(2)	65.5(7)	C(52)-Fe(2)-C(48)	43.6(8)
C(4)-Fe(1)-C(2)	67.3(8)	C(47)-Fe(2)-C(44)	67.4(5)
C(7)-Fe(1)-C(3)	118.6(6)	C(51)-Fe(2)-C(44)	124.5(7)
C(9)-Fe(1)-C(3)	124.7(6)	C(50)-Fe(2)-C(44)	111.2(6)
C(10)-Fe(1)-C(3)	162.5(7)	C(49)-Fe(2)-C(44)	123.3(7)
C(6)-Fe(1)-C(3)	154.8(6)	C(52)-Fe(2)-C(44)	157.2(7)
C(5)-Fe(1)-C(3)	68.6(6)	C(48)-Fe(2)-C(44)	158.2(8)
C(4)-Fe(1)-C(3)	42.7(7)	C(47)-Fe(2)-C(45)	66.5(6)
C(2)-Fe(1)-C(3)	38.2(7)	C(51)-Fe(2)-C(45)	155.0(8)
C(7)-Fe(1)-C(8)	40.0(6)	C(50)-Fe(2)-C(45)	122.3(7)
C(9)-Fe(1)-C(8)	40.4(6)	C(49)-Fe(2)-C(45)	107.4(7)
C(10)-Fe(1)-C(8)	68.8(6)	C(52)-Fe(2)-C(45)	162.5(8)
C(6)-Fe(1)-C(8)	69.7(6)	C(48)-Fe(2)-C(45)	124.4(8)
C(5)-Fe(1)-C(8)	159.9(6)	C(44)-Fe(2)-C(45)	37.8(5)
C(4)-Fe(1)-C(8)	121.3(7)	C(47)-Fe(2)-C(43)	43.0(5)
C(2)-Fe(1)-C(8)	122.5(7)	C(51)-Fe(2)-C(43)	111.3(7)
C(3)-Fe(1)-C(8)	105.6(7)	C(50)-Fe(2)-C(43)	126.2(7)
C(7)-Fe(1)-C(1)	125.2(7)	C(49)-Fe(2)-C(43)	158.8(8)
C(9)-Fe(1)-C(1)	157.8(6)	C(52)-Fe(2)-C(43)	121.1(6)
C(10)-Fe(1)-C(1)	122.1(6)	C(48)-Fe(2)-C(43)	160.6(9)
C(6)-Fe(1)-C(1)	107.3(6)	C(44)-Fe(2)-C(43)	39.7(6)

Table 3.10, Continued

C(45)-Fe(2)-C(43)	66.7(6)	C(32)-Fe(3)-C(27)	109.0(7)
C(47)-Fe(2)-C(46)	38.5(6)	C(35)-Fe(3)-C(27)	167.6(7)
C(51)-Fe(2)-C(46)	164.0(8)	C(36)-Fe(3)-C(27)	128.7(7)
C(50)-Fe(2)-C(46)	155.9(7)	C(29)-Fe(3)-C(34)	125.2(8)
C(49)-Fe(2)-C(46)	121.2(7)	C(31)-Fe(3)-C(34)	120.0(9)
C(52)-Fe(2)-C(46)	124.4(8)	C(30)-Fe(3)-C(34)	106.0(7)
C(48)-Fe(2)-C(46)	108.4(8)	C(33)-Fe(3)-C(34)	40.0(7)
C(44)-Fe(2)-C(46)	66.3(6)	C(28)-Fe(3)-C(34)	166.7(8)
C(45)-Fe(2)-C(46)	40.8(7)	C(32)-Fe(3)-C(34)	68.3(6)
C(43)-Fe(2)-C(46)	68.5(5)	C(35)-Fe(3)-C(34)	39.0(6)
C(29)-Fe(3)-C(31)	66.6(8)	C(36)-Fe(3)-C(34)	68.4(6)
C(29)-Fe(3)-C(30)	39.1(8)	C(27)-Fe(3)-C(34)	152.6(7)
C(31)-Fe(3)-C(30)	41.7(8)	C(23)-Fe(4)-C(26)	68.2(7)
C(29)-Fe(3)-C(33)	159.9(8)	C(23)-Fe(4)-C(19)	107.8(7)
C(31)-Fe(3)-C(33)	106.7(7)	C(26)-Fe(4)-C(19)	158.1(8)
C(30)-Fe(3)-C(33)	123.2(7)	C(23)-Fe(4)-C(24)	39.7(9)
C(29)-Fe(3)-C(28)	44.2(8)	C(26)-Fe(4)-C(24)	70.6(6)
C(31)-Fe(3)-C(28)	66.3(8)	C(19)-Fe(4)-C(24)	121.0(8)
C(30)-Fe(3)-C(28)	70.4(6)	C(23)-Fe(4)-C(18)	119.7(8)
C(33)-Fe(3)-C(28)	152.6(8)	C(26)-Fe(4)-C(18)	119.4(6)
C(29)-Fe(3)-C(32)	159.1(7)	C(19)-Fe(4)-C(18)	42.4(7)
C(31)-Fe(3)-C(32)	123.4(7)	C(24)-Fe(4)-C(18)	155.4(10)
C(30)-Fe(3)-C(32)	160.3(6)	C(23)-Fe(4)-C(20)	126.4(6)
C(33)-Fe(3)-C(32)	40.5(6)	C(26)-Fe(4)-C(20)	158.9(7)
C(28)-Fe(3)-C(32)	119.4(6)	C(19)-Fe(4)-C(20)	40.0(7)
C(29)-Fe(3)-C(35)	110.8(7)	C(24)-Fe(4)-C(20)	110.0(6)
C(31)-Fe(3)-C(35)	154.5(8)	C(18)-Fe(4)-C(20)	69.3(6)
C(30)-Fe(3)-C(35)	119.7(7)	C(23)-Fe(4)-C(22)	37.4(8)
C(33)-Fe(3)-C(35)	66.5(7)	C(26)-Fe(4)-C(22)	39.8(7)
C(28)-Fe(3)-C(35)	130.9(7)	C(19)-Fe(4)-C(22)	124.6(7)
C(32)-Fe(3)-C(35)	68.5(5)	C(24)-Fe(4)-C(22)	64.7(8)
C(29)-Fe(3)-C(36)	124.0(7)	C(18)-Fe(4)-C(22)	107.3(7)
C(31)-Fe(3)-C(36)	161.5(8)	C(20)-Fe(4)-C(22)	160.5(8)
C(30)-Fe(3)-C(36)	156.1(7)	C(23)-Fe(4)-C(21)	165.9(6)
C(33)-Fe(3)-C(36)	68.3(6)	C(26)-Fe(4)-C(21)	119.7(6)
C(28)-Fe(3)-C(36)	109.5(6)	C(19)-Fe(4)-C(21)	69.4(6)
C(32)-Fe(3)-C(36)	41.3(5)	C(24)-Fe(4)-C(21)	129.0(9)
C(35)-Fe(3)-C(36)	41.5(5)	C(18)-Fe(4)-C(21)	68.2(6)
C(29)-Fe(3)-C(27)	66.9(8)	C(20)-Fe(4)-C(21)	42.7(5)
C(31)-Fe(3)-C(27)	37.1(8)	C(22)-Fe(4)-C(21)	155.4(7)
C(30)-Fe(3)-C(27)	66.9(8)	C(23)-Fe(4)-C(17)	151.5(8)
C(33)-Fe(3)-C(27)	120.1(7)	C(26)-Fe(4)-C(17)	103.8(6)
C(28)-Fe(3)-C(27)	38.7(7)	C(19)-Fe(4)-C(17)	68.9(6)

Table 3.10, Continued

C(24)-Fe(4)-C(17)	165.9(10)	Fe(1)-C(5)-H(5)	125.2
C(18)-Fe(4)-C(17)	38.6(6)	C(7)-C(6)-C(10)	105.3(11)
C(20)-Fe(4)-C(17)	70.4(5)	C(7)-C(6)-Fe(1)	68.4(8)
C(22)-Fe(4)-C(17)	119.7(7)	C(10)-C(6)-Fe(1)	69.7(7)
C(21)-Fe(4)-C(17)	41.7(5)	C(7)-C(6)-H(6)	127.3
C(23)-Fe(4)-C(25)	70.2(8)	C(10)-C(6)-H(6)	127.4
C(26)-Fe(4)-C(25)	42.9(7)	Fe(1)-C(6)-H(6)	126.1
C(19)-Fe(4)-C(25)	158.0(9)	C(8)-C(7)-C(6)	110.7(13)
C(24)-Fe(4)-C(25)	43.6(9)	C(8)-C(7)-Fe(1)	72.3(9)
C(18)-Fe(4)-C(25)	158.0(7)	C(6)-C(7)-Fe(1)	69.5(7)
C(20)-Fe(4)-C(25)	122.6(7)	C(8)-C(7)-H(7)	124.6
C(22)-Fe(4)-C(25)	67.7(8)	C(6)-C(7)-H(7)	124.6
C(21)-Fe(4)-C(25)	106.9(7)	Fe(1)-C(7)-H(7)	125.2
C(17)-Fe(4)-C(25)	123.6(8)	C(7)-C(8)-C(9)	105.3(13)
C(5)-C(1)-C(2)	104.6(14)	C(7)-C(8)-Fe(1)	67.8(9)
C(5)-C(1)-Fe(1)	69.1(7)	C(9)-C(8)-Fe(1)	68.2(7)
C(2)-C(1)-Fe(1)	67.2(8)	C(7)-C(8)-H(8)	127.4
C(5)-C(1)-H(1)	127.7	C(9)-C(8)-H(8)	127.4
C(2)-C(1)-H(1)	127.7	Fe(1)-C(8)-H(8)	128.2
Fe(1)-C(1)-H(1)	127.4	C(10)-C(9)-C(8)	110.2(12)
C(3)-C(2)-C(1)	112.1(16)	C(10)-C(9)-Fe(1)	69.6(7)
C(3)-C(2)-Fe(1)	71.8(10)	C(8)-C(9)-Fe(1)	71.4(8)
C(1)-C(2)-Fe(1)	71.0(8)	C(10)-C(9)-H(9)	124.9
C(3)-C(2)-H(2)	124.0	C(8)-C(9)-H(9)	124.9
C(1)-C(2)-H(2)	123.9	Fe(1)-C(9)-H(9)	125.6
Fe(1)-C(2)-H(2)	124.9	C(9)-C(10)-C(6)	108.5(13)
C(2)-C(3)-C(4)	105.5(16)	C(9)-C(10)-C(11)	130.1(13)
C(2)-C(3)-Fe(1)	69.9(9)	C(6)-C(10)-C(11)	121.3(12)
C(4)-C(3)-Fe(1)	67.5(9)	C(9)-C(10)-Fe(1)	69.7(7)
C(2)-C(3)-H(3)	127.2	C(6)-C(10)-Fe(1)	69.7(8)
C(4)-C(3)-H(3)	127.3	C(11)-C(10)-Fe(1)	123.1(10)
Fe(1)-C(3)-H(3)	126.8	O(1)-C(11)-C(12)	117.9(13)
C(5)-C(4)-C(3)	104.3(16)	O(1)-C(11)-C(10)	120.4(13)
C(5)-C(4)-Fe(1)	69.4(9)	C(12)-C(11)-C(10)	121.0(12)
C(3)-C(4)-Fe(1)	69.9(9)	C(16)-C(12)-C(13)	112.3(12)
C(5)-C(4)-H(4)	127.9	C(16)-C(12)-C(11)	125.4(12)
C(3)-C(4)-H(4)	127.9	C(13)-C(12)-C(11)	122.2(11)
Fe(1)-C(4)-H(4)	124.6	C(12)-C(13)-C(14)	105.4(11)
C(1)-C(5)-C(4)	113.5(14)	C(12)-C(13)-H(13A)	110.7
C(1)-C(5)-Fe(1)	73.9(9)	C(14)-C(13)-H(13A)	110.7
C(4)-C(5)-Fe(1)	69.2(8)	C(12)-C(13)-H(13B)	110.7
C(1)-C(5)-H(5)	123.2	C(14)-C(13)-H(13B)	110.7
C(4)-C(5)-H(5)	123.2	H(13A)-C(13)-H(13B)	108.8

Table 3.10, Continued

C(15)-C(14)-C(13)	103.6(12)	C(20)-C(21)-H(21)	127.2
C(15)-C(14)-H(14A)	111.0	Fe(4)-C(21)-H(21)	127.9
C(13)-C(14)-H(14A)	111.0	C(23)-C(22)-C(26)	115.4(18)
C(15)-C(14)-H(14B)	111.0	C(23)-C(22)-Fe(4)	70.7(10)
C(13)-C(14)-H(14B)	111.0	C(26)-C(22)-Fe(4)	69.5(9)
H(14A)-C(14)-H(14B)	109.0	C(23)-C(22)-H(22)	122.2
C(14)-C(15)-C(16)	109.3(11)	C(26)-C(22)-H(22)	122.4
C(14)-C(15)-H(15A)	109.8	Fe(4)-C(22)-H(22)	129.6
C(16)-C(15)-H(15A)	109.8	C(22)-C(23)-C(24)	108.9(19)
C(14)-C(15)-H(15B)	109.8	C(22)-C(23)-Fe(4)	71.9(10)
C(16)-C(15)-H(15B)	109.8	C(24)-C(23)-Fe(4)	70.8(10)
H(15A)-C(15)-H(15B)	108.3	C(22)-C(23)-H(23)	125.7
C(17)-C(16)-C(12)	129.6(13)	C(24)-C(23)-H(23)	125.4
C(17)-C(16)-C(15)	121.5(12)	Fe(4)-C(23)-H(23)	123.3
C(12)-C(16)-C(15)	109.0(12)	C(23)-C(24)-C(25)	108.7(15)
C(16)-C(17)-C(18)	124.1(14)	C(23)-C(24)-Fe(4)	69.5(12)
C(16)-C(17)-C(21)	127.0(13)	C(25)-C(24)-Fe(4)	70.1(10)
C(18)-C(17)-C(21)	109.0(13)	C(23)-C(24)-H(24)	125.7
C(16)-C(17)-Fe(4)	128.4(10)	C(25)-C(24)-H(24)	125.6
C(18)-C(17)-Fe(4)	69.8(9)	Fe(4)-C(24)-H(24)	126.3
C(21)-C(17)-Fe(4)	69.3(8)	C(26)-C(25)-C(24)	100.9(19)
C(17)-C(18)-C(19)	109.9(13)	C(26)-C(25)-Fe(4)	66.0(9)
C(17)-C(18)-Fe(4)	71.6(10)	C(24)-C(25)-Fe(4)	66.3(12)
C(19)-C(18)-Fe(4)	68.7(9)	C(26)-C(25)-H(25)	129.5
C(17)-C(18)-H(18)	125.1	C(24)-C(25)-H(25)	129.6
C(19)-C(18)-H(18)	125.0	Fe(4)-C(25)-H(25)	129.4
Fe(4)-C(18)-H(18)	126.2	C(22)-C(26)-C(25)	105.7(16)
C(20)-C(19)-C(18)	107.7(12)	C(22)-C(26)-Fe(4)	70.6(9)
C(20)-C(19)-Fe(4)	69.8(9)	C(25)-C(26)-Fe(4)	71.1(9)
C(18)-C(19)-Fe(4)	68.9(9)	C(22)-C(26)-H(26)	127.2
C(20)-C(19)-H(19)	126.2	C(25)-C(26)-H(26)	127.1
C(18)-C(19)-H(19)	126.2	Fe(4)-C(26)-H(26)	122.8
Fe(4)-C(19)-H(19)	126.7	C(31)-C(27)-C(28)	112.9(19)
C(19)-C(20)-C(21)	108.0(13)	C(31)-C(27)-Fe(3)	69.6(10)
C(19)-C(20)-Fe(4)	70.1(9)	C(28)-C(27)-Fe(3)	69.3(8)
C(21)-C(20)-Fe(4)	69.9(6)	C(31)-C(27)-H(27)	123.5
C(19)-C(20)-H(20)	126.0	C(28)-C(27)-H(27)	123.6
C(21)-C(20)-H(20)	126.0	Fe(3)-C(27)-H(27)	129.4
Fe(4)-C(20)-H(20)	125.6	C(27)-C(28)-C(29)	102.0(16)
C(17)-C(21)-C(20)	105.5(13)	C(27)-C(28)-Fe(3)	72.0(9)
C(17)-C(21)-Fe(4)	69.0(7)	C(29)-C(28)-Fe(3)	66.0(8)
C(20)-C(21)-Fe(4)	67.4(7)	C(27)-C(28)-H(28)	129.0
C(17)-C(21)-H(21)	127.3	C(29)-C(28)-H(28)	129.0

Table 3.10, Continued

Fe(3)-C(28)-H(28)	124.7	C(35)-C(36)-C(32)	105.8(12)
C(30)-C(29)-C(28)	110.3(17)	C(35)-C(36)-C(37)	131.6(13)
C(30)-C(29)-Fe(3)	72.7(11)	C(32)-C(36)-C(37)	122.3(12)
C(28)-C(29)-Fe(3)	69.8(9)	C(35)-C(36)-Fe(3)	69.9(9)
C(30)-C(29)-H(29)	124.9	C(32)-C(36)-Fe(3)	69.1(8)
C(28)-C(29)-H(29)	124.9	C(37)-C(36)-Fe(3)	120.6(10)
Fe(3)-C(29)-H(29)	124.2	O(2)-C(37)-C(36)	122.4(13)
C(29)-C(30)-C(31)	104.1(16)	O(2)-C(37)-C(38)	120.7(13)
C(29)-C(30)-Fe(3)	68.2(10)	C(36)-C(37)-C(38)	116.4(12)
C(31)-C(30)-Fe(3)	68.8(10)	C(42)-C(38)-C(37)	129.7(12)
C(29)-C(30)-H(30)	128.0	C(42)-C(38)-C(39)	112.0(12)
C(31)-C(30)-H(30)	127.9	C(37)-C(38)-C(39)	118.3(12)
Fe(3)-C(30)-H(30)	126.5	C(40)-C(39)-C(38)	102.1(12)
C(27)-C(31)-C(30)	110.6(16)	C(40)-C(39)-H(39A)	111.3
C(27)-C(31)-Fe(3)	73.2(9)	C(38)-C(39)-H(39A)	111.3
C(30)-C(31)-Fe(3)	69.5(10)	C(40)-C(39)-H(39B)	111.4
C(27)-C(31)-H(31)	124.7	C(38)-C(39)-H(39B)	111.4
C(30)-C(31)-H(31)	124.7	H(39A)-C(39)-H(39B)	109.2
Fe(3)-C(31)-H(31)	124.1	C(39)-C(40)-C(41)	108.6(14)
C(33)-C(32)-C(36)	107.1(13)	C(39)-C(40)-H(40A)	110.0
C(33)-C(32)-Fe(3)	69.8(9)	C(41)-C(40)-H(40A)	109.9
C(36)-C(32)-Fe(3)	69.6(8)	C(39)-C(40)-H(40B)	110.0
C(33)-C(32)-H(32)	126.5	C(41)-C(40)-H(40B)	110.0
C(36)-C(32)-H(32)	126.4	H(40A)-C(40)-H(40B)	108.3
Fe(3)-C(32)-H(32)	125.7	C(42)-C(41)-C(40)	99.2(12)
C(32)-C(33)-C(34)	110.1(15)	C(42)-C(41)-H(41A)	111.9
C(32)-C(33)-Fe(3)	69.7(9)	C(40)-C(41)-H(41A)	111.9
C(34)-C(33)-Fe(3)	71.6(9)	C(42)-C(41)-H(41B)	111.9
C(32)-C(33)-H(33)	124.9	C(40)-C(41)-H(41B)	111.9
C(34)-C(33)-H(33)	124.9	H(41A)-C(41)-H(41B)	109.6
Fe(3)-C(33)-H(33)	125.3	C(38)-C(42)-C(41)	112.6(12)
C(35)-C(34)-C(33)	107.2(14)	C(38)-C(42)-C(43)	127.7(13)
C(35)-C(34)-Fe(3)	69.6(9)	C(41)-C(42)-C(43)	119.6(11)
C(33)-C(34)-Fe(3)	68.3(9)	C(44)-C(43)-C(47)	102.2(13)
C(35)-C(34)-H(34)	126.4	C(44)-C(43)-C(42)	132.3(13)
C(33)-C(34)-H(34)	126.4	C(47)-C(43)-C(42)	125.3(13)
Fe(3)-C(34)-H(34)	127.2	C(44)-C(43)-Fe(2)	69.4(9)
C(34)-C(35)-C(36)	109.7(14)	C(47)-C(43)-Fe(2)	66.6(8)
C(34)-C(35)-Fe(3)	71.4(9)	C(42)-C(43)-Fe(2)	123.0(10)
C(36)-C(35)-Fe(3)	68.7(8)	C(45)-C(44)-C(43)	112.3(13)
C(34)-C(35)-H(35)	125.2	C(45)-C(44)-Fe(2)	71.4(9)
C(36)-C(35)-H(35)	125.1	C(43)-C(44)-Fe(2)	70.8(8)
Fe(3)-C(35)-H(35)	126.4	C(45)-C(44)-H(44)	123.9

Table 3.10, Continued

C(43)-C(44)-H(44)	123.9	Fe(2)-C(48)-H(48)	127.2
Fe(2)-C(44)-H(44)	125.5	C(48)-C(49)-C(50)	105.8(18)
C(44)-C(45)-C(46)	108.8(13)	C(48)-C(49)-Fe(2)	70.0(9)
C(44)-C(45)-Fe(2)	70.8(9)	C(50)-C(49)-Fe(2)	70.3(11)
C(46)-C(45)-Fe(2)	69.5(8)	C(48)-C(49)-H(49)	127.0
C(44)-C(45)-H(45)	125.6	C(50)-C(49)-H(49)	127.1
C(46)-C(45)-H(45)	125.6	Fe(2)-C(49)-H(49)	124.2
Fe(2)-C(45)-H(45)	125.6	C(51)-C(50)-C(49)	113.1(19)
C(47)-C(46)-C(45)	107.1(12)	C(51)-C(50)-Fe(2)	72.0(11)
C(47)-C(46)-Fe(2)	69.1(8)	C(49)-C(50)-Fe(2)	71.5(10)
C(45)-C(46)-Fe(2)	69.7(9)	C(51)-C(50)-H(50)	123.5
C(47)-C(46)-H(46)	126.4	C(49)-C(50)-H(50)	123.4
C(45)-C(46)-H(46)	126.5	Fe(2)-C(50)-H(50)	124.7
Fe(2)-C(46)-H(46)	126.3	C(50)-C(51)-C(52)	113.1(18)
C(46)-C(47)-C(43)	109.6(14)	C(50)-C(51)-Fe(2)	71.0(11)
C(46)-C(47)-Fe(2)	72.4(9)	C(52)-C(51)-Fe(2)	70.3(10)
C(43)-C(47)-Fe(2)	70.4(8)	C(50)-C(51)-H(51)	123.5
C(46)-C(47)-H(47)	125.3	C(52)-C(51)-H(51)	123.4
C(43)-C(47)-H(47)	125.2	Fe(2)-C(51)-H(51)	127.0
Fe(2)-C(47)-H(47)	123.6	C(48)-C(52)-Fe(2)	67.3(9)
C(49)-C(48)-C(52)	110.4(18)	C(51)-C(52)-H(52)	131.3
C(49)-C(48)-Fe(2)	70.5(9)	C(48)-C(52)-H(52)	131.4
C(52)-C(48)-Fe(2)	69.1(8)	Fe(2)-C(52)-H(52)	124.4
C(49)-C(48)-H(48)	124.9	C(51)-C(52)-C(48)	97.3(17)
C(52)-C(48)-H(48)	124.7	C(51)-C(52)-Fe(2)	68.7(9)

Symmetry transformations used to generate equivalent atoms:

#1 -x+1,-y,-z

Table 3.11

Anisotropic Displacement Parameters ($\text{\AA}^2 \times 10^3$) for 1-ferrocenylcarbonyl-2-ferrocenylcyclopentene. The anisotropic displacement factor exponent takes the form: $-2 \pi^2 [h^2 a^{*2} U_{11} + \dots + 2 h k a^* b^* U_{12}]$

Atom Number	U11	U22	U33	U23	U13	U12
Fe(1)	38(1)	32(1)	49(1)	4(1)	2(1)	19(1)
Fe(2)	54(1)	28(1)	46(1)	-1(1)	-14(1)	-7(1)
Fe(3)	31(1)	45(1)	44(1)	1(1)	23(1)	-5(1)
Fe(4)	47(2)	49(1)	56(2)	16(1)	-4(1)	12(1)
O(1)	52(7)	102(9)	54(6)	27(6)	25(5)	35(6)
O(2)	47(6)	87(8)	42(6)	23(5)	3(4)	23(5)
C(1)	29(7)	56(8)	44(7)	-17(6)	-2(5)	-6(6)
C(2)	51(10)	61(10)	71(12)	-9(9)	-3(8)	-29(7)
C(3)	64(10)	38(7)	96(13)	1(8)	32(9)	12(7)
C(4)	65(12)	72(11)	86(13)	17(10)	4(9)	-1(9)
C(5)	42(7)	47(7)	46(7)	-26(5)	24(5)	-19(6)
C(6)	56(8)	35(6)	39(7)	28(5)	25(6)	7(5)
C(7)	42(10)	45(9)	72(12)	3(8)	15(8)	20(7)
C(8)	59(9)	43(7)	41(8)	-2(6)	12(6)	29(6)
C(9)	46(8)	71(9)	11(5)	-21(5)	5(5)	-24(6)
C(10)	40(2)	32(2)	32(3)	2(2)	9(2)	2(2)
C(11)	31(2)	33(2)	41(2)	8(2)	9(2)	-1(2)
C(12)	32(8)	30(7)	52(9)	2(6)	17(6)	4(6)
C(13)	45(7)	60(8)	46(8)	20(6)	21(6)	23(6)
C(14)	80(10)	46(7)	15(5)	3(5)	4(6)	-6(7)
C(15)	52(8)	36(7)	74(10)	24(6)	39(7)	18(6)
C(16)	32(2)	38(2)	32(2)	6(2)	10(2)	7(2)
C(17)	31(2)	40(2)	36(3)	12(2)	1(2)	5(2)
C(18)	61(9)	49(7)	35(7)	-12(6)	-13(6)	-9(6)
C(19)	55(11)	87(12)	95(14)	59(11)	17(9)	-5(9)
C(20)	39(8)	23(6)	85(11)	-5(7)	-43(7)	-8(5)
C(21)	63(8)	27(6)	23(6)	-3(5)	-22(5)	-8(5)
C(22)	73(12)	114(15)	36(8)	33(10)	-22(8)	31(11)
C(23)	84(13)	72(11)	59(10)	19(8)	-21(9)	-8(9)
C(24)	150(20)	52(10)	91(15)	-23(9)	-86(14)	14(11)
C(25)	103(16)	100(14)	86(15)	3(11)	-8(11)	73(13)
C(26)	60(9)	52(7)	42(8)	3(6)	-17(6)	-12(6)
C(27)	82(13)	25(7)	98(13)	17(7)	55(10)	-10(7)

Table 3.11, Continued

C(28)	62(9)	29(7)	135(15)	20(8)	19(9)	17(6)
C(29)	83(12)	55(10)	76(11)	-9(8)	27(9)	-8(8)
C(30)	25(8)	75(11)	117(16)	-24(10)	8(9)	21(7)
C(31)	58(10)	101(13)	92(14)	-10(11)	52(10)	-31(9)
C(32)	48(8)	30(6)	75(9)	17(6)	22(6)	29(6)
C(33)	48(9)	76(10)	69(11)	-31(8)	32(8)	-16(7)
C(34)	56(11)	41(8)	64(12)	1(8)	1(9)	16(7)
C(35)	40(7)	49(8)	58(9)	-3(6)	-10(6)	24(6)
C(36)	40(2)	32(2)	32(3)	2(2)	9(2)	2(2)
C(37)	31(2)	33(2)	41(2)	8(2)	9(2)	-1(2)
C(38)	36(8)	43(8)	14(6)	2(5)	0(5)	10(6)
C(39)	80(10)	43(8)	42(8)	-32(6)	3(7)	-28(7)
C(40)	93(13)	64(10)	67(11)	-11(8)	22(10)	3(9)
C(41)	57(9)	94(11)	10(5)	-6(6)	1(5)	6(7)
C(42)	32(2)	38(2)	32(2)	6(2)	10(2)	7(2)
C(43)	31(2)	40(2)	36(3)	12(2)	1(2)	5(2)
C(44)	31(6)	56(8)	57(9)	12(7)	19(6)	13(6)
C(45)	91(12)	68(11)	32(7)	8(7)	11(7)	20(9)
C(46)	26(7)	29(6)	97(12)	-9(7)	-25(7)	-8(5)
C(47)	26(6)	51(8)	79(10)	37(7)	21(6)	4(6)
C(48)	90(15)	33(8)	180(20)	62(12)	-23(15)	8(8)
C(49)	104(15)	61(11)	109(15)	2(10)	-13(11)	63(11)
C(50)	51(10)	90(13)	64(12)	18(10)	7(8)	13(9)
C(51)	54(9)	64(9)	84(12)	13(9)	-11(8)	35(7)
C(52)	100(15)	55(10)	74(12)	25(9)	6(10)	23(9)

Table 3.12

Hydrogen Coordinates ($\times 10^4$) and Isotropic Displacement Parameters ($\text{Å}^2 \times 10^3$) for
1-ferrocenylcarbonyl-2-ferrocenylcyclopentene

Atom Number	x	y	z	U(eq)
H(1)	2981	3783	4022	56
H(2)	5080	3057	2912	81
H(3)	4539	3695	996	76
H(4)	1892	4812	817	92
H(5)	1142	4815	2741	57
H(6)	780	815	3148	48
H(7)	2844	234	1978	62
H(8)	2064	895	34	55
H(9)	-453	1952	6	56
H(13A)	-1282	3943	3917	56
H(13B)	128	3115	4298	56
H(14A)	-915	2733	5883	59
H(14B)	-2440	3417	5429	59
H(15A)	-3902	1489	5029	58
H(15B)	-2343	811	5355	58
H(18)	-5171	-676	4271	65
H(19)	-6507	-2642	2859	94
H(20)	-5204	-2495	1186	70
H(21)	-3083	-353	1523	52
H(22)	-2290	-2318	5405	91
H(23)	-3747	-4122	4208	93
H(24)	-2589	-4297	2507	135
H(25)	-297	-2220	2610	113
H(26)	-461	-889	4513	69
H(27)	-1689	4170	10015	77
H(28)	-575	4159	8288	88
H(29)	-2619	5252	6890	87
H(30)	-4658	5961	7880	88
H(31)	-3894	5331	9871	101
H(32)	947	7035	10700	56
H(33)	-1563	8051	10699	79
H(34)	-2467	8821	8816	65
H(35)	-549	8278	7613	60
H(39A)	1443	4986	6783	74
H(39B)	240	5953	6303	74
H(40A)	1515	5916	4915	91

Table 3.12, Continued

H(40B)	3070	5498	5652	91
H(41A)	4228	7638	5637	66
H(41B)	2501	8117	5360	66
H(44)	3641	9427	9281	55
H(45)	5564	11423	9634	75
H(46)	6947	11698	7961	69
H(47)	5751	9851	6559	59
H(48)	4018	13336	6738	127
H(49)	2852	13147	8463	110
H(50)	779	11215	8116	82
H(51)	577	10110	6351	81
H(52)	2751	11191	5317	91

Table 3.13

Crystal Data and Structure Refinement for 1,6-diferrocenylnhexane

Empirical formula	C ₂₆ H ₃₀ Fe ₂
Formula weight	454.20
Temperature	293(2) K
Wavelength	0.71073 Å
Crystal system, space group	Monoclinic, P2(1)/c
Unit cell dimensions	a = 12.8908(11) Å alpha = 90° b = 8.3936(7) Å beta = 98.572(2)° c = 10.0431(9) Å gamma = 90°
Volume	1074.53(16) Å ³
Z, Calculated density	2, 1.404 Mg/m ³
Absorption coefficient	1.358 mm ⁻¹
F(000)	476
Crystal size	0.06 x 0.10 x 0.04 mm
Theta range for data collection	1.60 to 28.28 deg.
Limiting indices	-17 ≤ h ≤ 17, -10 ≤ k ≤ 10, -13 ≤ l ≤ 13
Reflections collected / unique	9429 / 2594 [R(int) = 0.0494]
Completeness to theta = 28.28	97.2 %
Absorption correction	None
Refinement method	Full-matrix least-squares on F ²
Hydrogen Atom Positions	Constrained
Data / restraints / parameters	2594 / 0 / 127
Goodness-of-fit on F ²	1.063
Final R indices [I > 2σ(I)]	R1(F) ^a = 0.0637, wR2(F ²) ^b = 0.1420
R indices (all data)	R1(F) ^a = 0.0960, wR2(F ²) ^b = 0.1552
Largest diff. peak and hole	0.426 and -0.424 e.Å ⁻³

$${}^a R_1(F) = \frac{\sum ||F_o| - |F_c||}{\sum |F_o|} \text{ with } F_o > 4.0\sigma(F).$$

$${}^b wR_2(F^2) = \left[\frac{\sum [w(F_o^2 - F_c^2)^2]}{\sum [w(F_o^2)^2]} \right]^{1/2} \text{ with } F_o > 4.0\sigma(F), \text{ and } w^{-1} = \sigma^2(F_o)^2 + (W \cdot P)^2 + T \cdot P, \text{ where } P = (\text{Max}(F_o^2, 0) + 2F_c^2)/3, W = 0.0600, \text{ and } T = 1.18.$$

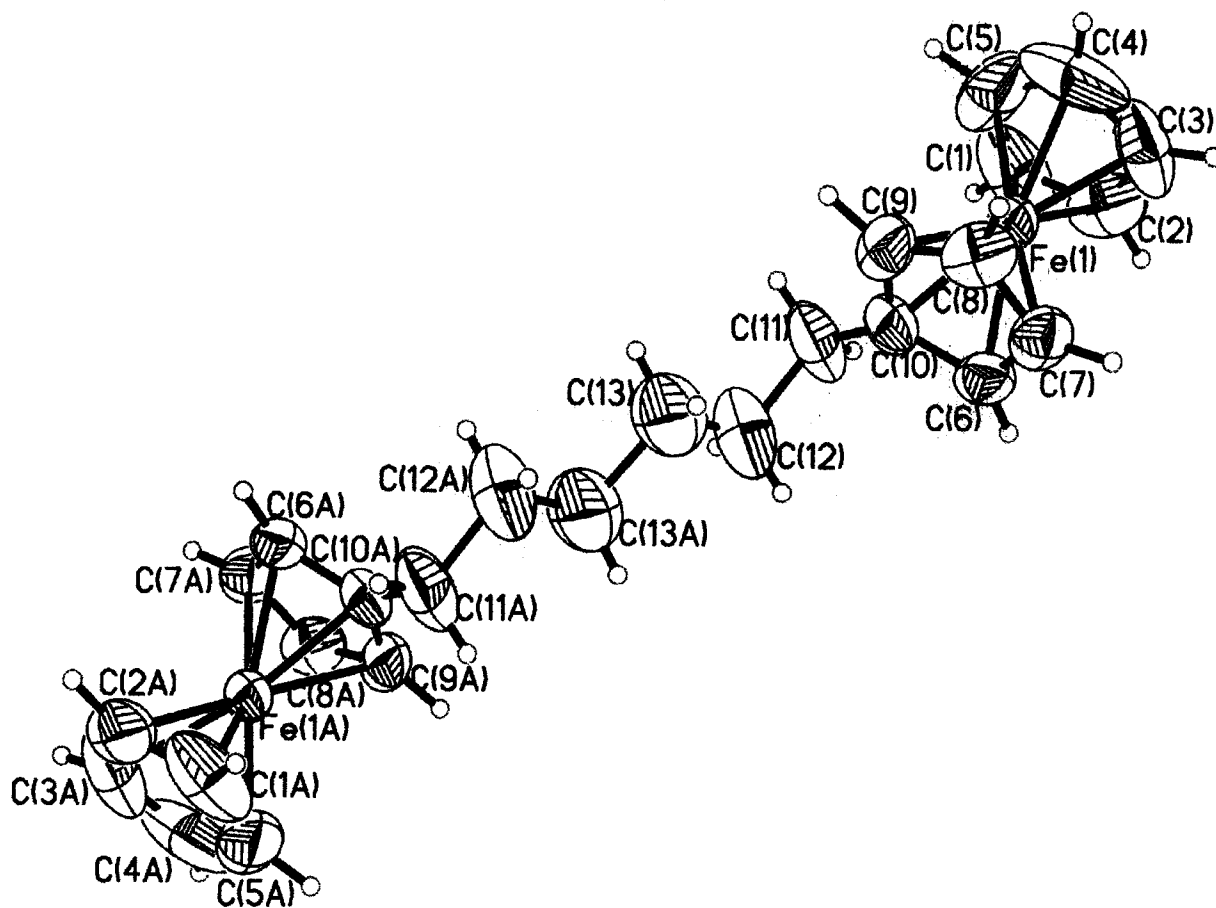


Figure 3.6: ORTEP plot of 1,6-diferrocenylhexane (50% ellipsoids)

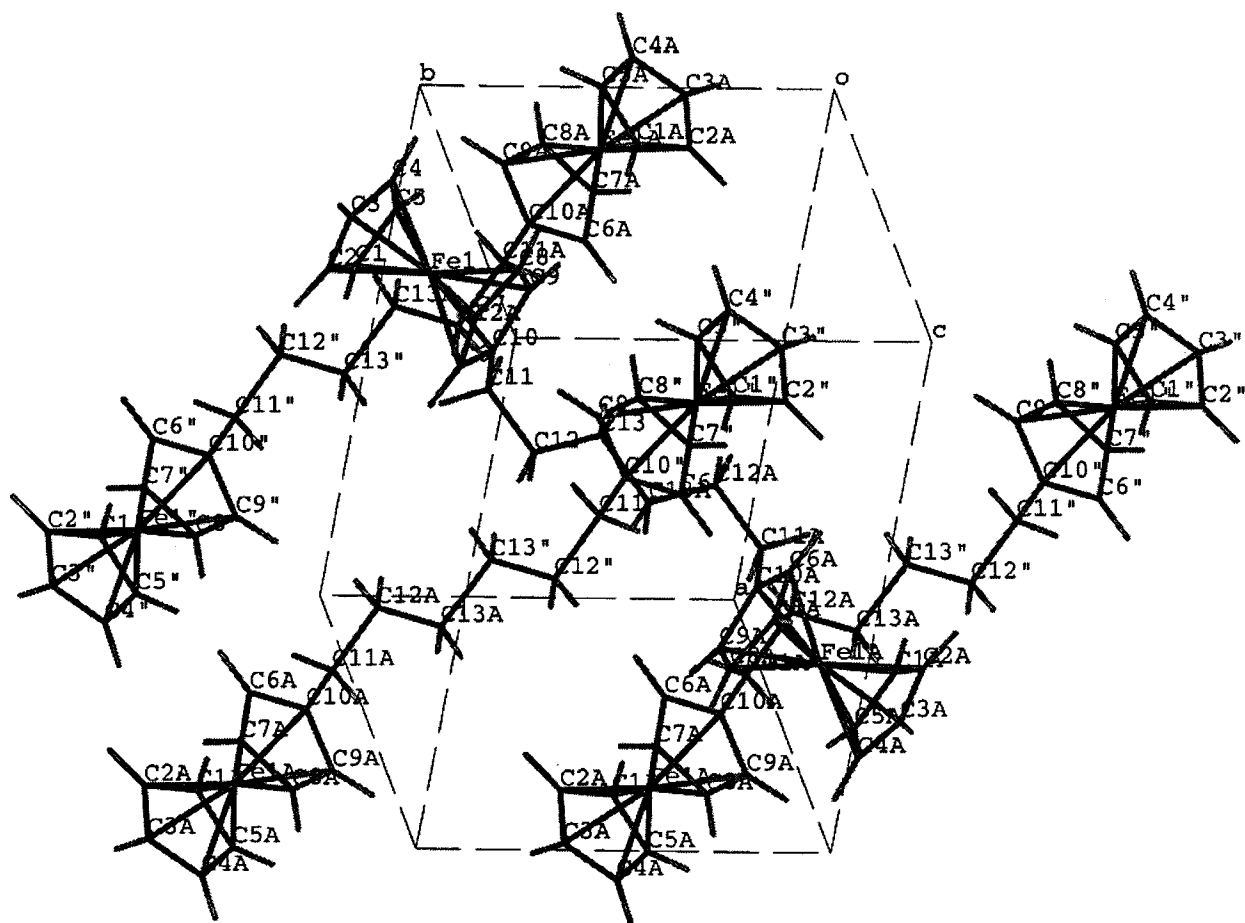


Figure 3.7: Unit cell of 1,6-diferrocenylhexane

Table 3.14

Atomic Coordinates ($\times 10^4$) and Equivalent Isotropic Displacement Parameters ($\text{\AA}^2 \times 10^3$) for 1,6-diferrocenylohexane. $U(\text{eq})$ is defined as one third of the trace of the orthogonalized U_{ij} tensor.

Atom Number	x	y	z	$U(\text{eq})$
Fe(1)	1894(1)	10132(1)	3653(1)	50(1)
C(1)	2444(5)	11477(10)	2270(9)	110(3)
C(2)	2071(7)	12438(6)	3194(6)	95(2)
C(3)	1050(7)	12117(9)	3138(8)	109(3)
C(4)	781(6)	10979(13)	2237(11)	138(4)
C(5)	1622(12)	10561(9)	1684(6)	138(4)
C(6)	2833(4)	9588(5)	5394(4)	64(1)
C(7)	1782(4)	9501(6)	5573(4)	67(1)
C(8)	1293(4)	8363(6)	4679(4)	71(1)
C(9)	2043(4)	7749(5)	3929(4)	69(1)
C(10)	3020(4)	8518(5)	4369(4)	64(1)
C(11)	4036(4)	8259(7)	3847(6)	100(2)
C(12)	4835(5)	7164(9)	4722(8)	128(3)
C(13)	4548(7)	5590(8)	4590(9)	137(3)

Table 3.15
Bond Lengths [Å] for 1,6-diferrocenylhexane

C(1)-C(5)	1.369(11)
C(1)-C(2)	1.370(9)
C(1)-Fe(1)	1.999(5)
C(1)-H(1)	0.9800
C(2)-C(3)	1.335(9)
C(2)-Fe(1)	2.010(5)
C(2)-H(2)	0.9800
C(3)-C(4)	1.326(11)
C(3)-Fe(1)	2.015(5)
C(3)-H(3)	0.9800
C(4)-C(5)	1.337(11)
C(4)-Fe(1)	1.995(6)
C(4)-H(4)	0.9800
C(5)-Fe(1)	1.990(6)
C(5)-H(5)	0.9800
C(6)-C(7)	1.395(7)
C(6)-C(10)	1.414(6)
C(6)-Fe(1)	2.025(4)
C(6)-H(6)	0.9800
C(7)-C(8)	1.396(6)
C(7)-Fe(1)	2.026(4)
C(7)-H(7)	0.9800
C(8)-C(9)	1.408(6)
C(8)-Fe(1)	2.026(4)
C(8)-H(8)	0.9800
C(9)-C(10)	1.426(6)
C(9)-Fe(1)	2.024(4)
C(9)-H(9)	0.9800
C(10)-C(11)	1.497(7)
C(10)-Fe(1)	2.036(4)
C(11)-C(12)	1.552(8)
C(11)-H(11A)	0.9700
C(11)-H(11B)	0.9700
C(12)-C(13)	1.373(10)
C(12)-H(12A)	0.9700
C(12)-H(12B)	0.9700
C(13)-C(13)#1	1.654(14)
C(13)-H(13A)	0.9700
C(13)-H(13B)	0.9700

Symmetry transformations used to generate equivalent atoms: #1 -x+1,-y,-z

Table 3.16

Bond Angles [degrees] for 1,6-diferrocenylnhexane

C(5)-C(1)-C(2)	107.1(6)	Fe(1)-C(7)-H(7)	126.1
C(5)-C(1)-Fe(1)	69.5(4)	C(7)-C(8)-C(9)	108.3(4)
C(2)-C(1)-Fe(1)	70.4(3)	C(7)-C(8)-Fe(1)	69.8(2)
C(5)-C(1)-H(1)	126.4	C(9)-C(8)-Fe(1)	69.6(2)
C(2)-C(1)-H(1)	126.4	C(7)-C(8)-H(8)	125.8
Fe(1)-C(1)-H(1)	126.4	C(9)-C(8)-H(8)	125.8
C(3)-C(2)-C(1)	107.2(6)	Fe(1)-C(8)-H(8)	125.8
C(3)-C(2)-Fe(1)	70.8(3)	C(8)-C(9)-C(10)	108.3(4)
C(1)-C(2)-Fe(1)	69.6(3)	C(8)-C(9)-Fe(1)	69.7(2)
C(3)-C(2)-H(2)	126.4	C(10)-C(9)-Fe(1)	69.9(2)
C(1)-C(2)-H(2)	126.4	C(8)-C(9)-H(9)	125.8
Fe(1)-C(2)-H(2)	126.4	C(10)-C(9)-H(9)	125.8
C(4)-C(3)-C(2)	109.3(7)	Fe(1)-C(9)-H(9)	125.8
C(4)-C(3)-Fe(1)	69.9(4)	C(6)-C(10)-C(9)	105.9(4)
C(2)-C(3)-Fe(1)	70.4(3)	C(6)-C(10)-C(11)	126.9(5)
C(4)-C(3)-H(3)	125.4	C(9)-C(10)-C(11)	127.2(5)
C(2)-C(3)-H(3)	125.4	C(6)-C(10)-Fe(1)	69.2(2)
Fe(1)-C(3)-H(3)	125.4	C(9)-C(10)-Fe(1)	69.0(2)
C(3)-C(4)-C(5)	109.1(8)	C(11)-C(10)-Fe(1)	126.0(3)
C(3)-C(4)-Fe(1)	71.5(4)	C(10)-C(11)-C(12)	115.5(5)
C(5)-C(4)-Fe(1)	70.2(4)	C(10)-C(11)-H(11A)	108.4
C(3)-C(4)-H(4)	125.5	C(12)-C(11)-H(11A)	108.4
C(5)-C(4)-H(4)	125.5	C(10)-C(11)-H(11B)	108.4
Fe(1)-C(4)-H(4)	125.5	C(12)-C(11)-H(11B)	108.4
C(4)-C(5)-C(1)	107.3(7)	H(11A)-C(11)-H(11B)	107.5
C(4)-C(5)-Fe(1)	70.6(4)	C(13)-C(12)-C(11)	111.6(7)
C(1)-C(5)-Fe(1)	70.3(4)	C(13)-C(12)-H(12A)	109.3
C(4)-C(5)-H(5)	126.3	C(11)-C(12)-H(12A)	109.3
C(1)-C(5)-H(5)	126.3	C(13)-C(12)-H(12B)	109.3
Fe(1)-C(5)-H(5)	126.3	C(11)-C(12)-H(12B)	109.3
C(7)-C(6)-C(10)	109.6(4)	H(12A)-C(12)-H(12B)	108.0
C(7)-C(6)-Fe(1)	69.9(3)	C(12)-C(13)-C(13)#1	111.6(9)
C(10)-C(6)-Fe(1)	70.1(2)	C(12)-C(13)-H(13A)	109.3
C(7)-C(6)-H(6)	125.2	C(13)#1-C(13)-H(13A)	109.3
C(10)-C(6)-H(6)	125.2	C(12)-C(13)-H(13B)	109.3
Fe(1)-C(6)-H(6)	125.2	C(13)#1-C(13)-H(13B)	109.3
C(6)-C(7)-C(8)	107.9(4)	H(13A)-C(13)-H(13B)	108.0
C(6)-C(7)-Fe(1)	69.8(2)	C(5)-Fe(1)-C(4)	39.2(3)
C(8)-C(7)-Fe(1)	69.9(2)	C(5)-Fe(1)-C(1)	40.2(3)
C(6)-C(7)-H(7)	126.1	C(4)-Fe(1)-C(1)	66.1(3)
C(8)-C(7)-H(7)	126.1	C(5)-Fe(1)-C(2)	66.9(3)

Table 3.16, Continued

C(4)-Fe(1)-C(2)	65.6(3)	C(3)-Fe(1)-C(7)	110.4(2)
C(1)-Fe(1)-C(2)	40.0(3)	C(9)-Fe(1)-C(7)	68.29(19)
C(5)-Fe(1)-C(3)	65.6(3)	C(6)-Fe(1)-C(7)	40.30(19)
C(4)-Fe(1)-C(3)	38.6(3)	C(5)-Fe(1)-C(8)	127.9(4)
C(1)-Fe(1)-C(3)	65.7(3)	C(4)-Fe(1)-C(8)	109.5(3)
C(2)-Fe(1)-C(3)	38.7(3)	C(1)-Fe(1)-C(8)	165.7(3)
C(5)-Fe(1)-C(9)	108.3(2)	C(2)-Fe(1)-C(8)	152.5(3)
C(4)-Fe(1)-C(9)	119.5(3)	C(3)-Fe(1)-C(8)	120.3(3)
C(1)-Fe(1)-C(9)	128.1(3)	C(9)-Fe(1)-C(8)	40.68(18)
C(2)-Fe(1)-C(9)	166.2(3)	C(6)-Fe(1)-C(8)	67.7(2)
C(3)-Fe(1)-C(9)	152.7(3)	C(7)-Fe(1)-C(8)	40.31(18)
C(5)-Fe(1)-C(6)	153.3(5)	C(5)-Fe(1)-C(10)	118.8(3)
C(4)-Fe(1)-C(6)	165.9(4)	C(3)-Fe(1)-C(10)	165.9(4)
C(1)-Fe(1)-C(6)	119.9(3)	C(9)-Fe(1)-C(10)	41.11(18)
C(2)-Fe(1)-C(6)	110.0(2)	C(6)-Fe(1)-C(10)	40.75(17)
C(3)-Fe(1)-C(6)	129.7(3)	C(7)-Fe(1)-C(10)	68.81(19)
C(9)-Fe(1)-C(6)	68.09(18)	C(2)-Fe(1)-C(10)	128.5(3)
C(5)-Fe(1)-C(7)	165.2(4)	C(4)-Fe(1)-C(10)	152.6(4)
C(4)-Fe(1)-C(7)	128.8(4)	C(1)-Fe(1)-C(10)	108.2(2)
C(1)-Fe(1)-C(7)	153.1(3)	C(8)-Fe(1)-C(10)	68.9(2)
C(2)-Fe(1)-C(7)	119.8(2)		

Symmetry transformations used to generate equivalent atoms:

#1 -x+1,-y,-z

Table 3.17

Anisotropic Displacement Parameters ($\text{\AA}^2 \times 10^3$) for 1,6-diferrocenylhexane. The anisotropic displacement factor exponent takes the form: $-2 \pi^2 [h^2 a^{*2} U_{11} + \dots + 2 h k a^* b^* U_{12}]$

Atom Number	U11	U22	U33	U23	U13	U12
Fe(1)	60(1)	42(1)	47(1)	4(1)	8(1)	4(1)
C(1)	100(5)	126(6)	117(5)	77(5)	62(4)	38(4)
C(2)	148(6)	53(3)	76(4)	19(3)	-13(4)	-21(3)
C(3)	127(6)	88(5)	127(6)	49(4)	64(5)	59(4)
C(4)	100(5)	128(8)	163(9)	81(7)	-58(6)	-17(5)
C(5)	287(14)	74(4)	45(3)	5(3)	1(5)	33(7)
C(6)	82(3)	52(2)	53(2)	4(2)	-9(2)	2(2)
C(7)	90(3)	66(3)	47(2)	5(2)	16(2)	3(2)
C(8)	84(3)	66(3)	61(3)	12(2)	10(2)	-21(2)
C(9)	110(4)	41(2)	55(3)	4(2)	9(3)	1(2)
C(10)	76(3)	50(2)	64(3)	11(2)	5(2)	17(2)
C(11)	94(4)	90(4)	120(5)	24(3)	27(4)	50(3)
C(12)	122(6)	98(5)	164(7)	4(5)	24(5)	45(4)
C(13)	183(8)	76(4)	139(6)	12(4)	-15(6)	13(5)

Table 3.18

Hydrogen Coordinates ($\times 10^4$) and Isotropic Displacement Parameters ($\text{Å}^2 \times 10^3$) for
1,6-diferrocenylhexane

Atom Number	x	y	z	U(eq)
H(1)	3160	11467	2053	132
H(2)	2472	13238	3767	114
H(3)	577	12633	3685	131
H(4)	75	10533	2000	166
H(5)	1639	9778	963	165
H(6)	3357	10302	5887	77
H(7)	1447	10125	6217	80
H(8)	553	8052	4582	85
H(9)	1914	6938	3223	83
H(11A)	4364	9287	3763	120
H(11B)	3885	7803	2952	120
H(12A)	5523	7299	4455	153
H(12B)	4883	7475	5660	153
H(13A)	4437	5305	3643	164
H(13B)	3891	5437	4934	164

International Tables of Crystallography and are in agreement.¹ Sp^2 hybridized carbon bond lengths were approximately 1.4 Å with the carbon-hydrogen bonds in agreement with the typical 1.0 Å. Sp^3 hybridized carbon-carbon bond lengths were consistent with the theoretical values of 1.5 Å. The iron bond lengths to the carbons in the cyclopentene rings were in agreement with one another, displaying lengths of 2.0 Å, which are typical of ferrocene derivatives. The bond angles between the iron and carbons in the ring above and below also demonstrated agreement with literature values.^{2,3} The carbon-carbon bond angles in the Cp rings were also in agreement with literature values.^{2,3}

The planarity of the top and bottom Cp rings was calculated in XSELL. The equation of the mean plane and atomic deviations from the planes are given in Table A-1 and A-2 of Appendix A. The plane defined by C1 to C5 had a maximum deviation of 0.0020 Å, attributed to C1. The top Cp ring, containing C6 to C10, had a maximum deviation of 0.0042 Å at C9.

The planarity of the Cp ring with respect to the carbonyl was also investigated. The plane that included O1 and C6 to C10 showed a maximum deviation of 0.0046 Å from the plane due to C8. It is interesting to note that the carbonyl lies in the plane of the Cp ring to maximize electronic interactions between the Cp ring and the carbonyl group.

Due to the symmetry of 1,6-diferrocenylohexane-1,6-dione, half of the structure was in the asymmetric unit and the grow command was used to generate the other half. Utilizing this command put the ferrocenes 180 °C out of phase with respect to one another. The planarity calculations for the Cp rings produced the same results as previously stated. In addition, the top and bottom Cp rings of the ferrocenes, were eclipsed with respect to one another.

Characterization of 1-ferrocenylcarbonyl-2-ferrocenylcyclopentene

The sp^2 carbon-carbon bonds in the Cp rings demonstrated the appropriate bond lengths, 2.0 Å from the iron centers, as well as with respect to each other, 1.4 Å. The carbon-carbon sp^2 and sp^3 bond lengths in the cyclopentene ring were consistent with literature values at 1.3 Å and 1.5 Å, respectively. The bond between C12 and C16 was longer than expected for a double bond, suggesting the presence of a single bond. However, the results from the mass spectrometry and ^{13}C NMR experiments clearly demonstrate the presence of a C=C double bond. In addition the bond angles associated with C12, C16, C38, and C42 are in accordance with sp^2 hybridized carbons, further indicating the presence of a carbon-carbon double bond. Thus, it was concluded that the cyclopentene ring contained a double bond.

The coplanarity of the Cp rings within the ferrocene with respect to the carbonyl group was calculated. The maximum deviation in the plane defined by C6 to C11 containing O1, occurred at O1 with a value of 0.0567 Å, while the plane defined by O2 and C32 to C37 was 0.0462 Å at C37. The carbonyl, as in 1,6-diferrocenylhexane-1,6-dione, is coplanar with the adjacent Cp ring to maximize electronic interactions. The equations for the plane, as well as the atom deviations from the plane, are shown in Tables B-1 and B-2 in Appendix B. Figure 3.8 displays an ORTEP plot illustrating the coplanarity of the carbonyl with the adjacent Cp ring.

The planarity of the cyclopentene ring with respect to the adjacent Cp ring was also calculated in XSELL. The maximum deviation from the plane was 0.1195 Å at C12 in the plane defined by C12 to C21. Thus, the cyclopentene group and the neighboring Cp ring are nearly coplanar with respect to one another. The plane that included C38 to C47

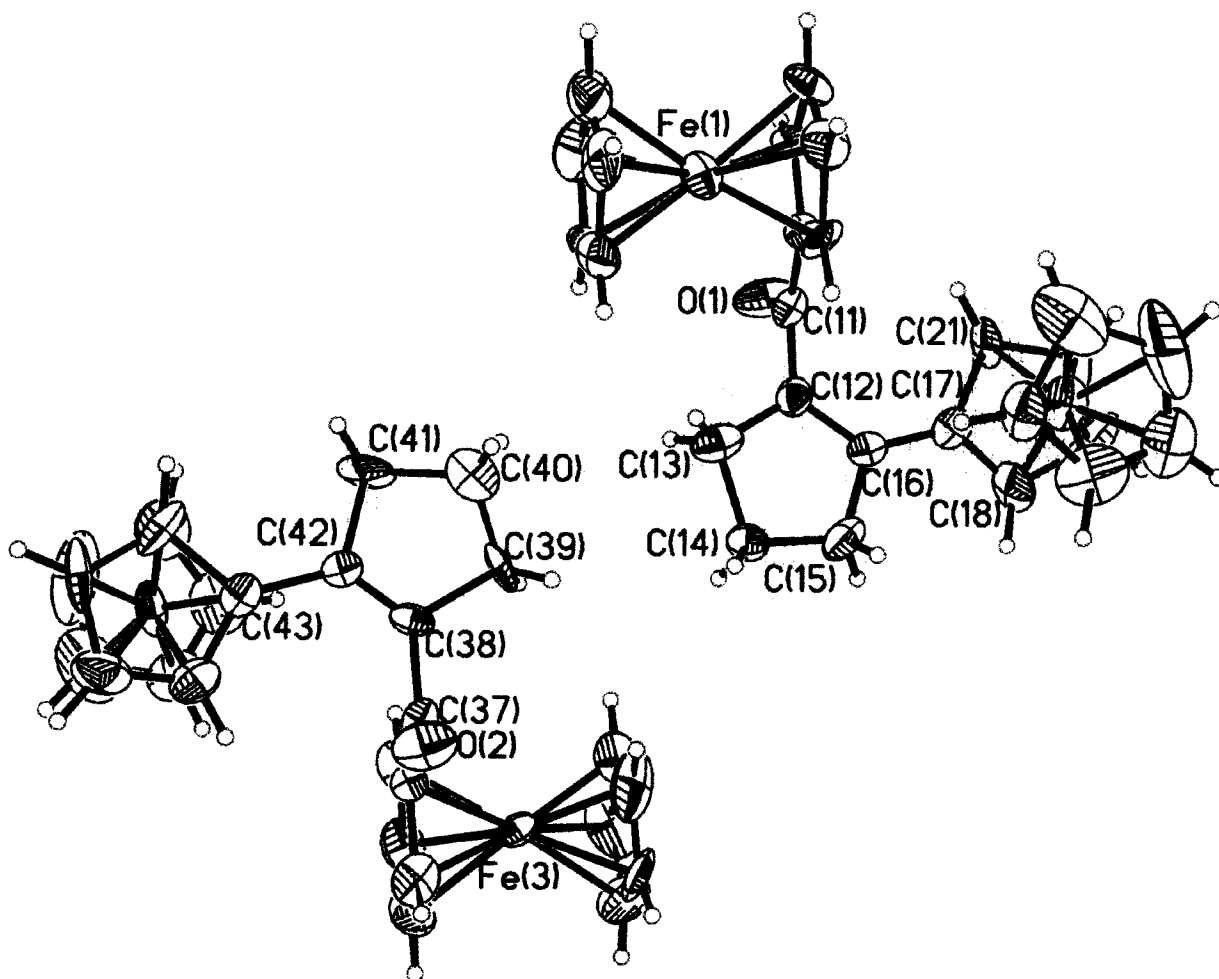


Figure 3.8: ORTEP plot of 1-ferrocenylcarbonyl-2-ferrocenylcyclopentene (50% ellipsoids) demonstrating coplanarity of carbonyl with adjacent Cp ring.

demonstrated a maximum deviation of 0.2523 Å at C41 also demonstrating the near coplanarity between the cyclopentene and Cp rings. An ORTEP plot shown in Figure 3.9 shows the coplanarity between the cyclopentene ring and the adjacent Cp ring. The equation of the planes for the five-membered ring, as well as atomic deviations from the plane can be found in Tables B-3 and B-4 in Appendix B.

The planarity of the Cp rings was calculated for the four ferrocenes 1-ferrocenyl-carbonyl-2-ferrocenylcyclopentene was also calculated. The equations of the mean planes and atomic deviations are located in Tables B-5 to B-12 for all eight Cp rings. The greatest deviation from planarity between all of the Cp rings occurred at C14 with a deviation of 0.0501 Å. Eclipsing of the top and bottom Cp rings was evident in all of the ferrocene groups.

The planarity of the cyclopentene rings were also determined and the deviations from the calculated plane are shown in Table B-13 and Table B-14 in Appendix B. The plane defined by C12 to C16 had a maximum deviation of 0.0501 Å at C14. The cyclopentene ring containing C38 to C42, deviated by 0.1300 Å from the plane at C40. Figure 3.9 gives an edge on view of the five membered ring and the maximum deviation at C40 is easily seen in this ORTEP plot.

Figure 3.9 also illustrates that the orientation of the carbonyl is out of the plane relative to the cyclopentene ring. This is attributed to steric interactions between the carbonyl group and the adjacent five-membered ring.

Characterization of 1,6-diferrocenylhexane

Bond lengths between the sp² carbon atoms in the Cp rings produced values of approximately 1.4 Å, which are typical of sp² hybridized carbons. The carbon-iron bond

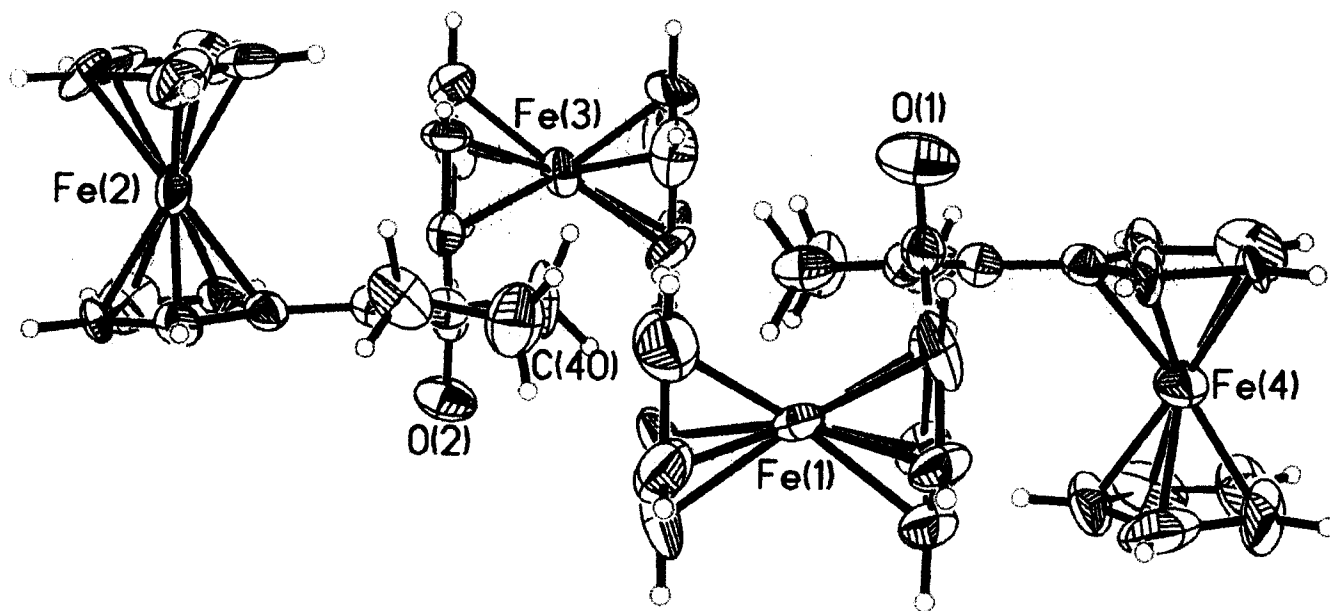


Figure 3.9: ORTEP plot of 1-ferrocenylcarbonyl-2-ferrocenylcyclopentene (50% ellipsoids) demonstrating coplanarity of cyclopentene ring with adjacent Cp ring.

bond lengths centers were also in agreement with theoretical values of 2.0 Å. The sp^3 hybridized carbon-carbon bonds in the six-carbon bridge were approximately 1.5 Å. The carbon-hydrogen bonds throughout the molecule produced typical 1.0 Å bond lengths. The bond angles were also investigated and were in agreement with those found in literature.^{2,3}

The maximum deviation from planarity for the bottom Cp ring was 0.0060 Å from the plane that included C1 to C5 and was due to C2. The planarity of the top ring only showed a 0.0040 Å deviation from the mean plane defined by C6 to C10 that was attributed to C6. Table C-1 and C-2 in Appendix C shown the equations of the mean plane and the atomic deviations for both the bottom and top rings. In addition, the top and bottom Cp rings were slightly staggered relative to one another, but not to an appreciable degree.

The grow command was also used to generate the remaining half of 1,6-diferrocenylhexane, not shown in the asymmetric unit. The ferrocenes were therefore 180° out of phase with respect to one another.

Conclusions

The crystal structures for the compounds, 1,6-diferrocenylhexane-1,6-dione, 1-ferrocenylcarbonyl-2-ferrocenylcyclopentene, and 1,6-diferrocenylhexane are presented. The structures of the fully oxidized and fully reduced compounds produced results that were consistent with literature values and refinement was straightforward. Since the structure of 1-ferrocenylcarbonyl-2-ferrocenylcyclopentane was not known prior to structure refinement, the results were surprising, i.e. chirality.

All three crystals produced bond lengths and angles that were similar with respect to one another, and were also in agreement with those reported in the literature.¹⁻³ The sp^2 carbon bond lengths were approximately 1.3 Å to 1.4 Å and sp^3 - sp^2 carbon bond lengths were 1.5 Å. The carbon bonds to the iron centers were all consistent at 2.0 Å and the carbon-hydrogen bonds were approximately 1.0 Å.

The top and bottom Cp rings were coplanar in all three crystal structures. The carbonyl moieties in both the 1,6-diferrocenylohexane-1,6-dione and 1-ferrocenylcarbonyl-2-ferrocenylcyclopentene were found to be coplanar with the adjacent Cp rings, allowing for maximization of electronic interactions between the two. The deviation from planarity of the oxygen in the 1,6-diferrocenylohexane-1,6-dione was compared to both oxygen's in 1-ferrocenylcarbonyl-2-ferrocenylcyclopentene. The plane defined by O1 and O2 in the chiral crystal, was 0.0552 Å and 0.0006 Å, respectively, different than the plane containing O1 in 1,6-diferrocenylohexane-1,6-dione.

The 1,6-diferrocenylohexane-1,6-dione and 1,6-diferrocenylohexane products both crystallized in the monoclinic crystal system. The space groups were different, with 1,6-diferrocenylohexane-1,6-dione belonged to the $P2(1)/n$ and 1,6-diferrocenylohexane to the $P2(1)/c$ space group. For these structures, it was observed that adjacent ferrocene groups in the molecule were rotated 180° out of phase relative to one another. The 1-ferrocenylcarbonyl-2-ferrocenylcyclopentene was observed to be in the triclinic crystal system with a space group of $P1$, the lowest symmetry possible.

In all three crystals the relative eclipsing of the Cp rings within the ferrocenes were investigated using XSELL. The top and bottom Cp rings in the fully oxidized and chiral crystals were eclipsed with respect to one another. The Cp rings in 1,6-

diferrocenyhexane were somewhat staggered, but to a negligible degree.

REFERENCES

1. Orpen, A.G., Brammer, L., Allen, F.H., Kennard, O., Wilson, D.G., Taylor, R., "Typical Interatomic Distances: Organometallic Compounds and Coordination Complexes of the d- and f- Block Metals." *International Tables for Crystallography, Volume C. Mathematical, Physical and Chemical Tables*, Wilson, A.J., ed., Kluwer Academic Publishers: Boston, **1995**.
2. Dong, T.Y., Ke, T.J., Peng, S.M., Yeh, S.K. *Inorg. Chem.* **1989**, 28, 2103-2106.
3. Ferguson, G., Glidewell, C., Opromolla, G., Zakaria, C.M., Zanello, P. *J. Organomet. Chem.* **1996**, 517, 183-190.

CHAPTER FOUR

ELECTROCHEMISTRY

Cyclic voltammetry was the principle electrochemical technique used to study the synthesized diferrocenes. A four-part synthesis was carried out, as stated in Chapter Two, to prepare 6-(diferrocenylhexanecarbonyl)pentanethiol. Solution CV was performed on four of the synthesized precursors, 1,6-diferrocenylhexane-1,6-dione, 1-ferrocenyl-carbonyl-2-ferrocenylcyclopentene, 1,6-diferrocenylhexane and 1,6-diferrocenylhexane-1-one. The redox potentials of the diferrocenes in solution were used to compare and assign the waves observed in the monolayer electrochemistry. Chemical and electrochemical reversibility, formal potentials, and ΔE_p values were investigated and compared to previous work performed on dimeric ferrocene complexes in solution.^{1,2} To demonstrate that solution voltammetry was a diffusion controlled process, graphs of peak current versus the square root of the scan rate (i_p v. $v^{1/2}$) were created.

The electrochemical investigation of monolayers constructed from 6-(diferrocenylhexanecarbonyl)pentanethiol was the ultimate goal of this project. The data presented is a preliminary study in diferrocene tagged alkanethiol monolayers. Rate constants, surface coverages and full width at half maximum (FWHM) values are reported for the monolayers. The values obtained for each are compared to previously reported work on 1,2-diferrocenylethane containing monolayers and the various monomeric ferrocene alkanethiol monolayers produced by Chidsey^{3,4}.

Chemicals

Acetonitrile (Fisher, HPLC grade, 99.9%), aluminium oxide (LECO Corp., 1.0 μm

powder), methylene chloride (Fisher, certified ACS, 99.9%), and perchloric acid (Fisher, certified ACS, 74%), were used as received.

Tetra-*n*-butylammonium perchlorate (Fluka, 98%) was recrystallized three times from ethanol.

Instrumentation

A Bio-Analytical Systems (BAS) 100B Potentiostat was used to perform the cyclic voltammetry experiments. The software used in data analysis was included in the potentiostat package. Platinum and gold disc (1.6 mm diameter) working electrodes, platinum wire counter electrodes, and aqueous Ag/AgCl and non-aqueous Ag/AgNO₃ electrodes were purchased from Bio-Analytical Systems.

Electrode Preparation

Solution voltammetry experiments were performed at a platinum disc working electrode. Before each use, the electrode was hand polished for fifteen minutes on a flocked twill polishing cloth with an aqueous suspension of 1.0 micron Al₂O₃, until a mirror finish was obtained. The electrode was sonicated for fifteen minutes in deionized water to remove residual aluminum oxide, rinsed with water and electrolyte before transferring it to the cell.

The polycrystalline gold electrodes used for monolayer electrochemistry were polished by hand on a flocked twill polishing cloth for one and a half hours using an aqueous suspension of 1.0 micron Al₂O₃. The electrode was sonicated for fifteen minutes in deionized water to ensure all of the Al₂O₃ was removed, followed by rinsing with water and electrolyte solution. Prior to soaking the electrode in the thiol coating solution, the gold electrode surface was electrochemically reduced in a 1.0 M HClO_{4(aq)} solution

by performing 50 cyclic voltammetric sweeps between -1500 mV and 1500 mV, ending at -1500 mV. The electrode was rinsed with deionized water and methylene chloride before immersing it in the monolayer coating solution.

Solution Voltammetry

Cyclic voltammetry was performed on four of the synthesized precursors; 1,6-diferrocenylohexane-1,6-dione, 1-ferrocenylcarbonyl-2-ferrocenylcyclopentene, 1,6-diferrocenylohexane, and 1,6-diferrocenylohexane-1-one. Solutions were prepared as 1.0 mM in the ferrocene compounds and 0.1 M in recrystallized tetra-*n*-butylammonium perchlorate (TBAP) in HPLC grade acetonitrile.

Data analysis was performed by constructing a spreadsheet in Microsoft Excel in which ΔE_p , $i_{p,a}/i_{p,c}$, and $E^{\circ'}$ values were calculated as a function of scan rate. These values are shown in Tables D-1 to D-4 in Appendix D. The data were then examined for chemical and electrochemical reversibility. Graphs of $i_{p,a}$ versus $v^{1/2}$ were constructed for all four solutions to demonstrate that electron transfer was diffusion controlled.

Monolayer Preparation

Monolayers were produced by preparing a 1.0 mM coating solution of 6-(diferrocenylohexanecarbonyl)pentanethiol (0.01 g, 0.017 mol) dissolved in methylene chloride. The electrodes were prepared as stated previously and soaked in the thiol solution overnight with gentle stirring.

Data analysis consisted of calculating ΔE_p , $i_{p,a}/i_{p,c}$, and $E^{\circ'}$ as a function of scan rate. The peak areas, used for surface coverage determinations, as well as FWHM values for each wave were determined using the BAS software. A spreadsheet was constructed in Microsoft Excel and the data is tabulated in Tables D-5 to D-7 of Appendix D. The data

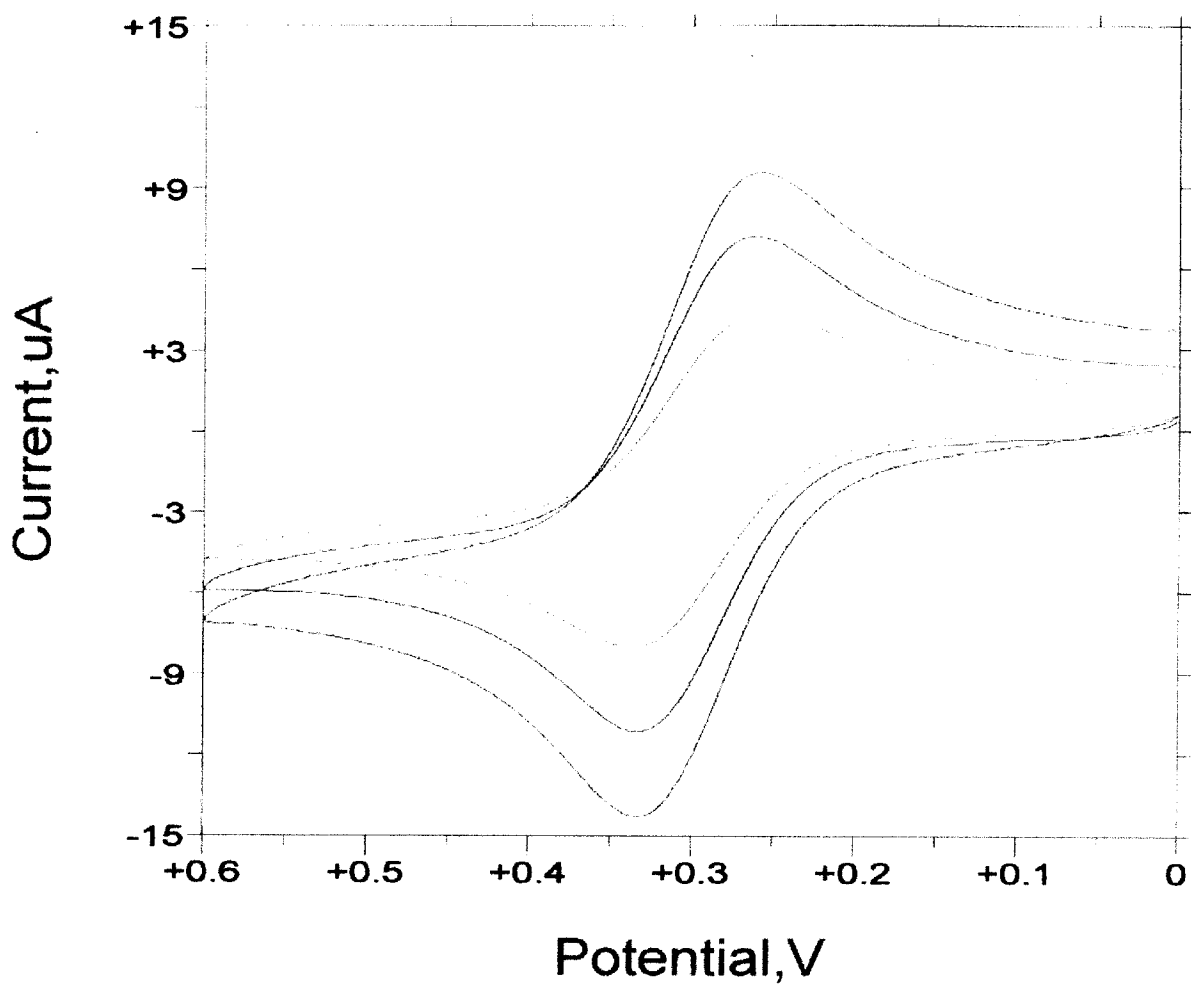
were examined for chemical and electrochemical reversibility, formal potentials and electrochemical accessibility. To illustrate that the thiol was a surface confined species, a plot of $i_{p,a}$ versus scan rate was constructed.

Solution Voltammetry of 1,6-diferrocenylhexane-1,6-dione

A scan rate study was performed on the solution from 25 mV/sec to 500 mV/sec at 25 mV/sec intervals and from 500 mV/sec to 1000 mV/sec at 50 mV/sec intervals. The data is tabulated in Appendix D in Table D-1. Shown in Figure 4.1, is a series of voltammograms at 150 mV/sec, 100 mV/sec, and 50 mV/sec scan rates. The voltammograms displayed a single, two-electron oxidation centered at an $E^{\circ'}$ of 271.5 mV. The cathodic and anodic waves were symmetrical with respect to each other, with minimal peak tailing and broadening. The ratio of $i_{p,a}/i_{p,c}$ was approximately one. ΔE_p was approximately 94.5 mV and independent of scan rate.

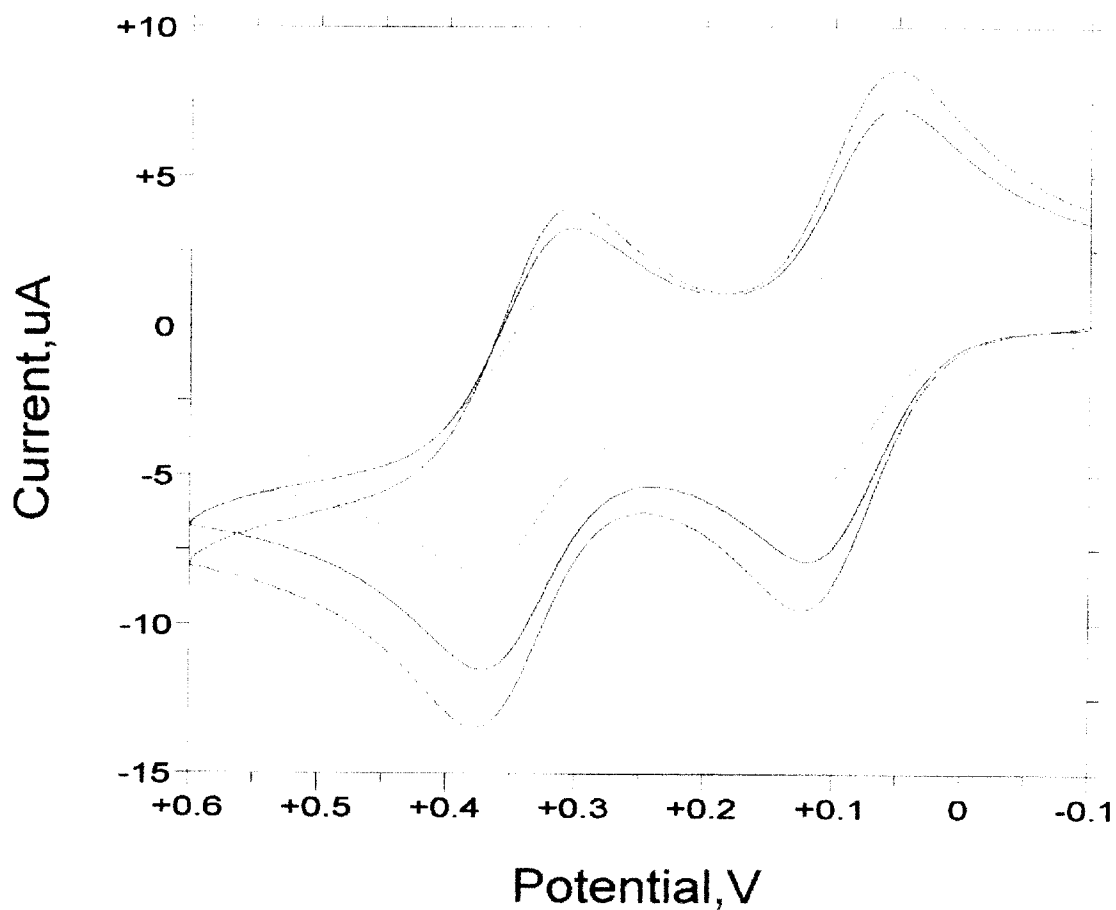
Solution Voltammetry of 1-ferrocenylcarbonyl-2-ferrocenylcyclopentene

A full scan rate study was performed on the 1-ferrocenylcarbonyl-2-ferrocenylcyclopentene and tabulated data is found in Table D-2 of Appendix D. Voltammograms at scan rates of 150 mV/sec, 100 mV/sec, and 50 mV/sec are shown in Figure 4.2. The voltammograms displayed two distinct one electron transfer waves, with $E^{\circ'}$'s centered at 87 mV for the first wave and 344 mV for the second wave. The waves were well defined and symmetrical in both the anodic and cathodic directions. The peak current ratios for both redox waves were approximately one at all scan rates. ΔE_p was approximately 80 mV for both redox waves and was independent of scan rate.



<u>Line Color</u>	<u>Scan Rate</u>
Blue	150 mV/sec
Red	100 mV/sec
Green	50 mV/sec

Figure 4.1: Cyclic voltammogram of 1.0 mM 1,6-diferrocenylhexane-1,6-dione with 0.1 M TBAP in CH_3CN . Working electrode: Platinum disc; Counter electrode: Platinum wire; Reference electrode: non-aqueous Ag/AgNO_3 ; Temperature: 25°C



<u>Line Color</u>	<u>Scan Rate</u>
Blue	150 mV/sec
Red	100 mV/sec
Green	50 mV/sec

Figure 4.2: Cyclic voltammogram of 1.0 mM 1-ferrocenylcarbonyl-2-ferrocenylcyclopentene with 0.1 M TBAP in CH₃CN. Working electrode; Platinum disc; Counter electrode; Platinum wire; Reference electrode: non-aqueous Ag/AgNO₃; Temperature: 25°C

Solution Voltammetry of 1,6-diferrocenylhexane

A full scan rate study was also performed on the fully reduced product, 1,6-diferrocenylhexane. The voltammograms for the 150 mV/sec, 100 mV/sec, and 50 mV/sec scan rates are shown in Figure 4.3. The remaining data is tabulated in Table D-3 of Appendix D. A single, two electron transfer wave was observed with $E^{\circ'}$ centered at -10.5 mV. The ratio of peak currents was approximately one and ΔE_p was 81.5 mV, both of which were independent of scan rate.

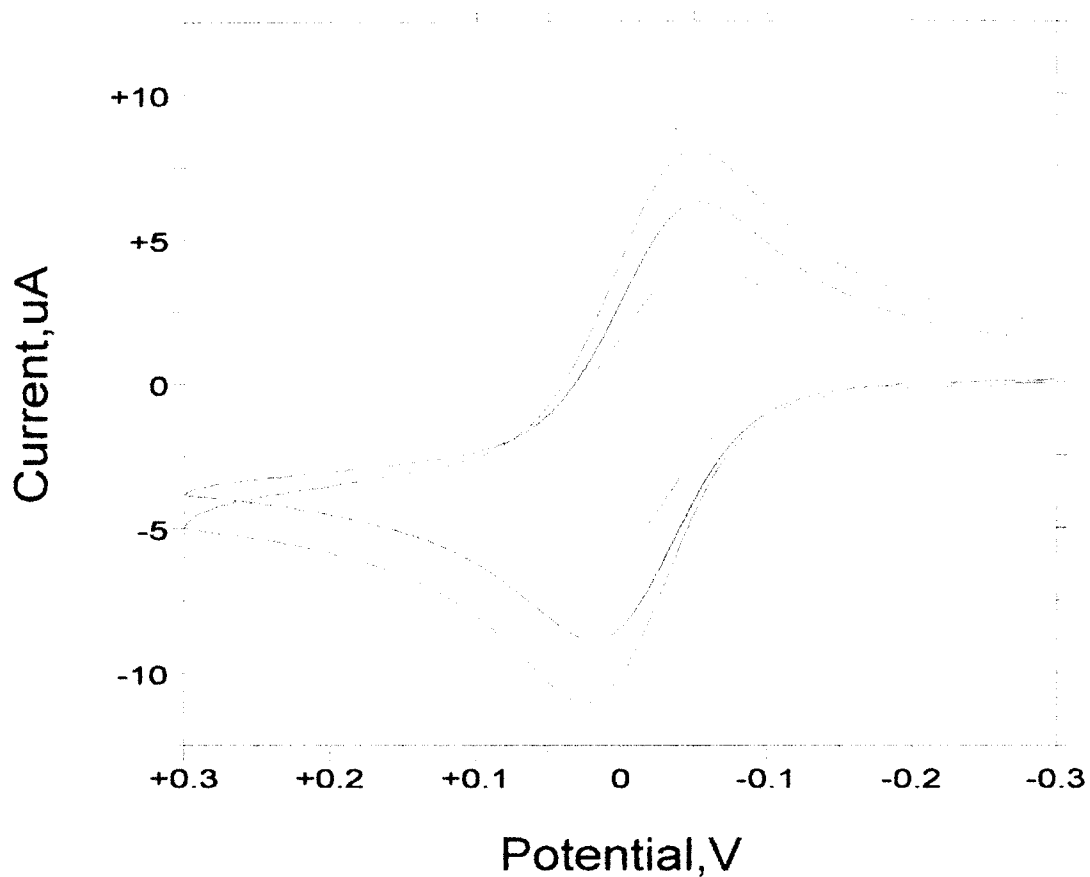
Solution Voltammetry of 1,6-diferrocenylhexane-1-one

A series of voltammograms for 150 mV/sec, 100 mV/sec, and 50 mV/sec scan rates are shown in Figure 4.4. The data for the remaining scan rates is located in Table D-4 of Appendix D. A full scan rate study displayed two, single electron transfer waves centered at 7 mV and 305 mV, respectively. The symmetrical waves produced peak current ratios equal to one at all scan rates. ΔE_p was 75 mV and 84 mV for the first and second redox waves, respectively, and was also independent of scan rate.

Monolayer Voltammetry of 6-(diferrocenylhexanylcarbonyl)pentanethiol

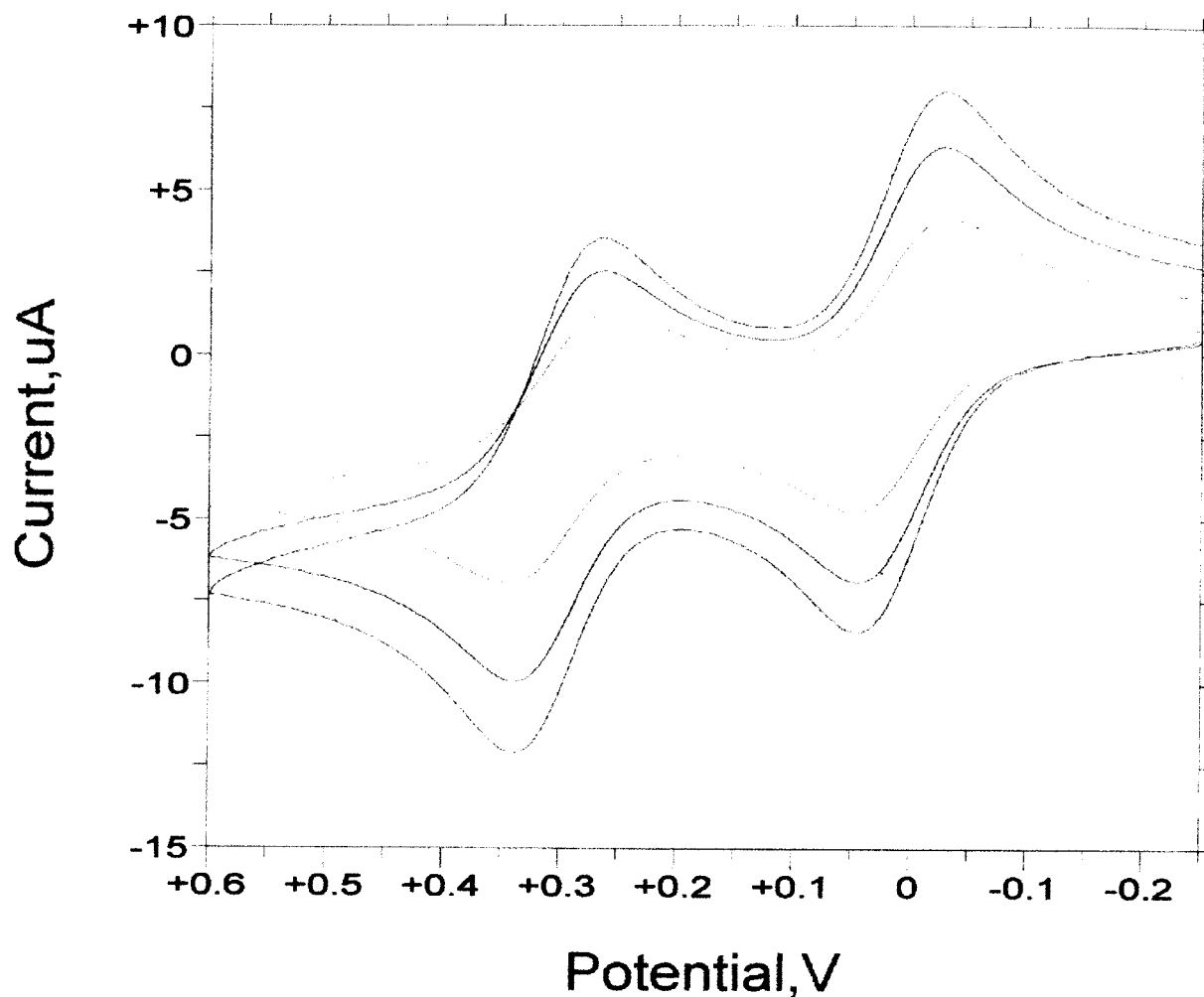
Scan rate studies from 25 mV/sec to 500 mV/sec were obtained between 0 mV and 800 mV. As a final step, the electrodes were cycled through the aforementioned potentials, for 100 sweeps. This was to determine if the monolayer was stable to extended cycling in perchloric acid. Three electrodes were prepared for the following monolayer study.

The first electrode did not produce well-defined peaks in the anodic direction but did produce well-defined peaks in the cathodic direction. Voltammograms at 150 mV/sec, 100 mV/sec and 50 mV/sec are shown in Figure 4.5, and illustrates the formation of a



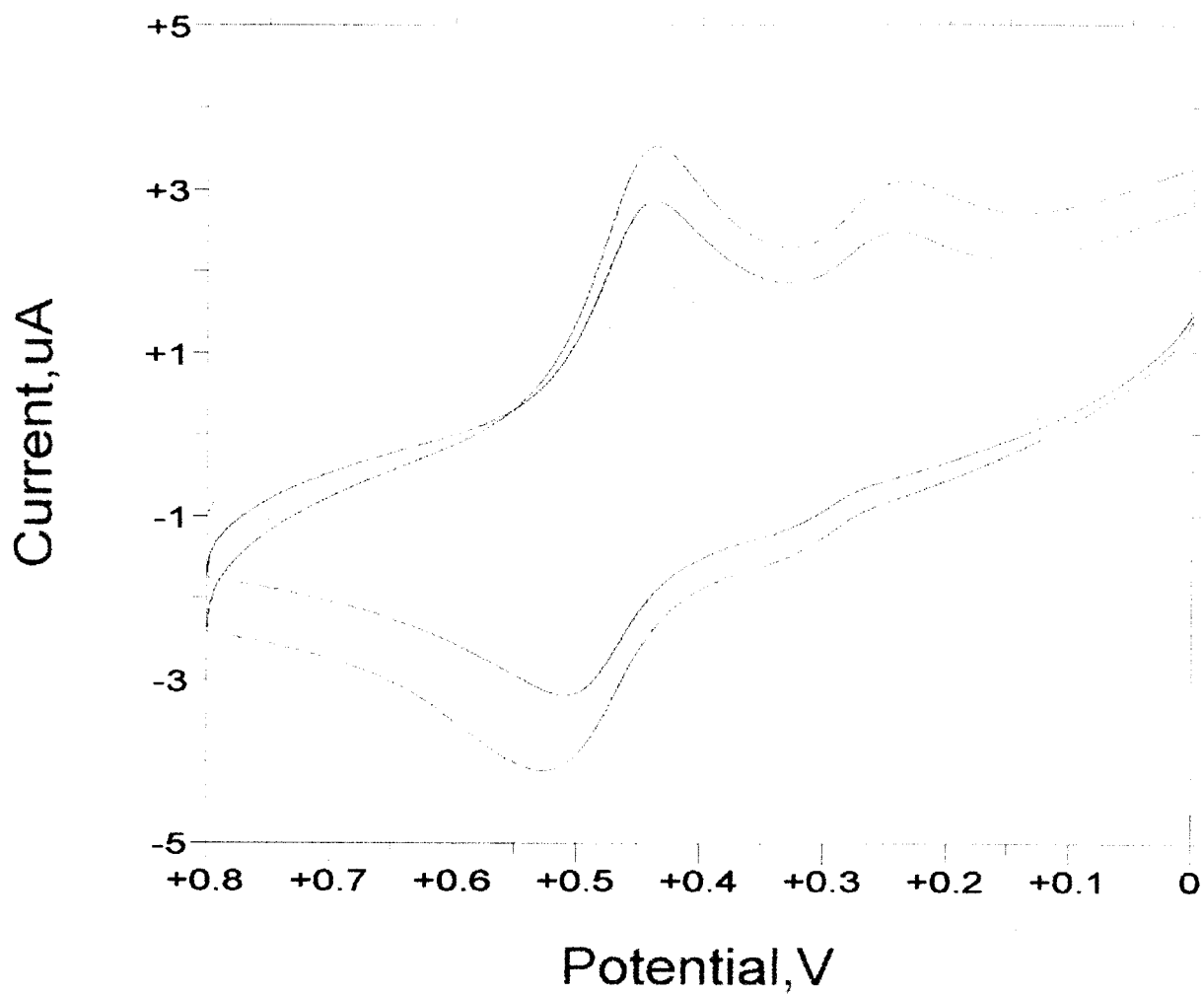
<u>Line Color</u>	<u>Scan Rate</u>
Blue	150 mV/sec
Red	100 mV/sec
Green	50 mV/sec

Figure 4.3: Cyclic voltammogram of 1.0 mM 1,6-diferrocenylhexane with 0.1 M TBAP in CH₃CN. Working electrode: Platinum disc; Counter electrode: Platinum wire; Reference electrode: non-aqueous Ag/AgNO₃; Temperature: 25°C



<u>Line Color</u>	<u>Scan Rate</u>
Blue	150 mV/sec
Red	100 mV/sec
Green	50 mV/sec

Figure 4.4: Cyclic voltammogram of 1.0 mM 1,6-diferrocenylhexane-1-one with 0.1 M TBAP in CH_3CN . Working electrode: Platinum disc; Counter electrode: Platinum wire; Reference electrode: non-aqueous Ag/AgNO_3 ; Temperature: 25°C

**Line Color**

Blue

Red

Green

Scan Rate

150 mV/sec

100 mV/sec

50 mV/sec

Figure 4.5: Poor cyclic voltammogram of 1.0 mM 6-(diferrocenylhexanylethyl)-pentanethiol self-assembled monolayer. Working electrode: Gold disc; Counter electrode: Platinum wire; Reference electrode: aqueous Ag/AgCl; Temperature: 25°C

poor monolayer on the electrode surface. Because the first anodic peak was not well defined, the determination of the peak potentials and currents was difficult. The cathodic sweep produced peaks that were broadened and tailed, therefore the data was not included in any of the reported values. Table D-5 contains the data obtained, as well as the relevant calculations.

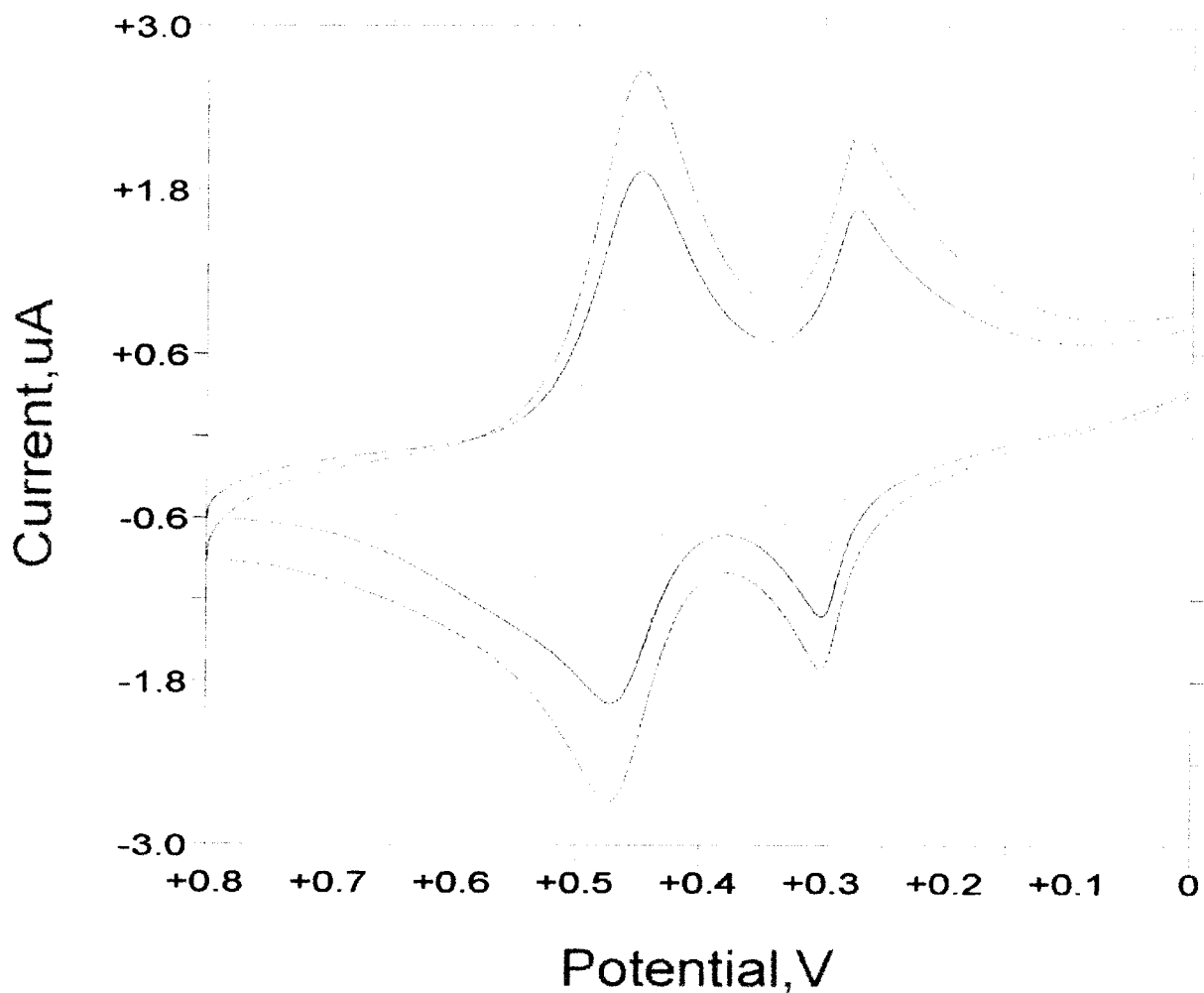
The second and third electrodes produced voltammograms, which displayed four well-defined peaks. The data produced from both electrodes were similar in nature, but the focus of analysis will be on the data obtained from the second electrode. The full data sets for both electrodes are located in Tables D-6 and D-7 of Appendix D.

Figure 4.6 displays a series of voltammograms at a variety of scan rates for the second electrode. Two, single electron transfer waves were observed in the cyclic voltammetry experiment. The first redox wave was centered at 285.5 mV, and the second wave was centered at 462.5 mV. Peak broadening and tailing did occur in the second anodic and first cathodic wave, but not to the degree seen with the first electrode. Peak current ratios were approximately one for both redox waves and are tabulated in Table D-6 in Appendix D. ΔE_p for the first redox wave was found to increase with increasing scan rate. The second redox wave produced ΔE_p values of approximately 27.5 mV that were independent of scan rate.

Surface coverages were calculated by integrating the area under the voltammetric waves. The formula used to calculate surface coverage was:

$$\Gamma = (\text{Area of peak}) / (0.0402 \text{ cm}^2 nFv)$$

where 0.0402 cm^2 is the electrode surface area corrected for surface roughness.⁵ The



<u>Line Color</u>	<u>Scan Rate</u>
Blue	150 mV/sec
Red	100 mV/sec
Green	50 mV/sec

Figure 4.6: Cyclic voltammogram of 1.0 mM of 6-(diferrocenylhexanoyl)-pentanethiol self-assembled monolayer. Working electrode: Gold disc; Counter electrode: Platinum wire; Reference electrode: aqueous Ag/AgCl; Temperature: 25°C

values obtained for each wave were tabulated and can be found in Table D-6 of Appendix D. The median surface coverages calculated from the anodic and cathodic peaks for the oxidation centered at 285.5 mV were 2.11×10^{-11} mol/cm² and 2.81×10^{-11} mol/cm², respectively. The redox wave centered at 462.5 mV displayed median surface coverages of 5.16×10^{-11} mol/cm² for the anodic wave and 7.29×10^{-11} mol/cm² for the cathodic wave. The surface coverage was also calculated for a CV taken after extended cycling. The surface coverage for the first anodic wave was determined to be 1.78×10^{-11} mol/cm².

FWHM values were obtained for all four waves displayed on the voltammogram. The peak centered at 285.5 mV displayed FWHM values of 44.9 mV and 85 mV for the anodic and cathodic waves, respectively. The peak centered at more anodic potentials displayed FWHM values of 80.2 mV and 86.8 mV for the anodic and cathodic waves, respectively. These values were obtained from the voltammogram at a scan rate of 200 mV/sec.

RESULTS AND DISCUSSION

Analysis of the Solution Voltammetry

The cyclic voltammograms for the symmetrically substituted compounds, 1,6-diferrocenylhexane-1,6-dione and 1,6-diferrocenylhexane, display single, two electron oxidations. While those that are asymmetrically substituted, 1-ferrocenylcarbonyl-2-ferrocenylcyclopentene and 1,6-diferrocenylhexane-1-one, display two, single electron oxidations. The formal potentials obtained from the solution voltammetry of the compounds containing carbonyl substituted ferrocenes were determined to be

approximately 300 mV, while those containing alkyl or alkene substituents were determined to be approximately 50 mV. These potentials are characteristic of ferrocene containing compounds. It is well documented that formal potentials for carbonyl substituted ferrocenes are shifted to more anodic potentials with respect to ferrocene, due to the electron withdrawing nature of the substituent. Electron donating alkyl groups, shift the formal potentials cathodically with respect to ferrocene. The formal potentials obtained in this study were shifted cathodically by approximately 200 mV relative to literature values obtained in methylene chloride. The shift in E° is attributed to the different solvent, acetonitrile, used in the current study.

The symmetrically substituted ferrocene compounds, 1,6-diferrocenylohexane-1,6-dione and 1,6-diferrocenylohexane, were investigated to determine if the ferrocenes were electronically communicating with one another. A study done by Ferguson⁶ et al., demonstrated that symmetrical dimeric ferrocenes can produce two one-electron transfers, indicating that the ferrocenes are electronically “talking” to one another. The study found that a single, two-electron transfer wave for symmetrical ferrocene dimers indicated that the ferrocenes were not communicating with one another. Compounds displaying this type of behavior were given a Robin-Day classification of I-II. In the case of 1,6-diferrocenylohexane-1,6-dione and 1,6-diferrocenylohexane, a single two-electron transfer wave was displayed for each compound. Since the ΔE_p values were observed to be larger than the theoretical value of $59/n$ mV, the effects of solution iR made it difficult to unambiguously assign a Robin-Day classification. The symmetric ferrocenes were thus given a Robin-Day classification of I-II.

The ratio of the peak currents was calculated for all four compounds and are reported

in Tables D-1 to D-4 in Appendix D. The ratios for the four compounds were approximately one at all scan rates, indicating that each oxidation was chemically reversible.

The difference in peak potentials for each wave was also calculated for all four sets of voltammograms. The cyclic voltammetry experiments for each solution produced ΔE_p values that were approximately 90 mV, and were independent of scan rate. The theoretical value of ΔE_p at all scan rates for an electrochemically reversible system in solution is $57/n$ mV. The ΔE_p values were larger than $57/n$ mV due to solution iR effects. Electrochemical reversibility was therefore demonstrated for all four solutions. The peak potentials for each individual scan rate for all four compounds are tabulated in Tables D-1 to D-4 located in Appendix D.

To demonstrate that the electron transfers were diffusion controlled, graphs of the anodic peak current versus the square root of the scan rate were constructed and are presented in Figures 4.7 to 4.10. The resulting linear plots indicate that the electron transfers were diffusion controlled. The best-fit line was calculated and the resulting correlation coefficients are shown in the figures.

Analysis of 6-(diferrocenylhexanylethyl)pentanethiol Self-Assembled Monolayer

Voltammetry

The cyclic voltammograms for monolayers containing 6-(diferrocenylhexanylethyl)pentanethiol display two, single electron transfer waves centered at 263 mV and 463 mV. Based on substituent effects, the wave centered at 263 mV was assigned to the outer ferrocene and the wave at 463 mV was assigned to the carbonyl substituted (inner)

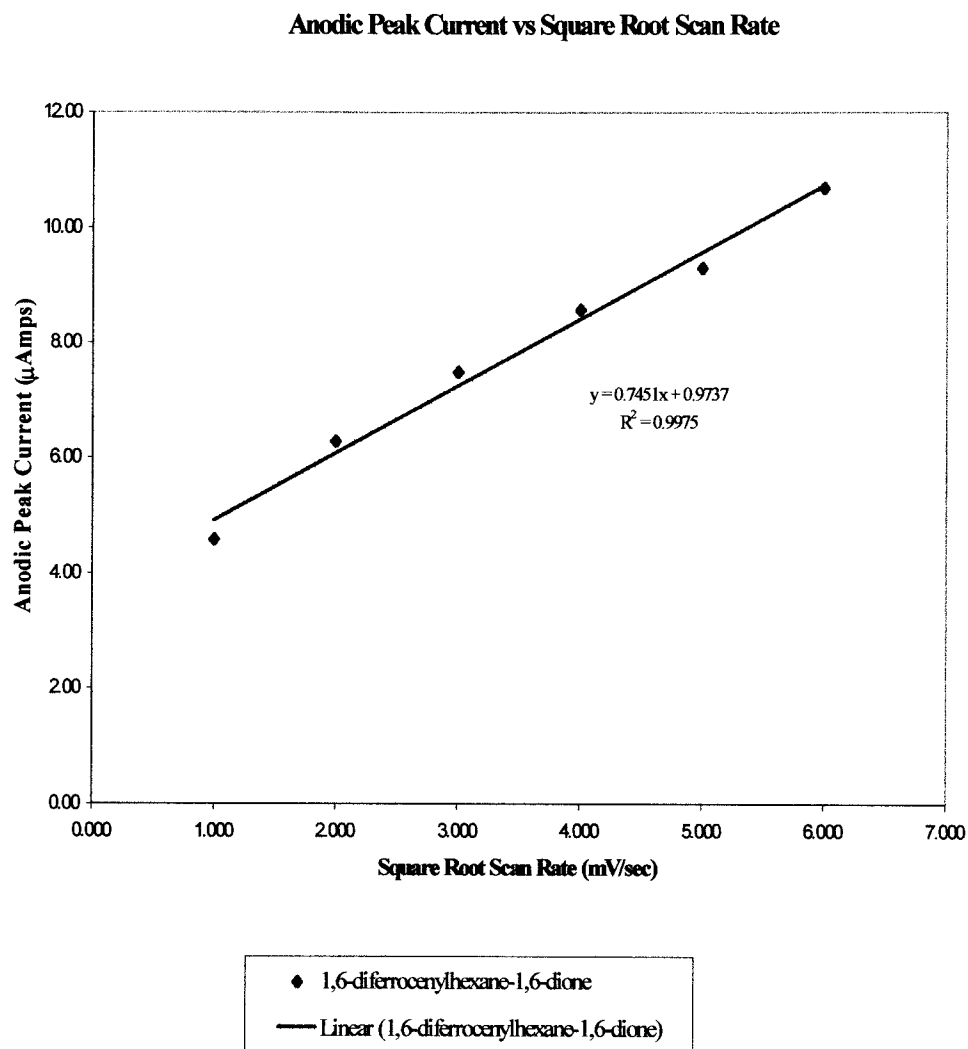


Figure 4.7: Plot of $i_{p,a}$ versus $v^{1/2}$ for 1,6-diferrocenylhexane-1,6-dione for the 25 mV/sec to 200 mV/sec scan rates.

Anodic Peak Current versus Square Root Scan Rate

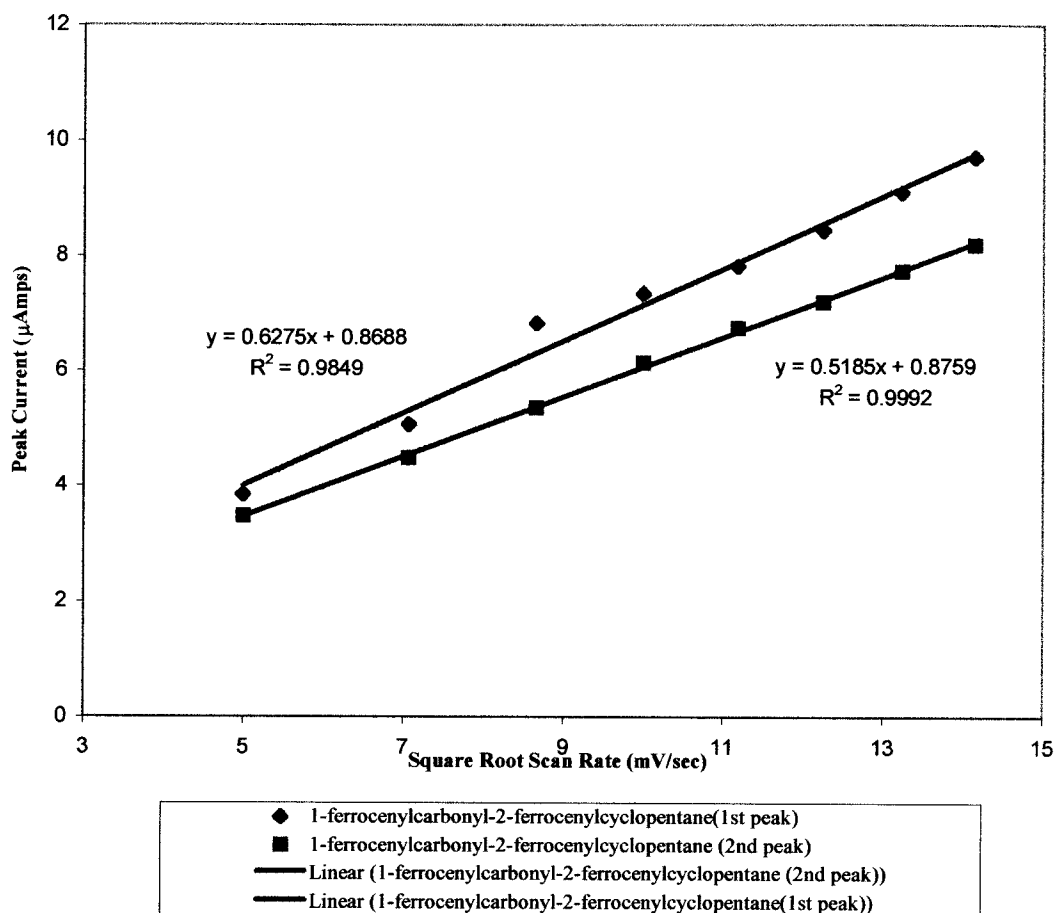


Figure 4.8: Plot $i_{p,a}$ versus $v^{1/2}$ for 1-ferrocenylcarbonyl-2-ferrocenylcyclopentane for the 25 mV/sec to 200 mV/sec scan

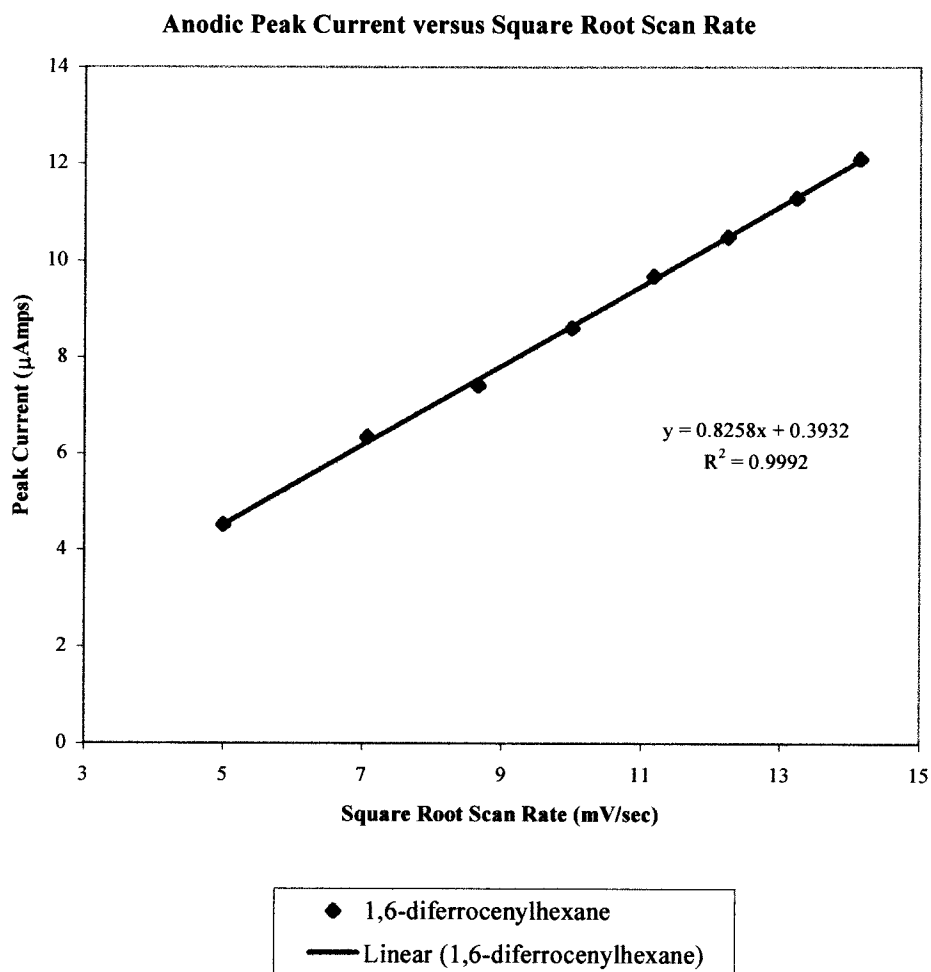


Figure 4.9: Plot $i_{p,a}$ versus $v^{1/2}$ for 1,6-diferrocenylhexane for the 25 mV/sec to 200 mV/sec scan rates

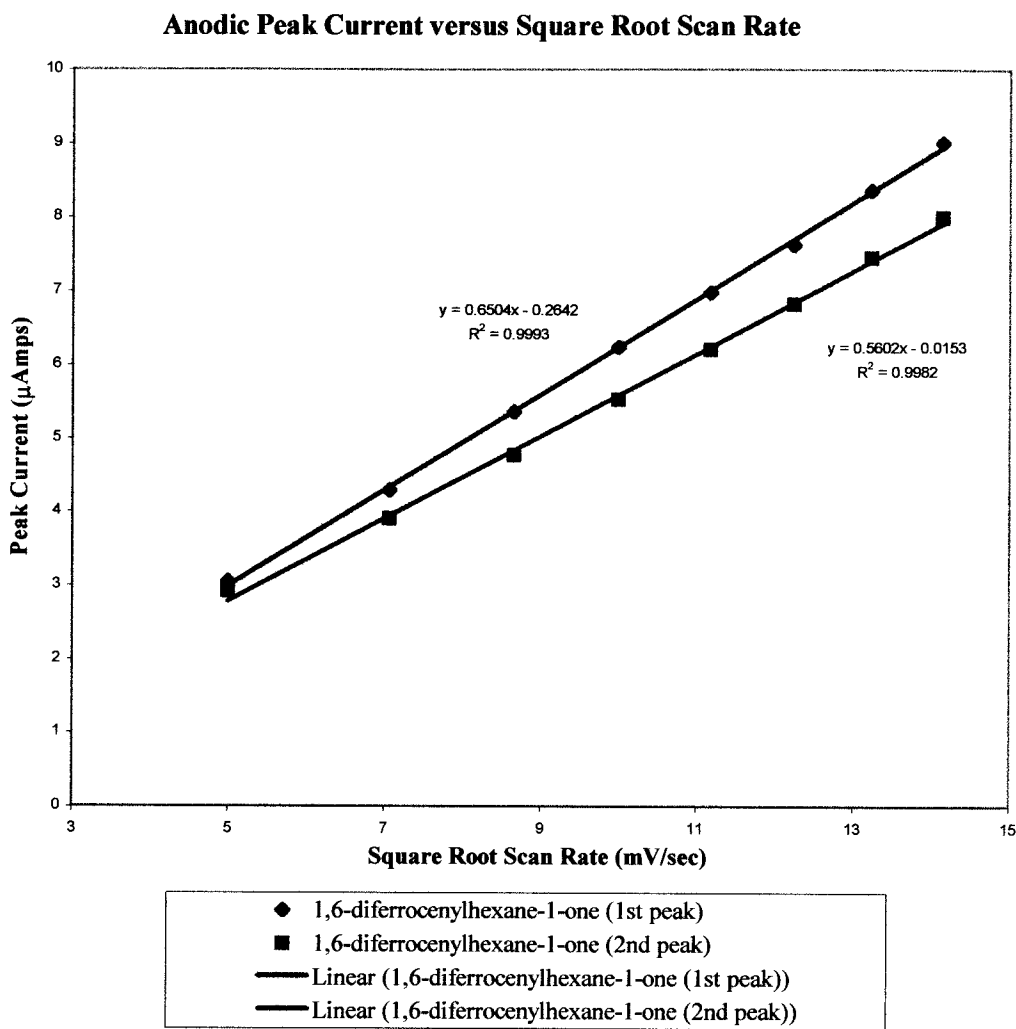


Figure 4.10: Plot $i_{p,a}$ versus $v^{1/2}$ for 1,6-diferrocenylhexane-1-one for the 25 mV/sec to 200 mV/sec scan rates.

ferrocene. The formal potentials are in good agreement with those reported by Kubo², but are significantly different than those reported by Filler because a different reference electrode was used. The redox waves were reasonably symmetric, but the waves associated with oxidation of the inner ferrocene and reduction of the outer ferrocene displayed significant tailing.

The peak current ratios were approximately one at all scan rates, indicating monolayers produced from 6-(diferrocenylhexanylethyl)pentanethiol were chemically reversible. The values for the ratios were similar to those obtained by Filler, but different than those seen by Kubo, because the monolayers containing biferrrocene were found to be chemically irreversible. These values are tabulated in Table D-6 in Appendix D.

The value of ΔE_p for oxidation of the inner ferrocene was approximately 27.5 mV and did not increase with increasing scan rate, indicating an electrochemically reversible process. A rate constant could not be calculated for the inner ferrocene because electron transfer was rapid on the voltammetric time scale. The outer ferrocene, however, demonstrated increasing ΔE_p values as the scan rate was increased from 25 mV/sec to 500 mV/sec. A plot of ΔE_p versus scan rate is shown in Figure 4.11. A heterogeneous electron transfer rate constant of $11.9 \text{ s}^{-1}(\pm 0.2)$ was obtained via the method of Laviron, indicating that the monolayer was ordered.

To determine if the the redox active species was surface confined, a plot of $i_{p,a}$ versus scan rate was constructed. The plot demonstrated a linear relationship, indicating that the electron transfer was for a covalently bonded species. The plot is shown in Figure 4.12.

The surface coverages were calculated for all four waves of the 6-(diferrocenylhexanylethyl)pentanethiol monolayer by integrating the charge under the

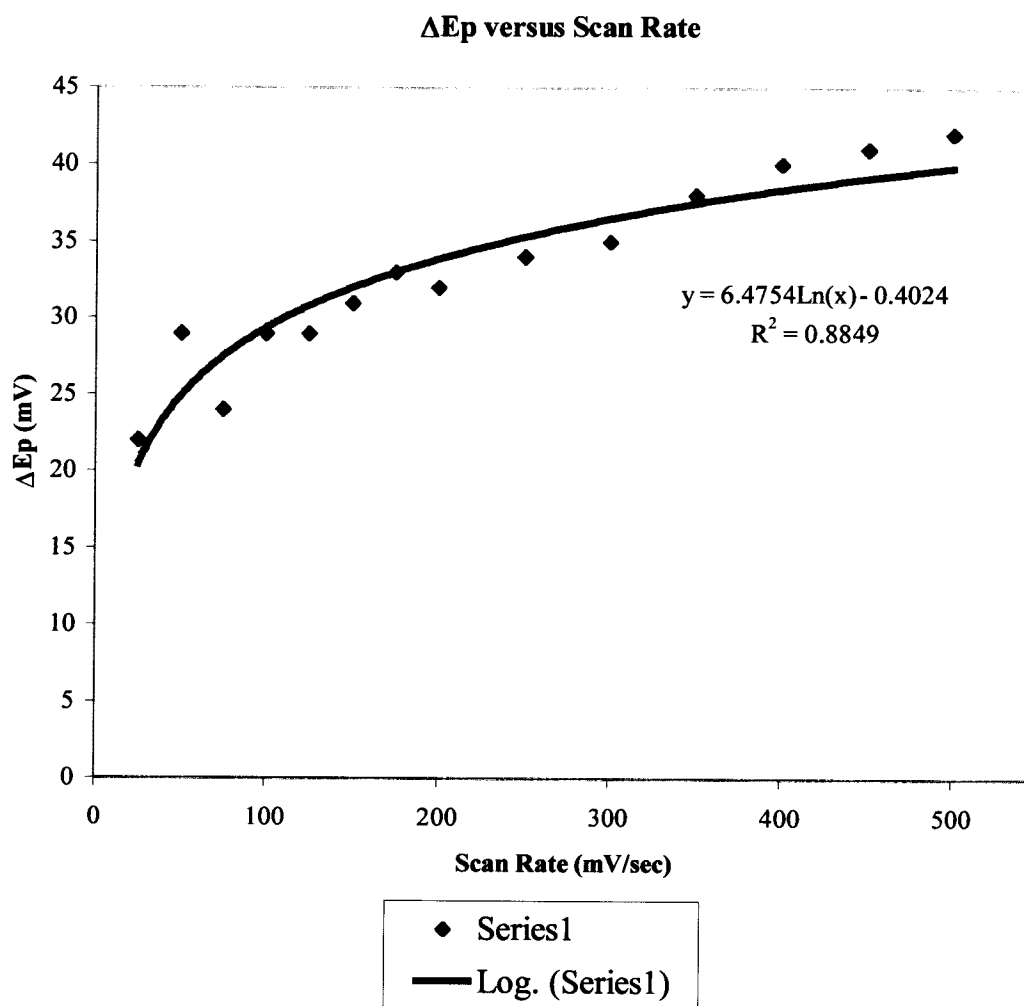


Figure 4.11: Plot of ΔE_p versus v for 6-(diferrocenylhexanylethynyl)pentanethiol

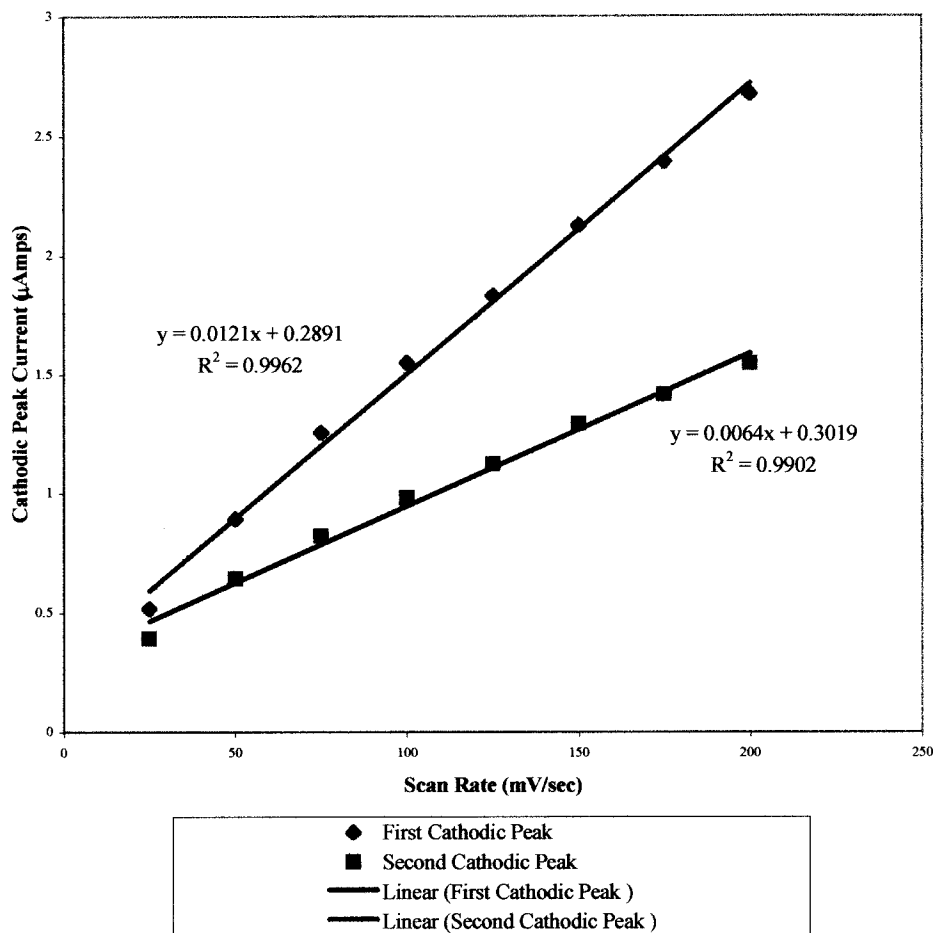
Thiol (2nd Electrode) Cathodic Peak Current versus Scan Rate

Figure 4.12: Plot of $i_{p,a}$ versus v for 6-(diferrocenylhexanylethynyl)pentanethiol for the 25 mV/sec to 200 mV/sec scan rates

voltammetric waves and are corrected for surface roughness.⁵ The inner ferrocene produced surface coverages of 7.29×10^{-11} mol/cm² and 5.16×10^{-11} mol/cm², for the anodic and cathodic waves, respectively. The difference in the surface coverages were attributed to tailing of the anodic wave. The outer ferrocene waves yielded surface coverages of 2.11×10^{-11} mol/cm² for the anodic wave and 2.81×10^{-11} mol/cm² for the cathodic wave. These values are lower than those reported by Chidsey and Filler for monomeric and dimeric ferrocene alkanethiol monolayers. This is attributed to the fact that the 6-(diferrocenylhexanylethyl)pentanethiol head group occupies a much larger volume than either ferrocene and diferrocenylethane. The surface coverages from the inner ferrocene group indicates a densely packed monolayer.

The surface coverages measured for the outer ferrocene are approximately 40% of that for the inner ferrocene. This indicates that 60% of the outer ferrocene groups are not electrochemically accessible. This behavior is very different than that observed by Filler¹ and Mirkin⁷. The surface coverage of the outer ferrocene groups in diferrocenylethane tagged alkanethiol monolayers was found to be the same as that of the inner ferrocenes, indicating that both of the redox active molecules were electrochemically accessible. Mirkin et.al constructed monolayer films containing an inner azobenzene moiety separated from an outer ferrocene group via a butane chain. The results demonstrated that the *outer* ferrocene groups were electrochemically accessible, but the inner azobenzenes were not. This was attributed to the dense packing in the monolayer, which did not allow charge-compensating cations to enter the film upon reduction. Monolayer films tagged with diferrocenylhexane groups display the opposite behavior with respect to the films reported by Mirkin.

A possible explanation for this unusual behavior is that the majority of the outer ferrocenes prefer to fold over into the non-polar hexane region of the film, rather than fully extending into the aqueous solution. In such a situation, oxidation of the majority of the outer ferrocene groups would be difficult because the resulting cations do not like the hydrophobic chain environment. This issue will be addressed by performing voltammetry in less polar solvents, such as acetonitrile or methylene chloride. Solvents such as these could prevent the outer ferrocene groups from folding over into the hydrophobic alkane region, resulting in greater electrochemical accessibility.

Surface coverages were also obtained for the monolayer at 100 mV/sec after extended cycling in perchloric acid and are displayed in Table D-6 of Appendix D. The coverage from the anodic wave for the outer ferrocene decreased by approximately 27% when compared with the 100 mV/sec scan. In addition, the voltammetric waves were considerably less well-defined after extended cycling, as shown in Figure 4.13. This data indicates that the monolayer was not stable with respect to extended cycling in perchloric acid.

The FWHM values were calculated by subtracting the potentials at half peak height. The FWHM values obtained for the second anodic wave and both cathodic waves were approximately 90/n mV. This was a strong indication that the ferrocene redox sites are isolated and not interacting with one another. The FWHM of 44.9 mV for the first anodic wave was not typical for a surface confined species. The wave was much sharper when compared to the other three, as seen in Figure 4.6. A structural rearrangement upon oxidation of the outer ferrocene could be an explanation for the narrow peaks, as observed in films containing polyvinyl ferrocene.⁸

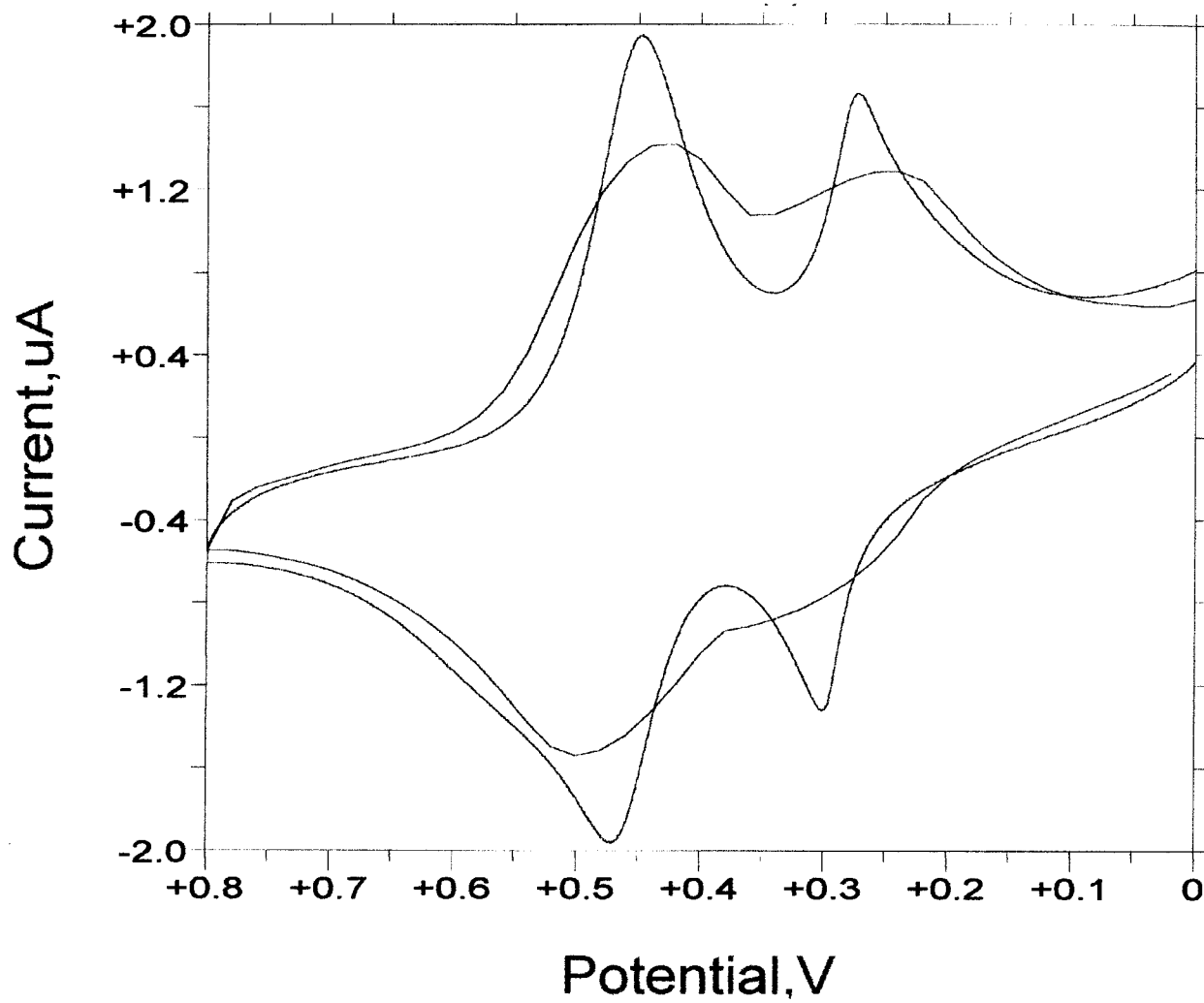


Figure 4.13: Cyclic voltammogram of 6-(diferrocenylhexanylcarbonyl)pentanethiol monolayer at 100 mV/sec (blue) and 100 sweeps (red) at 100 mV/sec. Blue: Before extended cycling; Red: After extended cycling.

Conclusion

The ultimate goal of this research endeavor was to determine the effects of including a long alkane chain between two ferrocene moieties on monolayer voltammetry. The results from solution voltammetry experiments demonstrated that all four of the compounds that were synthesized, displayed oxidations at the appropriate potentials and that they were chemically and electrochemically reversible. The fully oxidized and fully reduced symmetrical compounds were assigned a Robin-Day classification of I-II. This indicated that the ferrocenes were not electronically communicating.

The monolayer study provided preliminary data concerning rate constants, surface coverages, and FWHM values for diferrocene alkanethiol monolayers with a six-carbon chain separating the ferrocenes. Both ferrocene oxidations were determined to be chemically reversible. The oxidation of the inner ferrocene was found to be electrochemically reversible, whereas the outer ferrocene was electrochemically irreversible. A rate constant of 11.9 s^{-1} was calculated based on Laviron's method.

The calculated surface coverages concluded that approximately 40% of the outer ferrocenes were electrochemically accessible. This unexpected result could be due to the outer ferrocene groups folding over into the hydrophobic alkane bridge. Further experiments in which less polar solvents will be employed, should address this issue.

FWHM values agreed with the theoretical value of $90/n \text{ mV}$ for a surface confined species. This indicated that the ferrocene sites in the monolayer were ordered and non-interacting, a criterion for the extraction of a single rate constant. However, the first anodic wave produced a sharp, narrow peak and thus a small value of FWHM. This could possibly be due to a structural rearrangement upon oxidation of the outer ferrocene.

REFERENCES

1. Filler, William J. Characterization of Diferrocene Tagged Self-Assembled Alkanethiol Monolayers, M.S. Thesis, Temple University, Philadelphia, August 1996.
2. Kubo, K., Kondow, H., Nishihara, H. *Electrochemistry*, **1999**, 67, 1129-1131.
3. Chidsey, C.E.D., Bertozzi, C.R., Putvinski, T.M., Majsce, A.M. *J. Am. Chem. Soc.*, **1990**, 112, 4301-4306.
4. Chidsey, C.E.D. *Science*, **1991**, 251, 919-921.
5. Rodriguez, J.F., Mebrahtu, T., Soriaga, M.P. *J. Electroanal. Chem.* **1987**, 233, 283-289.
6. Ferguson, G., Glidewell, C., Opromolla, G., Zakaria, C.M., Zanello, P. *J. Organomet. Chem.* **1996**, 517, 183-190.
7. Campbell, D.J., Herr, B.R., Hulteen, J.C., Van Duyne, R.P., Mirkin, C.A. *J. Am. Chem. Soc.*, **1996**, 118, 10211-10219.
8. Murray, R. *Molecular Design of Electrode Surfaces*; Wiley: New York, **1992**.

APPENDIX A

Crystallography Data for 1,6-diferrocenylhexane-1,6-dione

Equations of Mean Plane for 1,6-diferrocenylhexane-1,6-dione

Table A-1

$$0.1396 * XO + 0.6041 * YO + 0.7846 * ZO = -1.1562$$

$$0.7877 * x + 13.7660 * y - 6.2742 * z = -1.1562$$

Deviation	Weight	Name
0.0020	1.00	C1
-0.0015	1.00	C2
0.0003	1.00	C3
0.0009	1.00	C4
-0.0017	1.00	C5

Table A-2

$$0.1297 * XO + 0.6044 * YO + 0.7861 * ZO = 2.1022$$

$$0.7318 * x + 13.7720 * y - 6.2982 * z = 2.1022$$

Deviation	Weight	Name
0.0016	1.00	C6
0.0010	1.00	C7
-0.0033	1.00	C8
0.0042	1.00	C9
-0.0035	1.00	C10

Table A-3

$$0.1287 * XO + 0.6037 * YO + 0.7867 * ZO = 2.0932$$

$$0.7262 * x + 13.7566 * y - 6.3049 * z = 2.0932$$

Deviation	Weight	Name
0.0029	1.00	C6
0.0004	1.00	C7
-0.0046	1.00	C8
0.0044	1.00	C9
-0.0016	1.00	C10
-0.0015	1.00	O1

Table A-4
Observed and Calculated Structure Factors for 1,6-diferrocenyhexane-1,6-dione

h	k	l	10Fo	10Fc	10a	h	k	l	10Fo	10Fc	10a	h	k	l	10Fo	10Fc	10a	h	k	l	10Fo	10Fc	10a						
2	0	0	520	581	8	2	12	0	453	427	6	0	26	0	197	193	18	2	4	1	221	220	5	-1	10	1	259	251	9
4	0	0	259	276	7	3	12	0	465	456	8	1	26	0	19	34	19	3	4	1	171	187	9	0	10	1	40	35	7
6	0	0	111	102	7	4	12	0	183	183	4	2	26	0	153	157	8	4	4	1	154	156	4	1	10	1	184	170	5
1	1	0	249	310	3	5	12	0	75	78	24	3	26	0	32	31	32	5	4	1	52	43	19	2	10	1	65	71	6
2	1	0	170	185	13	6	12	0	0	6	1	4	26	0	33	45	32	6	4	1	101	94	11	3	10	1	112	111	7
3	1	0	33	17	11	7	12	0	0	5	1	1	27	0	39	23	18	7	4	1	96	85	21	4	10	1	72	76	8
4	1	0	211	225	4	1	13	0	344	341	4	2	27	0	40	66	21	-7	5	1	26	6	25	5	10	1	141	131	17
5	1	0	156	157	6	2	13	0	14	18	14	-6	5	1	0	12	1	6	5	1	0	12	1	6	10	1	28	11	27
6	1	0	131	142	7	3	13	0	192	186	5	4	27	0	36	46	35	-5	5	1	78	87	6	7	10	1	125	115	29
7	1	0	70	49	11	4	13	0	21	7	21	0	28	0	40	39	15	-4	5	1	36	36	13	-7	11	1	19	10	18
0	2	0	134	437	134	5	13	0	114	123	8	1	28	0	100	112	11	-3	5	1	334	361	4	-6	11	1	20	33	20
1	2	0	1936	1659	5	6	13	0	17	2	17	2	28	0	0	7	1	-2	5	1	74	68	6	-5	11	1	69	70	13
2	2	0	231	234	4	7	13	0	54	74	17	3	28	0	21	54	20	-1	5	1	683	694	13	-4	11	1	64	65	8
3	2	0	353	395	11	0	14	0	591	585	8	1	29	0	18	8	18	0	5	1	70	26	5	-3	11	1	126	130	5
4	2	0	168	167	4	1	14	0	501	490	6	2	29	0	17	5	17	1	5	1	872	867	5	-2	11	1	183	180	4
5	2	0	244	226	13	2	14	0	324	316	4	3	29	0	47	48	15	2	5	1	126	123	3	-1	11	1	356	376	8
6	2	0	0	10	1	3	14	0	206	198	4	0	30	0	145	131	8	3	5	1	348	374	4	0	11	1	293	277	3
7	2	0	0	5	1	4	14	0	116	108	5	1	30	0	0	15	1	4	5	1	34	28	12	1	11	1	728	717	6
1	3	0	313	306	3	5	14	0	60	81	14	2	30	0	48	53	13	5	5	1	204	210	12	2	11	1	221	225	3
2	3	0	146	149	10	6	14	0	24	9	24	1	31	0	26	15	26	6	5	1	0	20	1	3	11	1	315	313	4
3	3	0	79	89	6	7	14	0	34	2	19	2	31	0	16	42	16	7	5	1	0	12	1	4	11	1	202	206	5
4	3	0	0	5	1	1	15	0	91	90	5	0	32	0	43	53	19	-7	6	1	73	83	13	5	11	1	64	65	12
5	3	0	291	290	4	2	15	0	43	48	11	-7	0	1	161	164	13	-6	6	1	107	92	8	6	11	1	12	19	12
6	3	0	20	12	20	3	15	0	85	81	7	-5	0	1	239	249	3	-5	6	1	263	260	8	7	11	1	0	17	1
7	3	0	100	104	10	4	15	0	170	162	7	-3	0	1	638	668	13	-4	6	1	169	164	4	-7	12	1	21	28	20
0	4	0	1681	1624	10	5	15	0	35	43	14	-1	0	1	806	1217	805	-3	6	1	243	270	9	-6	12	1	159	149	10
1	4	0	421	412	10	6	15	0	138	123	8	1	0	1	357	359	5	-2	6	1	207	193	11	-5	12	1	211	194	4
2	4	0	336	362	9	7	15	0	7	9	7	3	0	1	116	132	11	-1	6	1	288	289	5	-4	12	1	343	328	6
3	4	0	345	343	4	0	16	0	305	315	7	5	0	1	156	141	4	0	6	1	332	342	6	-3	12	1	172	152	4
4	4	0	130	133	7	1	16	0	213	205	4	7	0	1	123	111	10	1	6	1	51	58	7	-2	12	1	245	239	7
5	4	0	84	82	6	2	16	0	283	281	4	-8	1	1	43	7	17	2	6	1	92	95	5	-1	12	1	48	47	10
6	4	0	49	72	17	3	16	0	18	30	17	-7	1	1	34	5	24	3	6	1	152	167	13	0	12	1	213	220	2
7	4	0	29	5	28	4	16	0	211	210	5	-6	1	1	33	58	27	4	6	1	143	135	4	1	12	1	170	157	4
1	5	0	188	194	2	5	16	0	0	27	1	-5	1	1	74	76	7	5	6	1	123	124	5	2	12	1	37	39	13
2	5	0	351	342	6	6	16	0	0	5	1	-4	1	1	108	109	9	6	6	1	90	69	15	3	12	1	0	11	1
3	5	0	40	40	11	1	17	0	142	140	4	-3	1	1	331	341	4	7	6	1	53	84	18	4	12	1	113	111	5
4	5	0	222	217	4	2	17	0	36	29	15	-2	1	1	193	286	89	-7	7	1	35	7	25	5	12	1	46	34	14
5	5	0	75	77	7	3	17	0	121	117	6	-1	1	1	378	902	377	-6	7	1	24	10	23	6	12	1	140	124	16
6	5	0	161	155	11	4	17	0	51	59	14	0	1	1	465	561	4	-5	7	1	33	24	23	7	12	1	87	73	11
7	5	0	29	11	28	5	17	0	135	121	8	1	1	1	1008	950	5	-4	7	1	279	282	4	-7	13	1	10	1	10
0	6	0	584	537	13	6	17	0	43	64	43	2	1	1	195	208	4	-3	7	1	267	257	3	-6	13	1	29	0	28
1	6	0	161	147	5	0	18	0	100	102	6	3	1	1	181	202	8	-2	7	1	468	470	12	-5	13	1	39	71	23
2	6	0	424	433	6	1	18	0	308	313	4	4	1	1	230	242	3	-1	7	1	235	227	3	-4	13	1	55	48	19
3	6	0	192	207	3	2	18	0	34	39	23	5	1	1	236	240	3	0	7	1	198	193	2	-3	13	1	74	54	7
4	6	0	290	292	3	3	18	0	232	231	4	6	1	1	30	21	29	1	7	1	255	267	4	-2	13	1	311	313	8
5	6	0	149	142	9	4	18	0	53	53	13	7	1	1	0	5	1	2	7	1	827	836	10	-1	13	1	201	206	3
6	6	0	29	37	28	5	18	0	32	41	31	-8	2	1	139	105	9	3	7	1	151	157	4	0	13	1	751	772	5
7	6	0	0	32	1	6	18	0	10	0	10	-7	2	1	32	36	32	4	7	1	332	339	4	1	13	1	28	14	21
1	7	0	91	87	4	1	19	0	50	58	12	-6	2	1	198	188	5	5	7	1	0	8	1	2	13	1	536	518	6
2	7	0	108	112	5	2	19	0	79	82	19	-5	2	1	166	167	8	6	7	1	47	63	17	3	13	1	59	67	8
3	7	0	276	283	5	3	19	0	33	16	17	-4	2	1	374	389	14	7	7	1	6	12	5	4	13	1	92	96	7
4	7	0	31	46	20	4	19	0	118	120	17	-3	2	1	101	103	4	-7	8	1	19	26	19	5	13	1	21	31	20
5	7	0	194	194	7	5	19	0	114	109	8	-2	2	1	338	384	17	-6	8	1	176	180	9	6	13	1	72	74	39
6	7	0	40	61	21	6	19	0	71	78	14	-1	2	1	66	339	65	-5	8	1	48	47	24	7	13	1	0	6	1
7	7	0	82	99	12	0	20	0	179	181	9	0	2	1	458	444	6	-4	8	1	368	372	6	-7	14	1	51	68	20
0	8	0	430	457	6	1	20	0	174	165	8	1	2	1	259	262	10	-3	8	1	326	311	4	-6	14	1	96	93	10
1	8	0	796	811	7	2	20	0	300	307	14	2	2	1	32	9	9	-2	8	1	448	441	6	-5	14	1	143	140	7
2	8	0	49	53	7	3	20	0	0	19	1	3	2	1	109	113	12	-1	8	1	152	153	9	-4	14	1	247	230	10
3	8	0	506	514	12	4	20	0	160	164	15	4	2	1	162	164	4	0	8	1	74	76	4	-3	14	1	108	102</	

Table A-4, Continued
Observed and Calculated Structure Factors for 1,6-diferrocenylhexane-1,6-dione

h	k	l	IO _o	IO _c	IO _a	h	k	l	IO _o	IO _c	IO _a	h	k	l	IO _o	IO _c	IO _a	h	k	l	IO _o	IO _c	IO _a						
2	16	1	58	62	11	2	23	1	251	254	6	5	1	2	139	132	4	-2	7	2	206	195	3	-4	13	2	37	31	16
3	16	1	59	61	10	3	23	1	95	96	14	6	1	2	107	93	15	-1	7	2	0	35	1	-3	13	2	307	323	11
4	16	1	44	34	21	4	23	1	116	108	10	7	1	2	45	49	19	0	7	2	385	378	6	-2	13	2	95	102	6
5	16	1	151	134	7	5	23	1	0	22	1	-8	2	2	31	29	30	1	7	2	587	561	6	-1	13	2	394	408	6
6	16	1	31	38	30	-5	24	1	37	60	24	-7	2	2	55	67	16	2	7	2	223	231	3	0	13	2	62	58	4
-6	17	1	30	15	30	-4	24	1	122	103	9	-6	2	2	48	52	14	3	7	2	138	137	10	1	13	2	58	49	8
-5	17	1	26	48	26	-3	24	1	74	84	22	-5	2	2	83	92	8	4	7	2	115	113	5	2	13	2	146	139	4
-4	17	1	38	26	17	-2	24	1	137	121	20	-4	2	2	24	20	24	5	7	2	186	185	5	3	13	2	125	115	6
-3	17	1	163	157	5	-1	24	1	0	7	1	-3	2	2	158	192	62	6	7	2	36	29	16	4	13	2	56	57	8
-2	17	1	257	253	5	0	24	1	97	90	6	-2	2	2	11	13	10	7	7	2	108	86	17	5	13	2	39	41	20
-1	17	1	41	41	17	1	24	1	0	3	1	-1	2	2	115	102	8	-7	8	2	28	42	28	6	13	2	29	2	29
0	17	1	464	454	4	2	24	1	22	4	22	0	2	2	500	505	4	-6	8	2	37	11	14	-7	14	2	23	13	22
1	17	1	190	181	4	3	24	1	54	40	11	1	2	2	743	731	5	-5	8	2	55	46	10	-6	14	2	49	50	14
2	17	1	224	233	15	4	24	1	37	50	21	2	2	2	306	318	3	-4	8	2	55	32	9	-5	14	2	106	94	9
3	17	1	96	87	6	5	24	1	44	41	16	3	2	2	494	523	6	-3	8	2	0	18	1	-4	14	2	46	5	10
4	17	1	123	123	13	-5	25	1	29	26	28	4	2	2	149	166	15	-2	8	2	150	154	3	-3	14	2	103	100	9
5	17	1	65	79	13	-4	25	1	14	21	14	5	2	2	235	223	3	-1	8	2	438	453	6	-2	14	2	274	264	9
6	17	1	55	62	15	-3	25	1	36	48	36	6	2	2	41	30	13	0	8	2	233	218	2	-1	14	2	299	309	4
-6	18	1	82	93	17	-2	25	1	82	81	12	7	2	2	40	48	21	1	8	2	350	374	4	0	14	2	284	287	4
-5	18	1	20	13	19	-1	25	1	180	173	6	-8	3	2	34	5	26	2	8	2	18	42	17	1	14	2	229	226	3
-4	18	1	216	206	7	0	25	1	77	88	7	-7	3	2	139	134	7	3	8	2	388	396	6	2	14	2	234	228	8
-3	18	1	11	8	10	1	25	1	189	189	7	-6	3	2	0	4	1	4	8	2	0	6	1	3	14	2	113	109	5
-2	18	1	91	92	7	2	25	1	53	38	12	-5	3	2	239	252	3	5	8	2	127	134	7	4	14	2	223	213	5
-1	18	1	93	88	5	3	25	1	162	160	8	-4	3	2	101	107	5	6	8	2	10	29	10	5	14	2	122	113	7
0	18	1	188	186	3	4	25	1	64	59	14	-3	3	2	360	719	360	7	8	2	62	72	15	6	14	2	0	46	1
1	18	1	61	41	6	-4	26	1	20	6	20	-2	3	2	79	75	8	-7	9	2	59	68	14	-7	15	2	53	27	12
2	18	1	109	107	5	-3	26	1	144	127	11	-1	3	2	196	192	12	-6	9	2	152	138	6	-6	15	2	140	134	9
3	18	1	7	18	7	-2	26	1	12	6	11	0	3	2	911	901	11	-5	9	2	151	140	6	-5	15	2	73	78	15
4	18	1	128	127	8	-1	26	1	53	59	13	1	3	2	221	224	3	-4	9	2	336	326	4	-4	15	2	250	245	4
5	18	1	31	28	17	0	26	1	40	56	10	2	3	2	111	115	4	-3	9	2	171	180	8	-3	15	2	134	139	5
6	18	1	57	67	17	1	26	1	0	4	1	3	3	2	114	124	10	-2	9	2	388	408	7	-2	15	2	173	173	5
-6	19	1	14	7	14	2	26	1	0	32	1	4	3	2	49	42	8	-1	9	2	185	203	3	-1	15	2	90	93	5
-5	19	1	0	39	1	3	26	1	45	51	19	5	3	2	192	182	6	0	9	2	225	229	2	0	15	2	366	371	5
-4	19	1	107	102	10	4	26	1	0	16	1	6	3	2	21	30	21	1	9	2	160	145	4	1	15	2	106	96	13
-3	19	1	76	63	11	-4	27	1	0	11	1	7	3	2	98	92	21	2	9	2	113	109	4	2	15	2	96	93	5
-2	19	1	149	136	4	-3	27	1	42	39	42	-8	4	2	43	31	17	3	9	2	182	180	10	3	15	2	68	69	7
-1	19	1	208	195	4	-2	27	1	53	73	18	-7	4	2	42	38	17	4	9	2	139	135	4	4	15	2	69	80	19
0	19	1	226	221	3	-1	27	1	104	108	9	-6	4	2	39	59	24	5	9	2	0	12	1	5	15	2	18	14	18
1	19	1	229	232	4	0	27	1	161	150	4	-5	4	2	86	82	17	6	9	2	56	75	14	6	15	2	101	82	10
2	19	1	109	100	5	1	27	1	89	95	10	-4	4	2	47	46	8	7	9	2	69	76	15	-7	16	2	31	17	31
3	19	1	208	213	4	2	27	1	110	109	13	-3	4	2	61	195	60	-7	10	2	19	7	19	-6	16	2	0	29	1
4	19	1	96	98	11	3	27	1	86	68	11	-2	4	2	39	143	38	-6	10	2	66	75	12	-5	16	2	49	40	19
5	19	1	58	71	18	4	27	1	48	53	15	-1	4	2	543	504	5	-5	10	2	76	67	12	-4	16	2	40	12	16
6	19	1	27	27	27	-3	28	1	41	56	19	0	4	2	473	489	3	-4	10	2	40	39	16	-3	16	2	60	59	9
-6	20	1	0	22	1	-2	28	1	62	81	15	1	4	2	159	180	3	-3	10	2	26	2	25	-2	16	2	108	116	6
-5	20	1	175	159	19	-1	28	1	40	48	19	2	4	2	441	466	6	-2	10	2	241	246	12	-1	16	2	258	251	4
-4	20	1	3	34	2	0	28	1	0	18	1	3	4	2	255	274	5	-1	10	2	388	391	7	0	16	2	63	58	6
-3	20	1	124	131	8	1	28	1	0	8	1	4	4	2	105	111	5	0	10	2	370	375	3	1	16	2	108	98	5
-2	20	1	24	16	24	2	28	1	6	29	6	5	4	2	142	133	4	1	10	2	91	92	7	2	16	2	240	242	10
-1	20	1	83	91	7	3	28	1	12	1	12	6	4	2	110	98	8	2	10	2	607	621	6	3	16	2	47	57	10
0	20	1	159	156	3	-3	29	1	27	31	26	7	4	2	36	26	19	3	10	2	0	3	1	4	16	2	187	175	6
1	20	1	112	112	5	-2	29	1	42	62	21	-8	5	2	76	79	14	4	10	2	249	252	3	5	16	2	68	81	15
2	20	1	55	47	7	-1	29	1	86	82	11	-7	5	2	0	23	1	5	10	2	24	13	23	6	16	2	52	59	14
3	20	1	89	94	9	0	29	1	34	33	11	-6	5	2	174	179	15	6	10	2	135	127	21	-6	17	2	0	46	1
4	20	1	26	6	26	1	29	1	52	69	17	-5	5	2	12	16	12	7	10	2	20	38	20	-5	17	2	151	128	8
5	20	1	146	123	9	2	29	1	109	102	20	-4	5	2	475	488	10	-7	11	2	44	36	18	-4	17	2	148	136	12
6	20	1	13	8	13	3	29	1	56	60	17	-3	5	2	0	3	1	-6	11	2	188	161	6	-3	17	2	223	221	6
-6	21	1	40	23	14	-2	30	1	27	30	26	-2	5	2	665	705	6	-5	11	2	110	101	6	-2	17	2	98	90	16
-5	21	1	26	4	26	-1	30	1	39	56	20	-1	5	2	596	574	5	-4	11	2	203	202	4	-1					

Table A-4, Continued
Observed and Calculated Structure Factors for 1,6-diferrocenylhexane-1,6-dione

h	k	l	10Fo	10Fc	10o	h	k	l	10Fo	10Fc	10o	h	k	l	10Fo	10Fc	10o	h	k	l	10Fo	10Fc	10o
5	19	2	34	39	34	0	28	2	16	5	16	5	4	3	49	67	14	4	10	3	59	56	7
-6	20	2	16	24	15	1	28	2	136	121	10	6	4	3	25	35	25	5	10	3	34	39	33
-5	20	2	36	1	15	2	28	2	0	4	1	7	4	3	29	16	28	6	10	3	0	1	1
-4	20	2	35	57	22	3	28	2	34	61	33	-7	5	3	63	80	13	-7	11	3	64	65	16
-3	20	2	74	75	10	-3	29	2	64	63	15	-6	5	3	58	55	21	-6	11	3	34	45	19
-2	20	2	92	86	19	-2	29	2	33	50	27	-5	5	3	24	78	23	-5	11	3	63	52	12
-1	20	2	0	11	1	-1	29	2	13	8	12	-4	5	3	38	23	13	-4	11	3	0	2	1
0	20	2	96	103	4	0	29	2	29	24	14	-3	5	3	60	61	7	-3	11	3	113	116	5
1	20	2	120	116	5	1	29	2	40	50	19	-2	5	3	39	39	12	-2	11	3	70	43	10
2	20	2	246	247	10	2	29	2	22	10	22	-1	5	3	549	558	6	-1	11	3	453	448	14
3	20	2	38	25	16	-2	30	2	20	23	20	0	5	3	40	42	5	0	11	3	21	17	18
4	20	2	194	189	8	-1	30	2	0	18	1	1	5	3	451	445	10	1	11	3	175	167	9
5	20	2	35	34	21	0	30	2	103	112	7	2	5	3	188	179	6	2	11	3	199	216	6
-6	21	2	62	67	19	1	30	2	20	22	19	3	5	3	425	428	12	3	11	3	369	365	5
-5	21	2	51	62	17	2	30	2	43	56	17	4	5	3	0	21	1	4	11	3	112	103	6
-4	21	2	154	140	13	-1	31	2	48	47	17	5	5	3	218	215	5	5	11	3	136	130	8
-3	21	2	73	70	12	0	31	2	20	24	19	6	5	3	0	2	1	6	11	3	48	42	29
-2	21	2	136	123	5	1	31	2	35	13	18	7	5	3	110	98	32	-7	12	3	28	31	28
-1	21	2	200	196	4	-7	0	3	112	109	9	-7	6	3	52	72	22	-6	12	3	91	110	5
0	21	2	135	143	3	-5	0	3	148	180	15	-6	6	3	125	133	11	-5	12	3	57	60	24
1	21	2	0	20	1	-3	0	3	905	899	7	-5	6	3	135	126	33	-4	12	3	312	307	4
2	21	2	0	26	1	-1	0	3	481	502	9	-4	6	3	38	85	38	-3	12	3	105	84	8
3	21	2	13	1	13	1	0	3	426	438	6	-3	6	3	144	408	144	-2	12	3	385	404	6
4	21	2	62	68	13	3	0	3	180	185	4	-2	6	3	55	58	7	-1	12	3	128	129	4
5	21	2	29	4	28	5	0	3	0	4	1	-1	6	3	412	418	6	0	12	3	418	412	4
-5	22	2	0	7	1	7	0	3	41	41	14	0	6	3	403	417	11	1	12	3	153	166	4
-4	22	2	28	16	27	-8	1	3	27	34	26	1	6	3	72	78	7	2	12	3	186	182	4
-3	22	2	35	28	18	-7	1	3	68	69	16	2	6	3	248	254	10	3	12	3	117	121	5
-2	22	2	88	76	7	-6	1	3	89	85	9	3	6	3	41	41	11	4	12	3	42	51	13
-1	22	2	209	205	6	-5	1	3	54	138	53	4	6	3	243	245	3	5	12	3	43	39	17
0	22	2	143	140	3	-4	1	3	35	6	17	5	6	3	81	72	11	6	12	3	30	42	29
1	22	2	203	205	6	-3	1	3	65	41	8	6	6	3	0	3	1	-7	13	3	0	3	1
2	22	2	108	118	8	-2	1	3	109	150	37	7	6	3	27	39	26	-6	13	3	55	61	15
3	22	2	149	158	22	-1	1	3	145	148	4	-7	7	3	35	41	30	-5	13	3	15	26	15
4	22	2	55	61	17	0	1	3	58	62	4	-6	7	3	116	105	8	-4	13	3	125	128	10
5	22	2	65	80	15	1	1	3	480	479	5	-5	7	3	71	77	7	-3	13	3	34	30	17
-5	23	2	80	97	16	2	1	3	369	405	6	-4	7	3	31	56	13	-2	13	3	149	151	4
-4	23	2	24	34	24	3	1	3	342	340	6	-3	7	3	44	41	10	-1	13	3	57	53	7
-3	23	2	167	156	7	4	1	3	185	185	4	-2	7	3	106	103	4	0	13	3	343	351	5
-2	23	2	22	32	21	5	1	3	200	201	10	-1	7	3	121	108	4	1	13	3	112	108	10
-1	23	2	127	139	12	6	1	3	48	58	15	0	7	3	246	246	3	2	13	3	287	290	4
0	23	2	49	62	10	7	1	3	62	66	17	1	7	3	218	218	3	3	13	3	55	61	9
1	23	2	63	79	16	-8	2	3	42	39	18	2	7	3	514	543	8	4	13	3	205	210	14
2	23	2	23	38	22	-7	2	3	21	14	21	3	7	3	281	288	7	5	13	3	24	10	24
3	23	2	27	15	27	-6	2	3	169	171	8	4	7	3	293	294	8	6	13	3	121	111	10
4	23	2	0	25	1	-5	2	3	0	38	1	5	7	3	29	21	28	-7	14	3	41	37	21
5	23	2	23	38	23	-4	2	3	354	358	4	6	7	3	134	129	8	-6	14	3	48	27	14
-5	24	2	24	18	23	-3	2	3	216	213	3	7	7	3	39	25	20	-5	14	3	145	142	7
-4	24	2	0	22	1	-2	2	3	304	534	303	-7	8	3	0	10	1	-4	14	3	156	140	4
-3	24	2	0	6	1	-1	2	3	189	179	5	-6	8	3	179	153	6	-3	14	3	299	293	8
-2	24	2	25	27	24	0	2	3	509	522	6	-5	8	3	25	27	24	-2	14	3	375	368	6
-1	24	2	78	91	12	1	2	3	214	220	3	-4	8	3	250	244	4	-1	14	3	229	230	6
0	24	2	171	168	4	2	2	3	471	488	5	-3	8	3	79	84	7	0	14	3	27	34	11
1	24	2	183	176	8	3	2	3	14	18	14	-2	8	3	655	671	6	1	14	3	103	94	5
2	24	2	124	132	9	4	2	3	107	101	6	-1	8	3	233	234	3	2	14	3	113	98	5
3	24	2	136	128	8	5	2	3	25	5	25	0	8	3	301	306	6	3	14	3	92	85	7
4	24	2	39	75	38	6	2	3	57	39	11	1	8	3	68	61	5	4	14	3	13	44	13
-5	25	2	35	26	23	7	2	3	19	15	18	2	8	3	166	164	4	5	14	3	35	4	15
-4	25	2	99	91	22	-8	3	3	44	81	29	3	8	3	57	68	9	6	14	3	25	32	24
-3	25	2	96	108	10	-7	3	3	0	14	1	4	8	3	75	86	7	-7	15	3	60	63	14
-2	25	2	139	126	8	-6	3	3	57	59	12	5	8	3	16	13	15	-6	15	3	17	2	16
-1	25	2	0	15	1	-5	3	3	31	105	31	6	8	3	24	40	23	-5	15	3	45	15	14
0	25	2	33	36	12	-4	3	3	74	72	6	-7	9	3	62	62	20	-4	15	3	28	43	28
1	25	2	49	41	14	-3	3	3	110	97	5	-6	9	3	0	21	1	-3	15	3	51	45	11
2	25	2	55	62	15	-2	3	3	101	247	100	-5	9	3	91	91	8	-2	15	3	65	50	7
3	25	2	26	26	26	-1	3	3	502	502	5	-4	9	3	115	98	5	-1	15	3	35	51	17
4	25	2	0	21	1	0	3	3	187	200	2	-3	9	3	49	26	14	0	15	3	128	127	3
-4	26	2	32	15	32	1	3	3	22	8	22	-2	9	3	260	254	6	1	15	3	364	348	6
-3	26	2	0	4	1	2	3	3	582	618	6	-1	9	3	104	110	5	2	15	3	31	35	15
-2	26	2	37	32	17	3	3	3	0	19	1	0	9	3	525	516	8	3	15	3	333	320	6
-1	26	2	64	92	29	4	3	3	360	360	9	1	9	3	269	274	3	4	15	3	96	86	25
0	26	2	156	158	6	5	3	3	34	40	15	2	9	3	156	160	6	5	15	3	127	121	21
1	26	2	102	90	8	6	3	3	138	124	7	3	9	3	263	271	12	6	15	3	54	54	15
2	26	2	127	140	9	7	3	3	20	24	20	4											

Table A-4, Continued
Observed and Calculated Structure Factors for 1,6-diferrocenylnhexane-1,6-dione

h	k	l	10Fo	10Fc	10o	h	k	l	10Fo	10Fc	10o	h	k	l	10Fo	10Fc	10o	h	k	l	10Fo	10Fc	10o						
-3	25	3	0	10	1	2	3	4	32	6	12	5	9	4	0	3	1	-4	16	4	26	50	25	-5	24	4	48	25	14
-2	25	3	35	44	28	3	3	4	281	285	3	6	9	4	11	28	11	-3	16	4	62	55	7	-4	24	4	0	28	1
-1	25	3	123	123	9	4	3	4	21	16	21	-7	10	4	26	21	25	-2	16	4	48	47	9	-3	24	4	0	6	1
0	25	3	21	41	20	5	3	4	0	6	1	-6	10	4	116	116	10	-1	16	4	181	183	4	-2	24	4	0	3	1
1	25	3	64	86	15	6	3	4	0	3	1	-5	10	4	31	19	27	0	16	4	138	137	3	-1	24	4	0	4	1
2	25	3	53	59	11	-7	4	4	8	39	7	-4	10	4	62	65	8	1	16	4	91	89	6	0	24	4	12	28	12
3	25	3	85	81	10	-6	4	4	152	141	10	-3	10	4	0	3	1	2	16	4	187	174	4	1	24	4	84	86	14
4	25	3	61	71	15	-5	4	4	27	29	26	-2	10	4	31	9	17	3	16	4	59	44	11	2	24	4	41	46	13
-4	26	3	54	56	26	-4	4	4	87	82	7	-1	10	4	431	420	6	4	16	4	147	145	8	3	24	4	81	86	13
-3	26	3	77	68	13	-3	4	4	108	96	10	0	10	4	237	245	4	5	16	4	38	59	30	-4	25	4	85	85	17
-2	26	3	49	51	14	-2	4	4	49	39	20	1	10	4	0	24	1	-6	17	4	37	46	22	-3	25	4	63	55	14
-1	26	3	102	113	9	-1	4	4	70	65	4	2	10	4	187	199	4	-5	17	4	157	162	8	-2	25	4	146	151	7
0	26	3	40	58	11	0	4	4	359	377	7	3	10	4	0	21	1	-4	17	4	118	106	8	-1	25	4	67	71	14
1	26	3	95	104	10	1	4	4	239	235	3	4	10	4	265	253	5	-3	17	4	305	298	4	0	25	4	120	117	8
2	26	3	0	22	1	2	4	4	319	322	4	5	10	4	27	50	27	-2	17	4	267	253	7	1	25	4	62	59	12
3	26	3	42	8	16	3	4	4	120	122	4	6	10	4	81	95	24	-1	17	4	239	224	4	2	25	4	89	85	10
-4	27	3	44	26	15	4	4	4	146	155	8	-7	11	4	30	20	30	0	17	4	176	160	4	3	25	4	104	84	10
-3	27	3	35	6	35	5	4	4	74	81	16	-6	11	4	65	82	13	1	17	4	292	274	3	-4	26	4	0	12	1
-2	27	3	63	53	13	6	4	4	93	88	11	-5	11	4	30	36	29	2	17	4	139	127	4	-3	26	4	21	15	20
-1	27	3	117	105	25	-7	5	4	12	5	12	-4	11	4	171	161	4	3	17	4	64	83	12	-2	26	4	0	2	1
0	27	3	121	120	6	-6	5	4	140	157	7	-3	11	4	119	118	5	4	17	4	0	27	1	-1	26	4	9	34	8
1	27	3	0	47	1	-5	5	4	56	58	9	-2	11	4	364	365	5	5	17	4	0	6	1	0	26	4	39	38	11
2	27	3	35	24	13	-4	5	4	353	344	4	-1	11	4	247	248	4	-6	18	4	0	14	1	1	26	4	42	33	14
3	27	3	54	68	15	-3	5	4	65	62	10	0	11	4	415	416	6	-5	18	4	42	30	15	2	26	4	81	80	16
-3	28	3	14	2	14	-2	5	4	963	954	5	1	11	4	211	197	3	-4	18	4	69	80	12	3	26	4	38	24	38
-2	28	3	69	79	15	-1	5	4	0	7	1	2	11	4	334	322	4	-3	18	4	34	46	33	-3	27	4	112	123	18
-1	28	3	0	3	1	0	5	4	624	643	4	3	11	4	51	35	9	-2	18	4	0	1	1	-2	27	4	143	122	8
0	28	3	83	96	9	1	5	4	155	154	3	4	11	4	35	42	21	-1	18	4	145	141	4	-1	27	4	88	92	13
1	28	3	0	14	1	2	5	4	277	282	3	5	11	4	33	20	21	0	18	4	18	29	17	0	27	4	54	77	11
2	28	3	0	35	1	3	5	4	0	13	1	6	11	4	14	2	14	1	18	4	211	197	4	1	27	4	20	44	20
-3	29	3	48	14	12	4	5	4	103	101	5	-7	12	4	53	74	26	2	18	4	3	32	3	2	27	4	51	55	15
-2	29	3	43	47	18	5	5	4	0	24	1	-6	12	4	33	45	33	3	18	4	123	116	8	-3	28	4	0	26	1
-1	29	3	4	15	3	6	5	4	0	5	1	-5	12	4	102	120	8	4	18	4	0	12	1	-2	28	4	0	6	1
0	29	3	52	58	11	-7	6	4	49	67	14	-4	12	4	33	5	32	5	18	4	112	96	11	-1	28	4	0	7	1
1	29	3	29	41	29	-6	6	4	17	31	17	-3	12	4	57	54	8	-6	19	4	12	45	12	0	28	4	32	20	10
2	29	3	91	81	11	-5	6	4	0	7	1	-2	12	4	48	37	9	-5	19	4	94	74	40	1	28	4	36	61	35
-2	30	3	0	13	1	-4	6	4	47	32	9	-1	12	4	133	139	4	-4	19	4	163	136	7	2	28	4	0	29	1
-1	30	3	75	91	15	-3	6	4	75	155	74	0	12	4	151	138	4	-3	19	4	255	244	5	-2	29	4	42	49	41
0	30	3	37	30	14	-2	6	4	98	90	4	1	12	4	187	189	4	-2	19	4	161	156	4	-1	29	4	138	130	18
1	30	3	23	42	22	-1	6	4	297	290	4	2	12	4	0	26	1	-1	19	4	194	187	4	0	29	4	42	42	10
-8	0	4	74	69	11	0	6	4	378	379	6	3	12	4	213	209	4	0	19	4	242	239	5	1	29	4	64	73	16
-6	0	4	22	127	22	1	6	4	229	227	3	4	12	4	207	185	6	1	19	4	154	138	8	-1	30	4	0	18	1
-4	0	4	174	170	7	2	6	4	178	180	4	5	12	4	134	130	8	2	19	4	138	141	7	-7	0	5	34	38	34
-2	0	4	133	125	3	3	6	4	247	245	3	6	12	4	0	9	1	3	19	4	56	72	15	-5	0	5	195	192	7
0	0	4	455	449	5	4	6	4	225	217	12	-7	13	4	39	29	17	4	19	4	30	12	20	-3	0	5	318	342	11
2	0	4	345	364	4	5	6	4	19	39	19	-6	13	4	0	10	1	5	19	4	27	5	27	-1	0	5	407	421	8
4	0	4	178	175	4	6	6	4	72	70	11	-5	13	4	179	172	6	-6	20	4	25	42	25	1	0	5	481	478	5
6	0	4	135	134	8	-7	7	4	59	63	16	-4	13	4	40	32	16	-5	20	4	17	28	17	3	0	5	330	340	4
-8	1	4	0	10	1	-6	7	4	24	94	24	-3	13	4	308	308	4	-4	20	4	48	42	14	5	0	5	46	52	15
-7	1	4	36	27	23	-5	7	4	230	222	17	-2	13	4	0	18	1	-3	20	4	14	11	14	-7	1	5	89	77	11
-6	1	4	103	108	16	-4	7	4	92	86	7	-1	13	4	386	388	6	-2	20	4	45	39	13	-6	1	5	123	90	17
-5	1	4	121	118	11	-3	7	4	356	357	4	0	13	4	53	57	6	-1	20	4	84	82	6	-5	1	5	189	180	4
-4	1	4	258	255	3	-2	7	4	107	110	5	1	13	4	332	329	7	0	20	4	82	79	5	-4	1	5	69	49	8
-3	1	4	156	153	4	-1	7	4	1087	1071	5	2	13	4	48	51	26	1	20	4	124	136	7	-3	1	5	82	196	82
-2	1	4	590	622	5	0	7	4	357	357	3	3	13	4	201	192	10	2	20	4	152	153	8	-2	1	5	135	138	3
-1	1	4	336	349	13	1	7	4	453	445	6	4	13	4	20	30	19	3	20	4	29	54	28	-1	1	5	86	86	4
0	1	4	384	421	4	2	7	4	152	151	5	5	13	4	36	28	18	4	20	4	119	115	9	0	1	5	126	124	2
1	1	4	345	351	4	3	7	4	121	121	4	6	13	4	18	29	17	-5	21	4	26	22	25	1	1	5	123	121	4
2	1	4	374	384	6	4	7	4	20	22	19	-7	14	4	0	30	1	-4	21	4	135	115	8	2	1	5	180	178	3
3	1	4	136	137	4	5	7	4																					

Table A-4, Continued
Observed and Calculated Structure Factors for 1,6-diferrocenylhexane-1,6-dione

h	k	l	10Fo	10Fc	10o	h	k	l	10Fo	10Fc	10o	h	k	l	10Fo	10Fc	10o	h	k	l	10Fo	10Fc	10o
6	3	5	143	115	8	-5	10	5	43	131	42	-5	17	5	44	53	17	-2	26	5	49	50	15
-7	4	5	0	11	1	-4	10	5	152	146	4	-4	17	5	123	124	9	-1	26	5	77	94	14
-6	4	5	92	64	20	-3	10	5	264	254	3	-3	17	5	62	54	18	0	26	5	0	22	1
-5	4	5	199	185	4	-2	10	5	50	44	19	-2	17	5	30	34	15	1	26	5	104	87	9
-4	4	5	88	89	5	-1	10	5	530	525	5	-1	17	5	17	30	16	2	26	5	33	46	32
-3	4	5	125	239	124	0	10	5	59	52	6	0	17	5	39	38	8	-3	27	5	0	24	1
-2	4	5	249	256	3	1	10	5	291	276	4	1	17	5	36	41	35	-2	27	5	26	18	25
-1	4	5	519	537	7	2	10	5	19	21	19	2	17	5	118	113	8	-1	27	5	38	34	16
0	4	5	381	394	4	3	10	5	213	206	6	3	17	5	36	42	17	0	27	5	37	45	10
1	4	5	219	215	3	4	10	5	38	61	19	4	17	5	101	110	11	1	27	5	12	20	11
2	4	5	86	76	5	5	10	5	73	65	16	5	17	5	34	42	34	-2	28	5	80	83	32
3	4	5	202	202	4	-7	11	5	50	80	45	-6	18	5	43	49	16	-1	28	5	0	35	1
4	4	5	25	28	24	-6	11	5	40	15	7	0	18	5	0	36	1	0	28	5	71	88	9
5	4	5	0	23	1	-5	11	5	143	118	8	-4	18	5	143	134	11	1	28	5	37	45	22
6	4	5	21	14	21	-4	11	5	109	99	5	-3	18	5	11	6	10	-6	0	6	241	230	6
-7	5	5	113	103	9	-3	11	5	61	48	7	-2	18	5	247	236	6	-4	0	6	158	301	158
-6	5	5	30	26	22	-2	11	5	24	5	23	-1	18	5	18	27	18	-2	0	6	52	46	8
-5	5	5	219	213	7	-1	11	5	114	123	7	0	18	5	288	276	3	0	0	6	178	180	3
-4	5	5	35	23	13	0	11	5	24	16	12	1	18	5	24	17	24	2	0	6	70	66	5
-3	5	5	175	190	11	1	11	5	38	44	13	2	18	5	134	124	10	4	0	6	156	164	6
-2	5	5	0	27	1	2	11	5	75	67	6	3	18	5	20	14	20	-7	1	6	0	7	1
-1	5	5	32	20	12	3	11	5	203	196	5	4	18	5	38	27	16	-6	1	6	0	6	1
0	5	5	71	60	3	4	11	5	49	38	13	-6	19	5	67	68	16	-5	1	6	0	7	1
1	5	5	271	258	3	5	11	5	48	71	18	-5	19	5	49	56	18	-4	1	6	20	9	19
2	5	5	38	38	15	-7	12	5	0	4	1	-4	19	5	77	81	13	-3	1	6	41	31	11
3	5	5	120	117	9	-6	12	5	38	45	19	-3	19	5	40	59	19	-2	1	6	208	211	3
4	5	5	12	15	11	-5	12	5	80	88	14	-2	19	5	0	2	1	-1	1	6	190	192	3
5	5	5	192	170	11	-4	12	5	161	150	4	-1	19	5	0	7	1	0	1	6	158	160	2
6	5	5	0	17	1	-3	12	5	95	86	5	0	19	5	78	79	5	1	1	6	159	155	4
-7	6	5	8	10	8	-2	12	5	264	258	4	1	19	5	0	5	1	2	1	6	136	137	4
-6	6	5	51	40	39	-1	12	5	156	157	4	2	19	5	64	57	10	3	1	6	53	53	9
-5	6	5	144	134	5	0	12	5	381	375	11	3	19	5	131	121	8	4	1	6	95	102	9
-4	6	5	87	77	7	1	12	5	129	121	5	4	19	5	29	45	28	5	1	6	29	33	29
-3	6	5	299	307	9	2	12	5	231	233	4	-5	20	5	44	48	34	-7	2	6	133	109	9
-2	6	5	198	203	3	3	12	5	104	94	8	-4	20	5	54	52	14	-6	2	6	23	37	23
-1	6	5	555	561	5	4	12	5	141	125	7	-3	20	5	133	126	8	-5	2	6	274	265	5
0	6	5	326	342	4	5	12	5	0	4	1	-2	20	5	99	87	7	-4	2	6	27	20	27
1	6	5	229	223	7	-7	13	5	0	5	1	-1	20	5	231	236	5	-3	2	6	163	164	4
2	6	5	105	102	9	-6	13	5	120	133	10	0	20	5	101	90	6	-2	2	6	27	41	23
3	6	5	120	110	13	-5	13	5	36	32	20	1	20	5	242	231	7	-1	2	6	151	151	4
4	6	5	0	21	1	-4	13	5	116	109	9	2	20	5	65	68	11	0	2	6	66	66	4
5	6	5	26	12	25	-3	13	5	44	30	12	3	20	5	42	47	13	1	2	6	59	50	6
6	6	5	28	6	28	-2	13	5	59	41	8	4	20	5	0	2	1	2	2	6	26	30	26
-7	7	5	61	59	15	-1	13	5	245	252	3	-5	21	5	61	65	14	3	2	6	207	204	8
-6	7	5	144	136	7	0	13	5	0	4	1	-4	21	5	0	17	1	4	2	6	22	12	21
-5	7	5	0	25	1	1	13	5	0	1	1	-3	21	5	50	55	20	5	2	6	141	116	7
-4	7	5	93	97	10	2	13	5	96	88	5	-2	21	5	0	4	1	-7	3	6	0	8	1
-3	7	5	22	23	21	3	13	5	0	7	1	-1	21	5	22	7	22	-6	3	6	37	6	16
-2	7	5	304	298	4	4	13	5	152	142	12	0	21	5	8	31	8	-5	3	6	0	6	1
-1	7	5	67	66	6	5	13	5	27	31	27	1	21	5	77	82	13	-4	3	6	24	29	24
0	7	5	134	139	3	-6	14	5	21	4	20	2	21	5	26	3	26	-3	3	6	161	168	4
1	7	5	84	86	5	-5	14	5	57	53	12	3	21	5	27	47	27	-2	3	6	55	60	7
2	7	5	219	216	3	-4	14	5	184	182	6	4	21	5	55	59	17	-1	3	6	317	324	3
3	7	5	133	134	5	-3	14	5	178	169	4	-5	22	5	49	71	24	0	3	6	26	11	9
4	7	5	175	164	11	-2	14	5	195	189	4	-4	22	5	84	71	11	1	3	6	302	296	3
5	7	5	37	38	14	-1	14	5	191	191	4	-3	22	5	63	68	12	2	3	6	47	50	9
6	7	5	56	76	16	0	14	5	128	119	5	-2	22	5	169	174	7	3	3	6	139	138	5
-7	8	5	28	11	28	1	14	5	312	295	4	-1	22	5	63	85	14	4	3	6	79	86	18
-6	8	5	33	34	26	2	14	5	119	116	4	0	22	5	113	113	6	5	3	6	59	71	12
-5	8	5	13	43	12	3	14	5	109	111	9	1	22	5	127	119	8	-7	4	6	34	50	34
-4	8	5	124	275	123	4	14	5	87	77	23	2	22	5	99	101	10	-6	4	6	147	147	14
-3	8	5	75	74	6	5	14	5	44	34	13	3	22	5	53	64	14	-5	4	6	103	97	8
-2	8	5	500	495	10	-6	15	5	47	37	18	-5	23	5	37	30	18	-4	4	6	194	193	4
-1	8	5	78	78	6	-5	15	5	127	108	27	-4	23	5	54	49	15	-3	4	6	112	109	5
0	8	5	450	448	6	-4	15	5	31	13	31	-3	23	5	19	33	18	-2	4	6	93	99	4
1	8	5	109	112	5	-3	15	5	96	92	6	-2	23	5	44	49	18	-1	4	6	38	39	11
2	8	5	167	159	5	-2	15	5	128	136	5	-1	23	5	54	45	12	0	4	6	13	6	12
3	8	5	65	71	12	-1	15	5	44	37	8	0	23	5	41	44	10	1	4	6	24	3	24
4	8	5	149	138	6	0	15	5	31	42	10	1	23	5	11	16	10	2	4	6	120	117	4
5	8	5	30	11	24	1	15	5	124	112	5	2	23	5	31	42	31	3	4	6	78	79	8
6	8	5	23	7	22	2	15	5	47	35	12	3	23	5	51	62	17	4	4	6	121	128	11
-7	9	5	50	62	35	3	15	5	208	194	6	-4	24	5	59	59	18	5	4	6	88	81	10
-6	9	5	140	119	10	4	15	5	34	13	17	-3	24	5	96	91	13	-7	5	6	54	11	11
-5	9	5	101	100	15	5	15	5	96	77	12	-2	24	5	54	52	12	-6	5				

Table A-4, Continued
Observed and Calculated Structure Factors for 1,6-diferrocenylhexane-1,6-dione

h	k	l	IO _o	IO _c	IO _a	h	k	l	IO _o	IO _c	IO _a	h	k	l	IO _o	IO _c	IO _a	h	k	l	IO _o	IO _c	IO _a						
1	5	8	52	57	15	3	13	8	135	124	8	2	2	9	105	83	17	-4	12	9	34	39	17	-2	5	10	42	58	16
2	5	8	223	222	6	-5	14	8	31	46	31	3	2	9	27	28	27	-3	12	9	12	3	12	-1	5	10	0	28	1
3	5	8	58	64	11	-4	14	8	86	95	10	-6	3	9	81	89	14	-2	12	9	0	28	1	0	5	10	31	45	12
4	5	8	93	109	13	-3	14	8	88	96	9	-5	3	9	24	8	24	-1	12	9	32	38	23	1	5	10	19	7	18
-6	6	8	54	58	14	-2	14	8	224	219	9	-4	3	9	122	121	17	0	12	9	105	94	6	2	5	10	55	70	17
-5	6	8	13	80	13	-1	14	8	56	62	11	-3	3	9	31	29	21	1	12	9	33	26	24	-5	6	10	0	10	1
-4	6	8	170	159	7	0	14	8	80	71	6	-2	3	9	238	238	5	2	12	9	109	78	9	-4	6	10	0	24	1
-3	6	8	83	91	10	1	14	8	63	62	13	-1	3	9	92	91	10	-5	13	9	12	10	12	-3	6	10	99	90	10
-2	6	8	185	191	5	2	14	8	7	4	7	0	3	9	152	147	4	-4	13	9	104	94	9	-2	6	10	52	61	14
-1	6	8	122	116	4	3	14	8	0	16	1	1	3	9	0	21	1	-3	13	9	25	14	25	-1	6	10	36	33	15
0	6	8	170	166	4	-5	15	8	27	10	26	2	3	9	59	67	14	-2	13	9	144	144	8	0	6	10	101	106	7
1	6	8	69	80	12	-4	15	8	0	12	1	3	3	9	15	12	15	-1	13	9	0	4	1	1	6	10	31	15	22
2	6	8	89	81	8	-3	15	8	58	68	15	-6	4	9	0	9	1	0	13	9	56	69	9	2	6	10	30	45	29
3	6	8	24	2	24	-2	15	8	136	117	8	-5	4	9	21	40	21	1	13	9	0	17	1	-5	7	10	72	71	14
4	6	8	0	15	1	-1	15	8	62	78	12	-4	4	9	0	3	1	2	13	9	74	69	11	-4	7	10	26	36	26
-6	7	8	27	2	27	0	15	8	118	120	5	-3	4	9	18	14	17	-4	14	9	14	6	13	-3	7	10	32	41	31
-5	7	8	19	24	7	1	15	8	29	7	29	-2	4	9	36	31	14	-3	14	9	39	35	19	-2	7	10	0	2	1
-4	7	8	0	4	1	2	15	8	147	131	8	-1	4	9	98	81	22	-2	14	9	32	39	31	-1	7	10	0	16	1
-3	7	8	76	67	13	3	15	8	41	22	15	0	4	9	64	73	7	-1	14	9	39	29	13	0	7	10	15	15	14
-2	7	8	121	116	7	-5	16	8	49	41	15	1	4	9	45	53	14	0	14	9	0	18	1	1	7	10	47	49	15
-1	7	8	241	235	9	-4	16	8	71	77	14	2	4	9	57	53	12	1	14	9	89	88	11	2	7	10	23	15	22
0	7	8	69	70	8	-3	16	8	75	85	17	3	4	9	80	79	14	2	14	9	44	57	18	-4	8	10	24	10	24
1	7	8	242	228	9	-2	16	8	214	195	6	-6	5	9	34	20	17	-4	15	9	0	27	1	-3	8	10	43	53	42
2	7	8	81	87	13	-1	16	8	106	114	10	-5	5	9	89	103	11	-3	15	9	186	171	8	-2	8	10	0	4	1
3	7	8	85	87	10	0	16	8	58	64	8	-4	5	9	36	28	19	-2	15	9	25	32	24	-1	8	10	133	129	7
4	7	8	42	52	17	1	16	8	20	5	19	-3	5	9	194	183	11	-1	15	9	117	116	8	0	8	10	0	3	1
-6	8	8	2	17	2	2	16	8	22	24	21	-2	5	9	0	32	1	0	15	9	17	36	16	1	8	10	97	80	28
-5	8	8	65	120	65	-5	17	8	0	2	1	-1	5	9	253	253	5	1	15	9	78	60	9	2	8	10	4	18	4
-4	8	8	29	34	29	-4	17	8	8	14	8	0	5	9	54	63	9	2	15	9	30	15	29	-4	9	10	27	35	26
-3	8	8	209	204	12	-3	17	8	54	61	14	1	5	9	185	175	6	-4	16	9	24	2	23	-3	9	10	6	1	6
-2	8	8	105	107	8	-2	17	8	126	127	9	2	5	9	73	78	12	-3	16	9	16	8	15	-2	9	10	33	17	25
-1	8	8	187	190	8	-1	17	8	68	70	61	3	5	9	41	48	16	-2	16	9	35	43	20	-1	9	10	29	31	23
0	8	8	50	76	10	0	17	8	42	45	10	-6	6	9	49	32	12	-1	16	9	69	66	10	0	9	10	10	29	10
1	8	8	175	170	6	1	17	8	84	83	11	-5	6	9	1	17	1	0	16	9	25	40	22	1	9	10	47	38	13
2	8	8	40	27	28	2	17	8	66	81	16	-4	6	9	0	28	1	1	16	9	58	53	13	-4	10	10	56	52	15
3	8	8	30	27	22	-4	18	8	21	12	20	-3	6	9	29	6	26	-3	17	9	62	54	14	-3	10	10	0	9	1
4	8	8	0	31	1	-3	18	8	167	159	8	-2	6	9	59	71	13	-2	17	9	133	121	9	-2	10	10	120	119	16
-6	9	8	0	10	1	-2	18	8	44	40	16	-1	6	9	54	63	14	-1	17	9	62	74	13	-1	10	10	26	41	25
-5	9	8	21	14	21	-1	18	8	132	139	8	0	6	9	61	75	7	0	17	9	73	70	7	0	10	10	93	86	16
-4	9	8	0	10	1	0	18	8	0	15	1	1	6	9	91	84	10	1	17	9	54	54	14	1	10	10	0	5	1
-3	9	8	113	112	7	1	18	8	63	52	11	2	6	9	21	6	20	-3	18	9	0	11	1	-4	11	10	21	18	20
-2	9	8	92	90	8	2	18	8	48	36	15	3	6	9	75	71	17	-2	18	9	29	29	29	-3	11	10	18	11	17
-1	9	8	64	67	8	-4	19	8	7	29	7	-5	7	9	44	41	15	-1	18	9	0	5	1	-2	11	10	0	6	1
0	9	8	163	157	4	-3	19	8	56	63	14	-4	7	9	130	107	8	0	18	9	42	46	9	-1	11	10	0	25	1
1	9	8	141	127	7	-2	19	8	13	33	13	-3	7	9	114	106	7	-2	19	9	77	79	11	0	11	10	15	20	15
2	9	8	59	72	18	-1	19	8	103	92	16	-2	7	9	222	218	5	-1	19	9	50	50	14	1	11	10	35	40	15
3	9	8	135	117	8	0	19	8	27	41	19	-1	7	9	33	47	17	0	19	9	44	63	12	-4	12	10	0	17	1
4	9	8	60	60	22	1	19	8	61	58	13	0	7	9	202	196	4	-1	20	9	53	53	13	-3	12	10	103	87	16
-6	10	8	79	79	14	2	19	8	63	57	14	1	7	9	40	39	16	-4	0	10	81	92	13	-2	12	10	34	45	20
-5	10	8	29	1	29	-4	20	8	67	77	21	2	7	9	55	67	12	-2	0	10	106	101	10	-1	12	10	78	93	12
-4	10	8	165	161	9	-3	20	8	33	50	25	3	7	9	41	41	14	0	0	10	72	79	11	0	12	10	39	38	11
-3	10	8	92	85	8	-2	20	8	161	148	7	-5	8	9	17	3	17	2	0	10	64	81	15	1	12	10	22	51	21
-2	10	8	211	205	12	-1	20	8	14	17	14	-4	8	9	39	20	14	-5	1	10	28	31	27	-3	13	10	0	13	1
-1	10	8	16	45	16	0	20	8	52	59	9	-3	8	9	32	69	32	-4	1	10	28	36	23	-2	13	10	45	25	13
0	10	8	150	144	6	1	20	8	71	67	13	-2	8	9	53	45	13	-3	1	10	52	62	16	-1	13	10	0	16	1
1	10	8	0	2	1	-3	21	8	33	34	28	-1	8	9	0	8	1	-2	1	10	28	42	28	0	13	10	11	12	11
2	10	8	51	65	14	-2	21	8	83	73	11	0	8	9	71	85	8	-1	1	10	34	55	22	-3	14	10	0	8	1
3	10	8	44	45	17	-1	21	8	22	14	22	1	8	9	15	7	15	0	1	10	108	106	6	-2	14	10	48	71	17
4	10	8	28	5	28	0	21	8	70	70	9	2	8	9	81	86	18	1	1	10	47	43	14	-1	14	10	86	71	15
-6	11	8	0	3	1	1	21	8	0	8	1	3	8																

APPENDIX B

Crystallography Data for 1-ferrocenylcarbonyl-2-ferrocenylcyclopentene

Equations of Mean Plane for 1-ferrocenylcarbonyl-2-ferrocenylcyclopentene

Table B-1

$$0.5973 * XO + 0.7897 * YO - 0.1399 * ZO = 5.0788$$

$$4.8754 * x + 7.3446 * y + 3.1518 * z = 5.0788$$

Deviation	Weight	Name
0.0567	1.00	O1
0.0025	1.00	C6
0.0408	1.00	C7
0.0033	1.00	C8
-0.0227	1.00	C9
-0.0517	1.00	C10
-0.0289	1.00	C11

Table B-2

$$0.5888 * XO + 0.7985 * YO - 0.1250 * ZO = 7.6427$$

$$4.8062 * x + 7.4463 * y + 2.9649 * z = 7.6427$$

Deviation	Weight	Name
0.0021	1.00	O2
0.0300	1.00	C32
-0.0337	1.00	C33
-0.0129	1.00	C34
0.0150	1.00	C35
0.0456	1.00	C36
-0.0462	1.00	C37

Table B-3

$$0.7418 * XO - 0.6288 * YO - 0.2332 * ZO = 4.9937$$

$$6.0543 * x + -7.4372 * y + 3.5489 * z = 4.9937$$

Deviation	Weight	Name
-0.1195	1.00	C12
-0.0103	1.00	C13
0.0247	1.00	C14
0.1110	1.00	C15
-0.0200	1.00	C16
0.0076	1.00	C17
-0.0795	1.00	C18
-0.1635	1.00	C19
0.0592	1.00	C20
0.1022	1.00	C21

Table B-4

$$0.7408 * XO - 0.6273 * YO - 0.2402 * ZO = -1.0226$$

$$6.0465 * x + -7.4204 * y + 3.6331 * z = -1.0226$$

Deviation	Weight	Name
0.0919	1.00	C38
-0.0045	1.00	C39
0.1238	1.00	C40
-0.2523	1.00	C41
-0.0274	1.00	C42
0.0262	1.00	C43
-0.0823	1.00	C44
-0.0579	1.00	C45
0.0676	1.00	C46
0.1149	1.00	C47

Table B-5

$$0.5771 * XO + 0.8077 * YO - 0.1205 * ZO = 8.2036$$

$$4.7106 * x + 7.5563 * y + 2.8976 * z = 8.2036$$

Deviation	Weight	Name
-0.0023	1.00	C1
0.0032	1.00	C2
-0.0028	1.00	C3
0.0015	1.00	C4
0.0004	1.00	C5

Table B-6

$$0.5692 * XO + 0.8105 * YO - 0.1379 * ZO = 4.8214$$

$$4.6462 * x + 7.5955 * y + 3.0979 * z = 4.8214$$

Deviation	Weight	Name
0.0015	1.00	C6
0.0057	1.00	C7
-0.0108	1.00	C8
0.0120	1.00	C9
-0.0085	1.00	C10

Table B-7

$$0.7028 * XO - 0.6418 * YO - 0.3069 * ZO = 5.0311$$

$$5.7361 * x - 7.5200 * y + 4.3720 * z = 5.0311$$

Deviation	Weight	Name
-0.0073	1.00	C17
0.0133	1.00	C18
-0.0146	1.00	C19
0.0101	1.00	C20
0.0015	1.00	C21

Table B-8

$$0.6985 * XO - 0.6242 * YO - 0.3501 * ZO = 8.3183$$

$$5.7009 * x - 7.3331 * y + 4.9000 * z = 8.3183$$

Deviation	Weight	Name
0.0479	1.00	C22
-0.0381	1.00	C23
0.0117	1.00	C24
0.0124	1.00	C25
-0.0338	1.00	C26

Table B-9

$$0.5927 * XO + 0.7951 * YO - 0.1283 * ZO = 4.3803$$

$$4.8379 * x + 7.4063 * y + 3.0077 * z = 4.3803$$

Deviation	Weight	Name
-0.0150	1.00	C27
0.0154	1.00	C28
-0.0110	1.00	C29
0.0037	1.00	C30
0.0070	1.00	C31

Table B-10

$$0.5641 * XO + 0.8139 * YO - 0.1392 * ZO = 7.9375$$

$$4.6040 * x + 7.6370 * y + 3.1078 * z = 7.9375$$

Deviation	Weight	Name
0.0090	1.00	C32
-0.0119	1.00	C33
0.0101	1.00	C34
-0.0045	1.00	C35
0.0027	1.00	C36

Table B-11

$$0.7118 * XO - 0.6233 * YO - 0.3237 * ZO = -0.3885$$

$$5.8102 * x - 7.3412 * y + 4.6023 * z = -0.3885$$

Deviation	Weight	Name
0.0007	1.00	C43
-0.0005	1.00	C44
-0.0000	1.00	C45
0.0005	1.00	C46
-0.0008	1.00	C47

Table B-12

$$0.6881 * XO - 0.6403 * YO - 0.3414 * ZO = -3.8563$$

$$5.6163 * x - 7.4853 * y + 4.7679 * z = -3.8563$$

Deviation	Weight	Name
-0.0349	1.00	C48
0.0269	1.00	C49
-0.0023	1.00	C50
-0.0198	1.00	C51
0.0302	1.00	C52

Table B-13

$$0.7722 * XO - 0.6157 * YO - 0.1570 * ZO = 4.9119$$

$$6.3025 * x - 7.3422 * y + 2.6816 * z = 4.9119$$

Deviation	Weight	Name
-0.0332	1.00	C12
0.0500	1.00	C13
-0.0501	1.00	C14
0.0343	1.00	C15
-0.0009	1.00	C16

Table B-14

$$0.7995 * XO - 0.5724 * YO - 0.1818 * ZO = -0.9642$$
$$6.5259 * x - 6.9325 * y + 3.0543 * z = -0.9642$$

Deviation	Weight	Name
0.0477	1.00	C38
-0.1119	1.00	C39
-0.1300	1.00	C40
-0.0941	1.00	C41
0.0283	1.00	C42

Table B-15
Observed and Calculated Structure Factors for 1-ferrocenylcarbonyl-2-ferrocenylcyclopentene

h	k	l	IOFo	IOFc	IOs	h	k	l	IOFo	IOFc	IOs	h	k	l	IOFo	IOFc	IOs	h	k	l	IOFo	IOFc	IOs	h	k	l	IOFo	IOFc	IOs
2	0	-16	109	85	23	4	3	-14	77	73	31	5	1	-13	57	65	40	1	-5	-12	125	116	16	-2	3	-12	82	95	25
3	0	-16	85	25	35	5	3	-14	74	30	30	6	1	-13	0	36	1	2	-5	-12	0	54	1	-1	3	-12	39	25	39
1	1	-16	50	46	49	6	3	-14	72	35	39	7	1	-13	104	30	24	3	-5	-12	0	19	1	0	3	-12	167	165	10
2	1	-16	87	12	30	-3	4	-14	108	73	29	8	1	-13	50	49	50	4	-5	-12	0	28	1	1	3	-12	0	18	1
3	1	-16	0	13	1	0	4	-14	64	46	42	-4	2	-13	0	13	1	5	-5	-12	94	107	20	2	3	-12	114	110	14
1	2	-16	0	37	1	1	4	-14	36	26	36	-3	2	-13	113	84	19	6	-5	-12	77	29	25	3	3	-12	39	45	39
2	2	-16	0	85	1	2	4	-14	86	64	24	-2	2	-13	77	46	34	-2	-4	-12	67	57	66	4	3	-12	77	57	22
3	2	-16	88	70	34	3	4	-14	50	29	49	0	2	-13	41	59	40	-1	-4	-12	77	14	39	5	3	-12	72	51	24
3	-1	-15	80	74	32	4	4	-14	95	81	23	1	2	-13	26	36	25	0	-4	-12	158	127	14	6	3	-12	42	58	41
4	-1	-15	72	25	48	5	4	-14	0	41	1	2	2	-13	55	55	48	1	-4	-12	92	98	19	7	3	-12	58	77	57
5	-1	-15	61	71	61	0	5	-14	94	50	24	3	2	-13	57	52	41	2	-4	-12	144	129	13	8	3	-12	133	89	19
1	0	-15	0	31	1	1	5	-14	79	68	33	4	2	-13	53	78	53	3	-4	-12	85	84	21	-5	4	-12	100	50	27
2	0	-15	130	93	17	2	5	-14	0	33	1	5	2	-13	119	91	18	4	-4	-12	37	50	36	-4	4	-12	112	74	20
3	0	-15	0	21	1	3	5	-14	70	63	40	6	2	-13	0	42	1	5	-4	-12	71	33	29	-3	4	-12	141	126	14
4	0	-15	77	53	31	4	5	-14	100	101	27	7	2	-13	73	92	41	-2	-3	-12	43	66	43	-2	4	-12	69	49	37
5	0	-15	69	52	40	5	5	-14	95	41	30	8	3	-13	57	60	57	-1	-3	-12	98	74	23	-1	4	-12	77	81	23
1	1	-15	0	2	1	0	6	-14	50	24	50	-3	3	-13	0	21	1	0	-3	-12	76	66	26	0	4	-12	84	51	21
2	1	-15	51	32	51	1	6	-14	97	118	27	1	3	-13	96	63	23	1	-3	-12	122	111	16	1	4	-12	138	121	14
3	1	-15	74	71	40	2	6	-14	55	18	54	0	3	-13	103	108	16	2	-3	-12	74	66	22	2	4	-12	65	20	30
4	1	-15	85	72	31	3	6	-14	68	24	50	1	3	-13	72	51	26	3	-3	-12	104	91	16	3	4	-12	112	105	16
5	1	-15	110	91	23	4	6	-14	0	61	1	2	3	-13	20	19	20	4	-3	-12	37	36	37	4	4	-12	71	20	29
1	2	-15	48	29	47	0	7	-14	66	32	66	3	3	-13	35	45	34	-2	-2	-12	0	52	1	5	4	-12	41	55	40
2	2	-15	0	24	1	1	7	-14	58	43	58	4	3	-13	0	45	1	-1	-2	-12	0	65	1	6	4	-12	59	58	59
3	2	-15	29	20	28	2	7	-14	60	45	59	5	3	-13	103	59	20	0	-2	-12	58	43	44	7	4	-12	56	32	56
4	2	-15	80	58	29	1	-7	-13	0	43	1	6	3	-13	56	52	55	1	-2	-12	66	44	29	-5	5	-12	75	32	38
5	2	-15	0	23	1	2	-7	-13	66	18	42	7	3	-13	0	32	1	2	-2	-12	177	56	16	-4	5	-12	69	25	38
1	3	-15	57	62	57	3	-7	-13	19	48	18	-4	4	-13	0	19	1	3	-2	-12	107	97	15	-3	5	-12	51	56	50
2	3	-15	88	18	25	4	-7	-13	0	44	1	-3	4	-13	96	70	25	4	-2	-12	38	56	37	-1	5	-12	57	54	36
3	3	-15	0	26	1	0	-6	-13	0	36	1	0	4	-13	57	39	41	5	-2	-12	67	79	30	0	5	-12	95	102	18
4	3	-15	101	47	25	1	-6	-13	92	70	26	1	4	-13	152	136	14	6	-2	-12	0	50	1	1	5	-12	56	54	32
1	4	-15	0	34	1	2	-6	-13	74	85	32	2	4	-13	63	43	45	-5	-1	-12	0	24	1	2	5	-12	57	65	31
2	4	-15	67	83	53	3	-6	-13	35	42	35	3	4	-13	30	30	30	-4	-1	-12	0	18	1	3	5	-12	0	27	13
3	4	-15	52	17	51	4	-6	-13	41	42	40	4	4	-13	72	68	30	-1	-1	-12	85	67	21	4	5	-12	144	133	13
4	4	-15	64	41	63	5	-6	-13	31	11	31	5	4	-13	56	77	55	0	-1	-12	83	89	20	5	5	-12	0	19	1
1	5	-15	84	74	31	6	-6	-13	0	15	1	6	4	-13	83	62	26	1	-1	-12	19	21	19	6	5	-12	19	38	18
2	5	-15	0	55	1	-2	-5	-13	87	44	47	7	4	-13	98	65	25	2	-1	-12	62	36	28	7	5	-12	57	42	57
3	5	-15	67	88	66	-1	-5	-13	145	126	19	-4	5	-13	122	82	23	3	-1	-12	123	134	12	-4	6	-12	0	42	1
2	-6	-14	33	7	32	0	-5	-13	0	44	1	-3	5	-13	0	55	1	4	-1	-12	114	108	13	-3	6	-12	43	14	42
3	-6	-14	49	54	49	1	-5	-13	43	34	43	0	5	-13	98	119	21	5	-1	-12	82	106	18	-1	6	-12	119	121	17
0	-5	-14	98	53	31	2	-5	-13	47	39	46	1	5	-13	67	59	35	6	-1	-12	0	55	1	0	6	-12	0	43	1
1	-5	-14	121	96	22	3	-5	-13	103	119	21	2	5	-13	147	147	14	7	-1	-12	62	23	61	1	6	-12	173	157	12
2	-5	-14	65	57	54	4	-5	-13	0	10	1	3	5	-13	48	37	47	8	-1	-12	89	28	28	2	6	-12	48	21	48
3	-5	-14	43	57	43	5	-5	-13	113	95	18	4	5	-13	38	29	38	-5	0	-12	82	17	31	3	6	-12	74	76	29
-1	-4	-14	69	32	68	-2	-4	-13	101	65	30	5	5	-13	59	38	58	-4	0	-12	0	29	1	4	6	-12	40	45	39
0	-4	-14	89	11	40	1	-4	-13	18	63	17	6	5	-13	70	74	50	-3	0	-12	80	79	27	5	6	-12	127	124	15
1	-4	-14	55	26	55	0	-4	-13	72	71	40	0	6	-13	0	43	1	-2	0	-12	0	19	1	6	6	-12	57	60	57
2	-4	-14	54	90	54	1	-4	-13	34	51	33	1	6	-13	48	83	48	-1	0	-12	141	125	11	-4	7	-12	34	23	34
-1	-3	-14	26	51	25	2	-4	-13	0	27	1	2	6	-13	37	37	37	0	0	-12	160	135	10	-1	7	-12	0	29	1
0	-3	-14	69	34	69	3	-4	-13	50	45	49	3	6	-13	97	108	21	1	0	-12	158	170	12	0	7	-12	86	74	26
-1	-2	-14	16	14	16	4	-4	-13	106	81	18	4	6	-13	75	25	30	2	0	-12	27	35	27	1	7	-12	82	88	24
2	-1	-14	75	15	32	-2	-3	-13	82	8	47	5	6	-13	53	33	52	3	0	-12	75	54	24	2	7	-12	76	48	28
3	-1	-14	59	59	47	-1	-3	-13	122	123	25	0	7	-13	83	2	29	4	0	-12	136	134	14	3	7	-12	0	23	1
4	-1	-14	73	7	33	0	-3	-13	58	63	58	1	7	-13	46	41	45	5	0	-12	121	126	15	4	7	-12	82	82	31
5	-1	-14	51	95	50	1	-3	-13	76	65	30	2	7	-13	107	99	22	6	0	-12	30	50	29	5	7	-12	35	38	35
6	-1	-14	71	86	36	2	-3	-13	0	30	1	3	7	-13	0	19	1	7	0	-12	95	76	25	-1	8	-12	119	109	18
7	-1	-14	25	12	24	-1	-2	-13	69	88	58	4	7	-13	43	78	43	8	0	-12	97	74	22	0	8	-12	0	26	1
1	0	-14	35	30	35	0	-2	-13	125	110	18	0	8	-13	0	19	1	-5	1	-12	105	54	24	1	8	-12	126	107	17
2	0	-14	0	43	1	1	-2	-13	49	56	49	1	8	-13	0	10	1	-4	1	-12	76	47	31	2	8	-12	87	71	27
3	0	-14	58	52	38	-1	-1	-13	63	36	62	2	8	-13	35	8	35	-3	1	-12	0	25	1						

Table B-15, Continued
Observed and Calculated Structure Factors for 1-ferrocenylcarbonyl-2-ferrocenylcyclopentene

h	k	l	IOFo	IOFc	IOs	h	k	l	IOFo	IOFc	IOs	h	k	l	IOFo	IOFc	IOs	h	k	l	IOFo	IOFc	IOs	h	k	l	IOFo	IOFc	IOs
1	-6	-11	75	93	27	0	1	-11	0	43	1	1	7	-11	66	59	23	6	-4	-10	28	39	28	4	2	-10	25	57	25
2	-6	-11	148	152	14	1	1	-11	64	79	22	2	7	-11	79	82	20	7	-4	-10	113	123	16	5	2	-10	124	110	11
3	-6	-11	81	97	20	2	1	-11	203	207	9	3	7	-11	130	137	14	8	-4	-10	39	34	38	6	2	-10	154	155	11
4	-6	-11	0	26	1	3	1	-11	26	45	25	4	7	-11	0	24	1	-3	-3	-10	73	63	30	7	2	-10	108	105	16
5	-6	-11	56	47	39	4	1	-11	190	180	11	5	7	-11	53	23	52	-2	-3	-10	9	48	9	8	2	-10	106	82	19
6	-6	-11	0	84	1	5	1	-11	0	10	1	6	7	-11	91	49	29	-1	-3	-10	90	72	17	-7	3	-10	0	19	1
7	-6	-11	0	3	1	6	1	-11	111	101	18	-1	8	-11	46	67	45	0	-3	-10	170	150	11	-6	3	-10	0	35	1
8	-6	-11	64	65	48	7	1	-11	28	73	28	0	8	-11	80	16	25	1	-3	-10	0	63	1	-5	3	-10	142	158	14
-3	-5	-11	122	105	17	8	1	-11	150	139	15	1	8	-11	100	35	18	2	-3	-10	216	215	8	-4	3	-10	120	122	15
-2	-5	-11	0	81	1	9	1	-11	28	45	28	2	8	-11	145	132	14	3	-3	-10	31	59	31	-3	3	-10	89	65	21
-1	-5	-11	33	44	32	-6	2	-11	0	47	1	3	8	-11	49	75	48	4	-3	-10	60	50	24	-2	3	-10	42	74	41
0	-5	-11	59	14	39	-5	2	-11	16	56	16	4	8	-11	118	112	18	5	-3	-10	116	127	13	-1	3	-10	58	55	19
1	-5	-11	84	101	19	-4	2	-11	57	67	53	5	8	-11	73	74	33	6	-3	-10	70	75	21	0	3	-10	112	117	12
2	-5	-11	80	63	23	-3	2	-11	138	94	15	-1	9	-11	48	103	48	7	-3	-10	110	102	14	1	3	-10	193	194	8
3	-5	-11	169	180	10	-2	2	-11	79	42	20	0	9	-11	0	30	1	-6	-2	-10	33	45	33	2	3	-10	37	45	37
4	-5	-11	75	102	20	-1	2	-11	140	132	8	1	9	-11	86	64	30	-5	-2	-10	98	57	24	3	3	-10	86	87	14
5	-5	-11	48	24	47	0	2	-11	0	14	1	2	9	-11	0	20	1	-4	-2	-10	0	77	1	4	3	-10	0	45	1
6	-5	-11	0	30	1	1	2	-11	106	111	12	3	9	-11	0	44	1	-3	-2	-10	222	209	9	5	3	-10	56	41	34
7	-5	-11	113	84	19	2	2	-11	70	74	17	4	9	-11	46	28	46	-2	-2	-10	0	34	1	6	3	-10	93	101	20
8	-5	-11	85	44	28	3	2	-11	192	199	9	-1	10	-11	13	46	12	-1	-2	-10	91	91	10	7	3	-10	53	53	53
-3	-4	-11	131	91	19	4	2	-11	106	83	14	0	10	-11	80	63	36	0	-2	-10	57	44	25	8	3	-10	33	68	33
-2	-4	-11	80	92	34	5	2	-11	164	155	12	1	10	-11	48	15	47	1	-2	-10	143	141	10	-7	4	-10	19	26	18
-1	-4	-11	91	96	20	6	2	-11	65	41	29	2	10	-11	62	16	62	2	-2	-10	41	26	30	-6	4	-10	26	42	26
0	-4	-11	0	28	1	7	2	-11	36	35	36	-1	9	-10	0	31	1	3	-2	-10	131	121	7	-5	4	-10	0	22	1
1	-4	-11	43	26	42	8	2	-11	72	48	37	0	9	-10	79	26	25	4	-2	-10	48	80	20	-4	4	-10	194	215	11
2	-4	-11	89	92	18	9	2	-11	134	85	16	1	9	-10	51	60	51	5	-2	-10	87	82	11	-3	4	-10	74	71	23
3	-4	-11	164	129	10	-6	3	-11	46	101	46	2	9	-10	81	64	24	6	-2	-10	55	73	37	-2	4	-10	130	132	13
4	-4	-11	50	50	49	-5	3	-11	69	13	42	3	9	-10	44	53	43	7	-2	-10	102	93	18	-1	4	-10	116	126	10
5	-4	-11	96	112	17	-4	3	-11	14	21	14	4	9	-10	88	21	19	-6	-1	-10	45	34	44	0	4	-10	143	146	11
6	-4	-11	109	35	17	-3	3	-11	151	133	13	5	9	-10	38	49	37	-5	-1	-10	41	61	40	1	4	-10	163	162	10
7	-4	-11	81	43	22	-2	3	-11	194	208	10	6	9	-10	0	24	1	-4	-1	-10	130	125	15	2	4	-10	3	44	3
-2	-3	-11	203	184	14	-1	3	-11	139	137	12	-2	8	-10	56	36	56	-3	-1	-10	220	233	10	3	4	-10	216	212	9
-1	-3	-11	0	24	1	0	3	-11	117	110	13	-1	8	-10	0	11	1	-2	-1	-10	229	235	13	4	4	-10	19	31	18
0	-3	-11	103	89	17	1	3	-11	138	145	13	0	8	-10	0	58	1	-1	-1	-10	68	52	14	5	4	-10	35	11	35
1	-3	-11	78	33	28	2	3	-11	81	86	17	1	8	-10	133	135	13	0	-1	-10	130	128	14	6	4	-10	0	43	1
2	-3	-11	57	74	31	3	3	-11	102	95	16	2	8	-10	0	46	1	1	-1	-10	0	37	1	7	4	-10	157	149	14
3	-3	-11	89	93	15	4	3	-11	90	88	17	3	8	-10	44	78	43	2	-1	-10	255	268	5	8	4	-10	90	78	25
4	-3	-11	125	136	12	5	3	-11	27	45	27	4	8	-10	93	58	17	3	-1	-10	0	36	1	-6	5	-10	44	12	44
5	-3	-11	28	46	27	6	3	-11	0	57	1	5	8	-10	60	69	34	4	-1	-10	274	263	5	-5	5	-10	45	72	45
-2	-2	-11	21	65	20	7	3	-11	89	76	23	6	8	-10	47	59	47	5	-1	-10	102	100	15	-4	5	-10	64	30	34
-1	-2	-11	226	219	10	8	3	-11	0	44	1	7	8	-10	29	2	28	6	-1	-10	17	36	16	-3	5	-10	243	260	9
0	-2	-11	66	64	26	-6	4	-11	92	68	27	-3	7	-10	0	37	1	7	-1	-10	115	123	14	-2	5	-10	181	179	7
1	-2	-11	201	187	10	-5	4	-11	132	104	16	-2	7	-10	138	127	16	8	-1	-10	95	93	24	1	5	-10	154	151	10
2	-2	-11	0	31	1	-4	4	-11	54	51	54	-1	7	-10	23	55	23	9	-1	-10	82	52	33	0	5	-10	139	135	10
3	-2	-11	97	103	10	-3	4	-11	38	48	37	0	7	-10	0	40	1	-7	0	-10	76	59	41	1	5	-10	52	54	32
4	-2	-11	118	111	9	-2	4	-11	20	22	20	1	7	-10	33	50	33	-6	0	-10	34	67	34	2	5	-10	72	79	19
5	-2	-11	101	108	16	-1	4	-11	227	248	8	2	7	-10	54	51	36	-5	0	-10	63	77	54	3	5	-10	100	121	14
6	-2	-11	83	66	23	0	4	-11	85	70	17	3	7	-10	131	145	12	-4	0	-10	89	59	20	4	5	-10	57	39	36
7	-2	-11	82	97	24	1	4	-11	121	127	12	4	7	-10	118	103	12	-3	0	-10	89	52	18	5	5	-10	133	111	14
-6	-1	-11	121	79	25	2	4	-11	0	27	1	5	7	-10	54	24	34	-2	0	-10	84	67	15	6	5	-10	68	29	28
-5	-1	-11	0	7	1	3	4	-11	66	66	23	6	7	-10	17	22	17	-1	0	-10	262	275	4	7	5	-10	30	40	30
-4	-1	-11	220	215	12	4	4	-11	0	21	1	7	7	-10	63	54	32	0	0	-10	70	70	9	8	5	-10	40	54	40
-3	-1	-11	50	8	50	5	4	-11	115	133	17	8	7	-10	56	27	56	1	0	-10	168	167	6	-6	6	-10	32	53	31
-2	-1	-11	40	34	40	6	4	-11	48	41	47	-3	6	-10	90	68	29	2	0	-10	36	32	30	-5	6	-10	0	16	1
-1	-1	-11	28	48	28	7	4	-11	90	58	24	-2	6	-10	95	85	23	3	0	-10	269	276	7	-4	6	-10	49	55	48
0	-1	-11	78	81	11	8	4	-11	73	47	44	4	6	-10	131	143	14	4	0	-10	81	79	14	-3	6	-10	59	41	45
1	-1	-11	111	78	9	-6	5	-11	74	45	54	0	6	-10	32	29	31	5	0	-10	230	252	8	-2	6	-10	195	219	9
2	-1	-11	136	141	12	-5	5	-11	38	104	37	1	6	-10	46	54	46	6	0	-10	63	54	24	-1	6	-10	29	31	28
3	-1	-11	13	48	12	-4	5	-11																					

Table B-15, Continued
Observed and Calculated Structure Factors for 1-ferrocenylcarbonyl-2-ferrocenylcyclopentene

h	k	l	IOFo	IOFc	IOs	h	k	l	IOFo	IOFc	IOs	h	k	l	IOFo	IOFc	IOs	h	k	l	IOFo	IOFc	IOs	h	k	l	IOFo	IOFc	IOs
-5	9	-10	104	81	27	-3	-4	-9	208	209	11	4	1	-9	157	161	9	-5	7	-9	88	104	21	-3	-7	-8	62	80	33
-2	9	-10	0	31	1	-2	-4	-9	60	80	33	5	1	-9	92	68	13	-4	7	-9	87	71	20	-2	-7	-8	203	197	10
-1	9	-10	70	62	34	-1	-4	-9	17	48	17	6	1	-9	93	88	15	-3	7	-9	154	143	13	-1	-7	-8	35	44	34
0	9	-10	30	41	30	0	-4	-9	78	8	24	7	1	-9	114	125	14	-2	7	-9	44	39	44	0	-7	-8	38	34	38
1	9	-10	141	157	14	1	-4	-9	68	50	21	8	1	-9	74	82	27	-1	7	-9	126	105	12	1	-7	-8	0	58	1
2	9	-10	0	34	1	2	-4	-9	64	25	18	-7	2	-9	66	56	54	0	7	-9	47	27	47	2	-7	-8	131	125	11
3	9	-10	0	58	1	3	-4	-9	209	241	8	-6	2	-9	77	70	24	1	7	-9	276	281	8	3	-7	-8	0	41	1
4	9	-10	56	18	55	4	-4	-9	97	110	13	-5	2	-9	55	62	55	2	7	-9	88	82	16	4	-7	-8	38	40	37
5	9	-10	25	11	25	5	-4	-9	93	113	12	-4	2	-9	232	233	9	3	7	-9	143	151	13	5	-7	-8	63	50	19
-2	10	-10	0	51	1	6	-4	-9	77	63	19	-3	2	-9	81	76	16	4	7	-9	58	72	47	6	-7	-8	81	94	19
-1	10	-10	0	11	1	7	-4	-9	95	74	17	-2	2	-9	168	155	6	5	7	-9	78	47	23	7	-7	-8	89	57	19
0	10	-10	0	61	1	8	-4	-9	0	54	1	-1	2	-9	32	10	31	6	7	-9	77	36	29	8	-7	-8	86	91	24
1	10	-10	16	20	16	9	-4	-9	72	79	42	0	2	-9	43	44	35	7	7	-9	150	128	16	9	-7	-8	22	44	22
2	10	-10	82	75	29	-7	-3	-9	21	60	20	1	2	-9	32	37	32	-6	8	-9	0	22	1	-4	-6	-8	87	62	24
3	10	-10	71	46	45	-6	-3	-9	33	63	33	2	2	-9	279	278	7	-5	8	-9	109	55	19	-3	-6	-8	135	147	14
-2	11	-10	0	32	1	-5	-3	-9	124	83	18	3	2	-9	145	141	10	-4	8	-9	146	131	15	-2	-6	-8	144	135	12
-1	11	-10	0	59	1	-4	-3	-9	11	33	11	4	2	-9	262	270	7	-2	8	-9	153	177	12	-1	-6	-8	149	158	11
0	11	-10	73	7	47	-3	-3	-9	102	91	11	5	2	-9	40	51	40	-1	8	-9	41	46	41	0	-6	-8	68	46	17
1	11	-10	43	42	42	-2	-3	-9	134	136	13	6	2	-9	36	74	36	0	8	-9	102	83	15	1	-6	-8	65	59	19
0	10	-9	70	15	43	-1	-3	-9	66	38	20	7	2	-9	136	145	13	1	8	-9	0	35	1	2	-6	-8	96	82	15
1	10	-9	96	71	21	0	-3	-9	59	9	21	8	2	-9	76	78	27	2	8	-9	173	168	13	3	-6	-8	322	332	7
2	10	-9	0	28	1	1	-3	-9	15	4	15	-7	3	-9	177	135	15	3	8	-9	76	70	21	4	-6	-8	104	72	13
3	10	-9	35	57	35	2	-3	-9	222	232	7	-6	3	-9	50	37	50	4	8	-9	80	85	24	5	-6	-8	120	116	11
4	10	-9	56	37	52	3	-3	-9	163	159	9	-5	3	-9	60	69	36	5	8	-9	44	42	43	6	-6	-8	41	16	40
5	10	-9	49	50	49	4	-3	-9	57	81	21	-4	3	-9	73	47	21	6	8	-9	92	20	23	7	-6	-8	106	89	15
-2	-9	-9	102	88	22	5	-3	-9	128	119	10	-3	3	-9	195	203	9	7	8	-9	0	22	1	8	-6	-8	0	41	1
-1	-9	-9	0	45	1	6	-3	-9	70	60	18	-2	3	-9	149	142	6	-5	9	-9	0	8	1	9	-6	-8	128	99	18
0	-9	-9	66	52	52	7	-3	-9	80	81	20	-1	3	-9	232	236	7	-2	9	-9	136	103	14	-4	-5	-8	90	75	38
1	-9	-9	0	53	1	8	-3	-9	156	154	13	0	3	-9	88	78	11	-1	9	-9	88	93	20	-3	-5	-8	39	23	38
2	-9	-9	89	97	17	-7	-2	-9	44	19	43	1	3	-9	66	77	14	0	9	-9	57	80	56	-2	-5	-8	235	223	9
3	-9	-9	49	74	49	-6	-2	-9	121	100	20	2	3	-9	143	147	8	1	9	-9	93	81	19	-1	-5	-8	157	161	10
4	-9	-9	70	85	21	-5	-2	-9	76	107	27	3	3	-9	135	126	9	2	9	-9	60	79	46	0	-5	-8	261	272	7
5	-9	-9	51	56	51	4	-2	-9	64	58	33	4	3	-9	103	93	12	3	9	-9	117	125	17	1	-5	-8	53	28	23
6	-9	-9	50	48	50	-3	-2	-9	172	155	11	5	3	-9	148	150	11	4	9	-9	0	22	1	2	-5	-8	40	61	40
7	-9	-9	59	20	46	-2	-2	-9	145	140	7	6	3	-9	53	50	52	5	9	-9	122	79	20	3	-5	-8	93	109	10
-3	-8	-9	0	35	1	-1	-2	-9	311	321	4	7	3	-9	74	57	25	6	9	-9	47	19	47	4	-5	-8	89	92	12
-2	-8	-9	16	29	15	0	-2	-9	133	121	8	8	3	-9	128	117	15	-2	10	-9	132	132	18	5	-5	-8	98	110	14
-1	-8	-9	120	137	18	1	-2	-9	130	138	9	-7	4	-9	80	9	31	-1	10	-9	95	67	22	6	-5	-8	121	95	12
0	-8	-9	38	13	38	2	-2	-9	0	11	1	-6	4	-9	96	126	23	0	10	-9	149	123	15	7	-5	-8	82	47	18
1	-8	-9	42	37	42	3	-2	-9	346	352	4	-5	4	-9	79	94	24	1	10	-9	21	37	21	8	-5	-8	62	72	34
2	-8	-9	0	36	1	4	-2	-9	34	31	34	-4	4	-9	76	36	23	2	10	-9	68	5	36	9	-5	-8	0	40	1
3	-8	-9	49	51	49	5	-2	-9	320	333	6	-3	4	-9	0	8	1	3	10	-9	49	21	49	10	-5	-8	45	27	44
4	-8	-9	104	83	13	6	-2	-9	148	134	7	-2	4	-9	229	231	10	4	10	-9	116	83	21	-7	-4	-8	0	33	1
5	-8	-9	157	152	11	7	-2	-9	116	117	9	-1	4	-9	0	49	1	-2	11	-9	0	72	1	-6	-4	-8	103	127	25
6	-8	-9	41	5	40	-7	-1	-9	86	60	34	0	4	-9	152	169	9	-1	11	-9	0	40	1	-5	-4	-8	40	54	40
7	-8	-9	77	49	24	-6	-1	-9	120	107	19	1	4	-9	0	49	1	0	11	-9	116	97	22	-4	-4	-8	61	54	47
8	-8	-9	95	56	26	-5	-1	-9	166	166	13	2	4	-9	82	97	16	1	11	-9	70	19	39	-3	-4	-8	96	104	17
-4	-7	-9	90	41	34	-4	-1	-9	214	230	10	3	4	-9	189	188	9	2	11	-9	0	29	1	-2	-4	-8	152	150	10
-3	-7	-9	0	26	1	-3	-1	-9	0	9	1	4	4	-9	168	191	10	0	-11	-8	112	65	20	-1	-4	-8	70	57	22
-2	-7	-9	61	57	55	-2	-1	-9	35	26	35	5	4	-9	0	42	1	1	-11	-8	42	3	42	0	-4	-8	286	282	7
-1	-7	-9	0	34	1	-1	-1	-9	163	155	6	6	4	-9	180	171	10	2	-11	-8	0	34	1	1	-4	-8	87	80	12
0	-7	-9	207	221	9	0	-1	-9	314	316	3	7	4	-9	22	12	21	3	-11	-8	66	28	27	2	-4	-8	109	109	11
1	-7	-9	44	19	44	1	-1	-9	177	187	9	8	4	-9	43	25	43	4	-11	-8	81	45	21	3	-4	-8	276	276	7
2	-7	-9	114	130	11	2	-1	-9	153	152	6	-7	5	-9	136	89	18	-2	-10	-8	0	19	1	4	-4	-8	182	197	8
3	-7	-9	98	106	14	3	-1	-9	16	10	16	-6	5	-9	0	51	1	-1	-10	-8	93	75	26	5	-4	-8	175	175	9
4	-7	-9	55	27	24	4	-1	-9	92	79	8	-5	5	-9	174	178	12	0	-10	-8	49	48	49	6	-4	-8	129	123	11
5	-7	-9	123	104	13	5	-1	-9	25	67	25	-4	5	-9	0	41	1	1	-10	-8	73	81	25	7	-4	-8	89	89	20
6	-7	-9	89	104	15	6	-1	-9	78	98	16	-3	5	-9	70	53	22	2	-10	-8	56	13	31	8	-4	-8	24	58	23
7	-7	-9	63	30	32	7	-1	-9	145	106	10	-2	5	-9	0	21	1	3	-10	-8	21	14	21	9	-4	-8	78	92	31
8	-7	-9	78	55	30	8	-1	-9	98	75	18	-1	5	-9	276														

Table B-15, Continued
Observed and Calculated Structure Factors for 1-ferrocenylcarbonyl-2-ferrocenylcyclopentene

h	k	l	10Fo	10Fc	10s	h	k	l	10Fo	10Fc	10s	h	k	l	10Fo	10Fc	10s	h	k	l	10Fo	10Fc	10s	h	k	l	10Fo	10Fc	10s
6	-2	-8	35	45	35	8	3	-8	21	38	21	4	9	-8	0	7	1	3	-6	-7	63	52	19	1	-1	-7	160	168	5
7	-2	-8	143	136	12	-8	4	-8	65	31	65	5	9	-8	71	74	35	4	-6	-7	116	126	9	2	-1	-7	152	148	5
8	-2	-8	182	168	12	-7	4	-8	0	23	1	6	9	-8	56	26	55	5	-6	-7	103	113	12	3	-1	-7	152	149	5
-8	-1	-8	0	29	1	-6	4	-8	153	143	12	-2	10	-8	18	45	18	6	-6	-7	44	30	44	4	-1	-7	218	219	4
-7	-1	-8	85	73	30	-5	4	-8	117	123	15	-1	10	-8	56	56	55	7	-6	-7	117	112	14	5	-1	-7	326	338	4
-6	-1	-8	26	43	25	-4	4	-8	312	322	7	0	10	-8	62	62	37	8	-6	-7	100	69	17	6	-1	-7	60	40	14
-5	-1	-8	132	128	14	-3	4	-8	0	34	1	1	10	-8	181	179	13	9	-6	-7	0	21	1	7	-1	-7	65	40	13
-4	-1	-8	92	62	15	-2	4	-8	151	150	6	2	10	-8	68	77	32	10	-6	-7	0	12	1	8	-1	-7	77	71	14
-3	-1	-8	350	354	7	-1	4	-8	0	19	1	3	10	-8	87	39	25	-4	-5	-7	53	33	53	-8	0	-7	61	10	61
-2	-1	-8	153	153	6	0	4	-8	169	172	7	4	10	-8	71	31	38	-3	-5	-7	176	166	11	-7	0	-7	68	66	42
-1	-1	-8	150	153	5	1	4	-8	60	45	14	5	10	-8	38	42	38	-2	-5	-7	65	54	19	-6	0	-7	243	250	10
0	-1	-8	101	104	5	2	4	-8	366	378	6	-2	11	-8	120	136	19	-1	-5	-7	203	201	8	-5	0	-7	89	96	17
1	-1	-8	297	288	4	3	4	-8	70	67	15	-1	11	-8	78	12	28	0	-5	-7	0	14	1	-4	0	-7	162	157	10
2	-1	-8	196	204	8	4	4	-8	101	95	11	0	11	-8	0	18	1	1	-5	-7	360	358	6	-3	0	-7	78	83	14
3	-1	-8	226	234	4	5	4	-8	44	38	44	1	11	-8	58	7	57	2	-5	-7	213	221	7	-2	0	-7	336	323	5
4	-1	-8	146	147	6	6	4	-8	93	91	14	2	11	-8	69	66	41	3	-5	-7	207	213	7	-1	0	-7	58	49	7
5	-1	-8	242	242	9	7	4	-8	107	99	16	3	11	-8	0	67	1	4	-5	-7	54	33	19	0	0	-7	666	647	3
6	-1	-8	175	172	6	8	4	-8	128	123	16	-2	12	-8	32	16	31	5	-5	-7	0	35	1	1	0	-7	22	24	21
7	-1	-8	0	25	1	-8	5	-8	61	29	60	-1	12	-8	51	58	51	6	-5	-7	192	186	9	2	0	-7	71	68	7
8	-1	-8	63	53	31	-7	5	-8	61	59	60	0	12	-8	49	17	48	7	-5	-7	118	120	13	3	0	-7	26	23	26
-8	0	-8	0	76	1	-6	5	-8	52	70	51	1	12	-8	103	56	26	8	-5	-7	50	58	49	4	0	-7	89	100	7
-7	0	-8	69	26	41	-5	5	-8	100	78	17	-1	-11	-7	95	33	22	9	-5	-7	85	81	27	5	0	-7	118	114	6
-6	0	-8	132	143	14	-4	5	-8	157	155	11	0	-11	-7	30	50	30	10	-5	-7	64	23	64	6	0	-7	166	173	6
-5	0	-8	30	13	30	-3	5	-8	287	287	7	1	-11	-7	63	31	32	-7	-4	-7	0	32	1	7	0	-7	99	70	12
-4	0	-8	74	54	20	-2	5	-8	146	140	9	2	-11	-7	83	81	20	-6	-4	-7	149	146	14	8	0	-7	74	71	22
-3	0	-8	109	91	12	-1	5	-8	0	37	1	3	-11	-7	0	18	1	-5	-4	-7	0	22	1	-8	1	-7	0	39	1
-2	0	-8	285	294	5	0	5	-8	86	87	13	4	-11	-7	50	40	50	-4	-4	-7	223	191	9	-7	1	-7	0	25	1
-1	0	-8	133	133	5	1	5	-8	253	250	7	5	-11	-7	27	26	26	-3	-4	-7	0	40	1	-6	1	-7	117	100	15
0	0	-8	188	198	8	2	5	-8	73	66	17	-3	-10	-7	68	24	50	-2	-4	-7	98	98	10	-5	1	-7	197	197	8
1	0	-8	85	89	7	3	5	-8	178	184	9	-2	-10	-7	43	31	42	-1	-4	-7	70	80	16	-4	1	-7	168	179	10
2	0	-8	261	261	4	4	5	-8	119	117	11	-1	-10	-7	45	29	44	0	-4	-7	38	38	38	-3	1	-7	0	44	1
3	0	-8	303	308	4	5	5	-8	12	25	12	0	-10	-7	0	12	1	1	-4	-7	68	86	14	-2	1	-7	58	53	10
4	0	-8	219	229	10	6	5	-8	74	80	24	1	-10	-7	130	134	12	2	-4	-7	290	298	6	-1	1	-7	267	270	5
5	0	-8	45	41	19	7	5	-8	180	153	11	2	-10	-7	76	27	20	3	-4	-7	8	37	7	0	1	-7	425	427	4
6	0	-8	136	137	10	-7	6	-8	102	93	19	3	-10	-7	123	124	11	4	-4	-7	122	133	9	1	1	-7	462	468	3
7	0	-8	154	144	11	-6	6	-8	35	32	34	4	-10	-7	68	65	21	5	-4	-7	104	88	11	2	1	-7	92	97	7
8	0	-8	151	150	12	-5	6	-8	0	48	1	5	-10	-7	0	36	1	6	-4	-7	68	77	20	3	1	-7	161	168	5
-8	1	-8	52	22	51	-4	6	-8	142	160	13	6	-10	-7	86	65	18	7	-4	-7	261	267	8	4	1	-7	25	33	24
-7	1	-8	124	131	17	-3	6	-8	196	203	9	7	-10	-7	85	97	27	8	-4	-7	138	121	14	5	1	-7	355	360	6
-6	1	-8	71	25	33	-2	6	-8	233	215	7	-4	-9	-7	114	86	21	9	-4	-7	109	71	17	6	1	-7	144	124	9
-5	1	-8	47	10	47	-1	6	-8	194	194	8	-3	-9	-7	59	76	7	10	-4	-7	66	27	65	7	1	-7	172	163	10
-4	1	-8	72	59	19	0	6	-8	110	94	11	-2	-9	-7	123	128	15	-8	-3	-7	58	31	57	8	1	-7	123	117	12
-3	1	-8	267	267	7	1	6	-8	56	74	25	-1	-9	-7	68	42	26	-7	-3	-7	37	57	36	-8	2	-7	0	31	1
-2	1	-8	26	49	25	2	6	-8	271	276	7	0	-9	-7	76	51	17	-6	-3	-7	88	21	26	-7	2	-7	65	37	33
-1	1	-8	488	499	4	3	6	-8	0	47	1	1	-9	-7	20	8	19	-5	-3	-7	112	150	16	-6	2	-7	70	80	27
0	1	-8	119	115	5	4	6	-8	143	135	11	2	-9	-7	156	151	11	-4	-3	-7	74	91	23	-5	2	-7	251	266	8
1	1	-8	13	15	13	5	6	-8	90	80	16	3	-9	-7	0	28	1	-3	-3	-7	210	192	6	-4	2	-7	175	174	9
2	1	-8	91	84	7	6	6	-8	45	32	44	4	-9	-7	164	170	10	-2	-3	-7	120	109	17	-3	2	-7	273	273	7
3	1	-8	331	350	5	7	6	-8	0	33	1	5	-9	-7	31	64	31	-1	-3	-7	20	29	20	-2	2	-7	203	211	8
4	1	-8	103	118	10	-7	7	-8	68	70	39	6	-9	-7	14	6	14	0	-3	-7	100	105	6	-1	2	-7	36	57	20
5	1	-8	416	411	6	-6	7	-8	97	74	23	7	-9	-7	25	20	25	1	-3	-7	291	293	6	0	2	-7	111	115	6
6	1	-8	58	80	26	-5	7	-8	36	59	36	8	-9	-7	49	58	48	2	-3	-7	222	227	6	1	2	-7	266	252	4
7	1	-8	75	42	21	-4	7	-8	87	67	19	-4	-8	-7	61	71	47	3	-3	-7	482	484	6	2	2	-7	484	486	3
8	1	-8	123	117	13	-3	7	-8	103	97	17	-3	-8	-7	102	70	19	4	-3	-7	143	142	9	3	2	-7	295	309	6
-8	2	-8	70	93	51	-2	7	-8	165	177	9	-2	-8	-7	139	139	13	5	-3	-7	270	283	7	4	2	-7	200	209	7
-7	2	-8	21	47	21	-1	7	-8	72	45	17	-1	-8	-7	154	170	12	6	-3	-7	93	73	13	5	2	-7	162	145	9
-6	2	-8	269	281	10	0	7	-8	28	46	28	0	-8	-7	103	113	14	7	-3	-7	90	109	17	6	2	-7	210	211	8
-5	2	-8	0	36	1	1	7	-8	31	40	30	1	-8	-7	94	89	13	8	-3	-7	124	110	13	7	2	-7	174	188	9
-4	2	-8	81	63	18	2	7	-8	163	163	10	2	-8	-7	29	14	29	9	-3	-7	147	143	15	-8	3	-7	125	124	18
-3	2	-8	0	57	1	3	7	-8</																					

Table B-15, Continued
Observed and Calculated Structure Factors for 1-ferrocenylcarbonyl-2-ferrocenylcyclopentene

h	k	l	10Fo	10Fc	10s	h	k	l	10Fo	10Fc	10s	h	k	l	10Fo	10Fc	10s	h	k	l	10Fo	10Fc	10s	h	k	l	10Fo	10Fc	10s
-8	5	-7	140	108	17	-2	11	-7	100	123	21	4	-6	-6	167	180	8	-2	-1	-6	121	106	11	-3	4	-6	136	126	11
-7	5	-7	0	69	1	-1	11	-7	78	90	25	5	-6	-6	58	61	18	-1	-1	-6	161	159	3	-2	4	-6	42	53	14
-6	5	-7	181	209	11	0	11	-7	139	122	14	6	-6	-6	8	35	7	0	-1	-6	119	123	4	-1	4	-6	272	282	4
-5	5	-7	105	118	14	1	11	-7	70	8	33	7	-6	-6	123	126	14	1	-1	-6	347	355	4	0	4	-6	271	250	5
-4	5	-7	132	141	11	2	11	-7	29	50	28	8	-6	-6	72	104	26	2	-1	-6	186	167	4	1	4	-6	468	481	5
-3	5	-7	74	90	10	3	11	-7	39	21	38	9	-6	-6	0	28	1	3	-1	-6	125	136	5	2	4	-6	385	391	5
-2	5	-7	125	131	6	4	11	-7	137	126	18	10	-6	-6	48	37	48	4	-1	-6	152	135	7	3	4	-6	138	132	9
-1	5	-7	120	122	9	-3	12	-7	0	31	1	-7	-5	-6	60	101	60	5	-1	-6	187	174	5	4	4	-6	75	61	13
0	5	-7	220	225	6	-2	12	-7	0	8	1	-6	-5	-6	84	18	25	6	-1	-6	0	43	1	5	4	-6	113	110	9
1	5	-7	210	226	7	-1	12	-7	64	54	64	-5	-5	-6	0	51	1	7	-1	-6	132	132	7	6	4	-6	180	166	9
2	5	-7	14	43	13	0	12	-7	102	78	21	-4	-5	-6	0	48	1	8	-1	-6	0	19	1	7	4	-6	149	119	10
3	5	-7	156	159	9	1	12	-7	104	49	26	-3	-5	-6	268	256	5	9	-1	-6	115	115	15	-9	5	-6	103	23	23
4	5	-7	75	57	15	2	12	-7	61	22	61	-2	-5	-6	61	54	19	-9	0	-6	87	68	34	-7	5	-6	102	58	21
5	5	-7	191	192	8	0	-12	-6	0	42	1	-1	-5	-6	298	274	7	-8	0	-6	0	15	1	-8	5	-6	49	46	48
6	5	-7	31	41	30	1	-12	-6	0	44	1	0	-5	-6	90	117	11	-7	0	-6	112	71	16	-6	5	-6	134	137	14
7	5	-7	0	42	1	2	-12	-6	86	50	20	-6	0	-6	40	30	26	-6	0	-6	40	30	40	-5	5	-6	0	17	1
-8	6	-7	65	13	52	3	-12	-6	83	78	22	2	-5	-6	41	56	29	-5	0	-6	85	63	15	-4	5	-6	348	359	7
-7	6	-7	130	114	17	4	-12	-6	0	10	1	4	-5	-6	76	77	12	-4	0	-6	212	217	8	-3	5	-6	49	55	14
-6	6	-7	45	40	44	-2	-11	-6	82	64	29	5	-5	-6	179	200	8	-3	0	-6	315	337	6	-2	5	-6	169	173	5
-5	6	-7	175	160	10	-1	-11	-6	0	27	1	6	-5	-6	72	95	17	-2	0	-6	370	379	4	-1	5	-6	138	135	8
-4	6	-7	11	40	10	0	-11	-6	33	41	33	7	-5	-6	30	58	29	-1	0	-6	41	43	9	0	5	-6	370	368	6
-3	6	-7	73	66	11	1	-11	-6	0	7	1	8	-5	-6	134	138	13	0	0	-6	173	178	3	1	5	-6	189	203	7
-2	6	-7	62	73	13	2	-11	-6	17	53	17	9	-5	-6	109	64	18	1	0	-6	438	417	15	2	5	-6	393	401	6
-1	6	-7	272	292	7	3	-11	-6	0	15	1	10	-5	-6	98	18	68	2	0	-6	434	432	4	3	5	-6	24	13	23
0	6	-7	48	48	27	4	-11	-6	123	122	13	-8	-4	-6	97	84	31	3	0	-6	270	267	3	4	5	-6	0	13	1
1	6	-7	207	212	7	5	-11	-6	78	62	22	-7	-4	-6	51	41	50	4	0	-6	289	298	13	5	5	-6	80	74	16
2	6	-7	17	30	17	6	-11	-6	33	7	32	-6	-4	-6	134	155	17	5	0	-6	155	158	9	6	5	-6	131	126	10
3	6	-7	162	139	9	-3	-10	-6	110	55	20	-5	-4	-6	98	117	19	6	0	-6	263	261	5	7	5	-6	152	149	12
4	6	-7	99	93	13	-2	-10	-6	47	74	46	-4	-4	-6	59	36	29	7	0	-6	0	48	1	-9	6	-6	88	85	30
5	6	-7	178	174	10	-1	-10	-6	114	103	15	-3	-4	-6	61	38	23	8	0	-6	199	189	10	-8	6	-6	69	33	40
6	6	-7	181	160	10	0	10	-6	105	86	16	-2	-4	-6	315	305	4	-9	1	-6	78	49	46	-7	6	-6	92	103	21
7	6	-7	138	125	13	1	-10	-6	0	22	1	-1	-4	-6	138	125	5	-8	1	-6	178	185	15	-6	6	-6	53	64	53
-8	7	-7	0	35	1	2	-10	-6	29	22	28	0	-4	-6	353	353	8	-7	1	-6	72	85	29	-5	6	-6	118	116	12
-7	7	-7	2	23	2	3	-10	-6	60	75	26	1	-4	-6	188	195	8	-6	1	-6	89	81	18	-4	6	-6	98	80	14
-6	7	-7	186	198	12	4	-10	-6	46	81	46	2	-4	-6	175	173	7	-5	1	-6	84	76	15	-3	6	-6	304	316	4
-5	7	-7	63	51	37	5	-10	-6	126	119	14	3	-4	-6	108	103	8	-4	1	-6	211	212	7	-2	6	-6	50	44	14
-4	7	-7	246	248	8	6	-10	-6	65	34	32	4	-4	-6	371	364	6	-3	1	-6	216	214	4	-1	6	-6	31	36	31
-3	7	-7	22	20	21	7	-10	-6	49	29	49	5	-4	-6	128	119	10	-2	1	-6	517	509	16	0	6	-6	96	80	10
-2	7	-7	51	69	28	-4	-9	-6	0	20	1	6	-4	-6	160	161	9	-1	1	-6	440	446	8	1	6	-6	312	323	6
-1	7	-7	96	88	13	-3	-9	-6	2	47	2	7	-4	-6	102	93	13	0	1	-6	65	73	5	2	6	-6	77	84	14
0	7	-7	171	172	9	-2	-9	-6	68	70	26	8	-4	-6	71	85	26	1	1	-6	47	55	8	3	6	-6	241	253	7
1	7	-7	174	183	9	-1	-9	-6	135	138	14	9	-4	-6	125	115	16	2	1	-6	45	27	11	4	6	-6	56	63	23
2	7	-7	210	211	8	0	-9	-6	170	146	10	10	-4	-6	112	71	20	3	1	-6	362	366	3	5	6	-6	43	49	42
3	7	-7	0	17	1	1	-9	-6	119	142	10	-8	-3	-6	39	42	38	4	1	-6	285	285	10	6	6	-6	82	80	20
4	7	-7	0	36	1	2	-9	-6	69	25	17	-7	-3	-6	130	157	17	5	1	-6	199	210	7	7	6	-6	184	169	10
5	7	-7	122	111	15	3	-9	-6	0	8	1	-6	-3	-6	0	54	1	6	1	-6	46	34	16	-8	7	-6	131	143	18
6	7	-7	148	128	14	4	-9	-6	142	138	11	-5	-3	-6	131	132	13	7	1	-6	89	108	13	-7	7	-6	63	7	33
7	7	-7	57	59	56	5	-9	-6	189	217	9	-4	-3	-6	0	19	1	-9	2	-6	51	56	51	-6	7	-6	5	50	5
-7	8	-7	56	45	55	6	-9	-6	115	112	13	-3	-3	-6	36	42	36	-8	2	-6	0	9	1	-5	7	-6	59	13	30
-6	8	-7	58	63	51	7	-9	-6	107	115	16	-2	-3	-6	89	94	7	-7	2	-6	216	236	9	-4	7	-6	172	183	9
-5	8	-7	138	142	13	8	-9	-6	34	24	34	-1	-3	-6	358	370	4	-6	2	-6	131	125	12	-3	7	-6	148	139	6
-4	8	-7	0	25	1	-4	-8	-6	142	119	14	0	-3	-6	25	31	25	-5	2	-6	62	55	22	-2	7	-6	212	226	7
-3	8	-7	150	136	10	-3	-8	-6	70	36	31	-1	-3	-6	353	350	6	-4	2	-6	83	82	14	-1	7	-6	102	97	11
-2	8	-7	139	127	12	-2	-8	-6	49	48	49	2	-3	-6	140	138	8	-3	2	-6	230	243	4	0	7	-6	53	52	17
-1	8	-7	0	15	1	-1	-8	-6	96	86	18	3	-3	-6	240	247	6	-2	2	-6	227	240	3	1	7	-6	42	12	41
0	8	-7	56	39	26	0	-8	-6	185	188	9	4	-3	-6	102	95	8	-1	2	-6	355	338	5	2	7	-6	181	200	8
1	8	-7	172	197	9	1	-8	-6	102	104	11	5	-3	-6	457	463	6	0	2	-6	267	257	9	3	7	-6	58	71	26
2	8	-7	41	59	40	2	-8	-6	110	108	10	6	-3	-6	72	76	15	1	2	-6	211	203	3	4	7	-6	235	239	3
3	8	-7	142	138	12	3	-8	-6	0	34	1	7	-3	-6	184	186	9	2	2	-6	118	122	18	5	7	-6	46	30	45
4	8	-7	182	22	18																								

Table B-15, Continued
Observed and Calculated Structure Factors for 1-ferrocenylcarbonyl-2-ferrocenylcyclopentene

h	k	l	10Fo	10Fc	10s	h	k	l	10Fo	10Fc	10s	h	k	l	10Fo	10Fc	10s	h	k	l	10Fo	10Fc	10s	h	k	l	10Fo	10Fc	10s
-3	10	-6	101	83	19	1	-7	-5	77	103	13	-8	-2	-5	108	105	21	3	2	-5	518	530	3	-8	8	-5	0	30	1
-2	10	-6	40	41	39	2	-7	-5	50	34	20	-7	-2	-5	81	82	25	4	2	-5	177	190	7	-7	8	-5	0	21	1
-1	10	-6	151	149	14	3	-7	-5	235	253	6	-6	-2	-5	41	37	41	5	2	-5	204	208	6	-6	8	-5	184	174	11
0	10	-6	99	52	17	4	-7	-5	67	63	14	-5	-2	-5	72	54	19	6	2	-5	205	207	12	-5	8	-5	91	104	17
1	10	-6	224	209	10	5	-7	-5	151	153	9	-4	-2	-5	123	113	11	7	2	-5	203	195	9	-4	8	-5	123	119	8
2	10	-6	59	37	34	6	-7	-5	117	110	12	-3	-2	-5	360	348	6	-9	3	-5	0	54	1	-3	8	-5	135	131	11
4	10	-6	0	22	1	7	-7	-5	59	40	32	-2	-2	-5	554	547	5	-8	3	-5	125	129	16	-2	8	-5	82	61	15
5	10	-6	151	107	15	8	-7	-5	70	37	33	-1	-2	-5	295	307	4	-7	3	-5	0	34	1	-1	8	-5	130	132	11
6	10	-6	103	30	29	9	-7	-5	112	87	21	0	-2	-5	0	25	1	-6	3	-5	48	82	36	0	8	-5	14	15	14
-3	11	-6	76	82	33	10	-7	-5	19	18	19	2	-2	-5	314	333	3	-5	3	-5	37	34	37	1	8	-5	257	257	8
-2	11	-6	73	75	35	7	-6	-5	41	53	41	3	-2	-5	328	346	6	-4	3	-5	463	478	6	2	8	-5	170	161	10
-1	11	-6	0	40	1	-6	-6	-5	145	152	15	4	-2	-5	266	287	7	-3	3	-5	131	118	10	3	8	-5	133	137	9
0	11	-6	79	101	29	-5	-6	-5	141	115	13	5	-2	-5	98	100	6	-2	3	-5	404	407	12	4	8	-5	121	129	14
1	11	-6	159	119	14	-4	-6	-5	20	45	20	6	-2	-5	113	107	11	-1	3	-5	199	192	4	5	8	-5	164	161	12
2	11	-6	98	92	17	-3	-6	-5	120	111	12	7	-2	-5	0	19	1	0	3	-5	295	311	5	6	8	-5	0	21	1
3	11	-6	84	18	27	-2	-6	-5	170	370	7	8	-2	-5	75	70	20	1	3	-5	135	122	7	-7	9	-5	0	30	1
4	11	-6	45	27	44	-1	-6	-5	129	118	9	9	-2	-5	0	33	1	2	3	-5	518	549	5	-6	9	-5	0	24	1
-3	12	-6	125	63	22	0	-6	-5	360	343	6	10	-2	-5	52	53	52	3	3	-5	44	58	23	-5	9	-5	120	120	13
-2	12	-6	136	135	18	1	-6	-5	115	102	9	11	-2	-5	65	44	65	4	3	-5	205	202	6	-4	9	-5	141	132	12
-1	12	-6	79	20	33	2	-6	-5	26	41	26	5	3	-5	53	32	17	5	3	-5	53	32	17	-3	9	-5	175	171	9
0	12	-6	68	49	44	3	-6	-5	45	13	22	-8	-1	-5	160	151	16	6	3	-5	82	87	13	-2	9	-5	170	186	10
1	12	-6	93	83	25	4	-6	-5	150	178	8	-7	-1	-5	32	82	32	7	3	-5	162	157	10	-1	9	-5	55	15	28
2	12	-6	0	56	1	5	-6	-5	112	115	10	-6	-1	-5	61	64	26	-9	4	-5	105	90	20	0	9	-5	127	101	14
3	12	-6	128	91	19	6	-6	-5	177	180	9	-5	-1	-5	64	56	22	-8	4	-5	37	54	36	1	9	-5	82	78	18
-1	12	-5	76	57	30	7	-6	-5	87	92	19	-4	-1	-5	90	100	12	-7	4	-5	188	182	11	2	9	-5	167	144	11
0	12	-5	63	73	31	8	-6	-5	37	50	37	-3	-1	-5	148	157	8	-6	4	-5	38	44	38	3	9	-5	142	115	11
1	12	-5	40	45	39	9	-6	-5	107	79	19	-2	-1	-5	629	614	3	-5	4	-5	81	93	12	4	9	-5	134	115	13
2	12	-5	22	14	21	10	-6	-5	74	24	39	-1	-1	-5	403	390	4	-4	4	-5	29	38	29	5	9	-5	54	26	53
3	12	-5	27	10	26	-8	-5	-5	67	41	67	0	-1	-5	387	389	2	-3	4	-5	478	501	3	6	9	-5	64	43	50
4	12	-5	0	15	1	-7	-5	-5	94	79	26	1	-1	-5	316	308	3	-2	4	-5	107	103	6	-4	10	-5	140	123	13
5	12	-5	57	74	48	-6	-5	-5	108	124	17	2	-1	-5	92	86	4	-1	4	-5	258	285	8	-3	10	-5	90	101	18
-3	11	-5	90	78	25	-5	-5	-5	192	177	10	3	-1	-5	370	368	4	0	4	-5	24	35	23	-2	10	-5	180	191	10
-2	11	-5	69	13	37	-4	-5	-5	197	197	6	4	-1	-5	186	192	4	1	4	-5	485	470	5	-1	10	-5	86	81	21
-1	11	-5	89	79	22	-3	-5	-5	152	170	7	5	-1	-5	360	351	4	2	4	-5	177	176	6	0	10	-5	112	77	17
0	11	-5	90	74	21	-2	-5	-5	77	78	10	6	-1	-5	82	76	15	3	4	-5	444	466	5	1	10	-5	191	186	12
1	11	-5	124	132	12	-1	-5	-5	207	215	4	7	-1	-5	21	7	20	4	4	-5	107	93	9	2	10	-5	173	156	12
2	11	-5	86	86	20	0	-5	-5	139	131	8	8	-1	-5	23	31	22	5	4	-5	114	118	10	3	10	-5	142	138	12
3	11	-5	88	46	16	1	-5	-5	354	357	6	9	-1	-5	179	177	13	6	4	-5	61	48	20	4	10	-5	136	96	14
4	11	-5	0	46	1	2	-5	-5	16	43	15	10	-1	-5	107	61	20	7	4	-5	73	62	22	5	10	-5	46	20	46
5	11	-5	66	55	28	3	-5	-5	0	13	1	-9	0	-5	78	23	41	-9	5	-5	0	48	1	6	10	-5	81	40	36
6	11	-5	84	83	22	4	-5	-5	89	101	10	-8	0	-5	0	19	1	-8	5	-5	144	144	15	-4	11	-5	85	66	28
7	11	-5	0	31	1	5	-5	-5	239	231	7	-7	0	-5	218	238	10	-7	5	-5	117	76	13	-3	11	-5	171	165	11
4	10	-5	37	80	36	6	-5	-5	80	77	16	-6	0	-5	77	54	19	-6	5	-5	96	73	15	-2	11	-5	136	114	14
-3	10	-5	0	10	1	7	-5	-5	163	148	11	-5	0	-5	121	115	11	-5	5	-5	89	84	15	-1	11	-5	204	196	11
-2	10	-5	28	24	27	8	-5	-5	53	63	47	-4	0	-5	177	176	8	-4	5	-5	149	164	9	0	11	-5	62	82	43
-1	10	-5	72	27	32	9	-5	-5	50	18	50	-3	0	-5	347	354	5	-3	5	-5	163	170	5	1	11	-5	68	71	31
0	10	-5	105	92	15	10	-5	-5	56	56	56	-2	0	-5	431	436	3	-2	5	-5	559	547	9	2	11	-5	68	73	37
1	10	-5	129	135	10	-8	-4	-5	59	23	58	-1	0	-5	743	720	6	-1	5	-5	216	218	6	3	11	-5	107	84	17
2	10	-5	168	167	8	-7	-4	-5	89	58	28	0	0	-5	473	491	5	0	5	-5	330	329	5	4	11	-5	105	100	22
3	10	-5	72	87	16	-6	-4	-5	176	162	12	1	0	-5	35	36	9	1	5	-5	47	29	18	5	11	-5	36	37	35
4	10	-5	0	36	1	-5	-4	-5	163	172	10	2	0	-5	269	248	3	2	5	-5	216	227	6	-4	12	-5	21	45	21
5	10	-5	113	132	12	-4	-4	-5	134	122	9	3	0	-5	78	75	9	3	5	-5	67	70	13	-3	12	-5	82	18	32
6	10	-5	107	110	17	-3	-4	-5	85	72	9	4	0	-5	233	236	3	4	5	-5	221	232	7	-2	12	-5	85	85	28
7	10	-5	125	104	15	-2	-4	-5	0	47	1	5	0	-5	309	311	3	5	5	-5	99	88	11	-1	12	-5	0	27	1
8	10	-5	87	80	26	-1	-4	-5	117	118	5	6	0	-5	223	210	6	6	5	-5	66	68	21	0	12	-5	77	76	29
-4	9	-5	42	60	41	0	-4	-5	234	238	6	7	0	-5	130	114	16	-9	6	-5	58	49	58	1	12	-5	46	39	46
-3	9	-5	205	179	12	1	-4	-5	247	252	5	8	0	-5	60	17	32	-8	6	-5	75	97	26	2	12	-5	34	27	33
-2	9	-5	48	15	47	2	-4	-5	566	566	5	9	0	-5	0	49	1	-7	6	-5	166	155	11	3	12	-5	95	19	22
-1	9	-5	0	15	1	3	-4	-5	181	187	7	-9	1	-5	0	19	1	-6	6	-5	168	177	10	-3	1				

Table B-15, Continued
Observed and Calculated Structure Factors for 1-ferrocenylcarbonyl-2-ferrocenylcyclopentene

h	k	l	10Fo	10Fc	10s	h	k	l	10Fo	10Fc	10s	h	k	l	10Fo	10Fc	10s	h	k	l	10Fo	10Fc	10s	h	k	l	10Fo	10Fc	10s
3	-10	-4	43	7	42	-8	-4	-4	74	64	35	-5	0	-4	193	213	8	-8	5	-4	58	22	37	-2	11	-4	0	16	1
4	-10	-4	224	233	7	-7	-4	-4	182	159	12	-4	0	-4	36	10	36	-7	5	-4	41	73	40	-1	11	-4	196	174	12
5	-10	-4	35	42	34	-6	-4	-4	0	51	1	-3	0	-4	519	536	5	-6	5	-4	173	148	10	0	11	-4	36	30	36
6	-10	-4	32	45	31	-5	-4	-4	83	88	17	-2	0	-4	29	14	16	-5	5	-4	190	207	7	1	11	-4	225	210	10
7	-10	-4	71	43	28	-4	-4	-4	0	36	1	-1	0	-4	121	134	3	-4	5	-4	282	291	9	2	11	-4	0	25	1
8	-10	-4	75	69	35	-3	-4	-4	382	381	4	0	0	-4	136	132	3	-3	5	-4	31	23	31	3	11	-4	0	43	1
-4	-9	-4	0	44	1	-2	-4	-4	347	348	4	1	0	-4	661	650	8	-2	5	-4	71	75	6	4	11	-4	12	21	12
-3	-9	-4	103	103	17	-1	-4	-4	393	391	3	2	0	-4	189	194	3	-1	5	-4	360	332	5	5	11	-4	89	94	30
-2	-9	-4	51	49	51	0	-4	-4	38	17	24	3	0	-4	390	369	5	0	5	-4	552	581	5	-4	12	-4	117	110	20
-1	-9	-4	188	192	8	1	-4	-4	107	106	7	4	0	-4	58	59	7	1	5	-4	443	439	5	-3	12	-4	54	52	54
0	-9	-4	93	95	13	2	-4	-4	494	493	5	5	0	-4	251	239	4	2	5	-4	424	440	5	-2	12	-4	63	61	51
1	-9	-4	149	150	10	3	-4	-4	464	465	5	6	0	-4	241	228	4	3	5	-4	31	28	30	-1	12	-4	0	32	1
2	-9	-4	34	16	33	4	-4	-4	466	464	5	7	0	-4	211	204	12	4	5	-4	40	38	28	0	12	-4	126	113	14
3	-9	-4	147	155	10	5	-4	-4	203	207	7	8	0	-4	65	75	26	5	5	-4	30	34	30	1	12	-4	0	31	1
4	-9	-4	74	85	15	6	-4	-4	84	79	13	9	0	-4	158	158	13	6	5	-4	186	172	9	2	12	-4	102	105	21
5	-9	-4	210	236	8	7	-4	-4	0	10	1	10	0	-4	7	52	7	-9	6	-4	69	43	39	3	12	-4	0	24	1
6	-9	-4	60	25	27	8	-4	-4	123	120	12	-9	1	-4	24	94	24	-8	6	-4	95	71	19	-4	13	-4	73	26	48
7	-9	-4	34	56	33	9	-4	-4	40	15	39	-8	1	-4	101	98	17	-7	6	-4	0	22	1	-3	13	-4	45	72	44
8	-9	-4	93	58	24	10	-4	-4	84	82	27	-7	1	-4	0	11	1	-6	6	-4	66	64	25	-2	13	-4	0	13	1
9	-9	-4	20	69	20	11	-4	-4	78	71	43	-6	1	-4	105	106	12	-5	6	-4	69	76	20	-1	13	-4	59	28	59
-4	-8	-4	54	53	53	-9	-3	-4	0	25	1	-5	1	-4	52	23	22	-4	6	-4	265	267	13	0	13	-4	0	33	1
-3	-8	-4	60	78	26	-8	-3	-4	146	138	15	-4	1	-4	588	575	6	-3	6	-4	228	234	4	1	13	-4	93	67	30
-2	-8	-4	106	109	14	-7	-3	-4	170	168	13	-3	1	-4	196	196	4	-2	6	-4	212	210	5	2	-13	-3	0	21	1
-1	-8	-4	74	71	15	-6	-3	-4	188	193	10	-2	1	-4	488	472	3	-1	6	-4	214	221	6	3	-13	-3	102	79	18
0	-8	-4	192	196	8	-5	-3	-4	91	100	15	-1	1	-4	0	28	1	0	6	-4	165	176	7	4	-13	-3	38	16	37
1	-8	-4	94	93	11	-4	-3	-4	64	77	18	0	1	-4	98	81	3	1	6	-4	266	296	6	0	-12	-3	86	80	21
2	-8	-4	0	32	1	-3	-3	-4	55	58	12	2	1	-4	75	65	3	2	6	-4	276	290	6	1	-12	-3	0	13	1
3	-8	-4	6	9	6	-2	-3	-4	475	468	9	2	1	-4	472	468	3	3	6	-4	135	136	8	2	-12	-3	51	38	50
4	-8	-4	141	140	8	-1	-3	-4	239	247	3	3	1	-4	126	112	5	4	6	-4	59	73	18	3	-12	-3	32	20	32
5	-8	-4	25	28	25	0	-3	-4	559	537	2	4	1	-4	565	562	3	5	6	-4	230	249	7	4	-12	-3	76	54	25
6	-8	-4	180	156	11	1	-3	-4	0	6	1	5	1	-4	85	89	7	6	6	-4	77	79	21	5	-12	-3	0	52	1
7	-8	-4	29	21	28	2	-3	-4	18	31	17	6	1	-4	78	75	9	-9	7	-4	75	82	37	6	-12	-3	105	65	18
8	-8	-4	70	45	38	3	-3	-4	209	228	5	7	1	-4	160	165	9	-8	7	-4	92	83	23	-2	-11	-3	45	41	44
9	-8	-4	78	55	41	4	-3	-4	431	429	5	8	1	-4	246	247	8	-7	7	-4	60	38	43	-1	-11	-3	143	139	11
-4	-7	-4	102	100	15	5	-3	-4	152	158	8	-10	2	-4	84	38	33	-6	7	-4	107	123	13	0	-11	-3	16	57	16
-3	-7	-4	120	113	12	6	-3	-4	199	201	7	-9	2	-4	129	118	17	-5	7	-4	63	36	24	1	-11	-3	151	146	9
-2	-7	-4	105	109	13	7	-3	-4	50	60	29	-8	2	-4	174	150	13	-4	7	-4	174	183	6	2	-11	-3	22	22	21
-1	-7	-4	207	203	7	8	-3	-4	40	15	39	-7	2	-4	280	287	8	-3	7	-4	240	235	5	3	-11	-3	22	66	21
0	-7	-4	95	93	10	9	-3	-4	111	123	15	-6	2	-4	93	100	14	-2	7	-4	131	138	10	4	-11	-3	40	33	40
1	-7	-4	231	235	6	10	-3	-4	49	46	48	-5	2	-4	61	37	15	-1	7	-4	6	28	6	5	-11	-3	150	143	11
2	-7	-4	29	30	29	11	-3	-4	82	66	39	-4	2	-4	106	99	10	0	7	-4	50	32	19	6	-11	-3	0	27	1
3	-7	-4	38	24	33	9	-2	-4	62	70	62	-3	2	-4	449	477	7	1	7	-4	181	177	8	7	-11	-3	100	61	19
4	-7	-4	72	67	12	-8	-2	-4	96	58	22	-2	2	-4	53	50	24	2	7	-4	168	166	8	-3	-10	-3	48	52	48
5	-7	-4	70	91	15	-7	-2	-4	234	235	10	-1	2	-4	295	277	3	3	7	-4	264	276	7	-2	-10	-3	80	58	23
6	-7	-4	62	71	22	-6	-2	-4	46	46	45	0	2	-4	30	16	6	4	7	-4	250	252	7	-1	-10	-3	82	61	16
7	-7	-4	208	210	11	-5	-2	-4	151	135	9	1	2	-4	220	228	4	5	7	-4	87	75	16	0	-10	-3	231	235	7
8	-7	-4	0	35	1	-4	-2	-4	144	130	8	2	2	-4	155	146	6	6	7	-4	92	117	16	1	-10	-3	80	91	16
9	-7	-4	0	85	1	-3	-2	-4	125	103	8	3	2	-4	526	523	2	-8	8	-4	189	194	11	2	-10	-3	204	201	7
10	-7	-4	0	12	1	-2	-2	-4	48	48	9	4	2	-4	53	48	12	-7	8	-4	104	108	16	3	-10	-3	0	9	1
-8	-6	-4	59	30	59	-1	-2	-4	467	473	3	5	2	-4	359	349	3	-6	8	-4	93	86	17	4	-10	-3	114	105	13
-7	-6	-4	34	49	33	0	-2	-4	128	122	4	6	2	-4	28	25	28	-5	8	-4	24	33	23	5	-10	-3	39	54	39
-6	-6	-4	69	61	37	1	-2	-4	379	385	4	7	2	-4	59	52	21	-4	8	-4	130	119	9	6	-10	-3	197	205	10
-5	-6	-4	150	143	13	2	-2	-4	99	113	6	-10	3	-4	43	14	42	-3	8	-4	94	91	14	7	-10	-3	73	48	27
-4	-6	-4	195	193	6	3	-2	-4	160	169	6	-9	3	-4	31	52	31	-2	8	-4	265	258	8	8	-10	-3	0	43	1
-3	-6	-4	53	55	17	4	-2	-4	83	82	12	-8	3	-4	90	96	19	-1	8	-4	131	114	10	-4	-9	-3	202	197	11
-2	-6	-4	186	190	6	5	-2	-4	399	412	5	-7	3	-4	87	85	17	0	8	-4	61	52	18	-3	-9	-3	106	113	14
-1	-6	-4	26	32	25	6	-2	-4	211	206	7	-6	3	-4	242	236	8	1	8	-4	46	39	42	-2	-9	-3	54	25	34
0	-6	-4	182	195	7	7	-2	-4	203	210	9	-5	3	-4	19	27	19	2	8	-4	95	90	16	-1	-9	-3	67	28	17
1	-6	-4	201	203	6	8	-2	-4	131	133	12	-4	3	-4	42	44	22	3	8	-4	0	40	1	0	-9	-3	83	90	14
2	-6	-4	437	445	6																								

Table B-15, Continued
Observed and Calculated Structure Factors for 1-ferrocenylcarbonyl-2-ferrocenylcyclopentene

h	k	l	10Fo	10Fc	10s	h	k	l	10Fo	10Fc	10s	h	k	l	10Fo	10Fc	10s	h	k	l	10Fo	10Fc	10s	h	k	l	10Fo	10Fc	10s
1	-7	-3	46	36	17	10	-3	-3	0	18	1	-7	2	-3	71	88	20	-6	7	-3	88	46	18	7	-11	-2	77	110	36
2	-7	-3	174	188	6	11	-3	-3	70	70	63	-6	2	-3	214	230	7	-5	7	-3	145	133	9	-2	-10	-2	43	75	43
3	-7	-3	221	220	6	-9	-2	-3	161	147	16	-5	2	-3	382	381	6	-4	7	-3	78	73	10	-1	-10	-2	119	104	10
4	-7	-3	163	170	9	-8	-2	-3	0	60	1	-4	2	-3	341	317	5	-3	7	-3	137	130	10	0	-10	-2	15	22	15
5	-7	-3	147	154	10	-7	-2	-3	73	68	24	-3	2	-3	257	257	2	-2	7	-3	191	198	7	1	-10	-2	164	160	9
6	-7	-3	0	22	1	-6	-2	-3	30	32	30	-2	2	-3	217	216	3	-1	7	-3	308	319	6	2	-10	-2	155	155	9
7	-7	-3	32	58	31	-5	-2	-3	174	173	9	-1	2	-3	88	95	4	0	7	-3	192	196	8	3	-10	-2	124	135	9
8	-7	-3	77	76	24	-4	-2	-3	180	177	7	0	2	-3	306	272	4	1	7	-3	239	230	7	4	-10	-2	119	117	11
9	-7	-3	144	126	14	-3	-2	-3	782	795	5	1	2	-3	488	495	4	2	7	-3	149	143	8	5	-10	-2	64	64	26
10	-7	-3	81	35	38	-2	-2	-3	0	15	1	2	2	-3	387	389	6	3	7	-3	172	171	8	6	-10	-2	58	60	51
-8	-6	-3	34	16	34	-1	-2	-3	197	202	3	3	2	-3	238	236	3	4	7	-3	128	112	10	7	-10	-2	0	32	1
-7	-6	-3	132	120	17	0	-2	-3	52	47	5	4	2	-3	96	106	4	5	7	-3	265	275	7	8	-10	-2	95	79	25
-6	-6	-3	13	22	12	1	-2	-3	601	586	4	5	2	-3	460	459	3	6	7	-3	81	76	19	-4	-9	-2	107	120	15
-5	-6	-3	112	93	14	2	-2	-3	216	224	4	6	2	-3	141	143	5	-7	8	-3	90	73	18	-3	-9	-2	65	68	22
-4	-6	-3	107	108	7	3	-2	-3	450	488	4	7	2	-3	161	175	10	-6	8	-3	179	165	9	-2	-9	-2	204	193	9
-3	-6	-3	285	288	5	4	-2	-3	212	220	5	8	2	-3	75	75	20	-5	8	-3	87	81	16	-1	-9	-2	60	43	21
-2	-6	-3	246	245	5	5	-2	-3	101	93	9	-10	3	-3	39	24	39	-4	8	-3	260	243	6	0	-9	-2	249	250	7
-1	-6	-3	331	331	4	6	-2	-3	65	73	16	-9	3	-3	160	149	14	-3	8	-3	105	89	12	1	-9	-2	25	36	24
0	-6	-3	95	96	8	7	-2	-3	49	76	29	-8	3	-3	80	83	21	-2	8	-3	89	79	14	2	-9	-2	132	138	10
1	-6	-3	142	164	7	8	-2	-3	115	92	13	-7	3	-3	51	69	43	-1	8	-3	36	51	36	3	-9	-2	157	153	8
2	-6	-3	104	107	8	9	-2	-3	130	129	13	-6	3	-3	156	175	9	0	8	-3	183	194	8	4	-9	-2	225	240	8
3	-6	-3	208	215	6	10	-2	-3	0	11	1	-5	3	-3	341	332	6	1	8	-3	37	22	36	5	-9	-2	130	129	11
4	-6	-3	290	290	6	11	-2	-3	0	28	1	-4	3	-3	390	419	4	2	8	-3	219	230	7	6	-9	-2	72	73	23
5	-6	-3	153	156	9	-9	-1	-3	80	40	34	-3	3	-3	0	32	1	3	8	-3	79	73	15	7	-9	-2	50	71	50
6	-6	-3	123	105	10	-8	-1	-3	129	112	15	-2	3	-3	0	10	1	4	8	-3	102	85	13	8	-9	-2	45	7	45
7	-6	-3	109	97	13	-7	-1	-3	33	38	32	-1	3	-3	24	17	20	5	8	-3	149	133	11	9	-9	-2	125	96	21
8	-6	-3	115	101	17	-6	-1	-3	44	52	43	0	3	-3	474	497	4	-5	9	-3	176	177	10	-7	-8	-2	135	122	19
9	-6	-3	49	31	48	-5	-1	-3	131	124	10	1	3	-3	371	392	4	-4	9	-3	65	89	23	-6	-8	-2	70	17	33
10	-6	-3	75	79	37	-4	-1	-3	300	315	6	2	3	-3	456	461	4	-3	9	-3	136	123	11	-5	-8	-2	159	154	13
-8	-5	-3	71	100	44	-3	-1	-3	317	289	5	3	3	-3	191	190	4	-2	9	-3	66	37	22	-4	-8	-2	57	66	26
-7	-5	-3	0	42	1	-2	-1	-3	648	635	3	4	3	-3	21	36	21	-1	9	-3	114	108	11	-3	-8	-2	99	93	11
-6	-5	-3	256	261	9	-1	-1	-3	222	212	3	5	3	-3	88	93	7	0	9	-3	106	84	14	-2	-8	-2	0	33	1
-5	-5	-3	75	75	19	0	-1	-3	319	282	5	6	3	-3	143	143	5	1	9	-3	237	242	8	-1	-8	-2	174	181	8
-4	-5	-3	137	144	7	1	-1	-3	177	172	2	7	3	-3	157	166	9	2	9	-3	0	17	1	0	-8	-2	137	128	8
-3	-5	-3	102	106	7	2	-1	-3	510	492	3	-10	4	-3	63	71	63	3	9	-3	173	144	11	1	-8	-2	92	90	9
-2	-5	-3	467	477	8	3	-1	-3	180	189	3	-9	4	-3	0	39	1	4	9	-3	69	19	26	2	-8	-2	93	80	10
-1	-5	-3	357	355	3	4	-1	-3	500	481	3	-8	4	-3	121	121	14	5	9	-3	129	101	13	3	-8	-2	69	73	12
0	-5	-3	656	646	3	5	-1	-3	34	42	14	-7	4	-3	49	44	48	-4	10	-3	275	266	8	4	-8	-2	140	147	10
1	-5	-3	183	191	6	6	-1	-3	118	105	7	-6	4	-3	78	97	14	-3	10	-3	48	51	47	5	-8	-2	169	165	9
2	-5	-3	169	172	7	7	-1	-3	162	170	10	-5	4	-3	95	97	10	-2	10	-3	136	140	11	6	-8	-2	164	153	11
4	-5	-3	99	108	10	8	-1	-3	146	113	12	-4	4	-3	758	739	5	-1	10	-3	92	58	16	7	-8	-2	63	15	32
5	-5	-3	225	230	6	9	-1	-3	74	59	27	-3	4	-3	583	558	13	0	10	-3	176	157	12	8	-8	-2	0	25	1
6	-5	-3	193	193	9	10	-1	-3	98	99	22	-2	4	-3	433	418	3	1	10	-3	0	49	1	9	-8	-2	0	48	1
7	-5	-3	0	64	1	11	-1	-3	40	26	39	-1	4	-3	90	93	5	2	10	-3	236	227	8	-8	-7	-2	0	48	1
8	-5	-3	58	42	28	-10	0	-3	73	4	56	0	4	-3	219	225	4	3	10	-3	73	42	26	-7	-7	-2	73	25	40
9	-5	-3	112	113	15	-9	0	-3	155	122	15	1	4	-3	357	361	5	4	10	-3	31	89	30	-6	-7	-2	139	147	14
10	-5	-3	61	35	61	-8	0	-3	218	217	10	2	4	-3	365	381	2	5	10	-3	0	28	1	-5	-7	-2	19	24	18
-9	-4	-3	76	64	43	-7	0	-3	140	133	11	3	4	-3	236	247	3	-4	11	-3	114	134	17	-4	-7	-2	0	29	1
-8	-4	-3	29	23	29	-6	0	-3	172	156	10	4	4	-3	29	28	25	-3	11	-3	181	200	11	-3	-7	-2	209	215	5
-7	-4	-3	146	144	15	-5	0	-3	25	6	24	5	4	-3	9	33	8	-2	11	-3	37	86	36	-2	-7	-2	241	236	5
-6	-4	-3	51	51	51	-4	0	-3	79	54	11	6	4	-3	41	73	40	-1	11	-3	167	149	12	-1	-7	-2	33	45	33
-5	-4	-3	263	260	8	-2	0	-3	301	302	4	-10	5	-3	0	44	1	0	11	-3	26	16	26	0	-7	-2	519	492	6
-4	-4	-3	54	39	21	-1	0	-3	437	440	4	-9	5	-3	158	147	14	1	11	-3	121	127	13	1	-7	-2	53	45	16
-3	-4	-3	186	186	5	0	0	-3	340	309	1	-8	5	-3	0	45	1	2	11	-3	0	30	1	2	-7	-2	76	94	10
-2	-4	-3	257	250	4	1	0	-3	39	47	6	-7	5	-3	184	176	8	3	11	-3	153	141	14	3	-7	-2	123	119	8
-1	-4	-3	218	224	3	2	0	-3	152	161	3	-6	5	-3	171	169	9	4	11	-3	55	22	55	4	-7	-2	103	96	11
0	-4	-3	166	172	5	3	0	-3	604	604	7	-5	5	-3	113	136	10	5	11	-3	0	42	1	5	-7	-2	122	119	11
1	-4	-3	464	458	5	4	0	-3	179	185	6	-4	5	-3	50	22	11	-4	12	-3	88	60	27	6	-7	-2	177	176	9
2	-4	-3	337	339	4	5	0	-3	699	684	3	-3	5	-3	670	675	14	-3	12	-3	99	49	21	7	-7	-2	85	108	19

Table B-15, Continued
Observed and Calculated Structure Factors for 1-ferrocenylcarbonyl-2-ferrocenylcyclopentene

h	k	l	10Fo	10Fc	10s	h	k	l	10Fo	10Fc	10s	h	k	l	10Fo	10Fc	10s	h	k	l	10Fo	10Fc	10s	h	k	l	10Fo	10Fc	10s
0	-5	-2	314	311	3	3	-1	-2	186	165	3	6	3	-2	148	137	8	4	9	-2	42	48	41	5	-8	-1	157	139	11
1	-5	-2	145	164	4	4	-1	-2	366	347	3	7	3	-2	66	57	17	5	9	-2	109	109	16	6	-8	-1	0	56	1
2	-5	-2	702	720	5	5	-1	-2	53	45	8	8	3	-2	86	86	16	-5	10	-2	48	55	47	7	-8	-1	196	180	10
3	-5	-2	35	36	23	6	-1	-2	361	372	6	-10	4	-2	64	41	40	-4	10	-2	114	98	16	8	-8	-1	80	88	27
4	-5	-2	233	240	6	7	-1	-2	28	21	28	-9	4	-2	67	54	32	-3	10	-2	226	228	10	9	-8	-1	89	89	35
5	-5	-2	143	135	9	8	-1	-2	94	74	14	-8	4	-2	156	160	11	-2	10	-2	216	199	9	-8	-7	-1	103	81	25
6	-5	-2	182	184	8	9	-1	-2	41	43	40	-7	4	-2	71	87	16	-1	10	-2	188	199	10	-7	-7	-1	27	38	27
7	-5	-2	85	112	14	10	-1	-2	60	108	51	-6	4	-2	239	257	7	0	10	-2	262	256	8	-6	-7	-1	62	43	45
8	-5	-2	226	230	10	11	-1	-2	0	21	1	-5	4	-2	214	232	7	1	10	-2	104	99	14	-5	-7	-1	58	46	31
9	-5	-2	0	7	1	-10	0	-2	76	32	43	-4	4	-2	222	209	4	2	10	-2	49	59	48	-4	-7	-1	172	167	13
10	-5	-2	72	21	33	-9	0	-2	89	40	29	-3	4	-2	533	469	3	3	10	-2	59	31	25	-3	-7	-1	144	141	6
-9	-4	-2	96	96	29	-8	0	-2	40	46	40	-2	4	-2	604	585	4	4	10	-2	175	166	12	-2	-7	-1	259	272	4
-8	-4	-2	30	96	29	-7	0	-2	0	39	1	-1	4	-2	53	43	7	5	10	-2	107	69	19	-1	-7	-1	80	80	8
-7	-4	-2	137	116	15	-6	0	-2	153	150	9	0	4	-2	569	580	4	-5	11	-2	60	63	59	0	-7	-1	15	39	14
-6	-4	-2	130	107	11	-5	0	-2	285	301	6	1	4	-2	366	349	4	-4	11	-2	0	39	1	1	-7	-1	79	81	6
-5	-4	-2	105	110	11	-4	0	-2	518	551	5	2	4	-2	64	66	9	-3	11	-2	56	23	56	2	-7	-1	355	362	5
-4	-4	-2	236	237	7	-3	0	-2	211	207	5	3	4	-2	245	252	3	-2	11	-2	47	72	46	3	-7	-1	0	10	1
-3	-4	-2	702	705	8	-2	0	-2	202	208	4	4	4	-2	256	274	3	-1	11	-2	134	132	13	4	-7	-1	238	247	7
-2	-4	-2	475	473	3	-1	0	-2	630	628	6	5	4	-2	49	54	18	0	11	-2	182	195	10	5	-7	-1	0	52	1
-1	-4	-2	54	58	7	0	0	-2	1155	1142	6	6	4	-2	222	232	7	1	11	-2	109	113	18	6	-7	-1	80	100	17
0	-4	-2	154	167	5	1	0	-2	1739	1658	12	7	4	-2	35	38	35	2	11	-2	49	28	49	7	-7	-1	38	20	38
1	-4	-2	468	465	4	2	0	-2	530	505	14	-10	5	-2	68	64	39	3	11	-2	34	31	33	8	-7	-1	188	171	12
2	-4	-2	221	220	5	3	0	-2	94	83	5	-9	5	-2	0	35	1	4	11	-2	62	35	50	10	-7	-1	0	35	1
3	-4	-2	666	658	5	4	0	-2	67	70	8	-8	5	-2	54	53	38	-5	12	-2	109	99	22	10	-7	-1	82	53	32
4	-4	-2	61	51	13	5	0	-2	511	499	3	-7	5	-2	215	226	7	-4	12	-2	0	21	1	-8	-6	-1	60	58	60
5	-4	-2	57	30	14	6	0	-2	106	89	15	-6	5	-2	265	277	7	-3	12	-2	89	22	27	-7	-6	-1	54	81	54
6	-4	-2	158	136	10	7	0	-2	259	267	7	-5	5	-2	269	273	4	-2	12	-2	48	60	47	-6	-6	-1	51	69	50
7	-4	-2	235	228	8	8	0	-2	73	100	18	-4	5	-2	68	64	8	-1	12	-2	79	48	26	-5	-6	-1	65	29	24
8	-4	-2	93	105	20	9	0	-2	5	27	5	-3	5	-2	0	16	1	0	12	-2	118	119	16	-4	-6	-1	243	255	8
9	-4	-2	155	162	13	10	0	-2	0	45	1	-2	5	-2	181	173	4	1	12	-2	130	112	16	-3	-6	-1	365	381	4
10	-4	-2	0	30	1	11	0	-2	105	44	22	-1	5	-2	701	664	5	2	12	-2	103	79	18	-2	-6	-1	258	261	4
11	-4	-2	17	53	16	-10	1	-2	15	39	15	0	5	-2	33	28	33	3	12	-2	26	28	25	-1	-6	-1	385	379	3
-9	-3	-2	67	34	67	-9	1	-2	182	156	13	2	5	-2	90	88	8	4	12	-2	103	46	28	0	-6	-1	24	27	24
-8	-3	-2	188	184	13	-8	1	-2	58	35	29	3	5	-2	130	141	4	-4	13	-2	122	79	21	1	-6	-1	135	140	4
-7	-3	-2	95	115	18	-7	1	-2	36	45	35	4	5	-2	259	268	8	-3	13	-2	152	108	16	2	-6	-1	84	78	4
-6	-3	-2	139	139	11	-6	1	-2	193	191	8	5	5	-2	227	225	5	-2	13	-2	24	40	24	3	-6	-1	510	514	5
-5	-3	-2	0	25	1	-5	1	-2	287	287	6	-10	6	-2	70	45	36	-1	13	-2	79	8	30	4	-6	-1	120	119	8
-4	-3	-2	129	135	8	-4	1	-2	470	461	5	-9	6	-2	62	76	37	0	13	-2	127	75	17	5	-6	-1	162	180	9
-3	-3	-2	74	100	6	-3	1	-2	351	355	4	-8	6	-2	34	33	33	1	13	-2	86	45	25	6	-6	-1	64	65	17
-2	-3	-2	634	624	3	-2	1	-2	260	246	2	-7	6	-2	54	75	33	2	13	-2	38	53	37	7	-6	-1	126	114	11
-1	-3	-2	377	374	2	-1	1	-2	267	279	5	-6	6	-2	168	155	9	5	-13	-1	44	19	43	8	-6	-1	104	105	16
0	-3	-2	326	328	4	0	1	-2	707	656	13	-5	6	-2	0	7	1	3	-12	-1	67	68	29	9	-6	-1	200	174	12
1	-3	-2	280	273	4	1	1	-2	1107	1048	4	-4	6	-2	471	461	4	4	-12	-1	69	65	26	10	-6	-1	0	19	1
2	-3	-2	429	425	4	2	1	-2	747	733	2	-3	6	-2	57	49	10	5	-12	-1	73	41	29	-9	-5	-1	82	45	41
3	-3	-2	281	259	5	3	1	-2	459	457	3	-2	6	-2	51	28	19	6	-12	-1	55	37	55	-8	-5	-1	105	118	21
4	-3	-2	433	442	5	4	1	-2	431	420	6	-1	6	-2	64	65	14	1	-11	-1	47	31	47	-7	-5	-1	166	170	11
5	-3	-2	172	161	7	5	1	-2	63	58	7	0	6	-2	532	537	6	2	-11	-1	149	132	9	-6	-5	-1	107	112	15
6	-3	-2	105	121	11	6	1	-2	165	164	7	1	6	-2	98	95	9	3	-11	-1	45	45	45	-5	-5	-1	153	146	9
7	-3	-2	78	69	14	7	1	-2	148	157	9	2	6	-2	440	447	5	4	-11	-1	136	133	11	-4	-5	-1	99	92	11
8	-3	-2	59	76	25	8	1	-2	140	145	12	3	6	-2	99	89	10	5	-11	-1	139	98	12	-3	-5	-1	37	36	20
9	-3	-2	40	25	40	9	1	-2	88	103	20	4	6	-2	184	182	8	6	-11	-1	115	102	19	-2	-5	-1	932	909	10
10	-3	-2	75	92	28	10	1	-2	23	29	22	5	6	-2	85	82	13	7	-11	-1	82	71	32	-1	-5	-1	480	485	3
11	-3	-2	0	25	1	-10	2	-2	118	105	24	-8	7	-2	61	30	33	-1	-10	-1	227	211	7	0	-5	-1	559	575	8
-9	-2	-2	82	29	31	-9	2	-2	41	61	41	-7	7	-2	41	73	41	0	-10	-1	136	120	9	1	-5	-1	51	60	7
-8	-2	-2	200	183	12	-8	2	-2	187	188	10	-6	7	-2	55	39	35	1	-10	-1	167	189	8	2	-5	-1	194	200	5
-7	-2	-2	160	157	12	-7	2	-2	176	157	11	-5	7	-2	157	132	6	2	-10	-1	0	9	1	3	-5	-1	49	63	15
-6	-2	-2	156	149	10	-6	2	-2	114	107	11	-4	7	-2	62	54	13	3	-10	-1	0	12	1	4	-5	-1	421	422	6
-5	-2	-2	179	189	8	-5	2	-2	91	70	11	-3	7	-2	352	340	4	4	-10	-1	180	177	8	5	-5	-1	96	82	10
-4	-2	-2	141	159	8	-3	2	-2	72	59	4	-2	7	-2	81	83	14	5	-10	-1	186	191	11	6	-5	-1	209		

Table B-15, Continued
Observed and Calculated Structure Factors for 1-ferrocenylcarbonyl-2-ferrocenylcyclopentene

h	k	l	10Fo	10Fc	10s	h	k	l	10Fo	10Fc	10s	h	k	l	10Fo	10Fc	10s	h	k	l	10Fo	10Fc	10s	h	k	l	10Fo	10Fc	10s
-2	-3	-1	295	278	7	-1	1	-1	1684	1603	8	5	5	-1	98	83	8	1	13	-1	16	37	16	7	-6	0	160	152	11
-1	-3	-1	372	370	2	0	1	-1	86	107	3	6	5	-1	73	68	14	2	13	-1	0	40	1	8	-6	0	0	62	1
0	-3	-1	235	250	2	1	1	-1	159	167	3	-9	6	-1	105	85	17	4	-12	0	54	19	54	9	-6	0	0	62	1
1	-3	-1	162	165	2	2	1	-1	27	21	20	-8	6	-1	61	44	31	5	-12	0	97	100	20	10	-6	0	0	17	1
3	-3	-1	49	51	9	3	1	-1	595	585	3	-7	6	-1	162	181	9	6	-12	0	47	44	47	-9	-5	0	57	68	57
4	-3	-1	59	48	10	4	1	-1	371	345	3	-6	6	-1	183	192	8	2	-11	0	177	148	9	-8	-5	0	53	20	53
5	-3	-1	232	227	6	5	1	-1	623	597	4	-5	6	-1	85	75	8	3	-11	0	0	41	1	-7	-5	0	117	118	17
6	-3	-1	332	313	7	6	1	-1	99	108	10	-4	6	-1	362	364	4	4	-11	0	91	91	15	-6	-5	0	110	87	13
7	-3	-1	169	156	10	7	1	-1	0	37	1	-3	6	-1	250	250	13	5	-11	0	86	62	18	-5	-5	0	275	285	8
8	-3	-1	180	179	11	8	1	-1	195	203	9	-2	6	-1	571	546	5	6	-11	0	109	82	18	-4	-5	0	64	64	17
9	-3	-1	31	15	30	9	1	-1	75	83	24	-1	6	-1	115	102	8	7	-11	0	0	35	1	-3	-5	0	458	472	6
10	-3	-1	0	31	1	10	1	-1	95	92	23	0	6	-1	61	75	13	0	-10	0	34	35	33	-2	-5	0	363	389	5
11	-3	-1	0	25	1	-10	2	-1	0	31	1	1	6	-1	176	175	7	1	-10	0	303	300	6	-1	-5	0	125	137	5
-10	-2	-1	83	48	48	-9	2	-1	39	9	38	2	6	-1	614	621	5	2	-10	0	56	58	23	0	-5	0	274	282	8
-9	-2	-1	76	67	40	-8	2	-1	156	134	11	3	6	-1	138	129	8	3	-10	0	189	167	9	1	-5	0	537	529	6
-8	-2	-1	111	125	17	-7	2	-1	58	61	22	4	6	-1	420	432	13	4	-10	0	0	17	1	2	-5	0	384	370	5
-7	-2	-1	44	55	44	-6	2	-1	414	412	6	5	6	-1	36	10	29	5	-10	0	35	16	34	3	-5	0	282	286	5
-6	-2	-1	203	209	8	-5	2	-1	66	63	13	-7	7	-1	184	177	9	6	-10	0	75	47	24	4	-5	0	38	39	23
-5	-2	-1	174	170	8	-4	2	-1	244	240	2	-6	7	-1	158	139	9	7	-10	0	146	137	16	5	-5	0	97	101	10
-4	-2	-1	632	615	5	-3	2	-1	268	251	2	-5	7	-1	189	189	13	8	-10	0	37	28	37	6	-5	0	393	387	7
-3	-2	-1	456	456	4	-2	2	-1	287	256	12	-4	7	-1	77	86	9	-7	-9	0	37	48	37	7	-5	0	134	126	10
-2	-2	-1	149	145	3	-1	2	-1	548	543	7	-3	7	-1	256	250	4	-6	-9	0	109	27	20	8	-5	0	200	206	10
-1	-2	-1	906	926	4	0	2	-1	1018	951	4	-2	7	-1	273	254	6	-5	-9	0	46	39	46	9	-5	0	88	60	23
0	-2	-1	981	925	3	1	2	-1	763	768	3	-1	7	-1	283	293	6	-4	-9	0	192	185	11	10	-5	0	49	50	48
1	-2	-1	349	318	3	2	2	-1	48	56	5	0	7	-1	116	115	10	-2	-9	0	217	194	8	-9	-4	0	61	20	60
2	-2	-1	613	600	4	3	2	-1	74	76	8	1	7	-1	131	115	9	-1	-9	0	159	143	8	-8	-4	0	166	161	12
3	-2	-1	267	230	4	4	2	-1	353	355	7	2	7	-1	63	62	17	0	-9	0	45	31	32	-7	-4	0	74	111	24
4	-2	-1	0	44	1	5	2	-1	119	117	9	3	7	-1	139	150	9	1	-9	0	17	6	16	-6	-4	0	100	81	12
5	-2	-1	238	240	5	6	2	-1	213	237	7	4	7	-1	111	85	10	2	-9	0	201	218	7	-5	-4	0	198	203	8
6	-2	-1	0	12	1	7	2	-1	33	58	33	5	7	-1	209	187	9	3	-9	0	44	63	32	-4	-4	0	439	437	6
7	-2	-1	149	159	9	8	2	-1	95	98	15	-5	8	-1	161	154	10	4	-9	0	327	327	7	-3	-4	0	190	189	4
8	-2	-1	0	31	1	9	2	-1	96	94	19	-4	8	-1	66	69	11	5	-9	0	38	33	38	-2	-4	0	366	368	3
9	-2	-1	88	61	21	10	2	-1	31	46	30	-3	8	-1	0	41	1	6	-9	0	8	47	7	-1	-4	0	152	144	4
10	-2	-1	31	29	30	-10	3	-1	100	46	22	7	-9	0	80	58	12	7	-9	0	48	23	48	0	-4	0	377	359	17
11	-2	-1	61	63	61	-9	3	-1	82	94	24	-1	8	-1	206	194	8	8	-9	0	104	66	20	1	-4	0	203	216	5
-10	-1	-1	0	15	1	-8	3	-1	66	61	24	0	8	-1	206	210	8	9	-9	0	81	28	36	2	-4	0	336	341	4
-9	-1	-1	207	160	13	-7	3	-1	108	97	11	1	8	-1	132	103	10	-7	-8	0	138	92	16	3	-4	0	365	351	5
-8	-1	-1	133	108	13	-6	3	-1	103	101	11	2	8	-1	53	50	21	-6	-8	0	12	77	12	4	-4	0	51	32	13
-7	-1	-1	127	120	13	-5	3	-1	390	397	20	3	8	-1	116	103	11	-5	-8	0	62	75	33	5	-4	0	135	139	8
-6	-1	-1	22	34	21	-4	3	-1	129	118	6	4	8	-1	178	170	9	-4	-8	0	168	157	10	6	-4	0	64	64	19
-5	-1	-1	276	277	6	-3	3	-1	181	162	3	5	8	-1	125	114	12	-3	-8	0	55	45	19	7	-4	0	236	237	9
-4	-1	-1	179	202	6	-2	3	-1	354	338	7	-5	9	-1	173	170	10	-2	-8	0	135	129	6	8	-4	0	110	109	17
-3	-1	-1	521	529	4	-1	3	-1	247	254	2	-4	9	-1	188	187	9	-1	-8	0	211	226	15	9	-4	0	86	103	25
-2	-1	-1	216	224	4	0	3	-1	131	132	5	-3	9	-1	64	62	22	0	-8	0	83	86	12	10	-4	0	0	29	1
-1	-1	-1	70	62	3	1	3	-1	75	59	6	-2	9	-1	74	75	20	1	-8	0	79	85	11	-10	-3	0	79	25	44
0	-1	-1	486	491	7	2	3	-1	259	251	4	-1	9	-1	28	59	28	2	-8	0	59	54	14	-9	-3	0	123	104	21
1	-1	-1	909	873	3	3	3	-1	146	161	6	0	9	-1	204	199	9	3	-8	0	175	190	8	-8	-3	0	46	19	45
2	-1	-1	1085	1045	4	4	3	-1	39	42	10	1	9	-1	221	203	8	4	-8	0	107	85	11	-7	-3	0	150	127	14
3	-1	-1	373	378	4	5	3	-1	403	409	3	2	9	-1	68	48	18	5	-8	0	153	121	10	-6	-3	0	69	92	20
4	-1	-1	411	396	5	6	3	-1	70	73	15	3	9	-1	82	45	16	6	-8	0	54	34	31	-5	-3	0	202	209	8
5	-1	-1	174	181	7	7	3	-1	301	317	7	4	9	-1	55	59	34	7	-8	0	106	97	18	-4	-3	0	116	115	9
6	-1	-1	222	217	7	8	3	-1	15	59	15	5	9	-1	166	141	12	8	-8	0	37	37	37	-3	-3	0	557	561	5
7	-1	-1	51	53	24	9	3	-1	0	44	1	-5	10	-1	244	241	10	9	-8	0	162	135	15	-2	-3	0	110	106	4
8	-1	-1	188	197	9	-10	4	-1	138	73	16	-4	10	-1	6	54	6	-8	-7	0	42	26	42	-1	-3	0	284	281	2
9	-1	-1	152	147	11	-9	4	-1	62	81	32	-3	10	-1	86	76	18	-7	-7	0	131	118	17	0	-3	0	403	416	7
10	-1	-1	67	74	33	-8	4	-1	83	73	16	-6	-7	0	97	85	18	-6	-7	0	97	85	18	1	-3	0	351	363	3
11	-1	-1	73	46	42	-7	4	-1	0	34	1	-1	10	-1	94	55	15	-5	-7	0	91	92	17	2	-3	0	362	353	4
-10	0	-1	98	96	26	-6	4	-1	372	394	6	0	10	-1	117	91	14	-4	-7	0	64	69	21	3	-3	0	499	493	4
-9	0	-1	43	68	43	-5	4	-1	326	334	11	1	10	-1	273	247	8	-3	-7	0	173	176	5	4	-3	0	329	338	5

Table B-15, Continued
Observed and Calculated Structure Factors for 1-ferrocenylcarbonyl-2-ferrocenylcyclopentene

h	k	l	IOFo	IOFc	IOs	h	k	l	IOFo	IOFc	IOs	h	k	l	IOFo	IOFc	IOs	h	k	l	IOFo	IOFc	IOs	h	k	l	IOFo	IOFc	IOs
-6	-1	0	19	59	18	-3	3	0	516	493	4	4	8	0	155	157	9	1	-8	1	193	193	10	-10	-3	1	0	23	1
-5	-1	0	313	331	6	-2	3	0	384	353	4	-6	9	0	29	47	28	2	-8	1	60	58	10	-9	-3	1	98	44	24
-4	-1	0	66	59	9	-1	3	0	354	363	4	-5	9	0	82	33	19	3	-8	1	40	41	29	-8	-3	1	0	59	1
-3	-1	0	163	181	5	0	3	0	391	416	4	-4	9	0	342	327	7	4	-8	1	54	69	21	-7	-3	1	308	317	8
-2	-1	0	347	342	4	1	3	0	284	280	4	-3	9	0	82	63	18	5	-8	1	151	154	9	-6	-3	1	68	73	17
-1	-1	0	1021	952	7	2	3	0	107	106	6	-2	9	0	201	218	9	6	-8	1	103	105	14	-5	-3	1	408	409	6
0	-1	0	305	302	3	3	3	0	531	561	4	-1	9	0	37	7	36	7	-8	1	149	140	13	-4	-3	1	24	42	24
1	-1	0	285	250	2	4	3	0	130	115	6	0	9	0	0	31	1	8	-8	1	0	12	1	-3	-3	1	144	161	7
2	-1	0	715	685	4	5	3	0	214	209	4	1	9	0	149	143	11	9	-8	1	0	47	1	-2	-3	1	259	251	3
3	-1	0	448	409	4	6	3	0	79	92	13	2	9	0	209	194	8	-8	-7	1	19	38	18	-1	-3	1	62	58	4
4	-1	0	254	255	5	7	3	0	118	127	12	3	9	0	69	85	19	-7	-7	1	65	33	42	0	-3	1	120	132	3
5	-1	0	587	584	5	8	3	0	41	19	40	4	9	0	194	185	9	-6	-7	1	0	33	1	1	-3	1	238	254	3
6	-1	0	100	89	11	9	3	0	97	104	19	-6	10	0	0	47	1	-5	-7	1	199	187	10	2	-3	1	342	338	4
7	-1	0	32	39	31	10	3	0	64	25	52	-5	10	0	0	16	1	-4	-7	1	81	85	17	3	-3	1	188	162	5
8	-1	0	45	25	45	-10	4	0	0	29	1	-4	10	0	0	17	1	-3	-7	1	145	150	6	4	-3	1	127	118	7
9	-1	0	104	108	17	-9	4	0	69	103	29	-3	10	0	175	167	10	-2	-7	1	76	62	13	5	-3	1	396	397	6
10	-1	0	0	55	1	-8	4	0	117	109	13	-2	10	0	34	58	33	-1	-7	1	129	115	5	6	-3	1	112	101	10
-10	0	0	76	23	36	-7	4	0	244	237	7	-1	10	0	309	300	8	0	-7	1	107	116	5	7	-3	1	101	97	13
-9	0	0	105	104	21	-6	4	0	70	64	12	0	10	0	27	35	27	1	-7	1	283	293	7	8	-3	1	82	61	29
-8	0	0	94	108	19	-5	4	0	139	139	5	1	10	0	0	28	1	2	-7	1	260	254	7	9	-3	1	77	94	22
-7	0	0	0	17	1	-4	4	0	54	32	14	2	10	0	75	55	18	3	-7	1	253	250	6	10	-3	1	71	46	34
-5	0	0	137	156	8	-3	4	0	365	351	9	3	10	0	137	138	12	4	-7	1	86	85	11	-10	-2	1	0	46	1
-4	0	0	304	338	5	-2	4	0	349	341	11	4	10	0	73	66	23	5	-7	1	199	189	8	-9	-2	1	96	94	25
-3	0	0	149	156	6	-1	4	0	208	216	5	-6	11	0	79	82	28	6	-7	1	155	139	10	-8	-2	1	87	98	18
-2	0	0	887	870	4	0	4	0	366	359	4	-5	11	0	0	62	1	7	-7	1	175	177	11	-7	-2	1	68	58	24
-1	0	0	42	35	4	1	4	0	160	144	5	-4	11	0	100	91	17	8	-7	1	132	130	13	-6	-2	1	232	237	8
1	0	0	47	35	4	2	4	0	357	368	4	-3	11	0	44	41	43	9	-7	1	103	103	23	-5	-2	1	103	117	10
2	0	0	909	870	9	3	4	0	173	189	5	-2	11	0	149	148	12	-9	-6	1	0	16	1	-4	-2	1	347	355	5
3	0	0	157	156	2	4	4	0	440	437	13	-1	11	0	60	85	41	-8	-6	1	138	125	17	-3	-2	1	73	76	9
4	0	0	338	338	3	5	4	0	198	203	6	0	11	0	262	232	9	-7	-6	1	95	85	20	-2	-2	1	46	55	13
5	0	0	166	156	3	6	4	0	54	81	19	1	11	0	47	13	47	-6	-6	1	49	73	49	-1	-2	1	772	768	2
6	0	0	311	326	6	7	4	0	119	111	12	2	11	0	53	53	53	-5	-6	1	0	10	1	0	-2	1	1038	951	16
7	0	0	0	17	1	8	4	0	162	161	10	3	11	0	68	50	34	-4	-6	1	396	432	7	1	-2	1	524	543	3
8	0	0	121	108	12	9	4	0	65	20	41	4	11	0	188	160	10	-3	-6	1	142	129	11	2	-2	1	279	256	4
9	0	0	119	104	14	-10	5	0	10	50	9	-5	12	0	120	100	19	-2	-6	1	604	621	3	3	-2	1	275	251	5
10	0	0	21	23	20	-9	5	0	27	60	26	-4	12	0	0	19	1	-1	-6	1	176	175	7	4	-2	1	256	240	5
-10	1	0	63	55	48	-8	5	0	211	206	8	-3	12	0	0	21	1	0	-6	1	61	75	5	5	-2	1	75	63	12
-9	1	0	111	108	16	-7	5	0	156	126	9	-2	12	0	91	99	20	1	-6	1	95	102	5	6	-2	1	432	412	6
-8	1	0	0	25	1	-6	5	0	378	387	6	-1	12	0	174	153	15	2	-6	1	560	546	3	7	-2	1	58	61	26
-7	1	0	0	39	1	-5	5	0	111	101	7	0	12	0	30	56	29	3	-6	1	250	250	5	8	-2	1	105	134	15
-6	1	0	73	89	13	-4	5	0	24	39	23	1	12	0	138	121	14	4	-6	1	360	364	5	9	-2	1	0	9	1
-5	1	0	587	584	4	-3	5	0	288	286	6	2	12	0	0	29	1	5	-6	1	74	75	12	10	-2	1	84	31	27
-4	1	0	252	255	4	-2	5	0	397	370	5	3	12	0	0	37	1	6	-6	1	182	192	10	-10	-1	1	70	92	47
-3	1	0	461	409	11	-1	5	0	562	529	5	-5	13	0	65	46	64	7	-6	1	205	181	10	-9	-1	1	96	83	22
-2	1	0	690	685	10	0	5	0	288	282	5	-4	13	0	103	82	24	8	-6	1	61	44	33	-8	-1	1	96	203	9
-1	1	0	293	250	1	1	5	0	131	137	6	-3	13	0	0	30	1	9	-6	1	76	85	27	-7	-1	1	59	37	25
0	1	0	298	302	2	2	5	0	377	389	5	-2	13	0	83	15	28	10	-6	1	67	52	66	-6	-1	1	102	108	12
1	1	0	1019	952	4	3	5	0	460	472	5	-1	13	0	0	47	1	-9	-5	1	39	87	39	-5	-1	1	623	597	5
2	1	0	350	342	3	4	5	0	55	64	9	0	13	0	0	68	1	-8	-5	1	53	39	52	-4	-1	1	374	345	5
3	1	0	168	181	10	5	5	0	278	285	4	1	13	0	0	41	1	-7	-5	1	187	186	12	-3	-1	1	596	585	4
4	1	0	50	59	7	6	5	0	89	87	13	6	-12	1	0	32	1	-6	-5	1	40	68	39	-2	-1	1	0	21	1
5	1	0	343	331	11	7	5	0	100	118	15	4	-11	1	233	232	8	-5	-5	1	58	83	23	-1	-1	1	166	167	4
6	1	0	48	59	23	-8	6	0	66	63	23	5	-11	1	0	36	1	-4	-5	1	0	4	1	0	-1	1	81	107	2
7	1	0	177	189	8	-7	6	0	178	152	9	-3	-5	1	106	67	20	-3	-5	1	403	419	3	1	-1	1	1692	1603	5
8	1	0	32	43	31	-6	6	0	86	85	13	7	-11	1	95	50	27	-2	-5	1	36	41	36	2	-1	1	28	22	13
9	1	0	47	11	47	-5	6	0	177	183	5	2	-10	1	0	25	1	-1	-5	1	450	467	3	3	-1	1	398	375	3
10	1	0	73	48	33	-4	6	0	171	164	4	3	-10	1	74	76	16	0	-5	1	108	100	4	4	-1	1	138	140	7
5	-1	1	239	241	6	8	3	1	23	39	22	1	9	1	99	101	13	7	-8	2	94	79	18	-4	-3	2	365	370	6
6	-1	1	83	89	11	9	3	1	68	74	32	2	9	1	68	55	21	8	-8	2	148	156	15	-3	-3	2	371	373	5
7	-1	1	204	218																									

Table B-15, Continued
Observed and Calculated Structure Factors for 1-ferrocenylcarbonyl-2-ferrocenylcyclopentene

h	k	l	10Fo	10Fc	10s	h	k	l	10Fo	10Fc	10s	h	k	l	10Fo	10Fc	10s	h	k	l	10Fo	10Fc	10s	h	k	l	10Fo	10Fc	10s	h	k	l	10Fo	10Fc	10s
-2	1	1	1090	1045	12	0	5	1	575	575	5	2	12	1	80	77	26	3	-6	2	37	49	26	9	-2	2	69	61	29	10	-2	2	158	105	15
-1	1	1	912	873	7	1	5	1	479	485	5	3	12	1	151	132	16	4	-6	2	456	461	6	10	-2	2	158	105	15	10	-1	2	38	29	37
0	1	1	491	491	2	2	5	1	906	909	5	-5	13	1	100	19	27	5	-6	2	0	7	1	-10	-1	2	38	29	37	-9	-1	2	46	103	45
1	1	1	69	62	3	3	5	1	26	36	26	-4	13	1	65	84	51	6	-6	2	171	155	9	-8	-1	2	181	145	11	-7	-1	2	168	157	10
2	1	1	217	224	6	4	5	1	106	92	10	-3	13	1	43	22	43	7	-6	2	83	75	16	-6	-1	2	165	164	9	-6	-1	2	435	420	5
3	1	1	535	529	4	5	5	1	143	146	8	-2	13	1	77	105	29	8	-6	2	0	33	1	-5	-1	2	57	58	18	-4	-1	2	279	286	6
4	1	1	186	202	5	6	5	1	112	112	12	-1	13	1	6	69	6	9	-6	2	53	76	53	-4	-1	2	175	191	8	-4	-1	2	39	45	38
5	1	1	269	277	6	7	5	1	168	170	10	0	13	1	65	22	52	10	-6	2	14	45	14	-3	-1	2	464	457	4	-3	-1	2	746	733	4
6	1	1	0	34	1	8	5	1	109	118	17	1	13	1	27	27	26	-7	-5	2	210	209	12	-2	-1	2	1114	1048	4	-1	-1	2	722	657	3
7	1	1	127	120	11	-6	6	1	79	65	10	6	-11	2	72	63	31	-6	-5	2	98	100	15	0	-1	2	274	279	3	2	-1	2	265	246	4
8	1	1	82	108	18	-5	6	1	176	180	5	6	-11	2	130	114	17	-7	-5	2	212	225	9	3	-1	2	359	355	4	4	-1	2	468	461	5
9	1	1	159	160	13	-4	6	1	125	119	7	7	-11	2	112	55	25	-6	-5	2	272	268	7	0	-1	2	279	286	6	5	-1	2	279	286	6
10	1	1	46	15	46	-3	6	1	516	514	3	-6	-10	2	60	76	59	-5	-5	2	212	225	9	6	-1	2	175	191	8	6	-1	2	39	45	38
-11	2	1	105	63	26	-2	6	1	73	78	10	-5	-10	2	71	69	29	-4	-5	2	272	268	7	7	-5	2	222	226	9	-10	0	2	51	45	50
-10	2	1	23	29	22	-1	6	1	138	140	7	-4	-10	2	149	166	13	-3	-5	2	149	141	9	-9	0	2	59	27	10	2	-1	2	503	499	5
-9	2	1	46	61	46	0	6	1	38	27	25	-3	-10	2	41	31	41	-2	-5	2	88	88	4	-7	-4	2	50	38	49	-4	0	2	69	70	10
-8	2	1	59	31	28	1	6	1	392	379	6	3	-10	2	237	228	8	-1	-5	2	559	570	3	-3	0	2	516	505	3	-2	0	2	516	505	3
-7	2	1	151	159	10	2	6	1	260	261	6	4	-10	2	101	98	14	0	-5	2	31	28	18	-4	-4	2	255	274	7	-1	0	2	1712	1658	5
-6	2	1	31	12	30	3	6	1	378	381	6	5	-10	2	72	55	25	1	-5	2	684	664	8	2	-5	2	176	173	5	2	0	2	198	208	4
-5	2	1	240	240	5	4	6	1	250	255	5	6	-10	2	110	79	17	2	-5	2	176	173	5	7	-1	2	39	45	38	6	-1	2	175	191	8
-4	2	1	46	44	12	5	6	1	0	29	1	7	-10	2	144	127	16	3	-5	2	0	16	1	8	-1	2	42	35	42	8	-1	2	42	35	42
-3	2	1	267	230	9	6	6	1	92	69	16	8	-10	2	89	96	31	4	-5	2	54	64	15	9	-1	2	145	156	13	9	-1	2	145	156	13
-2	2	1	630	600	2	7	6	1	93	81	17	-7	-9	2	37	40	37	5	-5	2	288	273	7	10	-1	2	0	39	1	10	-1	2	0	39	1
-1	2	1	355	318	5	-6	7	1	83	100	15	-6	-9	2	56	12	56	6	-5	2	278	277	7	-11	0	2	79	44	46	-11	0	2	79	44	46
0	2	1	988	925	4	-5	7	1	34	51	33	-5	-9	2	113	109	17	7	-5	2	222	226	9	-10	0	2	51	45	50	-10	0	2	51	45	50
1	2	1	905	926	4	-4	7	1	238	247	7	-4	-9	2	0	48	1	8	-5	2	50	53	49	-9	0	2	59	27	10	-9	0	2	59	27	10
2	2	1	153	145	4	-3	7	1	0	10	1	-3	-9	2	165	188	10	9	-5	2	0	35	1	-8	0	2	109	107	14	-8	0	2	109	107	14
3	2	1	457	456	8	-2	7	1	360	362	6	-2	-9	2	35	31	35	10	-5	2	88	64	35	-7	0	2	272	267	8	-7	0	2	272	267	8
4	2	1	609	615	3	-1	7	1	86	81	11	-1	-9	2	129	122	11	-9	-4	2	138	90	19	-6	0	2	74	89	14	-6	0	2	74	89	14
5	2	1	161	170	7	0	7	1	0	39	1	0	-9	2	0	59	1	0	-9	2	0	59	1	-8	-4	2	64	51	38	-5	0	2	503	499	5
6	2	1	197	209	7	1	7	1	65	80	14	1	-9	2	100	115	16	-7	-4	2	50	38	49	-4	0	2	69	70	10	-4	0	2	69	70	10
7	2	1	20	55	20	2	7	1	285	272	6	2	-9	2	132	132	7	2	-9	2	132	132	7	-6	-4	2	224	232	9	-3	0	2	118	84	6
8	2	1	131	125	13	3	7	1	148	141	9	3	-9	2	173	162	9	3	-9	2	173	162	9	-5	-4	2	53	54	29	-2	0	2	516	505	3
9	2	1	24	67	24	4	7	1	176	167	8	4	-9	2	90	80	16	-4	-4	2	255	274	7	-4	-4	2	255	274	7	-1	0	2	1712	1658	5
10	2	1	33	48	33	5	7	1	16	46	16	5	-9	2	50	63	49	-3	-4	2	250	252	6	-3	-4	2	250	252	6	2	0	2	198	208	4
-11	3	1	25	25	25	6	7	1	0	43	1	6	-9	2	22	70	21	-2	-4	2	72	66	6	3	0	2	195	207	5	3	0	2	195	207	5
-10	3	1	0	31	1	-6	8	1	75	56	18	7	-9	2	116	114	19	-1	-4	2	366	349	5	4	0	2	527	551	5	4	0	2	527	551	5
-9	3	1	0	15	1	-5	8	1	135	139	10	8	-9	2	80	102	30	0	-4	2	563	580	4	5	0	2	282	301	6	5	0	2	282	301	6
-8	3	1	167	179	9	-4	8	1	140	129	9	9	-9	2	129	50	19	1	-4	2	45	43	9	6	0	2	154	150	8	6	0	2	154	150	8
-7	3	1	160	156	8	-3	8	1	194	193	8	-8	-8	2	131	85	20	2	-4	2	609	585	4	7	0	2	7	39	7	7	0	2	7	39	7
-6	3	1	313	313	5	-2	8	1	0	30	1	-7	-8	2	26	20	25	3	-4	2	515	469	5	8	0	2	72	46	21	8	0	2	72	46	21
-5	3	1	225	227	4	-1	8	1	334	338	7	-6	-8	2	49	45	49	4	-4	2	217	209	5	9	0	2	39	40	39	9	0	2	39	40	39
-4	3	1	67	49	19	0	8	1	96	79	12	-5	-8	2	54	25	53	5	-4	2	202	203	7	10	0	2	0	32	1	10	0	2	0	32	1
-3	3	1	54	51	6	1	8	1	0	18	1	-4	-8	2	183	184	10	6	-4	2	258	257	7	-11	1	2	60	21	60	-11	1	2	60	21	60
-2	3	1	395	379	5	2	8	1	0	8	1	-3	-8	2	0	36	1	7	-4	2	78	87	18	-10	1	2	139	108	17	-10	1	2	139	108	17
-1	3	1	168	165	4	3	8	1	124	112	11	-2	-8	2	161	183	9	8	-4	2	169	160	10	-9	1	2	47	43	47	-9	1	2	47	43	47
0	3	1	231	250	4	4	8	1	71	47	18	-1	-8	2	54	39	19	9	-4	2	63	53	41	-8	1	2	74	74	19	-8	1	2	74	74	19
1	3	1	376	369	4	-6	9	1	195	189	10	0	-8	2	46	43	14	10	-4	2	68	41	45	-7	1	2	28	21	27	-7	1	2	28	21	27
2	3	1	276	277	4	-5	9	1	75	82	20	1	-8	2	75	77	9	-10	-3	2	125	88	21	-6	1	2	369	372	3	-6	1	2	369	372	3
3	3	1	176	177	3	-4	9	1	46																										

Table B-15, Continued
Observed and Calculated Structure Factors for 1-ferrocenylcarbonyl-2-ferrocenylcyclopentene

h	k	l	10Fo	10Fc	10s	h	k	l	10Fo	10Fc	10s	h	k	l	10Fo	10Fc	10s	h	k	l	10Fo	10Fc	10s	h	k	l	10Fo	10Fc	10s	h	k	l	10Fo	10Fc	10s						
-8	3	2	88	76	15	-2	8	2	52	80	20	-2	-8	3	217	230	8	9	-4	3	0	39	1	-7	1	3	165	170	10	-7	1	3	100	105	10						
-7	3	2	42	68	41	-1	8	2	66	90	18	-1	-8	3	47	22	22	10	-4	3	73	71	41	-6	1	3	100	105	10	-5	1	3	16	42	16						
-6	3	2	129	121	5	0	8	2	149	128	9	0	-8	3	190	194	7	-10	-3	3	99	53	29	-5	1	3	182	189	5	-4	1	3	495	481	4						
-5	3	2	152	161	4	1	8	2	172	181	8	1	-8	3	47	51	15	-9	-3	3	0	16	1	-4	1	3	182	189	5	-2	1	3	526	492	3						
-4	3	2	418	442	5	2	8	2	0	33	1	2	-8	3	75	79	9	-8	-3	3	180	180	12	-3	1	3	175	172	3	-1	1	3	641	635	3						
-3	3	2	287	259	6	3	8	2	100	93	13	3	-8	3	108	89	11	-7	-3	3	175	166	11	-2	1	3	226	212	3	2	1	3	226	212	3						
-2	3	2	457	425	9	4	8	2	71	66	20	4	-8	3	257	243	7	-6	-3	3	149	143	10	2	1	3	641	635	3	2	1	3	291	315	6						
-1	3	2	274	273	4	5	8	2	154	154	12	5	-8	3	39	81	38	-5	-3	3	105	93	12	3	1	3	301	289	3	3	1	3	301	289	3						
0	3	2	335	328	4	-6	9	2	30	72	29	6	-8	3	190	165	10	-4	-3	3	46	36	20	4	1	3	126	124	8	5	1	3	126	124	8						
1	3	2	371	374	4	-5	9	2	120	129	12	7	-8	3	52	73	52	-3	-3	3	192	190	6	3	1	3	31	52	30	6	1	3	31	52	30						
2	3	2	625	624	4	-4	9	2	243	240	8	8	-8	3	0	37	1	-2	-3	3	448	461	4	4	1	3	291	315	6	5	1	3	291	315	6						
3	3	2	94	100	5	-3	9	2	163	153	9	9	-8	3	76	49	36	-1	-3	3	378	392	4	5	1	3	126	124	8	5	1	3	126	124	8						
4	3	2	143	135	4	-2	9	2	161	138	10	-8	-7	3	0	24	1	0	-3	3	479	497	2	6	1	3	31	52	30	7	1	3	31	52	30						
5	3	2	0	25	1	-1	9	2	27	36	26	-7	-7	3	77	109	31	1	-3	3	46	17	8	7	1	3	0	38	1	8	1	3	0	38	1	8					
6	3	2	132	139	10	0	9	2	248	250	8	-6	-7	3	82	76	24	2	-3	3	20	10	20	8	1	3	76	112	21	9	1	3	76	112	21						
7	3	2	98	115	15	1	9	2	64	43	19	-5	-7	3	247	275	8	3	-3	3	0	31	1	9	1	3	27	40	27	9	1	3	27	40	27						
8	3	2	181	184	12	2	9	2	201	193	9	-4	-7	3	112	112	12	4	-3	3	418	419	5	10	1	3	39	23	38	10	1	3	39	23	38						
9	3	2	65	34	45	3	9	2	93	68	16	-3	-7	3	169	171	10	5	-3	3	308	332	6	-11	2	3	42	28	42	-11	2	3	42	28	42						
-10	4	2	103	30	20	-6	10	2	71	60	29	-2	-7	3	148	143	9	6	-3	3	183	175	8	-10	2	3	46	11	46	-10	2	3	46	11	46						
-9	4	2	168	162	11	-5	10	2	80	64	21	-1	-7	3	232	230	6	7	-3	3	68	69	21	-9	2	3	120	129	15	-9	2	3	120	129	15						
-8	4	2	125	106	11	-4	10	2	98	117	16	0	-7	3	198	196	7	8	-3	3	81	83	20	-8	2	3	57	92	35	-8	2	3	57	92	35						
-7	4	2	220	228	7	-3	10	2	104	135	14	1	-7	3	301	319	8	9	-3	3	145	149	15	-6	2	3	71	73	8	-6	2	3	71	73	8						
-6	4	2	139	136	5	-2	10	2	166	155	11	2	-7	3	193	198	6	10	-3	3	44	24	44	-5	2	3	104	93	7	-5	2	3	104	93	7						
-5	4	2	33	30	17	-1	10	2	158	160	11	3	-7	3	134	130	9	-10	-2	3	95	24	27	-4	2	3	218	220	3	-4	2	3	218	220	3						
-4	4	2	47	51	9	0	10	2	0	22	1	4	-7	3	79	73	12	-9	-2	3	95	93	23	-3	2	3	454	488	2	-3	2	3	454	488	2						
-3	4	2	677	658	6	1	10	2	114	104	14	5	-7	3	138	133	11	-8	-2	3	79	75	20	-2	2	3	217	224	2	-2	2	3	217	224	2						
-2	4	2	230	220	5	2	10	2	102	75	16	6	-7	3	76	46	21	-7	-2	3	182	175	11	-1	2	3	594	586	4	-1	2	3	594	586	4						
-1	4	2	465	465	4	3	10	2	189	185	10	7	-7	3	188	201	10	-6	-2	3	145	143	10	0	2	3	60	47	7	0	2	3	60	47	7						
0	4	2	164	167	6	-6	11	2	0	64	1	8	-7	3	0	35	1	-5	-2	3	471	459	6	1	2	3	197	202	4	1	2	3	197	202	4						
1	4	2	54	58	9	-5	11	2	0	46	1	9	-7	3	73	49	36	-4	-2	3	98	106	9	2	2	3	0	15	1	2	2	3	0	15	1	2	2	3	0	15	1
2	4	2	474	474	4	-4	11	2	29	53	28	-9	-6	3	138	117	19	-3	-2	3	248	236	5	3	2	3	801	795	3	3	2	3	801	795	3						
3	4	2	687	705	4	-3	11	2	103	118	17	-8	-6	3	24	51	23	-1	-2	3	496	495	4	4	2	3	173	177	5	4	2	3	173	177	5						
4	4	2	229	238	13	-2	11	2	92	83	20	-7	-6	3	25	51	25	0	-2	3	303	272	2	5	2	3	170	173	9	5	2	3	170	173	9						
5	4	2	112	110	9	-1	11	2	225	232	10	-6	-6	3	87	92	18	1	-2	3	102	95	5	6	2	3	28	32	38	6	2	3	28	32	38						
6	4	2	102	107	13	0	11	2	0	50	1	-5	-6	3	234	253	8	2	-2	3	218	216	4	7	2	3	53	68	25	7	2	3	53	68	25						
7	4	2	106	116	12	1	11	2	0	17	1	-4	-6	3	192	207	9	3	-2	3	274	257	5	8	2	3	52	60	56	8	2	3	52	60	56						
8	4	2	90	96	21	2	11	2	107	75	19	-3	-6	3	191	225	8	4	-2	3	328	317	5	9	2	3	119	147	12	9	2	3	119	147	12						
9	4	2	35	96	35	3	11	2	131	97	15	-2	-6	3	183	181	4	5	-2	3	378	382	6	-10	3	3	60	18	44	-10	3	3	60	18	44						
-8	5	2	229	230	7	-6	12	2	96	93	28	-1	-6	3	114	131	5	6	-2	3	215	230	7	-9	3	3	90	69	20	-9	3	3	90	69	20						
-7	5	2	131	112	9	-5	12	2	46	32	46	0	-6	3	270	289	4	7	-2	3	78	88	16	-8	3	3	170	154	10	-8	3	3	170	154	10						
-6	5	2	185	184	9	-4	12	2	88	39	24	1	-6	3	18	39	17	8	-2	3	141	130	12	-7	3	3	131	105	9	-7	3	3	131	105	9						
-5	5	2	140	135	5	-3	12	2	83	54	22	2	-6	3	582	550	5	9	-2	3	35	13	35	-6	3	3	252	248	5	-6	3	3	252	248	5						
-4	5	2	243	240	7	-2	12	2	81	83	21	3	-6	3	100	91	8	10	-2	3	81	61	30	-5	3	3	109	107	8	-5	3	3	109	107	8						
-3	5	2	17	36	16	-1	12	2	59	82	34	4	-6	3	147	146	9	-10	-1	3	135	108	17	-4	3	3	42	52	20	-4	3	3	42	52	20						
-2	5	2	713	720	5	0	12	2	121	101	16	5	-6	3	159	164	10	-9	-1	3	52	61	52	-3	3	3	70	66	7	-3	3	3	70	66	7						
-1	5	2	157	164	6	1	12	2	65	59	38	6	-6	3	50	47	29	-8	-1	3	72	93	26	-2	3	3	787	783	4	-2	3	3	787	783	4						
0	5	2	315	311	5	2	12	2	0	22	1	7	-6	3	80	67	44	-7	-1	3	92	105	14	-1	3	3	64	59	7	-1	3	3	64	59	7						
1	5	2	157	150	6	3	12	2	0	45	1	8	-6	3	190	157	12	-6	-1	3	366	353	7	-3	3	3	427	422	4	-3	3	3	427	422	4						
2	5	2	181	178	6	-4	13	2	13	14	12	9	-6	3	176	161	8	-5	-1	3	175	161	8	0	3	3	23	1	4	0	3	3	23	1	4						
3	5																																								

Table B-15, Continued
Observed and Calculated Structure Factors for 1-ferrocenylcarbonyl-2-ferrocenylcyclopentene

h	k	l	10Fo	10Fc	10s	h	k	l	10Fo	10Fc	10s	h	k	l	10Fo	10Fc	10s	h	k	l	10Fo	10Fc	10s	h	k	l	10Fo	10Fc	10s
8	5	3	108	100	20	-2	13	3	0	21	1	-9	-5	4	72	20	52	-2	-1	4	485	468	4	8	3	4	131	138	16
-7	6	3	79	97	17	-1	13	3	61	31	42	-8	-5	4	86	73	28	-1	-1	4	74	65	7	9	3	4	0	25	1
-6	6	3	97	105	13	0	13	3	30	33	29	-7	-5	4	94	79	19	1	-1	4	44	28	10	-7	4	4	28	10	27
-5	6	3	153	156	8	-5	-11	4	94	94	26	-6	-5	4	194	172	11	2	-1	4	486	472	4	-6	4	4	73	79	8
-4	6	3	297	290	6	-4	-11	4	0	21	1	-5	-5	4	43	34	43	3	-1	4	195	196	6	-5	4	4	213	207	7
-3	6	3	218	215	6	-3	-11	4	0	43	1	-4	-5	4	34	38	33	4	-1	4	584	575	5	-4	4	4	468	464	3
-2	6	3	108	107	9	-2	-11	4	42	25	42	-3	-5	4	32	28	32	5	-1	4	33	23	33	-3	4	4	465	465	5
-1	6	3	169	164	7	-6	-10	4	46	35	45	-2	-5	4	412	440	5	6	-1	4	101	107	10	-2	4	4	502	493	5
0	6	3	103	96	9	-5	-10	4	90	69	21	-1	-5	4	452	439	5	7	-1	4	0	12	1	-1	4	4	118	106	7
1	6	3	323	331	6	-4	-10	4	102	102	15	0	-5	4	567	581	12	8	-1	4	75	98	24	0	4	4	32	17	26
2	6	3	250	245	6	-3	-10	4	34	33	33	1	-5	4	356	332	3	9	-1	4	83	94	25	1	4	4	399	391	5
3	6	3	277	288	6	-2	-10	4	63	54	25	2	-5	4	85	75	8	-11	0	4	142	27	23	2	4	4	347	348	5
5	6	3	83	93	18	-1	-10	4	110	95	13	3	-5	4	10	23	10	-10	0	4	52	52	51	3	4	4	385	381	5
6	6	3	0	22	1	0	-10	4	203	236	10	4	-5	4	292	291	6	-9	0	4	161	158	15	4	4	4	60	37	18
7	6	3	114	120	18	1	-10	4	108	114	12	5	-5	4	206	207	8	-8	0	4	42	75	41	5	4	4	104	88	14
8	6	3	0	16	1	2	-10	4	177	191	11	6	-5	4	160	148	10	-7	0	4	211	204	8	6	4	4	54	51	36
-7	7	3	23	58	22	7	-10	4	43	39	43	7	-5	4	79	73	18	-6	0	4	229	228	8	7	4	4	152	159	13
-6	7	3	0	22	1	-7	-9	4	0	52	1	8	-5	4	24	22	23	-5	0	4	249	239	7	8	4	4	45	64	45
-5	7	3	154	154	9	-6	-9	4	33	31	33	9	-5	4	61	75	49	-4	0	4	90	99	9	-7	5	4	289	313	6
-4	7	3	156	170	8	-5	-9	4	115	128	16	-10	-4	4	0	45	1	-3	0	4	399	369	4	-6	5	4	108	106	10
-3	7	3	227	220	7	-4	-9	4	145	146	15	-9	-4	4	0	10	1	-2	0	4	203	194	5	-5	5	4	0	20	1
-2	7	3	173	188	7	-3	-9	4	103	90	14	-8	-4	4	84	75	27	-1	0	4	660	650	4	-4	5	4	161	169	7
-1	7	3	43	36	19	-2	-9	4	113	120	12	-7	-4	4	185	181	11	2	0	4	0	14	1	-3	5	4	520	528	5
0	7	3	135	139	9	-1	-9	4	53	57	25	-6	-4	4	24	30	23	4	0	4	31	10	31	-2	5	4	211	224	6
1	7	3	178	177	7	0	-9	4	120	119	10	-5	-4	4	307	311	7	5	0	4	194	213	7	-1	5	4	224	224	6
2	7	3	107	102	11	1	-9	4	166	179	10	-4	-4	4	0	37	1	6	0	4	15	25	14	0	5	4	0	25	1
3	7	3	195	197	7	2	-9	4	69	89	18	-3	-4	4	210	207	7	7	0	4	42	29	42	1	5	4	48	60	15
5	7	3	51	33	50	3	-9	4	171	167	10	-2	-4	4	87	115	11	8	0	4	83	53	21	2	5	4	254	246	5
6	7	3	48	64	48	4	-9	4	34	27	33	-1	-4	4	573	591	5	9	0	4	98	90	19	3	5	4	205	202	6
7	7	3	40	43	39	5	-9	4	130	116	13	0	-4	4	285	314	3	-11	1	4	0	74	1	5	5	4	57	21	33
-7	8	3	28	61	28	6	-9	4	56	59	55	1	-4	4	534	517	3	-10	1	4	46	39	45	6	5	4	79	52	20
-6	8	3	76	46	20	7	-9	4	221	204	11	2	-4	4	251	247	5	-9	1	4	98	9	16	7	5	4	54	61	53
-5	8	3	26	45	26	8	-9	4	71	5	45	3	-4	4	140	126	8	-8	1	4	125	118	13	8	5	4	48	88	48
-4	8	3	89	83	12	-7	-8	4	0	41	1	4	-4	4	0	33	1	-7	1	4	187	187	8	-7	6	4	49	68	45
-3	8	3	215	222	7	-6	-8	4	0	35	1	5	-4	4	164	166	8	-6	1	4	161	148	9	-6	6	4	100	91	12
-2	8	3	190	193	8	-5	-8	4	68	89	24	6	-4	4	189	186	9	-5	1	4	248	239	6	-5	6	4	145	131	8
-1	8	3	193	203	8	-4	-8	4	178	185	11	7	-4	4	147	153	12	-4	1	4	166	153	7	-4	6	4	209	196	7
0	8	3	104	96	11	-3	-8	4	34	40	33	8	-4	4	95	65	19	-3	1	4	208	190	5	-3	6	4	135	144	8
1	8	3	124	102	10	-2	-8	4	99	90	12	9	-4	4	12	51	12	-2	1	4	312	314	3	-2	6	4	453	445	6
2	8	3	100	103	12	-1	-8	4	47	39	30	-10	-3	4	10	70	10	-1	1	4	156	157	4	-1	6	4	207	203	6
3	8	3	115	87	12	0	-8	4	46	52	28	-9	-3	4	39	29	38	1	1	4	147	151	4	0	6	4	185	195	7
5	8	3	90	87	19	1	-8	4	104	114	11	-8	-3	4	72	83	27	2	1	4	145	149	4	1	6	4	13	32	12
6	8	3	40	24	39	2	-8	4	262	258	7	-7	-3	4	52	60	48	3	1	4	12	36	12	2	6	4	189	190	7
-7	9	3	119	134	15	3	-8	4	93	91	8	-6	-3	4	150	147	11	4	1	4	494	480	5	3	6	4	61	55	19
-6	9	3	0	28	1	4	-8	4	122	119	11	-5	-3	4	0	31	1	5	1	4	50	48	20	5	6	4	155	143	11
-5	9	3	145	126	10	5	-8	4	34	33	33	-4	-3	4	340	367	6	6	1	4	260	281	7	6	6	4	42	61	41
-4	9	3	70	77	19	6	-8	4	104	86	15	-3	-3	4	103	99	9	7	1	4	60	11	28	7	6	4	21	49	21
-3	9	3	120	94	10	7	-8	4	113	108	19	-2	-3	4	119	122	8	8	1	4	50	10	49	8	6	4	69	30	50
-2	9	3	185	210	9	-7	-9	5	35	23	34	-9	-4	5	50	62	50	-1	0	5	35	35	16	-2	5	5	37	43	24
-1	9	3	81	71	15	-6	-9	5	0	43	1	-8	-4	5	68	41	34	2	0	5	435	436	4	-1	5	5	349	357	5
0	9	3	76	91	16	-5	-9	5	39	26	38	-7	-4	5	84	62	23	3	0	5	350	354	12	0	5	5	129	131	8
1	9	3	56	67	20	-4	-9	5	108	115	16	-6	-4	5	54	48	39	4	0	5	185	176	8	1	5	5	206	215	6
2	9	3	42	24	33	-3	-9	5	127	115	13	-5	-4	5	118	118	13	5	0	5	133	115	9	2	5	5	80	78	12
-2	7	4	0	30	1	-2	-9	5	132	144	12	-4	-4	5	103	93	11	6	0	5	61	54	23	3	5	5	157	170	8
-1	7	4	231	235	7	-1	-9	5	52	77	31	-3	-4	5	436	466	6	7	0	5	240	238	9	5	5	5	183	177	11
0	7	4	79	93	10	0	-9	5	102	101	10	-2	-4	5	170	176	8	8	0	5	0	19	1	6	5	5	153	124	13
1	7	4	214	203	7	1	-9	5	0	15	1	-1	-4	5	463	470	5	9	0	5	0	22	1	7	5	5	92	79	24
2	7	4	134	109	9	2	-9	5	170	186	10	0	-4	5	0	35	1	-11	1	5	23	82	22	8	5	5	33	41	33
3	7	4	123	113	10	3	-9	5	169	171	10	1	-4	5	275	285	4	-10	1	5	77	61	33	-7	6	5	51	92	35
5	7	4	156	153	12	4</																							

Table B-15, Continued
Observed and Calculated Structure Factors for 1-ferrocenylcarbonyl-2-ferrocenylcyclopentene

h	k	l	10Fo	10Fc	10s	h	k	l	10Fo	10Fc	10s	h	k	l	10Fo	10Fc	10s	h	k	l	10Fo	10Fc	10s	h	k	l	10Fo	10Fc	10s
-4	10	4	217	233	9	3	-7	5	35	36	34	-7	-2	5	206	195	10	3	2	5	352	348	4	-3	8	5	35	37	34
-3	10	4	0	7	1	4	-7	5	80	81	16	-6	-2	5	206	207	10	4	2	5	108	113	10	-2	8	5	161	165	9
-2	10	4	126	147	13	5	-7	5	101	94	13	-5	-2	5	204	208	8	5	2	5	68	54	16	-1	8	5	124	126	10
-1	10	4	63	42	27	6	-7	5	186	164	10	-4	-2	5	195	190	7	6	2	5	0	37	1	0	8	5	73	84	15
0	10	4	106	114	14	7	-7	5	151	135	15	-3	-2	5	518	530	5	7	2	5	68	82	27	1	8	5	46	35	42
1	10	4	0	33	1	8	-7	5	67	15	48	-2	-2	5	239	255	5	8	2	5	94	105	24	2	8	5	252	249	8
2	10	4	195	199	10	9	-7	5	44	43	44	0	-2	5	146	155	4	9	2	5	17	60	16	5	8	5	84	24	25
3	10	4	0	42	1	-9	-6	5	105	71	33	1	-2	5	188	181	5	-8	3	5	0	40	1	6	8	5	15	56	14
-7	11	4	89	49	27	-8	-6	5	79	39	39	2	-2	5	123	114	6	-7	3	5	231	224	4	-7	9	5	76	74	27
-6	11	4	96	93	21	-7	-6	5	99	70	23	3	-2	5	226	222	6	-6	3	5	0	29	1	-6	9	5	48	40	47
-5	11	4	27	28	27	-6	-6	5	0	17	1	4	-2	5	35	37	35	-5	3	5	40	16	16	-5	9	5	0	13	1
-4	11	4	49	61	48	-5	-6	5	292	308	9	5	-2	5	275	274	6	-4	3	5	86	78	11	-4	9	5	46	40	46
-3	11	4	121	121	14	-4	-6	5	8	10	8	6	-2	5	32	38	32	-3	3	5	570	546	12	-3	9	5	240	248	8
-2	11	4	75	84	25	-3	-6	5	137	143	10	7	-2	5	58	55	28	-2	3	5	311	325	5	-2	9	5	106	81	12
-1	11	4	88	85	19	-2	-6	5	84	98	13	8	-2	5	46	27	46	-1	3	5	483	478	5	-1	9	5	172	181	9
0	11	4	65	21	31	-1	-6	5	215	236	7	9	-2	5	55	75	54	0	3	5	88	95	8	0	9	5	99	110	13
1	11	4	50	26	50	0	-6	5	137	141	8	-10	-1	5	0	52	1	1	3	5	0	16	1	1	9	5	0	15	1
2	11	4	0	2	1	1	-6	5	338	343	20	-9	-1	5	123	111	16	2	3	5	165	161	6	2	9	5	0	15	1
-6	12	4	0	39	1	2	-6	5	138	147	8	-8	-1	5	166	146	12	3	3	5	295	310	4	5	9	5	90	117	28
-5	12	4	84	46	29	3	-6	5	198	191	7	-7	-1	5	116	113	13	4	3	5	231	230	7	-7	10	5	129	104	14
-4	12	4	41	49	41	4	-6	5	166	159	8	-6	-1	5	253	246	8	5	3	5	153	154	9	-6	10	5	86	110	21
-3	12	4	122	61	16	5	-6	5	19	48	18	-5	-1	5	399	373	6	6	3	5	75	104	22	-5	10	5	125	132	13
-2	12	4	132	122	17	6	-6	5	171	177	10	-4	-1	5	259	251	7	7	3	5	0	23	1	-4	10	5	56	36	27
-1	12	4	84	50	25	7	-6	5	168	155	12	-3	-1	5	309	279	5	8	3	5	97	70	23	-3	10	5	66	87	22
0	12	4	24	56	23	8	-6	5	95	97	21	-2	-1	5	259	268	5	-7	4	5	115	131	10	-2	10	5	180	167	10
1	12	4	55	42	55	9	-6	5	0	49	1	-1	-1	5	73	63	8	-6	4	5	405	409	6	-1	10	5	150	135	13
2	12	4	73	51	40	-9	-5	5	65	42	65	-1	-1	5	0	29	1	-5	4	5	50	45	25	0	10	5	110	92	15
-5	-11	5	64	37	64	-8	-5	5	128	120	19	2	-1	5	236	240	4	-4	4	5	29	36	28	1	10	5	66	27	28
-4	-11	5	82	100	33	-7	-5	5	120	105	18	3	-1	5	49	23	14	-3	4	5	169	187	6	2	10	5	89	24	19
-3	-11	5	0	84	1	-6	-5	5	74	68	22	4	-1	5	308	313	6	-2	4	5	567	566	5	-7	11	5	88	30	28
-2	-11	5	48	73	47	-5	-5	5	82	88	19	5	-1	5	295	294	8	-1	4	5	242	252	5	-6	11	5	67	83	37
-1	-11	5	42	71	41	-4	-5	5	225	232	7	6	-1	5	295	294	8	0	4	5	236	238	5	-5	11	5	36	55	36
0	-11	5	100	82	16	-3	-5	5	74	70	15	7	-1	5	0	35	1	1	4	5	125	118	8	-4	11	5	38	46	38
1	-11	5	185	196	11	-2	-5	5	216	227	7	8	-1	5	72	80	25	2	4	5	44	46	19	-3	11	5	24	46	23
-6	-10	5	0	40	1	-1	-5	5	0	29	1	9	-1	5	0	19	1	3	4	5	66	71	12	-2	11	5	101	86	15
-5	-10	5	35	20	35	0	-5	5	336	329	2	-11	0	5	107	52	29	4	4	5	123	122	11	-1	11	5	151	132	13
-4	-10	5	71	96	28	1	-5	5	228	218	4	-10	0	5	123	102	17	5	4	5	159	172	11	0	11	5	58	74	42
-3	-10	5	122	139	14	2	-5	5	563	547	4	-9	0	5	47	49	46	6	4	5	159	162	11	1	11	5	76	80	25
-2	-10	5	175	156	11	3	-5	5	165	170	7	-8	0	5	0	18	1	7	4	5	68	58	31	2	11	5	54	13	54
-1	-10	5	177	186	9	4	-5	5	170	164	9	-7	0	5	107	114	13	8	4	5	0	23	1	-5	12	5	41	74	41
0	-10	5	77	77	20	5	-5	5	94	84	14	-6	0	5	223	210	7	-7	5	5	147	148	11	-4	12	5	60	14	54
1	-10	5	76	81	21	6	-5	5	69	73	22	-5	0	5	325	311	6	-6	5	5	35	77	34	-3	12	5	71	10	37
2	-10	5	191	191	11	7	-5	5	93	76	18	-4	0	5	225	236	6	-5	5	5	217	231	6	-2	12	5	0	14	1
3	-10	5	98	101	19	8	-5	5	131	144	13	-3	0	5	73	75	11	-4	5	5	108	101	9	-1	12	5	46	45	45
4	-10	5	144	122	12	9	-5	5	92	48	26	-2	0	5	274	248	4	-3	5	5	29	13	28	0	12	5	74	73	31
1	12	5	93	57	26	-3	-5	6	0	12	1	6	-1	6	83	81	17	8	4	6	46	84	46	-2	-12	7	0	22	1
-3	-12	6	133	91	18	-2	-5	6	391	401	6	7	-1	6	67	85	26	-7	5	6	27	58	26	-1	-12	7	71	49	37
-2	-12	6	58	56	57	-1	-5	6	197	203	8	8	-1	6	191	185	11	-6	5	6	90	96	11	0	-12	7	86	78	30
-4	-11	6	45	27	44	0	-5	6	377	368	6	9	-1	6	4	49	4	-5	5	6	188	200	7	-4	-11	7	89	126	27
-3	-11	6	86	18	23	1	-5	6	133	135	7	-10	0	6	83	90	32	-4	5	6	62	77	13	-3	-11	7	0	21	1
-2	-11	6	104	92	19	2	-5	6	174	173	6	-9	0	6	133	112	14	-3	5	6	383	409	6	-2	-11	7	0	50	1
-1	-11	6	120	119	15	3	-5	6	53	56	18	-8	0	6	203	189	11	-2	5	6	73	56	13	-1	-11	7	0	8	1
0	-11	6	101	101	18	4	-5	6	368	359	6	-7	0	6	63	48	24	-1	5	6	18	31	18	0	-11	7	117	122	17
1	-11	6	51	40	51	5	-5	6	55	17	25	-6	0	6	283	261	8	0	5	6	113	117	8	1	-11	7	72	90	34
2	-11	6	57	75	56	6	-5	6	160	137	11	-5	0	6	164	158	8	1	5	6	285	274	6	2	-11	7	109	123	18
-6	-10	6	0	30	1	7	-5	6	0	46	1	-4	0	6	303	298	6	2	5	6	42	54	38	3	-11	7	62	36	57
-5	-10	6	128	107	16	8	-5	6	24	58	24	-3	0	6	275	267	5	5	5	6	76	51	27	4	-11	7	30	57	30
-4	-10	6	0	22	1	9	-5	6	26	23	26	-2	0	6	445	432	5	6	5	6	0	18	1	-5	-10	7	67	56	38
-3	-10	6	27	69	26	-9	-4	6	84	11	39	-1	0	6	420	417	4	7	5	6	113	101	24	-4	-10	7	0	44	1

Table B-15, Continued
Observed and Calculated Structure Factors for 1-ferrocenylcarbonyl-2-ferrocenylcyclopentene

h	k	l	10Fo	10Fc	10s	h	k	l	10Fo	10Fc	10s	h	k	l	10Fo	10Fc	10s	h	k	l	10Fo	10Fc	10s	h	k	l	10Fo	10Fc	10s
7	-8	6	207	208	12	3	-3	6	0	22	1	-3	2	6	185	160	5	-4	8	6	0	29	1	-8	-7	7	40	60	40
8	-8	6	73	64	47	4	-3	6	112	104	9	-2	2	6	325	339	4	-3	8	6	76	34	17	-7	-7	7	90	60	27
-8	-7	6	116	111	24	5	-3	6	89	80	12	-1	2	6	329	320	3	-2	8	6	88	108	12	-6	-7	7	147	128	14
-7	-7	6	74	78	44	6	-3	6	231	241	8	0	2	6	554	560	5	-1	8	6	81	104	14	-5	-7	7	109	111	18
-6	-7	6	34	33	33	7	-3	6	53	15	41	1	2	6	184	185	5	0	8	6	206	188	8	-4	-7	7	0	36	1
-5	-7	6	70	30	26	8	-3	6	88	98	19	2	2	6	148	158	6	1	8	6	101	86	12	-3	-7	7	52	17	28
-4	-7	6	208	239	9	9	-3	6	0	14	1	3	2	6	113	105	7	2	8	6	73	48	20	-2	-7	7	204	211	9
-3	-7	6	83	71	16	-10	-2	6	153	122	16	4	2	6	263	254	8	5	8	6	80	69	30	-1	-7	7	168	183	10
-2	-7	6	196	200	9	-9	-2	6	79	54	30	5	2	6	49	62	42	-8	9	6	87	24	30	0	-7	7	177	172	10
-1	-7	6	0	12	1	-8	-2	6	158	152	14	6	2	6	284	274	8	-7	9	6	121	115	17	1	-7	7	86	88	15
0	-7	6	46	52	46	-7	-2	6	90	97	19	7	2	6	128	123	14	-6	9	6	137	112	13	2	-7	7	77	69	21
1	-7	6	98	97	15	-6	-2	6	0	68	1	8	2	6	77	20	38	-5	9	6	204	217	9	5	-7	7	59	51	31
2	-7	6	218	226	10	-5	-2	6	343	335	7	-7	3	6	167	186	8	-4	9	6	156	138	11	6	-7	7	192	198	11
4	-7	6	210	183	8	-4	-2	6	188	187	8	-6	3	6	66	76	15	-3	9	6	62	8	21	7	-7	7	0	23	1
5	-7	6	66	13	23	-3	-2	6	250	243	6	-5	3	6	461	463	3	-2	9	6	27	25	27	8	-7	7	0	35	1
6	-7	6	66	50	31	-2	-2	6	124	122	9	-4	3	6	107	95	5	-1	9	6	147	142	11	-8	-6	7	87	74	37
7	-7	6	29	6	28	-1	-2	6	208	203	6	-3	3	6	251	247	11	0	9	6	154	146	11	-7	-6	7	115	125	19
8	-7	6	141	143	18	0	-2	6	276	257	4	-2	3	6	145	138	6	1	9	6	152	138	11	-6	-6	7	170	160	15
-8	-6	6	60	9	60	1	-2	6	355	338	4	-1	3	6	344	350	5	2	9	6	25	70	24	-5	-6	7	175	174	12
-7	-6	6	171	169	15	2	-2	6	237	240	5	0	3	6	0	31	1	-7	10	6	70	29	32	-4	-6	7	94	93	15
-6	-6	6	70	80	23	3	-2	6	233	243	5	1	3	6	363	370	5	-6	10	6	55	34	54	-3	-6	7	122	139	10
-5	-6	6	79	49	21	4	-2	6	78	82	11	2	3	6	99	94	7	-5	10	6	103	119	16	-2	-6	7	0	30	1
-4	-6	6	69	63	17	5	-2	6	49	55	28	3	3	6	49	42	18	-4	10	6	68	81	21	-1	-6	7	209	212	8
-3	-6	6	248	253	7	6	-2	6	152	125	10	4	3	6	43	19	43	-3	10	6	73	75	18	0	-6	7	39	49	38
-2	-6	6	99	84	12	7	-2	6	215	236	9	5	3	6	135	132	12	-2	10	6	0	22	1	1	-6	7	284	292	7
-1	-6	6	315	323	7	8	-2	6	0	9	1	6	3	6	0	54	1	-1	10	6	0	21	1	3	-6	7	61	67	15
0	-6	6	92	80	10	9	-2	6	38	56	38	7	3	6	169	157	13	0	10	6	92	86	17	4	-6	7	0	40	1
1	-6	6	0	36	1	-10	-1	6	0	56	1	8	3	6	68	42	54	1	10	6	90	103	19	5	-6	7	169	160	10
2	-6	6	36	44	35	-7	-4	6	164	158	12	-7	4	6	118	93	14	2	10	6	87	74	23	6	-6	7	53	40	53
3	-6	6	312	316	6	-8	-1	6	31	77	31	-6	4	6	161	161	8	-6	11	6	48	7	47	7	-6	7	127	114	15
4	-6	6	63	80	17	-7	-1	6	109	108	13	-5	4	6	131	119	9	-5	11	6	80	62	21	8	-6	7	0	13	1
5	-6	6	119	116	10	-6	-1	6	56	35	27	-4	4	6	378	364	6	-4	11	6	82	122	21	-9	-5	7	0	61	1
6	-6	6	79	64	17	-5	-1	6	233	210	9	-3	4	6	107	103	9	-3	11	6	40	15	39	-8	-5	7	0	24	1
7	-6	6	115	103	14	-4	-1	6	289	285	6	-2	4	6	177	173	7	-2	11	6	59	53	35	-7	-5	7	0	42	1
8	-6	6	0	33	1	-3	-1	6	360	366	5	-1	4	6	194	195	6	-1	11	6	44	7	44	-6	-5	7	61	41	44
9	-6	6	103	85	26	-2	-1	6	34	27	34	0	4	6	371	353	5	0	11	6	0	41	1	-5	-5	7	203	192	9
-9	-5	6	0	44	1	-1	-1	6	56	55	10	1	4	6	135	125	8	1	11	6	76	27	33	-4	-5	7	67	57	21
-8	-5	6	89	101	27	1	-1	6	438	446	4	2	4	6	326	305	6	-4	12	6	0	9	1	-3	-5	7	163	159	9
-7	-5	6	146	149	16	2	-1	6	503	510	5	4	4	6	66	36	23	-3	12	6	122	78	17	-2	-5	7	31	43	31
-6	-5	6	123	126	11	3	-1	6	213	214	7	5	4	6	137	117	13	-2	12	6	80	50	26	-1	-5	7	225	226	7
-5	-5	6	76	74	19	4	-1	6	197	212	7	6	4	6	145	155	13	-1	12	6	26	44	26	0	-5	7	241	225	7
-4	-5	6	0	13	1	5	-1	6	79	76	15	7	4	6	77	41	29	0	12	6	32	42	32	1	-5	7	136	122	11
2	-5	7	131	131	8	-4	0	7	119	100	9	-8	6	7	91	69	18	-5	-10	8	98	82	32	-3	-3	8	32	31	32
3	-5	7	94	90	10	-3	0	7	0	23	1	-7	6	7	103	112	15	-6	-9	8	24	26	24	-2	-3	8	37	49	37
4	-5	7	154	141	9	-2	0	7	52	68	16	-6	6	7	60	30	28	-5	-9	8	74	74	36	-1	-3	8	364	375	6
5	-5	7	118	118	11	-1	0	7	37	24	20	-5	6	7	98	113	14	-4	-9	8	90	7	20	0	-3	8	51	42	10
6	-5	7	196	209	11	2	0	7	322	323	5	-4	6	7	134	126	10	-3	-9	8	0	37	1	1	-3	8	312	320	5
7	-5	7	50	69	49	3	0	7	89	83	12	-3	6	7	67	52	15	-2	-9	8	44	21	44	2	-3	8	156	164	8
8	-5	7	82	108	33	4	0	7	161	157	10	-2	6	7	78	65	12	-1	-9	8	133	146	14	3	-3	8	41	22	33
-9	-4	7	0	35	1	5	0	7	81	96	16	-1	6	7	210	209	7	0	-9	8	107	85	17	4	-3	8	72	64	16
-8	-4	7	110	102	21	6	0	7	224	250	8	0	6	7	207	210	7	1	-9	8	60	84	35	5	-3	8	144	142	10
-7	-4	7	117	140	17	7	0	7	44	66	43	1	6	7	117	101	9	2	-9	8	0	47	1	6	-3	8	146	142	12
-6	-4	7	153	151	14	8	0	7	0	10	1	2	6	7	80	88	14	3	-9	8	91	86	20	7	-3	8	30	45	29
-5	-4	7	184	196	10	-9	1	7	86	82	24	5	6	7	78	63	28	4	-9	8	115	114	17	8	-3	8	63	26	62
-4	-4	7	210	221	9	-8	1	7	80	71	21	6	6	7	74	94	38	-7	-8	8	63	59	62	-10	-2	8	89	69	36
-3	-4	7	184	200	9	-7	1	7	65	39	23	-8	7	7	7	36	7	-6	-8	8	99	85	26	-9	-2	8	61	95	61
-2	-4	7	355	362	6	-6	1	7	0	39	1	-7	7	7	98	40	16	-5	-8	8	77	71	30	-8	-2	8	74	31	31
-1	-4	7	57	56	16	-5	1	7	341	338	6	-6	7	7	128	127	14	-4	-8	8	138	112	14	-7	-2	8	75	54	24
0	-4	7	179	171	8	-4	1	7	234	219	6	-5	7	7	0	26	1	-3	-8	8	44	30	43	-6	-2	8	131	105	14
1	-4	7	305	316	4	-3	1	7	161																				

Table B-15, Continued
Observed and Calculated Structure Factors for 1-ferrocenylcarbonyl-2-ferrocenylcyclopentene

h	k	l	10Fo	10Fc	10s	h	k	l	10Fo	10Fc	10s	h	k	l	10Fo	10Fc	10s	h	k	l	10Fo	10Fc	10s	h	k	l	10Fo	10Fc	10s	
-6	-2	7	226	211	8	-3	3	7	482	484	5	-6	10	7	38	65	38	-8	-5	8	0	49	1	8	-1	8	39	22	39	
-5	-2	7	162	145	11	-2	3	7	234	227	7	-5	10	7	84	36	24	-7	-5	8	131	153	16	-10	0	8	81	112	31	
-4	-2	7	208	209	8	-1	3	7	297	293	7	-4	10	7	91	65	17	-6	-5	8	56	79	55	-9	0	8	118	89	18	
-3	-2	7	284	309	7	0	3	7	109	105	8	-3	10	7	134	124	12	-5	-5	8	40	25	40	-8	0	8	172	150	12	
-2	-2	7	491	486	6	1	3	7	23	28	22	-2	10	7	45	27	45	-4	-5	8	114	117	14	-7	0	8	163	144	13	
-1	-2	7	255	252	6	2	3	7	115	109	8	-1	10	7	136	134	12	-3	-5	8	182	183	9	-6	0	8	167	137	10	
0	-2	7	118	115	5	4	3	7	95	91	13	0	10	7	0	12	1	-2	-5	8	77	66	15	-5	0	8	0	41	1	
1	-2	7	66	57	8	5	3	7	180	150	12	1	10	7	41	29	40	-1	-5	8	253	250	8	-4	0	8	226	229	8	
2	-2	7	209	211	6	6	3	7	26	21	26	0	-12	8	94	17	29	0	-5	8	99	87	12	-3	0	8	304	308	6	
3	-2	7	266	273	6	7	3	7	86	57	29	-5	11	7	0	26	1	1	-5	8	65	37	24	-2	0	8	264	261	6	
4	-2	7	185	174	8	-8	4	7	125	121	16	-4	11	7	54	40	53	3	-5	8	289	287	6	-1	0	8	106	89	8	
5	-2	7	256	266	7	-7	4	7	251	267	8	-3	11	7	19	18	18	4	-5	8	161	155	9	2	0	8	288	294	6	
6	-2	7	85	80	14	-6	4	7	66	77	19	-2	11	7	121	81	16	5	-5	8	86	78	16	3	0	8	90	91	14	
7	-2	7	0	37	1	-5	4	7	88	88	12	-1	11	7	73	31	28	6	-5	8	74	70	23	4	0	8	67	54	21	
8	-2	7	5	31	4	-4	4	7	145	133	8	0	11	7	86	50	24	7	-5	8	51	58	51	5	0	8	0	13	1	
-10	-1	7	62	92	62	-3	4	7	27	37	27	8	1	11	7	71	33	41	8	-5	8	0	29	1	6	0	8	142	143	13
-9	-1	7	69	81	40	-2	4	7	292	298	6	-1	-12	8	110	56	22	-9	-4	8	0	33	1	7	0	8	45	26	45	
-8	-1	7	145	117	13	-1	4	7	85	86	11	0	-12	8	94	17	29	-8	-4	8	103	123	23	8	0	8	9	76	8	
-7	-1	7	186	163	11	0	4	7	41	38	23	1	-12	8	56	58	55	-7	-4	8	76	99	27	-8	1	8	55	53	55	
-6	-1	7	143	124	11	1	4	7	89	80	10	2	-12	8	0	16	1	-6	-4	8	79	91	23	-7	1	8	32	25	32	
-5	-1	7	375	360	7	2	4	7	108	98	10	-4	-11	8	71	66	39	-5	-4	8	0	38	1	-6	1	8	207	172	9	
-4	-1	7	48	33	24	4	4	7	202	191	10	-3	-11	8	66	67	65	-4	-4	8	87	95	16	-5	1	8	258	242	8	
-3	-1	7	172	168	8	5	4	7	15	23	14	-2	-11	8	78	66	30	-3	-4	8	75	67	20	-4	1	8	160	147	8	
-2	-1	7	101	97	9	6	4	7	139	146	16	-1	-11	8	33	7	33	-2	-4	8	381	378	7	-3	1	8	222	234	7	
-1	-1	7	454	468	5	7	4	7	72	32	41	0	-11	8	0	18	1	-1	-4	8	46	45	24	-2	1	8	208	204	6	
1	-1	7	276	270	5	-8	5	7	69	58	24	1	-11	8	95	12	26	0	-4	8	167	172	9	-1	1	8	288	288	5	
2	-1	7	64	53	13	-7	5	7	119	120	12	2	-11	8	155	136	16	2	-4	8	147	150	8	2	1	8	157	153	7	
3	-1	7	59	43	16	-6	5	7	160	186	9	3	-11	8	0	39	1	3	-4	8	62	34	16	3	1	8	360	353	7	
4	-1	7	182	179	8	-5	5	7	20	35	20	4	-11	8	119	105	24	4	-4	8	322	322	6	4	1	8	71	62	18	
5	-1	7	194	197	8	-4	5	7	35	33	35	-5	-10	8	0	42	1	5	-4	8	127	123	11	5	1	8	125	128	13	
6	-1	7	89	100	17	-3	5	7	211	213	7	-4	-10	8	0	31	1	6	-4	8	156	143	12	6	1	8	33	43	33	
7	-1	7	47	24	47	-2	5	7	213	221	7	-3	-10	8	39	39	39	7	-4	8	0	23	1	7	1	8	116	73	19	
8	-1	7	0	39	1	-1	5	7	351	358	6	-2	-10	8	66	77	31	8	-4	8	0	31	1	8	1	8	71	29	47	
-10	0	7	63	57	63	0	5	7	37	14	37	-2	-10	8	197	179	12	-9	-3	8	88	49	30	-8	2	8	160	168	11	
-9	0	7	74	31	30	1	5	7	193	201	7	0	-10	8	76	62	27	-8	-3	8	0	38	1	-4	2	8	109	86	9	
-8	0	7	58	71	50	2	5	7	63	54	17	1	-10	8	7	56	7	-7	-3	8	233	243	11	-3	2	8	60	70	14	
-7	0	7	0	70	1	5	5	7	218	185	12	2	-10	8	66	45	35	-6	-3	8	49	69	48	-2	2	8	211	198	6	
-6	0	7	206	173	9	6	5	7	0	17	1	3	-10	8	108	57	22	-5	-3	8	282	278	8	-1	2	8	239	237	8	
-5	0	7	131	114	11	7	5	7	80	49	43	4	-10	8	89	15	26	-4	-3	8	106	81	13	0	2	8	199	197	6	
1	2	8	51	37	16	-4	9	8	56	54	37	5	-5	9	177	178	9	-3	-1	9	53	10	22	-1	8	9	27	37	27	
2	2	8	149	134	8	-3	9	8	65	51	22	6	-5	9	82	51	24	-2	-1	9	150	152	9	0	8	9	61	13	29	
3	2	8	156	145	11	-2	9	8	73	58	20	-1	-5	9	120	89	18	-1	-1	9	180	187	7	1	8	9	156	137	14	
4	2	8	226	221	9	-1	9	8	71	43	19	-9	-4	9	0	34	1	1	-1	9	168	155	7	-7	9	9	48	20	48	
5	2	8	67	76	26	0	9	8	168	162	11	-8	-4	9	0	25	1	2	-1	9	0	26	1	-6	9	9	0	48	1	
6	2	8	167	159	13	1	9	8	56	8	44	-7	-4	9	0	12	1	3	-1	9	49	9	32	-5	9	9	47	56	46	
7	2	8	0	38	1	-6	10	8	27	32	26	-6	-4	9	188	171	13	4	-1	9	231	230	8	-4	9	9	101	85	18	
-8	3	8	96	100	16	-5	10	8	89	85	23	-5	-4	9	0	42	1	5	-1	9	186	166	13	-3	9	9	97	74	17	
-7	3	8	118	121	12	-4	10	8	85	49	22	-4	-4	9	197	191	9	6	-1	9	93	107	21	-2	9	9	112	97	13	
-6	3	8	245	258	7	-3	10	8	0	14	1	-3	-4	9	177	188	10	7	-1	9	48	60	48	-1	9	9	66	53	26	
-5	3	8	18	47	18	-2	10	8	54	13	45	-2	-4	9	74	97	21	-8	-2	9	82	42	20	0	9	9	84	52	25	
-4	3	8	64	80	14	-1	10	8	92	81	17	-1	-4	9	74	49	15	-2	-2	9	0	11	1	1	9	9	0	45	1	
-3	3	8	0	64	1	0	10	8	78	48	23	0	-4	9	182	169	9	-1	-2	9	130	138	13	-5	10	9	90	50	24	
-2	3	8	149	140	7	1	10	8	116	75	17	3	-4	9	31	7	30	0	-2	9	133	121	8	-4	10	9	50	37	49	
-1	3	8	237	252	6	-4	11	8	0	45	1	4	-4	9	26	36	26	1	-2	9	306	321	5	-3	10	9	51	57	51	
0	3	8	303	292	6	-3	11	8	0	28	1	5	-4	9	103	94	14	2	-2	9	167	140	10	-2	10	9	35	28	35	
1	3	8	137	136	8	-2	11	8	82	34	22	6	-4	9	154	126	12	3	-2	9	180	155	10	-1	10	9	92	71	19	
2	3	8	159	166	8	-1	11	8	49	3	48	7	-4	9	45	9	45	4	-2	9	65	58	29	0	10	9	55	15	54	
3	3	8	93	101	17	0	11	8	78	65	30	-9	-3	9	0	50	1	5	-2	9	128	107	14	-1	-11	10	0	42	1	
4	3	8	212	181	11	-3	-11	9	35	15	34	-8	-3	9	101	117	24	6	-2	9	100	101	24	0	-11	10	0	7	1	
5	3	8	30	41	30	-2	-1																							

Table B-15, Continued
Observed and Calculated Structure Factors for 1-ferrocenylcarbonyl-2-ferrocenylcyclopentene

h	k	l	10Fo	10Fc	10s	h	k	l	10Fo	10Fc	10s	h	k	l	10Fo	10Fc	10s	h	k	l	10Fo	10Fc	10s	h	k	l	10Fo	10Fc	10s
-8	6	8	43	41	43	-1	-8	9	0	35	1	7	-2	9	80	56	30	-4	5	9	29	27	29	-6	-7	10	79	71	37
-7	6	8	91	89	18	0	-8	9	87	83	21	8	-2	9	70	65	47	-3	5	9	116	98	9	-5	-7	10	124	137	16
-6	6	8	78	16	17	1	-8	9	34	46	33	-10	-1	9	46	19	46	-2	5	9	313	331	7	-4	-7	10	83	63	26
-5	6	8	117	115	10	2	-8	9	188	177	12	-9	-1	9	89	74	29	-1	5	9	90	69	11	-3	-7	10	156	153	14
-4	6	8	78	72	16	3	-8	9	100	79	26	-8	-1	9	106	82	21	0	5	9	133	140	9	-2	-7	10	0	15	1
-3	6	8	321	332	7	-7	-7	9	95	128	25	-7	-1	9	126	125	14	1	5	9	0	11	1	-1	-7	10	171	166	12
-2	6	8	57	82	20	-6	-7	9	59	36	59	-6	-1	9	87	88	18	4	5	9	136	107	17	0	-7	10	0	43	1
-1	6	8	71	59	14	-5	-7	9	0	47	1	-5	-1	9	58	68	24	5	5	9	76	79	54	1	-7	10	161	145	14
0	6	8	23	46	22	-4	-7	9	81	72	24	-4	-1	9	182	161	9	-8	6	9	42	9	41	2	-7	10	0	23	1
1	6	8	172	158	9	-3	-7	9	147	151	11	-3	-1	9	261	254	7	-7	6	9	105	89	15	-7	-6	10	80	79	43
2	6	8	154	135	10	-2	-7	9	69	82	25	-2	-1	9	230	226	7	-6	6	9	0	22	1	-6	-6	10	0	77	1
5	6	8	15	22	15	-1	-7	9	262	281	9	-1	-1	9	406	410	6	-5	6	9	118	101	12	-5	-6	10	57	45	57
-8	7	8	95	91	21	0	-7	9	56	27	33	1	-1	9	39	21	38	-4	6	9	35	36	35	-4	-6	10	186	152	11
-7	7	8	98	57	18	1	-7	9	99	106	16	2	-1	9	113	106	11	-3	6	9	115	91	11	-3	-6	10	139	152	14
-6	7	8	94	94	16	2	-7	9	0	39	1	3	-1	9	153	152	9	-2	6	9	134	133	10	-2	-6	10	37	50	36
-5	7	8	38	50	37	-8	-6	9	0	33	1	4	-1	9	79	88	17	-1	6	9	189	176	8	-1	-6	10	56	44	34
-4	7	8	60	40	24	-7	-6	9	94	46	23	5	-1	9	166	148	10	0	6	9	71	37	17	0	-6	10	160	142	12
-3	7	8	38	41	37	-6	-6	9	166	152	15	6	-1	9	101	106	20	1	6	9	102	79	14	1	-6	10	0	31	1
-2	7	8	125	125	10	-5	-6	9	64	75	32	7	-1	9	0	15	1	5	6	9	145	111	21	2	-6	10	209	219	10
-1	7	8	46	58	31	-4	-6	9	129	149	13	-8	0	9	81	66	25	-8	7	9	23	55	23	-8	-5	10	124	54	21
0	7	8	0	34	1	-3	-6	9	41	61	40	-7	0	9	153	130	13	-7	7	9	58	30	40	-7	-5	10	39	40	39
1	7	8	75	44	18	-2	-6	9	105	122	11	-6	0	9	135	98	11	-6	7	9	89	104	18	-6	-5	10	84	29	29
5	7	8	52	49	52	-1	-6	9	0	66	1	-5	0	9	297	292	7	-5	7	9	127	104	12	-5	-5	10	106	111	18
-8	8	8	0	7	1	0	-6	9	0	40	1	-4	0	9	43	37	42	-4	7	9	4	27	4	-4	-5	10	67	39	26
-7	8	8	95	79	23	1	-6	9	90	113	15	-3	0	9	0	24	1	-3	7	9	97	106	12	-3	-5	10	111	121	16
-6	8	8	0	46	1	2	-6	9	40	37	40	-2	0	9	159	154	8	-2	7	9	145	130	10	-2	-5	10	61	79	32
-5	8	8	39	9	39	-8	-5	9	93	72	30	-1	0	9	167	171	8	-1	7	9	0	19	1	-1	-5	10	76	54	20
-4	8	8	78	83	18	-7	-5	9	160	138	13	2	0	9	0	17	1	0	7	9	210	221	9	0	-5	10	126	135	13
-3	8	8	169	170	9	-6	-5	9	66	58	44	3	0	9	0	31	1	1	7	9	0	34	1	1	-5	10	149	151	11
-2	8	8	42	50	42	-5	-5	9	129	138	13	4	0	9	294	281	8	-8	8	9	73	56	39	-8	-4	10	101	78	28
-1	8	8	212	215	8	-4	-5	9	72	83	22	5	0	9	75	73	25	-7	8	9	97	49	21	-7	-4	10	155	149	18
0	8	8	0	16	1	-3	-5	9	12	22	11	6	0	9	106	110	16	-6	8	9	51	5	50	-6	-4	10	67	43	37
1	8	8	75	69	19	-2	-5	9	84	103	16	7	0	9	96	22	26	-5	8	9	158	152	11	-5	-4	10	21	11	20
-7	9	8	95	9	25	-1	-5	9	297	305	8	-6	1	9	122	97	12	-4	8	9	91	83	16	-4	-4	10	75	31	19
-6	9	8	151	155	16	0	-5	9	0	42	1	-5	1	9	87	67	16	-3	8	9	70	51	20	-3	-4	10	180	212	10
-5	9	8	16	62	16	1	-5	9	264	278	9	-4	1	9	100	79	12	-2	8	9	54	36	30	-2	-4	10	33	44	33
-1	-4	10	166	162	9	-5	3	10	108	127	14	3	-9	11	81	73	41	3	-1	11	103	72	16	-3	8	11	27	29	26
0	-4	10	158	146	11	-4	3	10	0	50	1	-5	-8	11	57	74	57	4	-1	11	184	153	11	-2	8	11	38	39	38
1	-4	10	122	126	13	-3	3	10	66	59	15	-4	-8	11	90	112	31	5	-1	11	91	29	21	-1	8	11	67	64	35
5	-4	10	27	22	26	-2	3	10	209	215	7	-3	-8	11	65	76	51	6	-1	11	68	58	41	0	8	11	94	85	18
6	-4	10	56	42	55	-1	3	10	99	63	9	-2	-8	11	122	132	19	-4	0	11	42	25	42	-4	9	11	0	20	1
7	-4	10	91	26	28	0	3	10	162	150	9	-1	-8	11	50	35	50	-3	0	11	189	201	9	-3	9	11	83	77	26
-9	-3	10	0	39	1	1	3	10	95	72	11	0	-8	11	0	16	1	-2	0	11	86	87	15	-2	9	11	56	34	53
-8	-3	10	68	68	55	4	3	10	202	194	12	1	-8	11	76	67	34	-1	0	11	199	205	9	-1	9	11	87	18	24
-7	-3	10	98	53	24	5	3	10	102	119	20	2	-8	11	98	90	25	0	0	11	0	29	1	-2	-9	12	119	43	25
-6	-3	10	96	101	22	6	3	10	82	82	43	3	-8	11	86	68	33	2	0	11	9	42	8	-1	-9	12	92	59	33
-5	-3	10	0	41	1	-9	4	10	0	29	1	4	-8	11	50	45	50	3	0	11	158	158	11	0	-9	12	65	54	65
-4	-3	10	70	45	21	-8	4	10	71	34	34	-6	-7	11	47	49	47	4	0	11	0	47	1	1	-9	12	0	24	1
-3	-3	10	97	87	13	-7	4	10	122	123	14	-5	-7	11	0	23	1	5	0	11	124	116	18	2	-9	12	99	57	30
-2	-3	10	43	45	42	-6	4	10	0	38	1	-4	-7	11	0	24	1	6	0	11	0	10	1	-4	-8	12	67	12	66
-1	-3	10	198	194	9	-5	4	10	141	144	10	-3	-7	11	146	137	16	-1	1	11	85	78	13	-3	-8	12	64	29	63
0	-3	10	92	117	14	-4	4	10	0	15	1	-2	-7	11	77	82	26	2	1	11	63	48	21	-2	-8	12	43	71	42
3	-3	10	55	65	27	-3	4	10	61	63	18	-1	-7	11	61	59	53	-1	7	11	14	34	14	-1	-8	12	107	107	25
4	-3	10	114	122	12	-2	4	10	0	11	1	0	-7	11	56	31	56	3	1	11	0	8	1	0	-8	12	85	26	31
5	-3	10	149	158	11	-1	4	10	258	241	8	1	-7	11	63	21	63	4	1	11	197	215	11	1	-8	12	153	109	17
6	-3	10	0	35	1	0	4	10	72	41	15	2	-7	11	95	56	20	5	1	11	62	7	62	2	-8	12	65	17	64
7	-3	10	35	19	35	1	4	10	243	226	8	3	-7	11	54	91	53	6	1	11	110	79	24	3	-8	12	0	35	1
-9	-2	10	39	38	39	4	4	10	90	53	25	-7	-6	11	0	90	1	-9	2	11	0	27	1	-5	-7	12	0	38	1
-8	-2	10	34	82	34	5	4	10	61	86	60	-6	-6	11	45	31	44	-8	2	11	30	42	29	-4	-7	12	122	82	19

Table B-15, Continued
Observed and Calculated Structure Factors for 1-ferrocenylcarbonyl-2-ferrocenylcyclopentene

h	k	l	10Fo	10Fc	10s	h	k	l	10Fo	10Fc	10s	h	k	l	10Fo	10Fc	10s	h	k	l	10Fo	10Fc	10s	h	k	l	10Fo	10Fc	10s
7	-1	10	77	39	44	-1	7	10	60	51	26	-5	-3	11	89	45	22	0	4	11	13	28	13	-2	-4	12	0	20	1
-6	0	10	80	54	20	0	7	10	68	40	23	-4	-3	11	92	88	15	1	4	11	105	96	14	-1	-4	12	134	121	13
-5	0	10	257	252	8	1	7	10	0	55	1	-3	-3	11	73	95	19	4	4	11	80	25	40	0	-4	12	36	51	35
-4	0	10	70	79	18	-7	8	10	0	2	1	-2	-3	11	85	86	17	-8	5	11	0	44	1	1	-4	12	98	81	18
-3	0	10	261	276	7	-6	8	10	0	59	1	-1	-3	11	166	145	10	-7	5	11	0	83	1	-8	-3	12	160	89	18
-2	0	10	53	32	25	-5	8	10	52	69	52	0	-3	11	86	110	15	-6	5	11	42	30	42	-7	-3	12	82	77	32
-1	0	10	171	167	9	-4	8	10	0	58	1	5	-3	11	0	13	1	-5	5	11	0	24	1	-6	-3	12	0	57	1
2	0	10	70	67	17	-3	8	10	72	78	23	6	-3	11	115	101	18	-4	5	11	140	102	13	-5	-3	12	79	51	26
3	0	10	51	52	51	-2	8	10	55	46	28	-9	-2	11	105	85	32	-3	5	11	175	180	9	-4	-3	12	97	57	18
4	0	10	43	59	42	-1	8	10	150	135	12	-8	-2	11	16	48	15	-2	5	11	62	63	23	-3	-3	12	0	45	1
5	0	10	90	77	21	0	8	10	98	58	17	-7	-2	11	58	35	57	-1	5	11	98	101	12	-2	-3	12	143	110	12
6	0	10	66	67	35	-6	9	10	27	24	27	-6	-2	11	47	41	47	0	5	11	0	14	1	-1	-3	12	51	19	51
7	0	10	117	59	24	-5	9	10	40	49	39	-5	-2	11	162	155	12	4	5	11	25	61	25	0	-3	12	180	165	12
-3	1	10	48	36	29	-4	9	10	23	21	22	-4	-2	11	88	83	15	-8	6	11	34	65	33	1	-3	12	0	25	1
-2	1	10	253	268	7	-3	9	10	78	53	21	-3	-2	11	197	199	9	-7	6	11	0	3	1	-7	-2	12	102	88	27
-1	1	10	53	37	21	-2	9	10	82	64	19	-2	-2	11	57	74	26	-6	6	11	103	84	18	-6	-2	12	0	51	1
1	1	10	9	52	9	-1	9	10	80	60	24	-1	-2	11	120	111	13	-5	6	11	45	47	45	-5	-2	12	35	63	40
3	1	10	246	233	9	0	9	10	9	26	9	0	-2	11	73	14	18	-4	6	11	41	26	41	-4	-2	12	0	26	40
4	1	10	155	125	12	-3	10	10	68	11	33	2	-2	11	78	42	18	-3	6	11	89	97	15	-3	-2	12	132	112	12
5	1	10	99	61	22	-2	10	10	0	23	1	3	-2	11	100	94	14	-2	6	11	163	152	11	-2	-2	12	110	83	15
6	1	10	71	34	38	-1	10	10	81	84	28	4	-2	11	57	67	37	-1	6	11	98	93	13	-1	-2	12	202	218	9
-8	2	10	0	23	1	-2	-10	11	42	16	42	5	-2	11	0	56	1	0	6	11	106	105	13	0	-2	12	109	94	12
-1	2	10	150	141	9	-1	-10	11	83	15	35	6	-2	11	0	47	1	-7	7	11	122	88	17	5	-2	12	131	118	18
0	2	10	42	44	38	0	-10	11	130	63	21	-7	-1	11	55	73	55	-6	7	11	42	19	41	-5	-1	12	136	121	14
1	2	10	91	91	10	1	-10	11	62	46	61	-6	-1	11	120	101	16	-5	7	11	84	83	23	-4	-1	12	113	99	13
3	2	10	217	209	9	2	-10	11	75	66	41	-5	-1	11	0	10	1	-4	7	11	0	51	1	-3	-1	12	98	79	14
4	2	10	82	77	24	-4	-9	11	0	28	1	-4	-1	11	190	180	9	-3	7	11	49	59	49	-2	-1	12	137	117	11
5	2	10	71	57	33	-3	-9	11	72	44	43	-3	-1	11	0	45	1	-2	7	11	0	25	1	-1	-1	12	70	27	23
6	2	10	0	45	1	-2	-9	11	0	20	1	-2	-1	11	202	207	9	-1	7	11	41	42	41	0	-1	12	178	138	10
-9	3	10	57	13	56	-1	-9	11	58	64	57	-1	-1	11	40	79	40	0	7	11	52	54	51	2	-1	12	97	81	14
-8	3	10	99	113	19	0	-9	11	0	30	1	0	-1	11	0	42	1	-6	8	11	56	69	55	3	-1	12	41	25	41
-7	3	10	81	102	20	1	-9	11	129	103	18	1	-1	11	44	11	43	-5	8	11	77	5	23	4	-1	12	76	47	29
-6	3	10	68	75	22	2	-9	11	81	44	44	2	-1	11	160	156	9	-4	8	11	38	43	37	5	-1	12	9	54	9
-2	0	12	0	35	1	-1	6	12	0	11	1	-2	-3	13	0	19	1	-5	6	13	6	11	6	-2	2	14	82	74	17
-1	0	12	188	170	10	0	6	12	74	79	22	-1	-3	13	60	51	30	-4	6	13	0	42	1	-1	2	14	28	31	32
0	0	12	154	135	11	-6	7	12	70	37	41	0	-3	13	113	108	16	-3	6	13	28	42	27	2	2	14	86	90	28
1	0	12	140	125	12	-5	7	12	69	63	32	1	-3	13	121	113	17	-2	6	13	103	85	17	-6	3	14	89	77	23
2	0	12	45	19	44	-4	7	12	44	18	44	-6	-2	13	63	42	56	-1	6	13	108	70	16	-5	3	14	78	93	23
3	0	12	88	79	19	-3	7	12	52	68	51	-5	-2	13	99	91	21	-4	7	13	8	44	7	-4	3	14	64	23	27
4	0	12	47	29	47	-2	7	12	30	39	30	-4	-2	13	72	78	30	-3	7	13	74	48	24	-3	3	14	112	76	14
5	0	12	83	17	33	-1	7	12	40	29	39	-3	-2	13	70	52	26	-2	7	13	64	18	32	-2	3	14	0	46	1
0	1	12	33	90	14	0	7	12	45	45	44	-2	-2	13	77	55	24	-1	7	13	0	44	1	-1	3	14	0	49	1
2	1	12	192	189	10	-4	8	12	57	60	36	-1	-2	13	90	36	18	-2	-7	14	55	45	55	2	3	14	0	18	1
3	1	12	92	30	22	-3	8	12	66	41	31	0	-2	13	99	59	18	-1	-7	14	6	43	6	-5	4	14	77	28	26
4	1	12	0	18	1	-2	8	12	72	63	27	1	-2	13	137	106	17	0	-7	14	83	32	43	-4	4	14	28	58	28
5	1	12	65	24	64	-1	8	12	80	23	28	-3	-1	13	127	111	13	-4	-6	14	115	61	24	-3	4	14	0	21	1
-8	2	12	75	80	39	-3	-8	13	59	52	59	-2	-1	13	86	61	19	-3	-6	14	0	24	1	-2	4	14	113	90	15
-7	2	12	81	5	24	-2	-8	13	65	8	65	-1	-1	13	47	49	47	-2	-6	14	37	18	37	-1	4	14	0	26	1
-3	2	12	123	97	10	-1	-8	13	51	10	50	0	-1	13	72	45	25	-1	-6	14	152	118	18	-4	5	14	0	5	1
-2	2	12	53	56	26	0	-8	13	0	19	1	1	-1	13	132	118	14	0	-6	14	82	24	39	-3	5	14	61	57	35
-1	2	12	0	44	1	1	-8	13	92	70	32	3	0	13	121	110	17	1	-6	14	118	57	26	-2	5	14	74	57	23
0	2	12	41	43	40	-4	-7	13	72	78	39	4	0	13	42	86	41	2	-6	14	0	10	1	-1	5	14	95	96	18
3	2	12	213	188	12	-3	-7	13	0	19	1	0	1	13	65	65	25	-5	-5	14	78	41	43	-3	6	14	24	54	23
4	2	12	68	29	45	-2	-7	13	132	99	17	2	1	13	0	16	1	-4	-5	14	98	101	24	-2	6	14	18	8	18
5	2	12	107	60	30	-1	-7	13	77	41	43	3	1	13	56	68	56	-3	-5	14	0	62	1	-3	-5	15	73	88	73
-8	3	12	58	62	58	0	-7	13	73	2	47	4	1	13	85	68	34	-2	-5	14	0	33	1	-2	-5	15	53	55	53
-7	3	12	115	80	18	1	-7	13	0	39	1	-8	2	13	63	28	62	-1	-5	14	0	68	1	-1	-5	15	107	74	27
-6	3	12	0	25	1	2	-7	13	0	45	1	-7	2	13	88	51	27	0	-5	14	47	50	46	0	-5	15	57	38	57
-5	3	12	65	40	22	-5	-6	13	78	33	37	-6	2	13	99	99	20	1	-5	14									

Table B-15, Continued
Observed and Calculated Structure Factors for 1-ferrocenylcarbonyl-2-ferrocenylcyclopentene

h	k	l	10Fo	10Fc	10s	h	k	l	10Fo	10Fc	10s	h	k	l	10Fo	10Fc	10s	h	k	l	10Fo	10Fc	10s
-2	6	12	0	33	1	-3	-3	13	0	46	1	-1	5	13	68	34	25	-3	2	14	0	21	1

APPENDIX C

Crystallography Data for 1,6-diferrocenylhexane

Equations of Mean Plane for 1,6-diferrocenyhexane

Table C-1

$$-0.2261 * XO + 0.6969 * YO + 0.6806 * ZO = 4.7724$$

$$-2.8817 * x + 5.8496 * y - 7.2697 * z = 4.7724$$

Deviation	Weight	Name
0.0044	1.00	C1
-0.0060	1.00	C2
0.0053	1.00	C3
-0.0024	1.00	C4
-0.0014	1.00	C5

Table C-2

$$-0.2333 * XO + 0.7141 * YO + 0.6601 * ZO = 1.6922$$

$$-2.9738 * x + 5.9936 * y - 7.0773 * z = 1.6922$$

Deviation	Weight	Name
-0.0040	1.00	C6
0.0037	1.00	C7
-0.0019	1.00	C8
-0.0006	1.00	C9
0.0028	1.00	C10

Table C-3
Observed and Calculated Structure Factor Tables for 1,6-diferrocenylhexane

h	k	l	10Fo	10Fc	10s	h	k	l	10Fo	10Fc	10s	h	k	l	10Fo	10Fc	10s	h	k	l	10Fo	10Fc	10s	h	k	l	10Fo	10Fc	10s
1	0	0	472	449	8	7	5	0	65	65	3	4	1	1	524	502	5	-7	4	1	3	1	3	-7	7	1	135	136	3
2	0	0	1175	1141	4	8	5	0	23	12	11	5	1	1	247	233	1	-6	4	1	165	171	2	-6	7	1	31	16	18
3	0	0	1485	1540	5	9	5	0	118	101	4	6	1	1	627	618	1	-5	4	1	146	150	2	-5	7	1	95	92	3
4	0	0	78	81	3	10	5	0	50	34	8	7	1	1	209	204	1	-4	4	1	177	175	2	-4	7	1	155	150	2
5	0	0	565	547	3	11	5	0	62	63	7	8	1	1	350	350	2	-3	4	1	115	114	2	-3	7	1	50	51	5
6	0	0	319	321	3	12	5	0	0	24	1	9	1	1	358	371	2	-2	4	1	151	146	1	-2	7	1	140	138	2
7	0	0	195	207	3	13	5	0	0	7	1	10	1	1	72	69	3	-1	4	1	180	187	1	-1	7	1	131	140	2
8	0	0	464	476	3	14	5	0	41	32	16	11	1	1	180	184	2	0	4	1	339	332	2	0	7	1	200	210	2
9	0	0	122	132	10	0	6	0	323	321	8	12	1	1	83	73	4	1	4	1	89	76	2	1	7	1	164	157	3
10	0	0	295	309	5	1	6	0	104	106	2	13	1	1	79	64	6	2	4	1	114	116	2	2	7	1	0	15	1
11	0	0	168	188	4	2	6	0	251	242	3	14	1	1	92	86	4	3	4	1	215	211	2	3	7	1	219	211	4
12	0	0	36	42	9	3	6	0	176	175	2	15	1	1	48	20	7	4	4	1	98	103	2	4	7	1	134	140	2
13	0	0	113	129	8	4	6	0	52	42	3	16	1	1	52	46	8	5	4	1	187	197	2	5	7	1	26	18	13
14	0	0	58	57	11	5	6	0	195	189	4	-16	2	1	0	16	1	6	4	1	31	9	5	6	7	1	164	161	2
15	0	0	60	46	14	6	6	0	106	113	3	-15	2	1	27	0	18	7	4	1	48	47	3	7	7	1	94	109	3
16	0	0	61	61	18	7	6	0	33	6	14	-14	2	1	29	17	16	8	4	1	93	95	2	8	7	1	67	72	5
1	1	0	80	66	1	8	6	0	165	158	4	-13	2	1	21	3	21	9	4	1	17	6	17	9	7	1	109	94	3
2	1	0	523	500	1	9	6	0	63	62	7	-12	2	1	51	43	5	10	4	1	35	31	17	10	7	1	24	5	24
3	1	0	187	168	1	10	6	0	87	91	5	-11	2	1	47	42	4	11	4	1	2	8	2	11	7	1	37	41	21
4	1	0	164	163	1	11	6	0	74	74	7	-10	2	1	36	36	6	12	4	1	27	21	26	12	7	1	46	36	45
5	1	0	106	99	2	12	6	0	0	7	1	-9	2	1	25	28	9	13	4	1	24	7	24	-12	8	1	59	17	19
6	1	0	138	140	2	13	6	0	65	55	14	-8	2	1	142	153	2	14	4	1	0	17	1	-11	8	1	55	40	12
7	1	0	87	88	2	14	6	0	14	35	14	-7	2	1	82	57	1	15	4	1	30	27	30	-10	8	1	0	7	1
8	1	0	117	115	1	1	7	0	39	50	5	-6	2	1	79	63	2	-15	5	1	58	57	12	-9	8	1	68	59	8
9	1	0	16	4	15	2	7	0	112	110	3	-5	2	1	82	81	1	-14	5	1	37	19	17	-8	8	1	113	99	4
10	1	0	0	6	1	3	7	0	85	75	3	-4	2	1	32	45	2	-13	5	1	66	75	8	-7	8	1	0	9	1
11	1	0	56	54	4	4	7	0	116	109	3	-3	2	1	153	150	2	-12	5	1	106	104	5	-6	8	1	163	178	4
12	1	0	42	39	7	5	7	0	50	41	5	-2	2	1	230	203	1	-11	5	1	44	8	9	-5	8	1	107	93	4
13	1	0	21	14	21	6	7	0	125	124	3	-1	2	1	142	118	1	-10	5	1	154	169	3	-4	8	1	101	88	4
14	1	0	13	5	13	7	7	0	84	84	3	0	2	1	500	469	3	-9	5	1	106	96	2	-3	8	1	129	139	3
15	1	0	0	8	1	8	7	0	61	59	5	1	2	1	773	754	7	-8	5	1	136	133	3	-2	8	1	41	31	14
16	1	0	27	4	26	9	7	0	73	69	7	2	2	1	40	56	1	-7	5	1	208	210	3	-1	8	1	61	72	5
0	2	0	578	544	9	10	7	0	0	23	1	3	2	1	264	247	1	-6	5	1	73	76	3	0	8	1	93	100	4
1	2	0	315	328	2	11	7	0	0	14	1	4	2	1	236	224	1	-5	5	1	357	358	3	1	8	1	9	4	9
2	2	0	580	588	3	12	7	0	47	48	15	5	2	1	86	82	1	-4	5	1	277	278	4	2	8	1	149	163	3
3	2	0	555	520	4	13	7	0	0	10	1	6	2	1	160	140	1	-3	5	1	158	145	2	3	8	1	65	52	5
4	2	0	7	31	6	0	8	0	158	144	6	7	2	1	168	182	1	-2	5	1	501	518	3	4	8	1	151	141	10
5	2	0	532	535	2	1	8	0	67	79	5	8	2	1	72	67	3	-1	5	1	199	186	2	5	8	1	113	122	3
6	2	0	413	403	2	2	8	0	146	151	4	9	2	1	4	22	3	0	5	1	434	420	5	6	8	1	54	63	6
7	2	0	58	61	2	3	8	0	143	141	5	10	2	1	31	33	7	1	5	1	510	531	2	7	8	1	99	97	5
8	2	0	455	461	2	4	8	0	0	26	1	11	2	1	62	56	3	2	5	1	51	55	2	8	8	1	18	19	17
9	2	0	124	130	2	5	8	0	146	140	5	12	2	1	26	9	12	3	5	1	384	372	3	9	8	1	32	21	17
10	2	0	138	147	2	6	8	0	105	100	4	13	2	1	27	16	16	4	5	1	334	334	5	10	8	1	31	41	30
11	2	0	219	228	5	7	8	0	67	73	5	14	2	1	0	5	1	5	5	1	133	142	2	11	8	1	62	28	11
12	2	0	40	4	6	8	8	0	107	106	4	15	2	1	0	9	1	6	5	1	269	270	2	-10	9	1	64	43	21
13	2	0	114	118	5	9	8	0	23	4	22	16	2	1	0	0	1	7	5	1	78	67	4	-9	9	1	82	53	12
14	2	0	69	53	5	10	8	0	80	56	8	-16	3	1	37	22	17	8	5	1	141	145	2	-8	9	1	29	34	29
15	2	0	52	32	6	11	8	0	48	38	15	-15	3	1	56	64	6	9	5	1	168	176	4	-7	9	1	112	107	5
16	2	0	57	51	7	1	9	0	84	90	6	-14	3	1	38	18	8	10	5	1	0	22	1	-6	9	1	52	24	12
1	3	0	54	52	1	2	9	0	105	83	12	-13	3	1	102	93	3	11	5	1	128	133	9	-5	9	1	108	111	6
2	3	0	232	216	3	3	9	0	53	42	10	-12	3	1	111	113	3	12	5	1	70	61	7	-4	9	1	93	96	6
3	3	0	57	53	1	4	9	0	134	145	4	-11	3	1	77	90	7	13	5	1	16	28	16	-3	9	1	26	35	25
4	3	0	111	113	1	5	9	0	18	27	18	-10	3	1	191	200	2	14	5	1	62	60	9	-2	9	1	129	126	6
5	3	0	58	48	2	6	9	0	92	98	9	-9	3	1	77	85	3	-14	6	1	26	27	26	-1	9	1	57	68	15
6	3	0	243	251	2	7	9	0	71	59	7	-8	3	1	213	207	2	-13	6	1	38	29	16	0	9	1	59	61	9
7	3	0	54	48	2	8	9	0	42	21	16	-7	3	1	501	515	2	-12	6	1	19	8	19	1	9	1	140	135	4
8	3	0	84	70	2	9	9	0	0	30	1	-6	3	1	12	8	12	-11	6	1	86	71	6	2	9	1	42	33	11
9	3	0	51	49	5	10	9	0	25	24	25	-5	3	1	578	556	3	-10	6	1	51	67	9	3	9	1	118	124	4
10	3	0	48	38	4	0	1	0	33	21	32	-4	3	1	703	690	3	-9	6	1	49	40	13	4	9	1	95	87	5
11	3	0	30	17	8	1	1	0	71	33	9	-3	3	1	189	176	1	-8	6	1	140	143	2	5					

Table C-3, Continued
 Observed and Calculated Structure Factor Tables for 1,6-diferrocenylhexane

h	k	l	10Fo	10Fc	10s	h	k	l	10Fo	10Fc	10s	h	k	l	10Fo	10Fc	10s	h	k	l	10Fo	10Fc	10s	h	k	l	10Fo	10Fc	10s
-5	0	2	144	174	2	15	2	2	75	63	24	7	5	2	81	54	3	-6	9	2	80	50	8	8	2	3	24	4	7
-4	0	2	955	936	5	16	2	2	32	0	31	8	5	2	111	96	3	-5	9	2	108	114	15	9	2	3	54	53	3
-3	0	2	94	72	1	-16	3	2	33	13	14	9	5	2	39	44	7	-4	9	2	39	12	16	10	2	3	27	7	7
-2	0	2	215	201	2	-15	3	2	29	22	28	10	5	2	52	43	13	-3	9	2	83	75	6	11	2	3	62	75	12
-1	0	2	1755	1781	3	-14	3	2	25	16	18	11	5	2	50	37	10	-2	9	2	86	89	6	12	2	3	28	14	23
0	0	2	237	241	4	-13	3	2	16	32	16	12	5	2	39	4	14	-1	9	2	0	3	1	13	2	3	24	40	24
1	0	2	532	505	7	-12	3	2	33	25	27	13	5	2	37	37	21	0	9	2	121	123	4	14	2	3	0	20	1
2	0	2	561	576	3	-11	3	2	53	64	4	14	5	2	51	16	12	1	9	2	104	87	5	15	2	3	30	5	29
3	0	2	191	191	5	-10	3	2	93	92	3	-14	6	2	54	49	27	2	9	2	95	88	5	-16	3	3	68	60	6
4	0	2	778	751	1	-9	3	2	30	31	6	-13	6	2	0	17	1	3	9	2	136	138	4	-15	3	3	35	6	11
5	0	2	318	293	1	-8	3	2	126	129	2	-12	6	2	89	96	6	4	9	2	24	11	23	-14	3	3	86	72	5
6	0	2	597	589	1	-7	3	2	115	112	2	-11	6	2	69	70	6	5	9	2	97	99	4	-13	3	3	39	54	8
7	0	2	570	562	4	-6	3	2	151	154	1	-10	6	2	82	85	4	6	9	2	39	46	12	-12	3	3	53	57	6
8	0	2	65	46	5	-5	3	2	180	180	2	-9	6	2	171	181	3	7	9	2	30	34	30	-11	3	3	120	107	3
9	0	2	378	369	2	-4	3	2	39	47	2	-8	6	2	20	12	19	8	9	2	42	41	15	-10	3	3	14	17	14
10	0	2	103	94	4	-3	3	2	145	144	2	-7	6	2	116	124	2	9	9	2	68	32	7	-9	3	3	122	114	2
11	0	2	102	120	4	-2	3	2	186	177	2	-6	6	2	156	153	2	-7	10	2	58	57	22	-8	3	3	338	337	2
12	0	2	95	88	14	-1	3	2	203	206	2	-5	6	2	57	48	3	-6	10	2	56	49	16	-7	3	3	11	17	11
13	0	2	36	19	35	0	3	2	9	15	9	-4	6	2	181	184	2	-5	10	2	64	47	11	-6	3	3	507	497	3
14	0	2	81	70	6	1	3	2	199	192	1	-3	6	2	101	106	2	-4	10	2	66	76	11	-5	3	3	338	354	2
15	0	2	79	66	18	2	3	2	193	196	1	-2	6	2	186	193	1	-3	10	2	65	24	13	-4	3	3	238	250	2
16	0	2	0	5	1	3	3	2	45	54	2	-1	6	2	254	267	1	-2	10	2	59	48	12	-3	3	3	569	565	4
-17	1	2	43	8	42	4	3	2	95	87	2	0	6	2	26	12	7	-1	10	2	76	73	9	-2	3	3	82	84	2
-16	1	2	0	8	1	5	3	2	230	228	1	1	6	2	344	348	3	0	10	2	41	43	40	-1	3	3	364	358	3
-15	1	2	24	2	24	6	3	2	70	58	2	2	6	2	167	169	2	1	10	2	85	65	8	0	3	3	397	411	3
-14	1	2	16	2	15	7	3	2	34	33	4	3	6	2	24	35	9	2	10	2	79	78	11	1	3	3	92	83	2
-13	1	2	31	24	11	8	3	2	44	45	5	4	6	2	298	283	7	3	10	2	29	22	28	2	3	3	643	657	4
-12	1	2	49	17	5	9	3	2	99	94	3	5	6	2	114	129	3	4	10	2	83	64	7	3	3	3	240	248	3
-11	1	2	31	25	14	10	3	2	23	23	16	6	6	2	97	107	3	5	10	2	34	15	28	4	3	3	224	235	4
-10	1	2	0	14	1	11	3	2	22	31	22	7	6	2	195	190	2	6	10	2	54	40	12	5	3	3	305	319	3
-9	1	2	21	11	9	12	3	2	0	14	1	8	6	2	52	44	5	-17	1	3	32	31	31	6	3	3	0	11	1
-8	1	2	36	35	4	13	3	2	47	32	10	9	6	2	122	126	3	-16	1	3	51	53	8	7	3	3	205	209	2
-7	1	2	35	33	4	14	3	2	26	1	25	10	6	2	82	77	6	-15	1	3	24	2	24	8	3	3	122	116	3
-6	1	2	151	142	2	15	3	2	47	15	12	11	6	2	28	18	27	-14	1	3	116	104	5	9	3	3	53	49	4
-5	1	2	164	150	1	-15	4	2	47	50	11	12	6	2	58	45	10	-13	1	3	95	101	3	10	3	3	157	161	2
-4	1	2	7	10	7	-14	4	2	79	75	6	13	6	2	65	34	9	-12	1	3	64	64	4	11	3	3	81	78	6
-3	1	2	93	95	1	-13	4	2	0	7	1	-13	7	2	40	34	19	-11	1	3	227	232	3	12	3	3	101	86	5
-2	1	2	357	351	1	-12	4	2	113	101	3	-12	7	2	4	16	4	-10	1	3	120	131	2	13	3	3	104	93	11
-1	1	2	466	431	2	-11	4	2	104	93	3	-11	7	2	62	52	8	-9	1	3	221	238	2	14	3	3	20	4	20
0	1	2	339	328	2	-10	4	2	95	83	3	-10	7	2	81	74	6	-8	1	3	320	311	2	15	3	3	49	49	13
1	1	2	998	981	7	-9	4	2	154	173	2	-9	7	2	39	13	15	-7	1	3	23	20	11	-15	4	3	42	21	9
2	1	2	256	256	2	-8	4	2	147	130	3	-8	7	2	128	133	4	-6	1	3	449	458	7	-14	4	3	27	16	20
3	1	2	34	24	2	-7	4	2	319	315	2	-7	7	2	99	87	3	-5	1	3	363	327	2	-13	4	3	41	35	12
4	1	2	47	39	1	-6	4	2	446	440	1	-6	7	2	126	119	2	-4	1	3	316	320	2	-12	4	3	54	44	5
5	1	2	76	75	1	-5	4	2	56	60	3	-5	7	2	121	114	3	-3	1	3	612	614	4	-11	4	3	0	7	1
6	1	2	76	72	1	-4	4	2	692	679	2	-4	7	2	69	61	4	-2	1	3	50	42	2	-10	4	3	104	120	3
7	1	2	60	50	2	-3	4	2	319	310	2	-3	7	2	116	116	2	-1	1	3	149	137	1	-9	4	3	54	33	4
8	1	2	49	44	2	-2	4	2	400	396	1	-2	7	2	137	143	5	0	1	3	294	307	2	-8	4	3	99	89	2
9	1	2	0	2	1	-1	4	2	640	642	1	-1	7	2	17	3	16	1	1	3	207	227	1	-7	4	3	91	89	2
10	1	2	30	19	6	0	4	2	36	25	2	0	7	2	122	125	2	2	1	3	322	323	3	-6	4	3	111	107	2
11	1	2	63	59	5	1	4	2	507	491	3	1	7	2	135	132	3	3	1	3	314	321	3	-5	4	3	103	105	2
12	1	2	21	10	20	2	4	2	559	557	4	2	7	2	120	126	3	4	1	3	371	361	2	-4	4	3	168	162	2
13	1	2	24	23	23	3	4	2	200	197	3	3	7	2	116	116	3	5	1	3	653	659	3	-3	4	3	34	23	3
14	1	2	24	7	24	4	4	2	421	435	2	4	7	2	51	47	5	6	1	3	30	22	3	-2	4	3	168	168	2
15	1	2	35	2	13	5	4	2	161	162	3	5	7	2	115	105	4	7	1	3	354	354	2	-1	4	3	40	39	2
16	1	2	0	2	1	6	4	2	286	296	4	6	7	2	74	22	13	8	1	3	251	252	2	0	4	3	445	438	2
-16	2	2	37	19	12	7	4	2	206	212	4	7	7	2	75	67	4	9	1	3	110	111	2	1	4	3	100	117	2
-15	2	2	80	57	6	8	4	2	61	53	3	8	7	2	73	62	6	10	1	3	144	140	2	2	4	3	306	295	3
-14	2	2	65	70	5	9	4	2	208	216	2	9	7	2	20	9	19	11	1	3	58	39	5	3	4	3	297	298	1
-13	2	2	22	27	22	10	4	2	144	138	3	10	7	2	40	29	39</												

Table C-3, Continued
 Observed and Calculated Structure Factor Tables for 1,6-diferrocenylhexane

h	k	l	10Fo	10Fc	10s	h	k	l	10Fo	10Fc	10s	h	k	l	10Fo	10Fc	10s	h	k	l	10Fo	10Fc	10s	h	k	l	10Fo	10Fc	10s	
6	5	3	36	36	6	-1	9	3	134	134	4	-14	2	4	37	30	9	11	4	4	134	126	5	-6	8	4	52	56	8	
7	5	3	226	224	4	0	9	3	146	150	5	-13	2	4	124	114	3	12	4	4	27	5	26	-5	8	4	129	124	3	
8	5	3	149	143	3	1	9	3	28	9	18	-12	2	4	34	34	8	13	4	4	58	57	15	-4	8	4	68	80	5	
9	5	3	70	65	4	2	9	3	141	144	6	-11	2	4	118	122	4	14	4	4	39	38	39	-3	8	4	133	142	3	
10	5	3	147	153	3	3	9	3	77	64	10	-10	2	4	207	200	2	-15	5	4	7	5	7	-2	8	4	157	157	3	
11	5	3	69	48	7	4	9	3	64	67	6	-9	2	4	0	1	1	-14	5	4	35	29	15	-1	8	4	19	20	19	
12	5	3	47	38	27	5	9	3	73	69	6	-8	2	4	326	341	4	-13	5	4	0	3	1	0	8	4	155	158	3	
13	5	3	43	53	22	6	9	3	28	11	28	-7	2	4	300	305	3	-12	5	4	28	39	16	1	8	4	92	94	4	
-14	6	3	0	11	1	7	9	3	83	66	7	-6	2	4	278	267	2	-11	5	4	36	14	9	2	8	4	61	61	7	
-13	6	3	30	22	29	8	9	3	36	33	17	-5	2	4	419	423	5	-10	5	4	61	50	4	3	8	4	121	130	3	
-12	6	3	66	52	6	-6	1	0	3	32	19	32	-4	2	4	111	110	1	-9	5	4	40	39	7	4	8	4	57	53	6
-11	6	3	37	11	20	-5	1	0	3	52	34	20	-3	2	4	369	371	2	-8	5	4	24	31	12	5	8	4	91	82	4
-10	6	3	75	60	4	-4	1	0	3	39	48	23	-2	2	4	353	344	4	-7	5	4	14	20	14	6	8	4	86	95	4
-9	6	3	47	48	8	-3	1	0	3	32	5	31	-1	2	4	66	62	1	-6	5	4	65	62	3	7	8	4	0	3	1
-8	6	3	87	76	3	-2	1	0	3	57	60	14	0	2	4	514	521	4	-5	5	4	105	100	2	8	8	4	96	80	4
-7	6	3	45	45	4	-1	1	0	3	62	54	32	1	2	4	395	382	1	-4	5	4	73	68	3	9	8	4	162	125	15
-6	6	3	0	19	1	0	1	0	3	50	44	12	2	2	4	288	299	4	-3	5	4	130	129	2	-6	9	4	72	71	8
-5	6	3	35	36	4	1	1	0	3	73	80	7	3	2	4	655	681	7	-2	5	4	101	106	2	-5	9	4	18	8	17
-4	6	3	119	120	2	2	1	0	3	20	8	20	4	2	4	66	63	1	-1	5	4	156	167	4	-4	9	4	89	72	10
-3	6	3	36	33	5	3	1	0	3	57	53	11	5	2	4	250	252	1	0	5	4	80	76	3	-3	9	4	40	49	15
-2	6	3	185	183	2	4	1	0	3	44	50	16	6	2	4	290	296	4	1	5	4	239	243	2	-2	9	4	57	43	8
-1	6	3	144	142	2	5	1	0	3	41	15	20	7	2	4	18	26	12	2	5	4	28	22	7	-1	9	4	105	104	4
0	6	3	168	175	2	6	1	0	3	36	44	36	8	2	4	152	150	3	3	5	4	0	5	1	0	9	4	36	28	11
1	6	3	137	136	4	-16	0	4	52	46	21	9	2	4	116	102	2	4	5	4	163	165	2	1	9	4	90	93	6	
2	6	3	38	26	5	-15	0	4	60	63	25	10	2	4	66	55	4	5	5	4	69	73	3	2	9	4	81	83	5	
3	6	3	164	166	2	-14	0	4	40	32	16	11	2	4	137	135	4	6	5	4	69	73	3	3	9	4	43	22	10	
4	6	3	21	35	17	-13	0	4	148	146	4	12	2	4	46	27	25	7	5	4	148	138	3	4	9	4	67	65	6	
5	6	3	14	14	13	-12	0	4	116	126	5	13	2	4	83	82	14	8	5	4	22	13	22	5	9	4	46	44	12	
6	6	3	114	108	3	-11	0	4	140	139	4	14	2	4	59	58	10	9	5	4	111	111	3	6	9	4	56	32	8	
7	6	3	29	38	10	-10	0	4	321	332	3	15	2	4	33	16	32	10	5	4	32	26	13	7	9	4	60	48	8	
8	6	3	72	81	4	-9	0	4	57	40	5	-16	3	4	12	14	12	11	5	4	0	22	1	-6	10	4	47	42	21	
9	6	3	99	79	8	-8	0	4	430	425	6	-15	3	4	10	10	10	12	5	4	42	27	15	-5	10	4	66	54	11	
10	6	3	14	8	14	-7	0	4	289	299	2	-14	3	4	35	22	14	13	5	4	23	15	22	-4	10	4	0	2	1	
11	6	3	50	44	26	-6	0	4	169	166	5	-13	3	4	0	1	1	-14	6	4	56	26	11	-3	10	4	70	61	10	
12	6	3	43	36	16	-5	0	4	864	863	7	-12	3	4	34	38	10	-13	6	4	59	70	9	-2	10	4	58	57	9	
-13	7	3	33	28	32	-4	0	4	106	103	2	-11	3	4	45	38	6	-12	6	4	26	18	25	-1	10	4	0	6	1	
-12	7	3	52	46	12	-3	0	4	487	461	7	-10	3	4	45	45	5	-11	6	4	68	85	6	0	10	4	75	70	9	
-11	7	3	87	93	7	-2	0	4	770	764	4	-9	3	4	61	67	4	-10	6	4	125	136	3	1	10	4	45	38	15	
-10	7	3	54	9	9	-1	0	4	118	119	1	-8	3	4	27	19	8	-9	6	4	33	28	10	2	10	4	53	44	11	
-9	7	3	117	129	4	0	0	4	645	602	7	-7	3	4	116	110	2	-8	6	4	131	142	3	3	10	4	0	41	1	
-8	7	3	124	123	4	1	0	4	350	362	4	-6	3	4	95	98	2	-7	6	4	118	114	3	4	10	4	0	2	1	
-7	7	3	55	50	5	2	0	4	378	381	5	-5	3	4	95	85	2	-6	6	4	74	62	3	-16	1	5	23	19	23	
-6	7	3	116	117	2	3	0	4	755	748	12	-4	3	4	201	196	2	-5	6	4	196	199	2	-15	1	5	73	65	6	
-5	7	3	131	133	2	4	0	4	228	227	2	-3	3	4	50	35	3	-4	6	4	61	58	4	-14	1	5	60	41	6	
-4	7	3	95	91	5	5	0	4	579	570	3	-2	3	4	253	241	2	-3	6	4	184	188	3	-13	1	5	81	77	4	
-3	7	3	166	169	7	6	0	4	442	452	5	-1	3	4	51	51	2	-2	6	4	167	173	2	-12	1	5	152	149	3	
-2	7	3	70	72	3	7	0	4	95	92	3	0	3	4	327	317	6	-1	6	4	46	36	7	-11	1	5	24	22	14	
-1	7	3	220	233	2	8	0	4	283	282	5	1	3	4	399	404	1	0	6	4	219	229	3	-10	1	5	239	250	2	
0	7	3	132	133	2	9	0	4	112	112	3	2	3	4	102	88	2	1	6	4	45	48	4	-9	1	5	212	219	2	
1	7	3	48	44	5	10	0	4	110	109	4	3	3	4	268	270	3	2	6	4	73	76	5	-8	1	5	181	173	2	
2	7	3	206	197	5	11	0	4	121	131	8	4	3	4	160	156	6	3	6	4	177	176	6	-7	1	5	448	448	3	
3	7	3	112	125	3	12	0	4	51	43	11	5	3	4	30	26	6	4	6	4	46	47	7	-6	1	5	164	158	1	
4	7	3	61	74	4	13	0	4	86	87	8	6	3	4	65	59	3	5	6	4	175	180	2	-5	1	5	434	423	4	
5	7	3	193	195	2	-16	1	4	0	1	1	7	3	4	47	39	4	6	6	4	170	165	7	-4	1	5	592	609	4	
6	7	3	73	89	4	-15	1	4	17	0	17	8	3	4	17	1	16	7	6	4	18	22	18	-3	1	5	44	43	2	
7	7	3	118	117	3	-14	1	4	29	7	14	9	3	4	76	71	3	8	6	4	155	160	3	-2	1	5	600	578	2	
8	7	3	127	126	3	-13	1	4	10	23	9	10	3	4	31	4	11	9	6	4	80	79	4	-1	1	5	517	512	3	
9	7	3	21	15	21	-12	1	4	30	16	10	11	3	4	46	60	10	10	6	4	43	45	9	0	1	5	418	432	3	
10	7	3	83	65	4	-11	1	4	0	4	1	12	3	4	56	38	11	11	6	4	60	55	9	1	1	5	670	663	5	
11	7	3	30	34	30	-10	1	4	39	47																				

Table C-3, Continued
Observed and Calculated Structure Factor Tables for 1,6-diferrocenyhexane

h	k	l	10Fo	10Fc	10s	h	k	l	10Fo	10Fc	10s	h	k	l	10Fo	10Fc	10s	h	k	l	10Fo	10Fc	10s	h	k	l	10Fo	10Fc	10s
3	2	5	18	3	7	1	5	5	255	265	5	0	9	5	32	39	19	1	2	6	399	410	3	3	5	6	98	87	3
4	2	5	70	65	2	2	5	5	61	54	5	1	9	5	100	89	4	2	2	6	427	444	5	4	5	6	97	97	3
5	2	5	24	34	7	3	5	5	180	185	6	2	9	5	34	26	15	3	2	6	79	75	2	5	5	6	66	72	4
6	2	5	69	68	5	4	5	5	175	176	2	3	9	5	78	68	10	4	2	6	258	272	1	6	5	6	64	64	5
7	2	5	23	19	10	5	5	5	80	76	3	4	9	5	54	49	12	5	2	6	183	185	5	7	5	6	46	51	6
8	2	5	25	3	13	6	5	5	213	218	8	5	9	5	32	4	32	6	2	6	97	88	2	8	5	6	72	71	7
9	2	5	41	22	5	7	5	5	118	102	3	6	9	5	76	58	8	7	2	6	198	205	3	9	5	6	23	5	22
10	2	5	41	42	7	8	5	5	90	84	3	-5	10	5	61	43	12	8	2	6	75	74	3	10	5	6	28	10	20
11	2	5	27	10	26	9	5	5	141	147	6	-4	10	5	0	15	1	9	2	6	126	126	3	11	5	6	57	19	15
12	2	5	54	33	10	10	5	5	25	23	24	-3	10	5	42	49	27	10	2	6	136	131	3	12	5	6	52	21	22
13	2	5	36	7	20	11	5	5	74	65	5	-2	10	5	48	30	24	11	2	6	28	20	17	-13	6	6	33	5	33
14	2	5	0	1	1	12	5	5	15	42	14	-1	10	5	35	33	22	12	2	6	93	85	9	-12	6	6	34	56	21
-16	3	5	0	20	1	-13	6	5	40	33	13	0	10	5	52	50	12	13	2	6	44	26	26	-11	6	6	74	59	6
-15	3	5	79	68	5	-12	6	5	8	14	8	1	10	5	28	2	27	-15	3	6	41	13	13	-10	6	6	30	35	30
-14	3	5	32	33	31	-11	6	5	23	23	23	2	10	5	48	36	17	-14	3	6	21	13	21	-9	6	6	91	107	7
-13	3	5	52	63	6	-10	6	5	2	5	2	3	10	5	56	33	23	-13	3	6	30	22	15	-8	6	6	48	55	17
-12	3	5	120	121	3	-9	6	5	27	23	25	-15	0	6	52	37	13	-12	3	6	41	20	8	-7	6	6	85	82	3
-11	3	5	17	12	17	-8	6	5	17	15	17	-14	0	6	70	76	8	-11	3	6	34	23	9	-6	6	6	161	184	5
-10	3	5	153	159	2	-7	6	5	23	1	23	-13	0	6	15	6	14	-10	3	6	49	68	5	-5	6	6	31	32	9
-9	3	5	176	180	2	-6	6	5	50	40	6	-12	0	6	123	110	5	-9	3	6	71	52	4	-4	6	6	207	210	4
-8	3	5	111	120	2	-5	6	5	78	67	5	-11	0	6	98	103	5	-8	3	6	78	72	3	-3	6	6	148	155	2
-7	3	5	315	316	3	-4	6	5	59	49	4	-10	0	6	67	89	6	-7	3	6	111	127	2	-2	6	6	58	59	4
-6	3	5	35	35	4	-3	6	5	107	123	4	-9	0	6	256	245	3	-6	3	6	25	8	7	-1	6	6	167	175	2
-5	3	5	212	228	1	-2	6	5	43	33	7	-8	0	6	45	38	11	-5	3	6	129	128	2	0	6	6	28	15	10
-4	3	5	248	246	2	-1	6	5	113	106	3	-7	0	6	208	214	5	-4	3	6	55	49	3	1	6	6	104	97	4
-3	3	5	21	1	6	0	6	5	39	38	6	-6	0	6	481	477	15	-3	3	6	72	81	2	2	6	6	92	83	3
-2	3	5	437	465	1	1	6	5	85	80	3	-5	0	6	51	46	4	-2	3	6	92	85	2	3	6	6	32	17	10
-1	3	5	435	426	2	2	6	5	47	41	7	-4	0	6	544	558	11	-1	3	6	59	51	3	4	6	6	157	155	4
0	3	5	192	189	5	3	6	5	81	78	5	-3	0	6	604	563	3	0	3	6	148	158	2	5	6	6	105	87	5
1	3	5	746	772	6	4	6	5	11	5	10	-2	0	6	216	217	2	1	3	6	65	60	5	6	6	6	61	63	6
2	3	5	222	236	7	5	6	5	114	114	3	-1	0	6	666	656	6	2	3	6	62	72	5	7	6	6	119	114	4
3	3	5	383	397	4	6	6	5	27	8	14	0	0	6	163	181	3	3	3	6	92	96	2	8	6	6	31	33	14
4	3	5	314	324	4	7	6	5	95	112	4	1	0	6	372	382	2	4	3	6	21	22	12	9	6	6	58	56	7
5	3	5	0	14	1	8	6	5	68	55	5	2	0	6	333	350	5	5	3	6	56	48	4	10	6	6	67	46	11
6	3	5	203	207	3	9	6	5	53	41	7	3	0	6	25	25	6	6	3	6	7	14	7	11	6	6	20	0	19
7	3	5	142	145	2	10	6	5	27	30	26	4	0	6	313	324	6	7	3	6	56	53	4	-11	7	6	0	15	1
8	3	5	65	58	3	11	6	5	37	13	19	5	0	6	170	173	3	8	3	6	33	28	8	-10	7	6	50	47	12
9	3	5	148	162	4	-12	7	5	57	47	13	6	0	6	183	183	5	9	3	6	38	31	7	-9	7	6	57	38	10
10	3	5	64	56	4	-11	7	5	50	12	21	7	0	6	215	221	6	10	3	6	22	28	22	-8	7	6	60	62	17
11	3	5	103	101	4	-10	7	5	61	72	9	8	0	6	50	40	6	11	3	6	23	9	22	-7	7	6	75	64	6
12	3	5	76	73	8	-9	7	5	70	68	18	9	0	6	188	190	3	12	3	6	0	0	1	-6	7	6	51	50	9
13	3	5	28	29	28	-8	7	5	54	41	45	10	0	6	141	151	7	13	3	6	42	3	19	-5	7	6	114	110	3
14	3	5	52	49	13	-7	7	5	96	99	5	11	0	6	17	12	16	-15	4	6	66	37	10	-4	7	6	10	15	9
-15	4	5	29	16	28	-6	7	5	110	99	3	-15	1	6	25	1	25	-14	4	6	66	63	8	-3	7	6	113	122	3
-14	4	5	30	26	18	-5	7	5	96	89	3	-14	1	6	0	1	1	-13	4	6	42	20	10	-2	7	6	86	80	3
-13	4	5	43	12	9	-4	7	5	151	156	2	-13	1	6	8	9	7	-12	4	6	100	94	4	-1	7	6	24	29	20
-12	4	5	40	24	8	-3	7	5	29	26	10	-12	1	6	31	17	11	-11	4	6	105	108	3	0	7	6	74	75	4
-11	4	5	37	54	8	-2	7	5	152	162	4	-11	1	6	45	53	6	-10	4	6	43	44	10	1	7	6	61	53	5
-10	4	5	44	3	6	-1	7	5	69	59	4	-10	1	6	31	34	9	-9	4	6	191	191	2	2	7	6	46	44	7
-9	4	5	74	66	4	0	7	5	69	63	4	-9	1	6	65	70	5	-8	4	6	77	69	5	3	7	6	94	89	3
-8	4	5	52	57	4	1	7	5	92	86	3	-8	1	6	39	31	6	-7	4	6	173	189	2	4	7	6	27	1	26
-7	4	5	86	75	4	2	7	5	36	33	8	-7	1	6	22	15	21	-6	4	6	196	191	2	5	7	6	79	77	5
-6	4	5	79	69	2	3	7	5	91	82	5	-6	1	6	17	14	17	-5	4	6	69	59	4	6	7	6	58	55	6
-5	4	5	157	160	3	4	7	5	128	124	3	-5	1	6	47	46	2	-4	4	6	228	244	3	7	7	6	18	20	18
-4	4	5	28	28	5	5	7	5	21	7	21	-4	1	6	90	79	2	-3	4	6	229	227	2	8	7	6	42	35	13
-3	4	5	108	113	2	6	7	5	118	119	3	-3	1	6	22	19	5	-2	4	6	122	119	2	9	7	6	26	6	26
-2	4	5	32	24	5	7	7	5	74	77	5	-2	1	6	30	30	3	-1	4	6	352	375	2	-10	8	6	81	11	14
-1	4	5	210	214	2	8	7	5	27	35	25	-1	1	6	133	124	1	0	4	6	181	189	2	-9	8	6	51	50	25
0	4	5	24	30	8	9	7	5	69	63	11	0	1	6	55	50	2	1	4	6	242	259	2	-8	8	6	30	39	29
1	4	5	158	158	2	10	7	5	21	15	21	1	1	6	128	127	2	2	4	6	265	277	6	-7	8	6	51	43	11
2																													

Table C-3, Continued
Observed and Calculated Structure Factor Tables for 1,6-diferrocenylhexane

h	k	l	10Fo	10Fc	10s	h	k	l	10Fo	10Fc	10s	h	k	l	10Fo	10Fc	10s	h	k	l	10Fo	10Fc	10s	h	k	l	10Fo	10Fc	10s
-12	1	7	37	38	10	-7	4	7	117	113	3	-8	8	7	0	5	1	-6	2	8	3	8	2	7	5	8	46	34	8
-11	1	7	118	117	3	-6	4	7	70	76	6	-7	8	7	80	77	7	-5	2	8	188	182	3	8	5	8	28	22	27
-10	1	7	32	36	10	-5	4	7	90	93	4	-6	8	7	50	29	18	-4	2	8	131	130	2	9	5	8	32	11	18
-9	1	7	114	114	3	-4	4	7	103	100	3	-5	8	7	32	46	32	-3	2	8	147	143	4	-11	6	8	18	30	17
-8	1	7	154	155	2	-3	4	7	23	4	11	-4	8	7	70	66	5	-2	2	8	210	210	3	-10	6	8	60	54	25
-7	1	7	35	30	6	-2	4	7	77	72	4	-3	8	7	42	0	19	-1	2	8	17	10	17	-9	6	8	0	4	1
-6	1	7	215	217	2	-1	4	7	105	107	2	-2	8	7	70	75	5	0	2	8	189	195	2	-8	6	8	79	68	7
-5	1	7	316	307	2	0	4	7	40	44	6	-1	8	7	54	59	7	1	2	8	160	162	2	-7	6	8	84	92	7
-4	1	7	106	108	2	1	4	7	78	78	3	0	8	7	61	60	6	2	2	8	85	83	3	-6	6	8	6	17	6
-3	1	7	400	389	2	2	4	7	100	99	3	1	8	7	116	113	7	3	2	8	194	200	2	-5	6	8	159	161	4
-2	1	7	185	184	3	3	4	7	20	20	19	2	8	7	0	4	1	4	2	8	106	101	4	-4	6	8	80	89	5
-1	1	7	280	277	3	4	4	7	68	69	4	3	8	7	112	103	5	5	2	8	127	130	2	-3	6	8	92	92	3
0	1	7	274	295	4	5	4	7	59	53	4	4	8	7	45	50	10	6	2	8	188	182	3	-2	6	8	147	165	6
1	1	7	24	24	6	6	4	7	73	67	4	5	8	7	27	19	27	7	2	8	5	1	5	-1	6	8	33	29	10
2	1	7	192	198	1	7	4	7	33	25	10	6	8	7	56	46	18	8	2	8	123	128	4	0	6	8	141	139	3
3	1	7	164	174	2	8	4	7	42	35	8	-6	9	7	64	58	18	9	2	8	75	64	8	1	6	8	123	130	3
4	1	7	115	120	3	9	4	7	29	26	16	-5	9	7	33	32	33	10	2	8	49	37	10	2	6	8	34	22	11
5	1	7	186	190	2	10	4	7	36	3	12	-4	9	7	49	29	10	11	2	8	69	51	9	3	6	8	155	158	4
6	1	7	51	40	4	11	4	7	46	5	10	-3	9	7	75	60	6	-14	3	8	16	15	16	4	6	8	71	74	7
7	1	7	174	175	2	-13	5	7	58	43	9	-2	9	7	25	21	24	-13	3	8	30	1	21	5	6	8	65	70	5
8	1	7	148	145	3	-12	5	7	24	10	23	-1	9	7	41	46	13	-12	3	8	39	37	11	6	6	8	76	75	5
9	1	7	44	36	10	-11	5	7	90	88	5	0	9	7	81	78	7	-11	3	8	38	41	10	7	6	8	18	2	18
10	1	7	126	121	4	-10	5	7	53	45	10	1	9	7	40	15	13	-10	3	8	27	27	18	8	6	8	61	47	12
11	1	7	40	52	39	-9	5	7	92	86	5	2	9	7	90	82	5	-9	3	8	94	83	6	-9	7	8	57	53	16
-15	2	7	29	17	29	-8	5	7	134	140	5	3	9	7	39	53	38	-8	3	8	22	17	21	-8	7	8	24	32	23
-14	2	7	14	2	13	-7	5	7	15	2	15	-14	0	8	23	6	23	-7	3	8	76	65	3	-7	7	8	64	44	9
-13	2	7	11	10	11	-6	5	7	179	196	3	-13	0	8	103	83	7	-6	3	8	55	51	5	-6	7	8	70	61	8
-12	2	7	44	17	8	-5	5	7	171	183	5	-12	0	8	31	37	30	-5	3	8	41	36	7	-5	7	8	27	5	27
-11	2	7	13	17	12	-4	5	7	107	94	3	-11	0	8	36	57	17	-4	3	8	64	56	4	-4	7	8	51	61	7
-10	2	7	0	2	1	-3	5	7	239	249	3	-10	0	8	99	89	6	-3	3	8	33	25	8	-3	7	8	63	55	5
-9	2	7	36	47	8	-2	5	7	114	113	3	-9	0	8	0	14	1	-2	3	8	58	52	4	-2	7	8	54	36	7
-8	2	7	7	20	6	-1	5	7	158	153	4	-8	0	8	107	98	4	-1	3	8	101	110	3	-1	7	8	83	88	5
-7	2	7	61	48	3	0	5	7	153	166	3	-7	0	8	183	172	10	0	3	8	0	5	1	0	7	8	0	4	1
-6	2	7	14	22	13	1	5	7	51	43	4	-6	0	8	37	34	9	1	3	8	116	123	2	1	7	8	112	119	5
-5	2	7	48	42	3	2	5	7	143	146	3	-5	0	8	304	302	2	2	3	8	52	58	4	2	7	8	75	78	5
-4	2	7	28	18	5	3	5	7	98	85	3	-4	0	8	151	147	3	3	3	8	77	77	3	3	7	8	82	74	5
-3	2	7	102	97	2	4	5	7	76	72	4	-3	0	8	200	200	3	4	3	8	85	84	3	4	7	8	108	92	4
-2	2	7	28	23	5	5	5	7	141	160	3	-2	0	8	260	247	9	5	3	8	32	15	10	5	7	8	47	15	10
-1	2	7	70	66	2	6	5	7	52	55	7	-1	0	8	30	31	7	6	3	8	64	59	5	6	7	8	33	26	18
0	2	7	42	38	4	7	5	7	82	78	4	0	0	8	157	157	2	7	3	8	52	43	6	-7	8	8	51	44	13
1	2	7	142	150	2	8	5	7	93	92	4	1	0	8	150	152	2	8	3	8	0	2	1	-6	8	8	21	20	21
2	2	7	22	20	9	9	5	7	3	9	3	2	0	8	21	8	21	9	3	8	38	20	13	-5	8	8	65	65	28
3	2	7	30	41	6	10	5	7	79	63	9	3	0	8	158	167	3	10	3	8	0	19	1	-4	8	8	37	27	13
4	2	7	26	29	8	11	5	7	55	22	10	4	0	8	95	92	4	11	3	8	37	6	17	-3	8	8	65	49	6
5	2	7	11	18	11	-12	6	7	52	32	15	5	0	8	163	163	4	-13	4	8	61	50	10	-2	8	8	86	80	6
6	2	7	29	18	16	-11	6	7	4	19	4	6	0	8	114	125	6	-12	4	8	55	50	8	-1	8	8	26	23	26
7	2	7	31	24	9	-10	6	7	55	24	10	7	0	8	56	37	11	-11	4	8	35	41	13	0	8	8	75	76	7
8	2	7	18	3	18	-9	6	7	24	47	24	8	0	8	128	126	7	-10	4	8	119	115	4	1	8	8	100	103	5
9	2	7	38	31	8	-8	6	7	34	14	34	9	0	8	57	50	15	-9	4	8	26	35	25	2	8	8	38	2	21
10	2	7	26	19	26	-7	6	7	74	81	8	10	0	8	53	35	16	-8	4	8	121	132	3	3	8	8	81	95	6
11	2	7	53	3	9	-6	6	7	56	41	8	11	0	8	52	53	17	-7	4	8	146	148	4	-14	1	9	63	48	12
12	2	7	39	3	39	-5	6	7	101	85	6	12	0	8	0	16	1	-6	4	8	63	46	6	-13	1	9	32	34	20
-13	3	7	0	7	1	-4	6	7	94	97	5	-14	1	8	0	5	1	-5	4	8	176	192	2	-12	1	9	99	88	6
-14	3	7	59	43	8	-3	6	7	27	19	13	-13	1	8	0	0	1	-4	4	8	131	120	3	-11	1	9	39	34	10
-13	3	7	79	76	9	-2	6	7	73	62	4	-12	1	8	12	8	12	-3	4	8	130	128	2	-10	1	9	86	84	4
-12	3	7	0	18	1	-1	6	7	58	60	5	-11	1	8	10	4	9	-2	4	8	196	199	2	-9	1	9	125	123	3
-11	3	7	136	135	3	0	6	7	73	71	4	-10	1	8	26	7	15	-1	4	8	0	2	1	-8	1	9	0	7	1
-10	3	7	92	98	3	1	6	7	69	51	4	-9	1	8	0	2	1	0	4	8	158	171	2	-7	1	9	185	177	2
-9	3	7	87	98	3	2	6	7	66	72	5	-8	1	8	22	5	21	1	4	8	111	97	3	-6	1	9	132	131	3
-8	3	7	207	198	3	3	6	7	33	42	17	-7	1	8	14	10	14	2	4	8	87	86	3	-5	1	9	155	148	6
-7	3	7	22	14	17	4	6</																						

Table C-3, Continued
Observed and Calculated Structure Factor Tables for 1,6-diferrocenyhexane

h	k	l	10Fo	10Fc	10s	h	k	l	10Fo	10Fc	10s	h	k	l	10Fo	10Fc	10s	h	k	l	10Fo	10Fc	10s
3	2	9	28	26	10	1	6	9	28	34	16	2	2	10	190	208	3	-6	1	11	121	120	5
4	2	9	44	38	6	2	6	9	87	91	4	3	2	10	45	47	8	-5	1	11	106	107	5
5	2	9	35	42	11	3	6	9	37	26	12	4	2	10	128	140	3	-4	1	11	19	37	18
6	2	9	39	22	10	4	6	9	39	47	11	5	2	10	123	118	5	-3	1	11	133	137	4
7	2	9	28	34	21	5	6	9	54	40	8	6	2	10	0	26	1	-2	1	11	109	101	4
8	2	9	33	46	16	6	6	9	0	15	1	7	2	10	89	92	7	-1	1	11	78	75	6
9	2	9	28	3	27	-8	7	9	40	1	39	8	2	10	48	41	15	0	1	11	171	175	3
10	2	9	0	17	1	-7	7	9	69	52	10	-11	3	10	0	6	1	1	1	11	56	49	10
-13	3	9	0	23	1	-6	7	9	28	37	27	-10	3	10	48	25	29	2	1	11	135	136	5
-12	3	9	82	74	5	-5	7	9	46	35	14	-9	3	10	6	1	6	3	1	11	116	112	6
-11	3	9	45	42	9	-4	7	9	74	69	8	-8	3	10	0	23	1	4	1	11	46	30	13
-10	3	9	69	72	5	-3	7	9	37	16	13	-7	3	10	20	14	19	5	1	11	99	85	9
-9	3	9	147	139	8	-2	7	9	69	64	6	-6	3	10	33	22	18	6	1	11	52	41	27
-8	3	9	13	18	13	-1	7	9	86	91	5	-5	3	10	31	42	30	-11	2	11	28	7	27
-7	3	9	150	155	7	0	7	9	39	13	16	-4	3	10	18	5	17	-10	2	11	12	13	12
-6	3	9	111	122	4	1	7	9	108	105	4	-3	3	10	62	67	5	-9	2	11	43	19	15
-5	3	9	81	55	16	2	7	9	104	92	5	-2	3	10	62	58	7	-8	2	11	46	2	36
-4	3	9	196	193	2	3	7	9	45	34	10	-1	3	10	50	45	7	-7	2	11	33	24	29
-3	3	9	65	59	4	4	7	9	91	83	7	0	3	10	83	76	5	-6	2	11	16	29	16
-2	3	9	152	158	2	-4	8	9	50	2	23	1	3	10	0	5	1	-5	2	11	28	8	27
0	3	9	144	148	2	-3	8	9	45	44	14	2	3	10	45	46	7	-4	2	11	64	48	7
1	3	9	47	47	5	-2	8	9	43	25	14	3	3	10	22	26	21	-3	2	11	25	29	24
2	3	9	166	178	2	-1	8	9	61	57	10	4	3	10	37	1	14	-2	2	11	26	17	23
3	3	9	103	101	3	0	8	9	59	61	12	5	3	10	36	25	15	-1	2	11	23	14	23
4	3	9	159	159	2	-13	0	10	35	25	35	6	3	10	39	30	20	0	2	11	15	7	14
5	3	9	17	42	16	-12	0	10	56	53	13	7	3	10	25	9	25	1	2	11	23	15	22
6	3	9	120	122	3	-11	0	10	99	86	6	8	3	10	42	23	15	2	2	11	42	4	18
7	3	9	104	96	4	-10	0	10	31	14	30	-10	4	10	42	18	18	3	2	11	0	21	1
8	3	9	32	31	21	-9	0	10	125	132	7	-9	4	10	86	85	7	4	2	11	30	10	30
9	3	9	87	68	8	-8	0	10	107	85	8	-8	4	10	63	53	7	5	2	11	41	16	41
10	3	9	63	24	12	-7	0	10	124	119	5	-7	4	10	67	63	8	6	2	11	0	18	1
-11	4	9	0	1	1	-6	0	10	196	194	10	-6	4	10	121	118	5	-10	3	11	46	35	17
-12	4	9	18	23	18	-5	0	10	12	19	12	-5	4	10	32	44	18	-9	3	11	53	38	14
-10	4	9	34	15	34	-4	0	10	200	197	3	-4	4	10	98	102	9	-8	3	11	80	81	22
-9	4	9	38	25	37	-3	0	10	128	124	22	-3	4	10	137	133	3	-7	3	11	30	23	29
-8	4	9	26	27	25	-2	0	10	44	49	9	-2	4	10	9	15	8	-6	3	11	89	69	7
-7	4	9	0	18	1	-1	0	10	215	195	3	-1	4	10	127	132	3	-5	3	11	119	112	5
-6	4	9	65	67	7	0	0	10	161	150	6	0	4	10	77	71	6	-4	3	11	0	19	1
-5	4	9	48	13	8	1	0	10	99	100	8	1	4	10	69	73	6	-3	3	11	130	133	3
-4	4	9	85	90	4	2	0	10	222	225	5	2	4	10	117	103	4	-2	3	11	117	116	4
-3	4	9	86	85	4	3	0	10	69	60	10	3	4	10	38	18	10	-1	3	11	64	50	5
-2	4	9	12	10	12	4	0	10	155	158	6	4	4	10	83	75	4	0	3	11	132	136	3
-1	4	9	99	105	3	5	0	10	95	100	9	5	4	10	83	70	6	1	3	11	52	41	7
0	4	9	70	74	4	6	0	10	47	20	26	6	4	10	0	22	1	2	3	11	95	85	5
1	4	9	53	50	6	7	0	10	67	62	15	7	4	10	71	62	7	3	3	11	77	78	6
2	4	9	76	79	4	8	0	10	31	43	30	-9	5	10	52	12	14	4	3	11	30	12	26
3	4	9	25	15	24	9	0	10	35	11	35	-8	5	10	45	9	16	5	3	11	72	73	7
4	4	9	47	52	7	-13	1	10	30	1	30	-7	5	10	0	16	1	6	3	11	33	37	32
5	4	9	59	44	5	-12	1	10	0	5	1	-6	5	10	0	5	1	-9	4	11	49	14	31
6	4	9	1	6	1	-11	1	10	26	14	26	-5	5	10	43	39	14	-8	4	11	0	21	1
7	4	9	19	18	19	-10	1	10	0	9	1	-4	5	10	0	12	1	-7	4	11	0	11	1
8	4	9	0	24	1	-9	1	10	7	12	7	-3	5	10	41	35	11	-6	4	11	33	29	33
9	4	9	0	6	1	-8	1	10	27	24	18	-2	5	10	57	51	6	-5	4	11	36	18	19
-11	5	9	46	8	22	-7	1	10	32	4	10	-1	5	10	46	8	8	-4	4	11	54	41	10
-10	5	9	50	58	13	-6	1	10	30	13	14	0	5	10	47	50	8	-3	4	11	0	1	1
-9	5	9	78	60	7	-5	1	10	22	15	21	-2	4	11	40	35	11	-2	4	11	40	38	10
-8	5	9	33	29	27	-4	1	10	46	39	6	2	5	10	26	14	25	-1	4	11	37	31	12
-7	5	9	117	114	5	-3	1	10	36	38	8	3	5	10	43	42	9	0	4	11	0	5	1
-6	5	9	84	77	5	-2	1	10	20	9	19	1	4	11	60	20	7	1	4	11	51	24	7
-5	5	9	87	85	9	-1	1	10	27	9	12	5	5	10	20	6	19	2	4	11	23	26	23
-4	5	9	141	150	3	0	1	10	39	21	9	6	5	10	16	20	16	3	4	11	38	2	13
-3	5	9	42	31	8	1	1	10	29	12	16	-7	6	10	8	25	8	4	4	11	16	28	15
-2	5	9	129	125	4	2	1	10	0	2	1	-6	6	10	82	66	8	5	4	11	0	9	1
						3	1	10	20	17	20	-5	6	10	0	12	1	-7	5	11	0	9	1

APPENDIX D

Electrochemical Data for Solution and Monolayer Voltammetry

Table D-1
Solution Voltammetry Data for 1,6-diferrocenylhexane-1,6-dione

scan rate (mV/s)	E_{pa}	E_{pc}	i_{pa}	i_{pc}	ΔE_p	E'	i_{pa}/i_{pc}	$Sq Rt$	scan rate
25	308	230	4.58	3.99	78.0	269.0	1.148		5.000
50	308	231	6.28	5.35	77.0	269.5	1.174		7.071
75	308	235	7.48	6.58	73.0	271.5	1.137		8.660
100	308	236	8.58	7.97	72.0	272.0	1.077		10.000
125	309	233	9.31	8.50	76.0	271.0	1.095		11.180
150	312	222	19.10	18.80	90.0	267.0	1.016		12.247
175	311	234	10.70	10.00	77.0	272.5	1.070		13.229
200	314	221	21.60	21.40	93.0	267.5	1.009		14.142
225	314	230	12.10	11.40	84.0	272.0	1.061		15.000
250	313	231	12.80	12.40	82.0	272.0	1.032		15.811
275	314	232	13.50	12.90	82.0	273.0	1.047		16.583
300	315	229	13.80	13.40	86.0	272.0	1.030		17.321
325	317	229	14.50	14.10	88.0	273.0	1.028		18.028
350	317	228	14.70	14.40	89.0	272.5	1.021		18.708
375	319	225	15.00	14.90	94.0	272.0	1.007		19.365
400	319	227	15.30	15.30	92.0	273.0	1.000		20.000
425	319	225	15.60	15.80	94.0	272.0	0.987		20.616
450	319	224	16.00	16.20	95.0	271.5	0.988		21.213
475	321	222	16.10	16.50	99.0	271.5	0.976		21.794
500	322	221	16.40	16.80	101.0	271.5	0.976		22.361
525	320	220	16.50	17.20	100.0	270.0	0.959		22.913
550	320	224	16.80	17.50	96.0	272.0	0.960		23.452
575	322	222	16.90	17.60	100.0	272.0	0.960		23.979
600	319	219	17.10	18.00	100.0	269.0	0.950		24.495
625	325	219	17.20	18.20	106.0	272.0	0.945		25.000
650	322	222	17.40	18.50	100.0	272.0	0.941		25.495
675	324	218	17.40	18.80	106.0	271.0	0.926		25.981
700	328	221	17.60	18.90	107.0	274.5	0.931		26.458
750	328	215	17.90	19.40	113.0	271.5	0.923		27.386
800	327	213	18.30	19.70	114.0	270.0	0.929		28.284
850	327	215	18.70	20.40	112.0	271.0	0.917		29.155
900	330	212	18.70	20.60	118.0	271.0	0.908		30.000
950	327	216	19.20	21.10	111.0	271.5	0.910		30.822
1000	329	213	19.40	21.50	116.0	271.0	0.902		31.623
					94.5	271.5			

Table D-2

Solution Voltammetry Data for 1-ferrocenylcarbonyl-2-ferrocenylcyclopentene

scan rate (mV/s)	E_{pa1}	E_{pc2}	E_{pa1}	E_{pc2}	i_{pa1}	i_{pa2}	i_{pc1}	i_{pc2}
25	119	375	307	51	3.85	3.48	3.72	3.45
50	123	374	308	49	5.06	4.48	4.93	4.49
75	121	376	308	53	6.82	5.35	5.94	5.44
100	120	373	309	51	7.34	6.13	6.86	6.24
125	119	375	307	53	7.82	6.74	7.44	6.85
150	122	377	307	51	8.44	7.20	8.04	7.48
175	124	378	307	50	9.09	7.72	8.64	8.01
200	124	380	308	51	9.69	8.18	9.14	8.54
250	126	381	306	51	10.70	8.99	10.10	9.44
300	126	381	307	47	11.60	9.72	11.00	10.30
350	127	385	305	49	12.50	10.40	11.70	11.00
400	130	386	302	46	13.30	11.00	12.40	11.70
450	130	387	302	46	14.10	11.50	13.10	12.40
500	132	388	302	44	14.70	12.00	13.60	13.00
550	128	384	307	48	15.50	12.60	14.20	13.60
600	129	389	305	45	16.20	13.20	14.60	14.10
650	133	385	303	44	16.70	13.30	15.10	14.60
700	129	392	306	42	17.20	13.60	15.40	15.00
750	135	395	298	45	17.70	13.90	15.80	15.50
800	133	396	301	46	18.20	14.20	16.20	15.90
850	131	396	299	41	18.70	14.50	16.60	16.30
900	133	389	298	40	19.10	14.80	16.90	16.80
950	140	397	301	44	19.50	14.90	17.20	17.10

ΔE_{pa1}	ΔE_{pc2}	E_p^0	E_p^0	i_{pa1}/i_{pc2}	i_{pc1}/i_{pa2}	Sq Rt scan rate
68	324	85.0	341.0	1.116	0.935	5.000
74	325	86.0	341.0	1.127	0.909	7.071
68	323	87.0	342.0	1.254	0.901	8.660
69	322	85.5	341.0	1.176	0.894	10.000
66	322	86.0	341.0	1.142	0.906	11.180
71	326	86.5	342.0	1.128	0.896	12.247
74	328	87.0	342.5	1.135	0.894	13.229
73	329	87.5	344.0	1.135	0.895	14.142
75	330	88.5	343.5	1.133	0.890	15.811
79	334	86.5	344.0	1.126	0.884	17.321
78	336	88.0	345.0	1.136	0.889	18.708
84	340	88.0	344.0	1.137	0.887	20.000
84	341	88.0	344.5	1.137	0.878	21.213
88	344	88.0	345.0	1.131	0.882	22.361
80	336	88.0	345.5	1.140	0.887	23.452
84	344	87.0	347.0	1.149	0.904	24.495
89	341	88.5	344.0	1.144	0.881	25.495
87	350	85.5	349.0	1.147	0.883	26.458
90	350	90.0	346.5	1.142	0.880	27.386
87	350	89.5	348.5	1.145	0.877	28.284
90	355	86.0	347.5	1.147	0.873	29.155
93	349	86.5	343.5	1.137	0.876	30.000
96	353	92.0	349.0	1.140	0.866	30.822
80	336	87.0	344.0			

Table D-3
Solution Voltammetry Data for 1,6-diferrocenylhexane

<u>scan rate (mV/s)</u>	E_{pa}	E_{pc}	i_{pa}	i_{pc}	ΔE_p	E'	i_{pa}/i_{pc}	<u>Sq Rt Scan Rate</u>
25	20	-50	4.52	4.19	70.0	-15.0	1.079	5.000
50	22	-52	6.34	5.75	74.0	-15.0	1.103	7.071
75	19	-50	7.41	7.04	69.0	-15.5	1.053	8.660
100	18	-52	8.61	8.19	70.0	-17.0	1.051	10.000
125	23	-49	9.69	8.92	72.0	-13.0	1.086	11.180
150	22	-49	10.50	9.69	71.0	-13.5	1.084	12.247
175	27	-46	11.30	10.60	73.0	-9.5	1.066	13.229
200	26	-46	12.10	11.20	72.0	-10.0	1.080	14.142
250	30	-45	13.40	13.00	75.0	-7.5	1.031	15.811
300	25	-53	14.70	14.40	78.0	-14.0	1.021	17.321
350	28	-53	16.20	15.50	81.0	-12.5	1.045	18.708
400	30	-52	17.10	16.70	82.0	-11.0	1.024	20.000
450	31	-53	18.30	17.70	84.0	-11.0	1.034	21.213
500	34	-53	19.10	18.60	87.0	-9.5	1.027	22.361
550	33	-48	20.10	19.70	81.0	-7.5	1.020	23.452
600	31	-56	21.10	20.40	87.0	-12.5	1.034	24.495
650	37	-54	21.80	21.30	91.0	-8.5	1.023	25.495
700	35	-51	22.50	22.30	86.0	-8.0	1.009	26.458
750	32	-51	23.50	23.10	83.0	-9.5	1.017	27.386
800	37	-50	24.10	23.70	87.0	-6.5	1.017	28.284
850	32	-57	24.90	24.50	89.0	-12.5	1.016	29.155
900	40	-50	25.60	25.30	90.0	-5.0	1.012	30.000
950	37	-56	26.40	25.90	93.0	-9.5	1.019	30.822
1000	40	-53	27.00	26.60	93.0	-6.5	1.015	31.623
					81.5	-10.5		

Table D-4
Solution Voltammetry Data for 1,6-diferrocenylhexane-1-one

scan rate (mV/s)	E_{pa1}	E_{pc1}	E_{pa2}	E_{pc2}	i_{pa1}	i_{pc1}	i_{pa2}	i_{pc2}
25	41	348	264	-31	3.05	2.91	2.56	2.94
50	47	344	260	-28	4.29	3.90	3.85	4.10
75	44	338	266	-29	5.36	4.76	4.85	5.06
100	44	339	267	-27	6.24	5.52	5.82	5.86
125	44	339	270	-28	6.98	6.21	6.60	6.54
150	44	339	267	-28	7.62	6.82	7.30	7.15
175	43	337	269	-26	8.36	7.44	8.02	7.75
200	44	338	271	-29	9.01	7.99	8.47	8.25
225	44	340	269	-28	9.22	8.27	9.00	8.75
250	44	340	270	-26	9.88	8.92	9.42	9.27
275	43	341	269	-29	10.10	9.05	9.93	9.70
300	42	341	270	-29	10.90	9.73	10.30	10.10
325	46	340	268	-29	11.30	10.10	10.80	10.50
350	61	360	251	-51	8.86	6.64	7.79	9.86
375	61	364	252	-53	9.24	6.61	7.79	10.10
400	63	364	246	-58	8.98	6.50	8.00	10.30
425	68	369	246	-58	9.29	6.52	8.01	10.60
450	66	367	246	-60	9.06	6.45	8.11	10.80
475	73	369	244	-63	9.24	6.42	8.17	11.00
500	73	367	244	-63	8.89	6.34	8.56	11.30
550	75	361	248	-64	9.01	6.45	8.99	11.80
600	74	365	249	-62	9.20	6.54	9.11	12.20
650	82	362	247	-66	9.34	6.61	9.35	12.60

ΔE_{pa}	ΔE_{pc}	E_p^*	E_c^*	i_{pa}/i_{pc}	i_{pa}/i_{pc}	Sq Rt scan rate
72	84	5.0	306.0	1.037	1.137	5.000
75	84	9.5	302.0	1.046	1.013	7.071
73	72	7.5	302.0	1.059	0.981	8.660
71	72	8.5	303.0	1.065	0.948	10.000
72	69	8.0	304.5	1.067	0.941	11.180
72	72	8.0	303.0	1.066	0.934	12.247
69	68	8.5	303.0	1.079	0.928	13.229
73	67	7.5	304.5	1.092	0.943	14.142
72	71	8.0	304.5	1.054	0.919	15.000
70	70	9.0	305.0	1.066	0.947	15.811
72	72	7.0	305.0	1.041	0.911	16.583
71	71	6.5	305.5	1.079	0.945	17.321
75	72	8.5	304.0	1.076	0.935	18.028
112	109	5.0	305.5	0.899	0.852	18.708
114	112	4.0	308.0	0.915	0.849	19.365
121	118	2.5	305.0	0.872	0.813	20.000
126	123	5.0	307.5	0.876	0.814	20.616
126	121	3.0	306.5	0.839	0.795	21.213
136	125	5.0	306.5	0.840	0.786	21.794
136	123	5.0	305.5	0.787	0.741	22.361
139	113	5.5	304.5	0.764	0.717	23.452
136	116	6.0	307.0	0.754	0.718	24.495
148	115	8.0	304.5	0.741	0.707	25.495
75	84	7.0	305.0			

Table D-5
Monolayer Voltammetry Data for Thiol -First Electrode

scan rate (mV/s)	E_{pa1}	E_{pc1}	E_{pa2}	E_{pc2}	i_{pa1}	i_{pc1}	i_{pa2}	i_{pc2}
25	322	495	446	259	0.090	0.765	0.033	0.213
26	316	492	446	264	0.125	0.089	0.976	0.253
50	321	507	442	252	0.092	1.130	1.203	0.321
75	322	522	443	248	0.122	1.462	1.537	0.431
100	326	506	443	245	0.102	1.638	1.772	0.488
125	425	529	443	245	0.127	1.806	2.035	0.557
150	323	523	443	240	0.120	2.081	2.252	0.593
175	323	530	441	237	0.159	2.017	2.400	0.662
200	319	526	442	242	0.232	3.032	3.455	1.034
250	318	531	442	238	0.278	3.195	3.955	1.173
300	315	531	441	236	0.274	3.463	4.348	1.288
350	318	534	439	234	0.319	3.405	4.675	1.383
400	317	536	439	231	0.270	3.657	4.993	1.467
450	316	537	439	229	0.323	3.708	5.267	1.517
500	315	540	438	228	0.365	3.807	5.536	1.539

ΔE_{pa}	ΔE_{pc}	i_{pa}/i_{pc}	i_{pa}/i_{pc}	E_{pa}	E_{pc}	Area 1	Area 2	Area 3	Area 4
63	236	0.421	23.454	290.5	470.5	2.44E-09	3.52E-08	3.26E-08	5.87E-09
52	228	0.493	0.091	290.0	469.0	3.05E-09	4.06E-08	4.14E-08	7.44E-09
69	255	0.287	0.939	286.5	474.5	2.50E-09	5.86E-08	5.23E-08	1.01E-08
74	274	0.284	0.951	285.0	482.5	3.46E-09	9.16E-03	7.07E-08	1.55E-08
81	261	0.208	0.944	285.5	474.5	2.87E-09	8.82E-08	7.72E-08	1.85E-08
180	284	0.229	0.887	315.0	486.0	3.91E-09	1.20E-07	9.19E-08	2.08E-08
83	283	0.201	0.924	281.5	483.0	3.57E-09	1.35E-07	1.04E-07	2.34E-08
86	293	0.240	0.840	280.0	485.5	5.50E-09	1.31E-07	1.16E-07	2.81E-08
77	284	0.224	0.878	280.5	484.0	6.62E-09	1.96E-07	1.63E-07	4.29E-08
80	293	0.237	0.808	278.0	486.5	7.78E-09	2.16E-07	1.86E-07	5.33E-08
79	295	0.213	0.796	275.5	486.0	6.73E-09	2.33E-07	2.09E-07	5.69E-08
84	300	0.231	0.728	276.0	486.5	9.13E-09	2.30E-07	2.32E-07	6.30E-08
86	305	0.184	0.732	274.0	487.5	5.96E-09	2.67E-07	2.48E-07	6.81E-08
87	308	0.213	0.704	272.5	488.0	8.40E-09	2.58E-07	2.55E-07	7.10E-08
87	312	0.237	0.688	271.5	489.0	9.65E-09	2.81E-07	2.75E-07	7.01E-08
81	284			280.5	485.5	5.99E-10	1.98E-07	1.05E-07	3.80E-08

scan rate (V/s)	C1	C2	C3	C4	FWHM	FWHM	FWHM	FWHM
0.025	1.26E-11	1.81E-10	1.68E-10	3.03E-11	54.5	112.2	83.4	61
0.050	7.87E-12	1.05E-10	1.07E-10	1.92E-11				
0.075	4.30E-12	1.01E-10	8.99E-11	1.78E-11				
0.100	4.47E-12	1.18E-09	9.11E-11	2.00E-11				
0.125	2.96E-12	9.09E-11	7.96E-11	1.91E-11				
0.150	3.36E-12	1.03E-10	7.90E-11	1.79E-11				
0.175	2.61E-12	9.96E-11	7.63E-11	1.72E-11				
0.200	3.55E-12	8.42E-11	7.45E-11	1.81E-11	59.3	189.2	95.7	96.2
0.250	3.41E-12	1.01E-10	8.42E-11	2.21E-11				
0.300	3.34E-12	9.27E-11	8.01E-11	2.29E-11				
0.350	2.48E-12	8.60E-11	7.69E-11	2.10E-11				
0.400	2.94E-12	7.43E-11	7.47E-11	2.03E-11				
0.450	1.71E-12	7.66E-11	7.10E-11	1.95E-11				
0.500	2.16E-12	6.64E-11	6.57E-11	1.83E-11	44.9	234	107.4	102.6
	3.35E-12	9.61E-11	7.93E-11	1.94E-11				
0.200	3.86E-13	1.28E-10	6.77E-11	2.45E-11				

Table D-6
Monolayer Voltammetry Data for Thiol-Second Electrode

scan rate (mV/s)	E_{pa}	E_{pc}	E_{pa}	E_{pc}	i_{pa}	i_{pc}	i_{pa}	i_{pc}
25	298	476	449	276	0.386	0.477	0.516	0.391
50	302	474	446	273	0.688	0.809	0.892	0.641
75	298	472	449	274	0.701	1.033	1.257	0.821
100	301	471	450	272	0.831	1.264	1.552	0.981
125	301	472	449	272	0.934	1.486	1.833	1.122
150	301	473	450	270	1.037	1.708	2.128	1.292
175	302	475	450	269	1.141	1.869	2.394	1.416
200	302	475	450	270	1.231	2.058	2.675	1.548
250	302	476	447	268	1.435	2.433	3.158	1.775
300	303	479	448	268	1.568	2.785	3.632	2.035
350	304	479	448	266	1.747	3.133	4.075	2.279
400	305	479	446	265	1.957	3.435	4.545	2.492
450	305	482	446	264	2.131	3.779	4.966	2.669
500	305	481	447	263	2.282	4.089	5.376	2.925

ΔE_p	ΔE_p	i_{pa}/i_{pc}	i_{pa}/i_{pc}	E_p	E_p	Area 1	Area 2	Area 3	Area 4
22	200	0.986	0.924	287.0	462.5	5.935E-09	2.014E-08	2.062E-08	7.959E-09
23	201	1.072	0.907	287.5	460.0	1.268E-08	3.149E-08	3.626E-08	1.437E-08
24	198	0.854	0.822	286.0	460.5	1.333E-08	3.944E-08	5.283E-08	2.009E-08
29	199	0.847	0.814	286.5	460.5	1.892E-08	4.614E-08	6.302E-08	2.577E-08
29	200	0.832	0.811	286.5	460.5	2.179E-08	5.506E-08	7.67E-08	2.835E-08
31	203	0.803	0.803	283.5	461.5	2.658E-08	6.488E-08	8.757E-08	3.651E-08
33	206	0.806	0.781	283.5	462.5	2.97E-08	7.209E-08	9.958E-08	4.025E-08
32	205	0.795	0.769	286.0	463.5	3.158E-08	7.779E-08	1.123E-07	4.185E-08
34	208	0.808	0.770	285.0	461.5	3.873E-08	9.338E-08	1.399E-07	4.944E-08
35	211	0.771	0.767	283.5	463.5	4.126E-08	1.128E-07	1.539E-07	5.783E-08
38	213	0.767	0.769	285.0	463.5	4.951E-08	1.252E-07	1.694E-07	6.734E-08
40	214	0.785	0.756	285.0	463.5	5.963E-08	1.351E-07	1.994E-07	7.484E-08
41	218	0.798	0.761	284.5	464.0	6.703E-08	1.595E-07	2.203E-07	7.902E-08
42	218	0.780	0.761	284.0	464.0	7.098E-08	1.655E-07	2.322E-07	9.055E-08
32.3	205.5			285.5	462.5	6.91E-09	5.92E-08	3.59E-08	2.94E-08

scan rate (V/s)	Γ_1	Γ_2	Γ_3	Γ_4	FWHM	FWHM	FWHM	FWHM
0.025	3.06E-11	1.04E-10	1.06E-10	4.10E-11	40.1	110.6	78.6	54.5
0.050	3.27E-11	8.12E-11	9.35E-11	3.70E-11				
0.075	2.29E-11	6.78E-11	9.08E-11	3.45E-11				
0.100	2.44E-11	5.95E-11	8.12E-11	3.32E-11				
0.125	2.25E-11	5.68E-11	7.91E-11	2.92E-11				
0.150	2.28E-11	5.58E-11	7.53E-11	3.14E-11				
0.175	2.19E-11	5.31E-11	7.34E-11	2.96E-11				
0.200	2.04E-11	5.01E-11	7.24E-11	2.70E-11	44.9	80.2	86.6	85
0.250	2.00E-11	4.82E-11	7.21E-11	2.55E-11				
0.300	1.77E-11	4.85E-11	6.61E-11	2.48E-11				
0.350	1.82E-11	4.61E-11	6.44E-11	2.48E-11				
0.400	1.92E-11	4.35E-11	6.43E-11	2.41E-11				
0.450	1.92E-11	4.57E-11	6.31E-11	2.26E-11				
0.500	1.83E-11	4.27E-11	5.99E-11	2.35E-11	54.5	107.4	85	89.8
	2.11E-11	5.16E-11	7.29E-11	2.81E-11				
0.100	1.78E-11	1.53E-10	9.26E-11	7.58E-11				

Table D-7
Monolayer Voltammetry Data for Thiol-Third Electrode

scan rate (mV/s)	E_{pa1}	E_{pc1}	E_{pa2}	E_{pc2}	i_{pa1}	i_{pc1}	i_{pa2}	i_{pc2}
25	295	468	448	270	0.319	0.375	0.433	0.258
50	298	473	444	266	0.475	0.647	0.737	0.428
75	296	471	447	268	0.647	0.854	1.043	0.569
100	296	471	447	267	0.800	1.026	1.265	0.725
125	296	473	449	265	0.943	1.213	1.503	8.508
150	298	473	448	265	1.071	1.393	1.778	0.972
175	298	476	448	264	1.227	1.540	1.996	1.115
200	299	476	446	263	1.347	1.667	2.191	1.242
250	301	476	446	263	1.579	1.995	2.686	1.457
300	302	478	444	259	1.818	2.238	3.138	1.714
350	302	476	444	258	2.036	2.505	3.505	1.933
400	304	479	444	258	2.207	2.731	3.823	2.101
450	305	480	445	258	2.383	2.942	4.179	7.839
500	306	482	444	256	2.587	3.164	4.678	2.478

ΔE_p	ΔE_p	i_{pa1}/i_{pc1}	i_{pa2}/i_{pc2}	E_p	E_p	Area 1	Area 2	Area 3	Area 4
25	198	1.236	0.866	282.5	458.0	6.72E-09	1.41E-08	1.94E-08	5.90E-09
32	207	1.110	0.877	282.0	458.5	1.08E-08	2.50E-08	3.37E-08	1.16E-08
28	203	1.137	0.819	282.0	459.0	1.78E-08	3.23E-08	5.00E-08	1.47E-08
29	204	1.103	0.811	281.5	459.0	2.14E-08	3.90E-08	5.76E-08	2.07E-08
31	208	0.111	0.407	280.5	461.0	2.51E-08	4.81E-08	6.38E-08	2.52E-08
33	208	1.102	0.783	281.5	460.5	3.06E-08	5.48E-08	8.19E-08	2.76E-08
34	212	1.100	0.772	281.0	462.0	3.60E-08	6.33E-08	8.78E-08	3.26E-08
36	213	1.085	0.761	281.0	461.0	3.99E-08	6.90E-08	9.94E-08	3.83E-08
38	213	1.084	0.743	282.0	461.0	4.77E-08	8.07E-08	1.25E-07	4.23E-08
43	219	1.061	0.713	280.5	461.0	5.87E-08	9.10E-08	1.51E-07	5.81E-08
44	218	1.053	0.715	280.0	460.0	6.35E-08	9.61E-08	1.66E-07	6.60E-08
46	221	1.050	0.714	281.0	461.5	6.99E-08	1.13E-07	1.80E-07	6.83E-08
47	222	0.304	0.704	281.5	462.5	7.56E-08	1.21E-07	2.03E-07	7.84E-08
50	226	1.044	0.676	281.0	463.0	8.64E-08	1.34E-07	2.19E-07	8.31E-08
36	212.5			281.3	461.0	1.68E-08	6.89E-08	7.70E-07	3.53E-08

scan rate (V/s)	I.1	I.2	I.3	I.4	FWHM	FWHM	FWHM	FWHM
0.025	3.47E-11	7.27E-11	9.98E-11	3.04E-11	38.4	39.8	83.4	65.8
0.050	2.78E-11	6.44E-11	8.70E-11	2.98E-11				
0.075	3.06E-11	5.34E-11	8.60E-11	4.53E-11				
0.100	2.76E-11	5.03E-11	7.42E-11	2.67E-11				
0.125	2.59E-11	4.96E-11	6.58E-11	2.59E-11				
0.150	4.63E-11	4.71E-11	7.04E-11	2.37E-11				
0.175	2.65E-11	4.66E-11	6.47E-11	2.40E-11				
0.200	2.57E-11	4.45E-11	6.41E-11	2.47E-11	43.3	125.0	83.4	93.0
0.250	2.46E-11	4.16E-11	6.46E-11	2.18E-11				
0.300	2.82E-11	3.91E-11	6.50E-11	2.50E-11				
0.350	2.34E-11	3.54E-11	6.11E-11	2.43E-11				
0.400	2.25E-11	3.63E-11	5.79E-11	2.30E-11				
0.450	2.17E-11	3.48E-11	5.82E-11	2.25E-11				
0.500	2.23E-11	3.46E-11	5.64E-11	2.14E-11	52.9	152.3	89.8	88.2
	2.58E-11	4.56E-11	6.48E-11	2.45E-11				
0.200	1.08E-11	4.44E-11	4.96E-10	2.28E-11				

